Analysis and Reduction of Cellular Heterogeneity in Strain Optimization of *Bacillus licheniformis*

I n a u g u r a l d i s s e r t a t i o n

zur

Erlangung des akademischen Grades eines

Doktors der Naturwissenschaften (Dr. rer. nat.)

der

Mathematisch-Naturwissenschaftlichen Fakultät

der

Universität Greifswald

vorgelegt von

Mathis Appelbaum

Greifswald, Juli 2021

Dekan:	Prof. Dr. Gerald Kerth
1. Gutachter:	Prof. Dr. Thomas Schweder
2. Gutachter:	Prof. Dr. Erhard Bremer
3. Gutachter:	Prof. Dr. Peter Neubauer

Tag der Promotion: 29.09.2021

Table of Contents

Abbreviations, tables and figures

Abbreviations	
DNA	Deoxyribonucleic acid
BLAP	Bacillus lentus alkaline protease
AAPF	N-Succinyl-L-alanyl-L-alanyl-L-prolyl-para-nitroanilide
AU	Arbitary units
Cas	CRISPR associated (protein)
CDW	Cellular dry weight
CRISPR	Clustered regularly interspaced short palindromic repeats
DAPI	4’,6-diamidino-2-phenylindole
EFSA	European Food Safety Authority
Eps	Extracellular polysaccharides
FDA	Food and Drug Administration (USA)
FITC	Fluorescein isothiocyanate, here: GFP intensity
gDNA	Genomic DNA
GFP	Green fluorescent protein
HDR	Homology directed repair
HTH	Helix-turn-helix (motif)
IPTG	Isopropyl β- d-1-thiogalactopyranoside
mRFP	Red fluorescent protein
mRNA	Messenger RNA (ribonucleic acid)
mScarletI	Red fluorescent protein
MTP	Microtiter plate
OD	Optical density
ori	Origin of replication
PAGE	Polyacrylamide gel electrophoresis
PBS	Phosphate buffered saline
RBS	Ribosome binding site
SDS	Sodium dodecyl sulfate
SEVA	Standardiozed european vector architecture
SOE	Splicing by overlap extension (PCR)
SsrA	SsrA proteolysis tag
UV	Ultra violet (radiation)
X-Gal	5-bromo-4-chloro-3-indolyl-β-D-galactopyranoside
γ-PGA	Poly-gamma-glutamic acid

Tables

Figures

1 Introduction

Microbial life has evolved under nearly all environmental conditions found on Earth. The high diversity of ecological niches microorganisms have adapted to is best reflected by extremophiles growing in presence of geochemical and physical parameters that are harsh from an anthropocentric point of view. This includes growth from below 0 °C to above 120 °C, in the range of pH 0 to 13, high salinity, UV and gamma radiation or combinations thereof (Coker 2019). Although the number of species adapted to extreme conditions is impressively high, the highest microbial diversity in the biosphere is found in soil with 10^2 to 10^6 bacterial phylotypes per gram of soil (Thompson *et al.* 2017; Bahram *et al.* 2018; Delgado-Baquerizo *et al.* 2018). Unlike the ecological niches of extremophiles, life in soil is not extreme at first glance. However, strong changes in physical and geochemical parameters and heterogeneous micro-environments render soil a harsh environment. The abiotic and biotic factors shaping life in this habitat comprise temperature, pH, osmolarity, availability of nutrients and inter- and intra-species competition (Pittelkow and Bremer 2011; Xu *et al.* 2013; Kaiser *et al.* 2016; Bahram *et al.* 2018). The ability to cope with these factors, and to adapt to changing environmental conditions in general, determines a species' fitness. Consequently, the selective pressure by fluctuating environmental conditions has favored greater complexity in the physiology of soil-dwelling bacteria compared to microorganisms facing rather homeostatic environments (Aizawa *et al.* 2002; Szurmant and Ordal 2004). The Gram-positive model organism *Bacillus subtilis* represents one of the best studied soil bacteria and microorganisms in general. Moreover, cellular mechanisms of how *B. subtilis* adapts to limiting environmental conditions are well understood at the molecular level. However, these adaption mechanisms are not limited to the natural habitat of *Bacillus* but also occur under optimized, constant growth conditions, which has strong implications for industrial application of members of this genus (Veening *et al.* 2006; Xiao *et al.* 2016; González-Cabaleiro *et al.* 2017; Fernandez-de-Cossio-Diaz *et al.* 2019). Following a brief overview on *B. subtilis* as a Gram-positive model organism as well as its industrial relevance, cellular adaptation processes and underlying physiological mechanisms are described in this introduction. Subsequently, the regulatory circuits controlling exoenzyme production, motility and biofilm formation are described. These adaptation mechanisms represent the focus of the strain engineering approach within this thesis.

1.1 The genus *Bacillus* in basic research and biotechnology

Members of the genus *Bacillus* are Gram-positive, rod-shaped, aerobic to facultative anaerobic bacteria from the phylum *Firmicutes* ubiquitously found in soil. *Bacillus* species are characterized by peritrichous flagella, except for *B. anthracis*, and a low GC-content (Spencer 2003). Their diverse morphology and the ability to form endospores has gained interested of researchers from the late 19th century on

(Cohn 1870; Drews 2000). This phenomenon, the differentiation of vegetative cells into dormant endospores, has been extensively investigated ever since (Leaver *et al.* 2009). However, it was the ability for uptake of exogeneous DNA from the environment, and the resulting possibility for genetic modification, that established *B. subtilis* as a Gram-positive model organism (Anagnostopoulos and Spizizen, 1961). The 4.2 Mbp large genome of *B. subtilis* was published in 1997 and encodes more than 4100 genes, 370 of which encode proteins of unknown function, making *B. subtilis* one of the best characterized organisms (Kunst *et al.* 1997; Barbe *et al.* 2009; Caspi *et al.* 2014; Borriss *et al.* 2018). The biochemistry and physiology of *Bacillus*, in particular *B. subtilis*, is well characterized including transcriptome (Rasmussen *et al.* 2009; Nicolas *et al.* 2012), proteome (Tjalsma *et al.* 2004b; Otto *et al.* 2010; Kohlstedt *et al.* 2014; Maaβ *et al.* 2014; Muntel *et al.* 2014), and metabolome analysis (Fischer and Sauer 2005; Liu *et al.* 2017) under a variety of conditions. The comprehensive genetical, biochemical, and physiological characterization of *B. subtilis* provides a strong basis for synthetic biology approaches, including the construction of minimal cells, with great potential to elucidate the essence of life as well as to design improved cell chassis for industrial applications (Westers *et al.* 2003; Manabe *et al.* 2011; Reuß *et al.* 2017; Aguilar Suárez *et al.* 2019).

In addition to the importance of *B. subtilis* for basic research, members of the genus *Bacillus* are major workhorses in industrial biotechnology. The ability to secret proteins at a g/L scale simplifies product purification and has made *Bacillus* a preferred host for production of degradative enzymes, including proteases and amylases (Schallmey *et al.* 2004). In fact, homo- and heterologous expressed enzymes using *Bacillus* production platforms account for approximately 50 % of the global enzyme market, with an estimated turnover of $7.1 billion in 2018 (Schallmey *et al.* 2004; Hohmann *et al.* 2017). Moreover, most *Bacillus* species are non-pathogenic and were applied in different areas of life for many decades (Mitsui *et al.* 2009). Consequently, selected species obtained the GRAS (*generally regarded as safe*) and QPS (*qualified presumption of safety*) status by the FDA and EFSA, reducing regulatory hurdles. Although the inherently high secretion capacity is the main driving force for the success of *Bacillus* expression hosts, their biotechnological application is not limited to enzyme production. Two examples of non-enzymatic products produced at industrial scale are vitamins, foremost riboflavin, and nucleotides used as flavoring agents (Hohmann *et al.* 2017; Acevedo-Rocha *et al.* 2019). Moreover, *Bacillus* strains were engineered for improved production of antibiotics (Kumpfmüller *et al.* 2016; Wang *et al.* 2019), pharmaceutical proteins (Lakowitz *et al.* 2017; Aguilar Suárez *et al.* 2019) and platform chemicals such as 2,3-butanediol (Yang *et al.* 2015; Fu *et al.* 2016) among others (Gu *et al.* 2018). Finally, *Bacillus* and related strains are becoming increasingly important as probiotics in food and feed applications as well as in biological control and plant growth promoting agents (Bais *et al.* 2004; Cutting

2011; Chowdhury *et al.* 2013; Rabbee *et al.* 2019). Among all *Bacillus* species, *B. subtilis*, *B. licheniformis*, *Bacillus clausii*, *Bacillus amyloliquefaciens* and *Bacillus pumilus* represent the currently most relevant hosts for biotechnological production of extracellular enzymes, but also peptide antibiotics, vitamins and biochemicals like poly-γ-glutamic acid (Froyshov and Laland 1974; Schallmey *et al.* 2004). The success story of many *Bacillus* species in industrial biotechnology is based on the production of alkaline serine proteases (subtilisin) used in the detergent industry. Two of the most capable producers of alkaline serine proteases are *B. licheniformis* and *B. pumilus*. Both species belong to the *B. subtilis* subgroup and show strong homology to this comprehensively characterized Gram-positive model species (Rey *et al.* 2004; Veith *et al.* 2004; Küppers *et al.* 2014).

1.2 Cellular heterogeneity

1.2.1 Cellular heterogeneity is a widespread phenomenon in procaryotes

The unicellular appearance of prokaryotes and their reproduction by binary fission led to the assumption, that all cells behave identical when facing the same environmental conditions. In contrast to this view, the diversity of microbial life is not limited to species- or strain-specific differences but rather includes cellular heterogeneity. Cellular heterogeneity describes the differentiation of genetically identical (isogenic) cells into phenotypically distinguishable cell types (Avery 2006). *B. subtilis* serves as a model organism for sporulation and bacterial cellular differentiation processes. In fact, *Bacillus* has gained interest of researchers already in the late 19th century due to its diverse morphology and cell types (see 1.2.2; Cohn 1870; Nakamura *et al.* 1999). However, there are further well-known examples of cellular heterogeneity in procaryotes that include Cyanobacteria, *Caulobacter crescentus* and Myxobacteria (Thaxter 1892; Lopez *et al.* 2009). Cyanobacteria, such as *Anabaena*, form heterocysts for nitrogen fixation within filaments of photosynthetically active, vegetative cells. Under nitrogen limitation, this division of labor is crucial to protect nitrogenases from oxygen generated by photosynthesis in vegetative cells. Heterocysts supply nitrogen to neighboring cells, which in return provide carbohydrates to the specialized cells (Adams 2000). *C. crescentus* differentiates into stalked and swarmer cells representing an adaptation to its aquatic lifestyle. Only stalked cells attached to surfaces can replicate, whereas swarmer cells allow for exploration of new habitats in this low nutrient environment (Ely 1991). Finally, multicellular communities represent even more complex forms of cellular differentiation allowing for cooperative behavior and division of labor. Biofilm formed by *B. subtilis* can be considered as multicellular structures, since differentiated cells provide common goods that benefit the whole population within this enclosed microenvironment (Aguilar *et al.* 2007). However, one of the most tangible examples for multicellularity and cooperative behavior are Myxobacteria, which coordinate swarming to allow for predation on other microorganisms. Moreover, when nutrients become

scarce, Myxobacteria form fruiting bodies in which the whole population contributes to efficient formation of myxospores by a fraction of cells. These elevated structures allow for efficient dispersal of spores, thereby increasing biological fitness of the species (Muñoz-Dorado *et al.* 2016). The examples described highlight the advantage of cellular heterogeneity when facing changing environmental conditions. Importantly, while environmental stimuli promote cellular adaptation processes, stochastic fluctuation in cellular components and gene expression is considered the main source for phenotypic heterogeneity (Veening and Kuipers 2010; Russell *et al.* 2017). Depending on the degree of phenotypic variation, heterogeneous and bistable (bimodal) expression patterns are distinguished. While phenotypic heterogeneity follows Gaussian distribution, bistability refers to distinct subpopulations co-existing in either an ON or OFF state regarding a certain phenotype (Dubnau and Losick 2006; Delvigne *et al.* 2014; Mustafi *et al.* 2014). The establishment of bistability requires positive and double-negative feedback loops to amplify the noise in gene expression (Lopez *et al.* 2009). These principles resulted in the widely accepted view, that cellular differentiation has evolved as a strategy for pre-adaptation to limiting conditions rather than responding to them and is therefore called a bet-hedging strategy (Veening *et al.* 2006; Xiao *et al.* 2016; González-Cabaleiro *et al.* 2017; Fernandez-de-Cossio-Diaz *et al.* 2019).

1.2.2 The regulatory network governing cellular heterogeneity in *Bacillus*

In its natural habitat as well as under laboratory conditions *B. subtilis* faces strong changes in the environmental conditions. The physiological response to these conditions results in coexistence of distinct cell types, including a motile, chemotactic subpopulation to migrate towards more favorable environments, development of genetic competence for uptake of extracellular DNA, formation of biofilms by synthesis of extracellular matrix components and the secretion of extracellular degradative enzymes to utilize macromolecules (López and Kolter 2010). Finally, as mentioned above, members of the genus *Bacillus* form dormant endospores to endure harsh environmental conditions (Piggot and Hilbert 2004). A schematic overview of these subpopulations is shown in Figure 1. The underlying regulatory network governing cellular heterogeneity in *B. subtilis* is intriguingly complex and yet follows only a few general principles including bistability, the use of regulators with dual function and different threshold levels required to trigger a certain cellular response (Fujita *et al.* 2005; Verhamme *et al.* 2007; Veening *et al.* 2008b; Chai *et al.* 2010b; Marlow *et al.* 2014b). Remarkably, only three major response regulators, Spo0A, DegU and ComA, and their cognate sensor kinases determine cell fate in *B. subtilis* (López and Kolter 2010). During exponential growth, Spo0A-P and DegU-P levels are low, enabling differentiation of the motile subpopulation. As growth conditions become limiting, Spo0A is phosphorylated by the so called phosphorelay. Five sensor kinases KinA, KinB, KinC, KinD and KinE

undergo autophosphorylation and subsequent phosphotransfer to the intermediate response regulator Spo0F. Spo0F functions as a phosphodonor for Spo0B, which transfers the phosphate group to Spo0A (Burbulys *et al.* 1991; Jiang *et al.* 2000). KinC also acts in parallel to this cascade by directly phosphorylating Spo0A (López *et al.* 2009a). Low to intermediate levels of Spo0A-P trigger biofilm formation (see section 1.3; Hamon and Lazazzera 2001; Fujita *et al.* 2005). As the Spo0A-P level further increases, biofilm formation is repressed and cells commence to sporulation by activating a regulatory cascade comprising the sporulation-specific sigma factors SigE, SigF, SigG, SigK as well as SigH (Hoon *et al.* 2010). In addition, Spo0A-P triggers expression of cannibalism factors Skf and Sdp for killing of sibling cells. This mechanism is supposed to lead to the release of nutrients thereby delaying entry into sporulation as well as to feed the sporulating subpopulation to finalize the energy intensive developmental process (González-Pastor *et al.* 2003; González-Pastor 2011; Shank and Kolter 2011). Finally, the Spo0A master regulator controls expression of exoenzyme synthesis, including the major extracellular alkaline protease AprE (Olmos *et al.* 1996). Transcription of *aprE* is repressed by SinR, ScoC, AbrB and CodY all of which, except for the latter, are under direct or indirect control of Spo0A-P (Perego *et al.* 1988; Strauch *et al.* 1989; Shafikhani *et al.* 2002). More recent data suggest that Spo0A-P also acts as a direct transcriptional activator of *aprE* as shown for *B. licheniformis* (Zhou *et al.* 2020a). In addition to Spo0A-P, expression of *aprE* requires phosphorylation of DegU (DegU-P) by its cognate sensor kinase DegS (Henner *et al.* 1988a; Shimane and Ogura 2004; Veening *et al.* 2008a). The regulatory network controlling intracellular levels of DegU-P is described in detail in section 1.5. Intermediate levels of DegU-P also promote biofilm formation, while high levels of the response regulator inhibit biofilm formation (Kobayashi 2007b; Verhamme *et al.* 2007; Marlow *et al.* 2014b). Finally, the ComP-ComA two-component regulatory system controls formation of surfactin producing cells, a small number of which develops natural genetic competence, while others initiate matrix synthesis (Nakano *et al.* 1991; López *et al.* 2009b). ComP senses the extracellular signaling peptide ComX and undergoes autophosphorylation following activation of ComA. ComA-P eventually leads to expression of the competence master regulator ComK (Weinrauch *et al.* 1990; Magnuson *et al.* 1994; Hamoen *et al.* 2003).

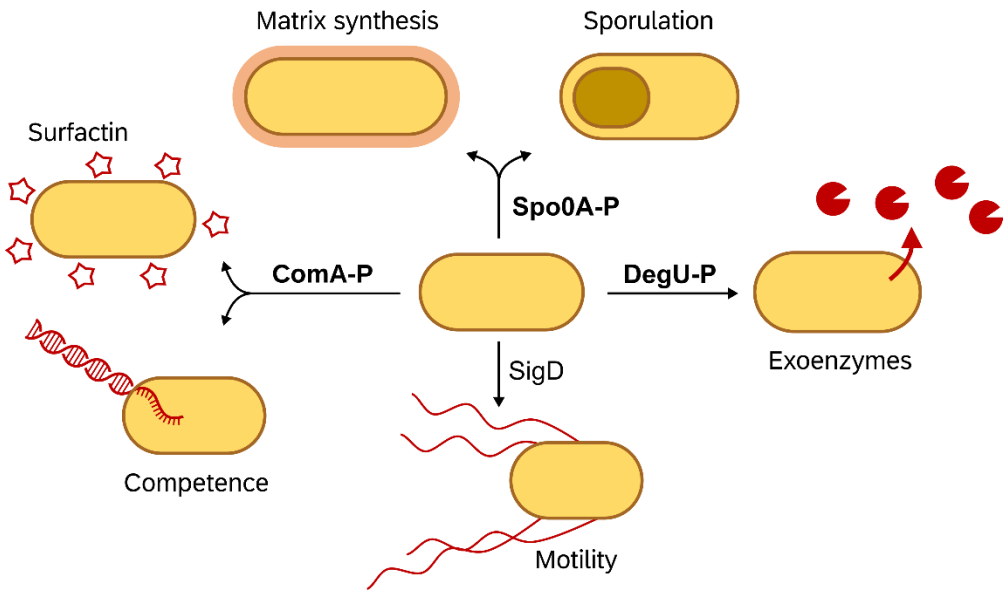

Figure 1: Illustration of distinct cell types formed by *B. subtilis*. Central regulators controlling the cellular differentiation process are indicated next to the corresponding developmental pathway. Note that matrix synthesis and sporulation require intermediate and high levels of Spo0A-P respectively. Moreover, the formation of cannibalistic cells (not shown) represents an intermediate step when initiating spore formation. Figure adapted from Lopez *et al.* (2009).

The environmental stimuli triggering all three response regulators, Spo0A, DegU and ComA are of diverse nature. One shared mechanism is their activation in response to cell density (Kalamara *et al.* 2018). Whereas the effect of ComX on the membrane bound sensor kinase ComP represents a direct interaction of the signaling molecule with its target sensor kinase, most *quorum sensing* mechanisms in *B. subtilis* occur by an indirect mechanism that involves response regulator aspartate phosphatases (Rap). Rap proteins modulate the activity of two-component signal transduction systems by two different mechanisms (Ogura *et al.* 2003; Pottathil and Lazazzera 2003; Gallego del Sol and Marina 2013; Kalamara *et al.* 2018). The first subgroup comprises Rap proteins exerting phosphatase activity over the target response regulator, such as RapA, which modulates the phosphorelay by dephosphorylating Spo0F-P (Perego and Hoch 1996; Gallego del Sol and Marina 2013). The second subset, including RapG, blocks DNA binding of the corresponding response regulator by direct interaction with its DNA binding domain (Ogura *et al.* 2003; Gallego del Sol and Marina 2013). Cell density dependent regulation of Rap protein activity occurs via secretion and uptake of pentapeptides. These so called Phr proteins antagonize Rap protein function, thereby promoting activity of the respective response regulator (Gallego del Sol and Marina 2013).

1.2.3 Cellular heterogeneity in the context of industrial biotechnology

The inherent ability of *Bacillus* to form phenotypically different subpopulations provides a fitness advantage under changing environmental conditions by enabling rapid adaptation (Avery 2006; Veening

et al. 2008b). While fluctuations in the (mirco) environment, including those observed in bioreactors, promote cellular differentiation, intrinsic noise in gene expression levels is considered the main source for phenotypic heterogeneity and bistability (Schweder *et al.* 1999; Enfors *et al.* 2001; Lara *et al.* 2006; Veening *et al.* 2008b). Consequently, even in homogeneous environments phenotypical variations at the single-cell level are observed, which has major implications for industrial biotechnology (Veening *et al.* 2006; Xiao *et al.* 2016; González-Cabaleiro *et al.* 2017; Fernandez-de-Cossio-Diaz *et al.* 2019). Single-cell analysis is widely used to address the complexity of biological systems by improving spatio-temporal analysis. But, unlike in basic research, only a limited number of studies used single cell techniques to investigate the formation of subpopulations in the context of industrial fermentation processes (Delvigne *et al.* 2014). Common global analysis of product formation represents population average values only, while productivity and metabolic capacity varies at the single-cell level (Delvigne *et al.* 2014). Similarly, proteomic, metabolomic, and transcriptomic profiling mask individual physiological differences leading to a loss of information. However, the impact of cell differentiation on process performance and economical success cannot be neglected (Delvigne and Goffin 2014; Xiao *et al.* 2016). Depending on the degree of phenotypic variation, heterogeneous and bistable (bimodal) expression patterns are distinguished both contributing to reduced productivity due to low- or non-producing cell types (Figure 2; Delvigne *et al.* 2014; Mustafi *et al.* 2014).

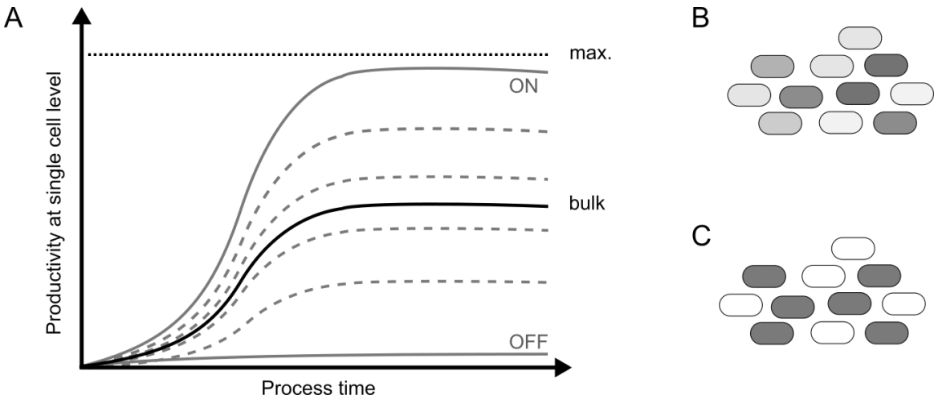

Figure 2: Cellular heterogeneity in industrial fermentation processes. A) Grey curves represent the productivity for a single cell or a subpopulation of cells. The resulting productivity at population level (bulk analysis) and the theoretical maximum productivity are depicted in black (solid and dotted line). Depending on the degree of phenotypic variation heterogeneous (dashed lines; B) or bistable (ON and OFF state; C) expression patterns are distinguished both resulting in non-optimal productivity at population level. Figure modified after Delvigne *et al.* (2014).

Cell heterogeneity was analyzed in selected industrially relevant species under process close conditions including procaryotic hosts (*E. coli*, *Clostridium*, *Pseudomonas, Corynebacterium*, *B. subtilis*) and yeasts (*Saccharomyces cervisiae*, *Pichia*, *Kluyveromyces*) (Veening *et al.* 2006; Tracy *et al.* 2008; Love *et al.* 2010; Alonso *et al.* 2012; Lee *et al.* 2013; Mustafi *et al.* 2014; Wyre and Overton 2014; Delvigne

et al. 2015; Ploss *et al.* 2016; Xiao *et al.* 2016). While the technological progress including mathematical modeling (González-Cabaleiro *et al.* 2017), on-line flow cytometry (Díaz *et al.* 2010; Baert *et al.* 2015; Milias-Argeitis *et al.* 2016), microfluidics (Fiore *et al.* 2016; Cabeen *et al.* 2017), genetically encoded biosensors (Mustafi *et al.* 2014), and semi-automated evaluation of fluorescence microscopy data (Piersma *et al.* 2013; Syvertsson *et al.* 2016) has improved analysis of phenotypic heterogeneity, only a limited number of studies developed and applied strategies to reduce cell heterogeneity from the strain engineering point of view. The aim of this thesis was to analyze and modify cellular adaptations that underly bistable control in the industrially relevant *B. licheniformis*.

1.3 Biofilm formation in *B. subtilis*

In nature, biofilms represent the predominant way of bacterial and archaeal life (Flemming and Wuertz 2019). The coordinated formation of multicellular communities embedded in an extracellular matrix provides several advantages by increasing the stress resistance against biotic and abiotic environmental factors. This includes predation, desiccation, limited availability of nutrients, and increased tolerance towards chemicals and antibiotics (Davey and O'toole 2000; Branda *et al.* 2005; Epstein *et al.* 2011; Flemming and Wuertz 2019). In addition, the enclosed microenvironment in biofilms allows for division of labor with subpopulations providing common goods that benefit the whole population (Branda *et al.* 2006; López *et al.* 2009a; Bartolini *et al.* 2018; Dragoš *et al.* 2018).

Bacteria of the genus *Bacillus* are frequently found in the rhizosphere and were shown to promote plant growth (Bais *et al.* 2004; Earl *et al.* 2008). Besides the diverse secondary metabolism of *Bacilli*, the ability to form biofilms is crucial for colonization of plant root surfaces and thus the function as a biological control agent in nature and agricultural settings (Bais *et al.* 2004; Beauregard *et al.* 2013; Fira *et al.* 2018). The underlying physiological processes governing biofilm formation in *B. subtilis* have been investigated in detail (Vlamakis *et al.* 2013; Cairns *et al.* 2014). The two main components of the extracellular matrix of *B. subtilis* are exopolysaccharides (Eps) and protein fibers formed by TasA (Branda *et al.* 2001; Kearns *et al.* 2005; Branda *et al.* 2006). In addition, the biofilm surface layer protein BslA confers hydrophobicity to *Bacillus* biofilms and is required for complex colony architecture (Kobayashi 2007b; Arnaouteli *et al.* 2017; Morris *et al.* 2017). Further structural components that contribute to biofilm formation in *B. subtilis* include the lipoprotein YvcA, the BslA paralogue YweA, levan and poly-γ-glutamic acid (γ-PGA). Although not essential for complex colony architecture and the extracellular matrix *per se*, YvcA, YweA, Levan and γ-PGA were shown to promote biofilm formation in certain *B. subtilis* strains (Stanley and Lazazzera 2005; Branda *et al.* 2006; Verhamme *et al.* 2007; Verhamme *et al.* 2009; Dogsa *et al.* 2013; Yu *et al.* 2016; Morris *et al.* 2017).

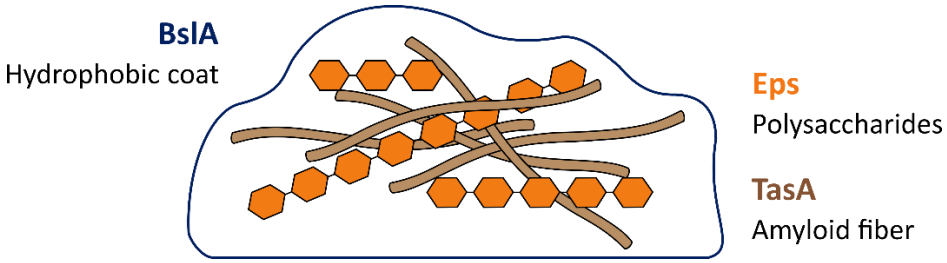

Figure 3: The *B. subtilis* biofilm matrix consists of three main components. Extracellular polysaccharides (Eps) are synthesized by genes in the *epsA-O* operon. Amyloid fibers formed by TasA are synthesized and secreted by the genes encoded in the *tapA-sipW-tasA* operon. BslA forms a hydrophobic coat at the outer surface of the biofilm.

It is important to note, that the microbial community in *B. subtilis* biofilms comprises all differentiated cell types described above (motile, spore-forming, exoenzyme producing and, although not experimentally shown, likely genetically competent cells), while only a subpopulation contributes to matrix synthesis (Chai *et al.* 2008; Vlamakis *et al.* 2008). Furthermore, the formation and size of subpopulations underlies a spatio-temporal differentiation process (Vlamakis *et al.* 2008).

1.3.1 Regulation of Eps and TasA biosynthesis

The genes for directing synthesis of the two major biofilm matrix components are encoded in the 15-gene operon *epsABCDEFGHIJKLMNO* and the *tapA-sipW-tasA* operon (hereafter *eps* and *tasA*) (Stöver and Driks 1999b; Branda *et al.* 2001; Branda *et al.* 2004; Kearns *et al.* 2005; Chu *et al.* 2006). While TapA most likely has an accessory function in the formation of TasA fibers, the type I signal peptidase SipW is required for secretion and processing of TasA and TapA (Serrano *et al.* 1999; Stöver and Driks 1999b; Romero *et al.* 2011; Erskine *et al.* 2018). In addition, SipW has a bifunctional role by promoting expression of *eps* encoded proteins independent from its catalytically active signal-peptidase domain (Terra *et al.* 2012).

Expression of *tasA* and *eps* is under transcriptional control of the biofilm master regulator SinR, the activator RemA and the transition state regulator AbrB (Stöver and Driks 1999a; Kearns *et al.* 2005; Chu *et al.* 2006; Winkelman *et al.* 2009; Chumsakul *et al.* 2011; Winkelman *et al.* 2013). SinR and AbrB repress transcription of biofilm matrix genes during vegetative growth under non-limiting conditions. Activation (phosphorylation) of the response regulator Spo0A triggered by environmental signals antagonizes SinR and AbrB mediated repression (Branda *et al.* 2001; Hamon and Lazazzera 2001). In addition to the regulation of *abrB*/AbrB by Spo0A-P (see “Introduction”), the global response regulator induces expression of the SinR antagonist SinI (Gaur *et al.* 1988; Bai *et al.* 1993; Shafikhani *et al.* 2002; Fujita *et al.* 2005; Kearns *et al.* 2005). Subsequent formation of the SinR-SinI heterodimer complex prevents SinR from tetramerization and thereby relieves target promoters from SinR (Bai *et al.* 1993;

Scott *et al.* 1999; Colledge *et al.* 2011; Newman *et al.* 2013; Kampf *et al.* 2018; Milton *et al.* 2020). While SinR is expressed constitutively by (nearly) all cells, SinI has been shown to be expressed only by cells reaching Spo0A-P levels sufficient to trigger biofilm formation (Gaur *et al.* 1988; Shafikhani *et al.* 2002; Chai *et al.* 2008). Consequently, only a subpopulation of cells contributes to matrix synthesis (Chai *et al.* 2008; Vlamakis *et al.* 2008).

In addition to SinI, SinR is antagonized by SlrA, a paralogue of SinI (Kobayashi 2008; Chai *et al.* 2009; Cozy *et al.* 2012). Regulation of *slrA* underlies the transcriptional repressor YwcC, which incorporates a so far unknown signal independent from Spo0A-P thereby adding another layer of regulation to the cost-intensive but ecologically crucial process of biofilm formation (Kobayashi 2008; Chai *et al.* 2009; Cairns *et al.* 2014).

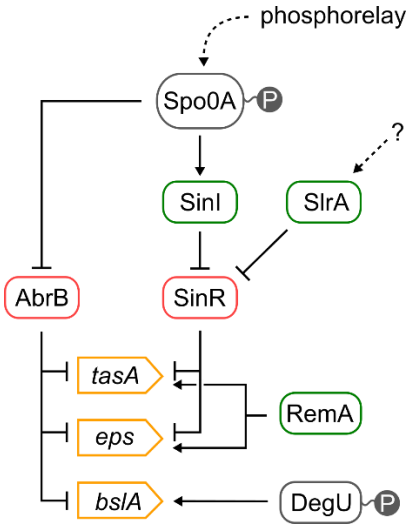

Figure 4: The regulatory network controlling biofilm matrix synthesis is *B. subtilis*. Transcriptional regulators of the major matrix components *epsA-O* (*eps*), *tapA-sipW-tasA* (*tasA*) and the hydrophobic coat protein *bslA* are shown. Repressor are depicted in red. Activators or anti-repressors are shown in green. Spo0A-P and DegU-P both activate biofilm formation at intermediate levels but repressing biofilm formation at high levels are marked in grey. Regulatory links to expression of early and late motility genes are omitted from this schema (see text for further explanation). Figure modified after Cairns *et al.* (2014) and Winkelmann *et al.* (2008).

As motility and matrix production are fundamentally contrasting adaptations several regulatory and mechanistic links have evolved to exclude the respective other developmental process in an isogenic population (Kearns *et al.* 2005; Cairns *et al.* 2014). This includes expression of the EpsE flagellar clutch, as well as proteins for surface sensing and DegU-P dependent inhibition of motility as described below (section 1.4.2). Another regulatory link, that directly involves SinR, is mediated by SlrR (Chai *et al.* 2010b). SlrR binds to SinR with high affinity and excludes SinR from binding to the *eps* and *tasA* promoter regions (Chai *et al.* 2010b; Newman *et al.* 2013). Interestingly, the SinR-SlrR heterodimer is able

to bind to the promoter core region of genes related to autolysis and motility thereby suppressing a planktonic lifestyle while simultaneously enabling biofilm formation (Chai *et al.* 2010b). Thus, SlrR is required to re-purpose SinR regarding its target promoters. More importantly, formation of the SinR-SlrR complex is crucial for long-term commitment to matrix synthesis (Chai *et al.* 2010b). Although stochastic fluctuations in SinI and SinR levels are sufficient to initiate biofilm formation, SlrR is important to promote and maintain this physiological state over several generations (Norman *et al.* 2013; Lord *et al.* 2019). The underlying bistable switch is characterized by a self-reinforcing double-negative feedback loop whereby SinR represses transcription of *slrR* while SlrR prevents SinR from binding to its own promoter (Chu *et al.* 2008; Chai *et al.* 2010b). Consequently, cells can exist in either a SlrR-high or SlrR-low state. Switching from one state to the other depends on Spo0A-P controlled expression of SinI regulating SinR and proteolytic degradation of SlrR (Fujita *et al.* 2005; Chai *et al.* 2008; Chai *et al.* 2010b; Chai *et al.* 2010a). Further regulators of *slrR* are AbrB and its homologue Abh with the latter incorporating external stimuli independent from Spo0A-P via the extracytoplasmic function sigma factors SigX, SigV, SigM (Murray *et al.* 2009b; Chumsakul *et al.* 2011).

In addition to derepression of SinR and AbrB, transcription of biofilm matrix genes requires RemA and RemB, both acting in parallel to SinR and AbrB (Winkelman *et al.* 2009; Winkelman *et al.* 2013). RemA was shown to bind to the *eps*, *tasA* and *slrR* promoter thereby activating biofilm formation directly as well as by promoting the SinR-SlrR bistable switch (Winkelman *et al.* 2013). Regulation and signaling upstream of RemA is unknown but possibly related to the nutrient limitation as indicated by its highly conserved chromosomal location (Winkelman *et al.* 2013). RemA is further involved in long-term adaptation to osmotic stress by controlling transcription of the *opuA*, *opuB* and *opuC* operons for uptake of compatible solutes (Winkelman *et al.* 2013; Hoffmann and Bremer 2017).

The importance to incorporate various environmental signals to regulate the cost-intensive but ecologically crucial process of biofilm formation is reflected by the still increasing complexity of the regulatory network in *B. subtilis* (López *et al.* 2009a; Irnov and Winkler 2010; Chai *et al.* 2012; Gerwig *et al.* 2014; İrigül-Sönmez *et al.* 2014; Gao *et al.* 2015; Dubnau *et al.* 2016; Gundlach *et al.* 2016; Bartolini *et al.* 2018; DeLoughery *et al.* 2018; Arnaouteli *et al.* 2019). Although the stimuli triggering these (newly identified) regulatory cascades or their cellular targets are largely unknown, many of them were shown to act upstream of SinR including YmdB, RNase Y-associated proteins, cyclic di-AMP, SigB and YwcC (Chai *et al.* 2008; Kobayashi 2008; Diethmaier *et al.* 2011; DeLoughery *et al.* 2016; Dubnau *et al.* 2016; Gundlach *et al.* 2016; Bartolini *et al.* 2018). Thus, still two conditions have to be met to initiate transcription of the biofilm matrix genes *eps* and *tasA*: Activation by RemA and anti-repression of AbrB and SinR (Cairns *et al.* 2014).

1.3.2 Regulation of BslA expression

The amphiphilic biofilm-surface layer protein BslA (YuaB) confers hydrophobicity to biofilms formed by *B. subtilis* and related strains, including *B. licheniformis* (Kobayashi and Iwano 2012; Morris *et al.* 2017). BslA has a bifunctional role and is required for complex colony architecture independent from its function in forming the hydrophobic coat (Kobayashi 2007b; Arnaouteli *et al.* 2017). Unlike *tasA* and *eps*, *bslA* shows an unimodal, homogeneous expression pattern at the single cell level (Kovács and Kuipers 2011; Hobley *et al.* 2013) and undergoes self-assembly into a hydrophobic layer located at the outer surface of the biofilm only (Kobayashi and Iwano 2012; Hobley *et al.* 2013).

Transcription of *bslA* and the similarly regulated *yvcA* requires DegU-P and is repressed by AbrB (Kobayashi 2007b; Verhamme *et al.* 2009). Deletion of *sinR* enhanced *yvcA* and *bslA* transcription in the undomesticated *B. subtilis* NCIB3610, but neither of the two genes is directly regulated by SinR. Instead, this results from enhanced expression of *eps* in SinR deletion mutants (Verhamme *et al.* 2009; Kobayashi and Iwano 2012). Similarly, deletion of *tasA* delays transcription of *bslA* demonstrating the requirement of *eps* and *tasA* synthesis prior to expressing the hydrophobic coat (Kobayashi and Iwano 2012). However, the increased *yvcA* and *bslA* transcription in the Δ*sinR* strain used by Verhamme *et al.* (2009) is most likely also due to reduced transcriptional repression of *degU* upon deletion of *sinR* (Newman *et al.* 2013; Ogura *et al.* 2014). In contrast to *B. subtilis* NCIB3610, transcription of *bslA* is increased in the domesticated *B. subtilis* 168 Δ*epsG* and *ΔsinI* mutants indicating strain dependent differences in the regulation of biofilm formation (Kovács and Kuipers 2011; McLoon *et al.* 2011; Gallegos-Monterrosa *et al.* 2016). In addition, the transcriptional repressor Rok is indirectly involved in expression of *bslA* in *B. subtilis* 168 via a yet unknown mechanism (Kovács and Kuipers 2011).

1.4 Motility and Chemotaxis

Many bacteria respond to changing environmental conditions by developing a motile, chemotactic state (Moens and Vanderleyden 1996). The ability to move towards higher concentrations of attractants or lower concentrations of repellents provides a fitness advantage (Aizawa *et al.* 2002). In addition, motility has been associated with surface sensing and virulence in pathogenic bacteria, including *E. coli* and *Salmonella* (Moens and Vanderleyden 1996). With the exception of *Bacillus anthracis*, all *Bacillus* species are considered to be conditionally motile by forming peritrichous flagella (Spencer 2003). Moreover, selective pressure by constantly changing environmental conditions in the natural habitat has favored greater complexity of the *B. subtilis* chemotaxis system compared to organisms facing rather homeostatic environments such as *E. coli* (Aizawa *et al.* 2002; Szurmant and Ordal 2004). In *B. subtilis*, motility and chemotaxis requires expression of more than 40 different structural proteins (Mukherjee and Kearns 2014). The main component of flagella is the filament, which is assembled from

approximately 12,000 monomeric subunits of flagellin (Hag protein) with an average number of 26 flagella per cell (Guttenplan *et al.* 2013). The so-called hook attaches the filament to the basal body, which anchors the flagellar in the cytoplasmic membrane (Kubori *et al.* 1997; Courtney *et al.* 2012). Moreover, the basal body is required for secretion and polymerization of Hag monomers and includes the rotor structure (Mukherjee and Kearns 2014). The rotor interacts with the stator composed of the motor protein MotA and the proton channel MotB to generate the torque that drives flagellar rotation (Shioi *et al.* 1978; Ito *et al.* 2005; Mukherjee and Kearns 2014). In addition to MotA/MotB, *B. subtilis* encodes a second, but minor set of stator proteins MotP/MotS driven by a Na^+ gradient (Hirota *et al.* 1981; Ito *et al.* 2004). Due to the high amount of cellular resources required for flagella synthesis, motility is strictly regulated at the transcriptional and post-transcriptional level (Moens and Vanderleyden 1996; Mukherjee and Kearns 2014).

Most of the structural genes for motility and chemotaxis in *B. subtilis* are located within the 27-kb *fla*/*che* operon (Aizawa *et al.* 2002; Mukherjee and Kearns 2014). This includes the genes encoding the flagellar basal body, the rotor, the secretion apparatus, and the hook hereafter referred as *early flagellar genes*. Furthermore, the *fla*/*che* operon encodes the core components of the chemotaxis machinery, the two-component regulatory system genes *cheA* and *cheY* and modulators required for adaptation and sensitivity of the methyl-accepting chemotaxis proteins (Aizawa *et al.* 2002). Unlike the *early flagellar* genes, the *late flagellar genes* for flagellin, motor protein and filament cap synthesis are not located in the *fla/che* operon, but distributed across the chromosome (Aizawa *et al.* 2002). However, transcription of *hag*, *motA*-*motB* and *fliD* is synchronized by the alternative sigma factor SigD (σ^D, σ^{28}) (Mirel and Chamberlin 1989; Serizawa *et al.* 2004). SigD was shown to regulate over 150 genes related to motility, chemotaxis and autolysis (*lytC*, *lytD*, *lytF*) grouped in the SigD regulon (Helmann *et al.* 1988; Mirel and Chamberlin 1989; Márquez *et al.* 1990; Serizawa *et al.* 2004). The *sigD* coding sequence itself is the penultimate gene of the *fla*/*che* operon and thus expression of the *early flagellar genes* including *sigD* is a prerequisite for expression of the *late flagellar genes* and synthesis of the cost-intensive Hag filament (Helmann *et al.* 1988; Mukherjee and Kearns 2014).

1.4.1 Transcriptional regulation of the *flalche* operon and motility

Transcription of the *fla*/*che* operon is initiated from two promoters P_{D3} and $P_{fla/che}$, which require the alternative sigma factor SigD and the housekeeping sigma factor SigA respectively (Estacio *et al.* 1998). In addition to P_{D3} and $P_{fla/che}$, two distally located promoters P_{sigD} and P_{yxlF} guide transcription of a subset of genes of the *fla/che* operon including *sigD* and the adjacent *swrB* (Allmansberger 1997; West *et al.* 2000; Cozy and Kearns 2010; Mordini *et al.* 2013). SigA-dependent transcription initiation at $P_{fla/che}$ is essential for expression of the *early flagellar genes* and *sigD* (Estacio *et al.* 1998; Kearns and

Losick 2005). But, due to an imperfect -10 promoter region, transcription initiation is rather week and efficient expression of the *fla*/*che* operon requires the transcriptional activator SwrA (Calvio *et al.* 2005; Kearns and Losick 2005). Consequently, cells deficient in *swrA* show a two-fold reduced number of basal bodies (Kearns and Losick 2005; Guttenplan *et al.* 2013). Recent findings have shown that SwrA regulates *fla*/*che* upon interaction with DegU-P, converting DegU-P from an repressor to an activator of the *fla*/*che* operon (Amati *et al.* 2004; Tsukahara and Ogura 2008; Ogura and Tsukahara 2012; Mordini *et al.* 2013). Transcription of *swrA* in turn depends on SigD (and SigA) and thus SwrA and SigD constitute a positive feedback loop (Calvio *et al.* 2008). Moreover, SigD-dependent transcription initiation at P_{sigD}, P_{D3} and P_{yxlF} promotes a second autoregulatory loop further stabilizing the SigD ON state required for motility (Allmansberger 1997; Estacio *et al.* 1998; West *et al.* 2000; Cozy *et al.* 2012; Mordini *et al.* 2013).

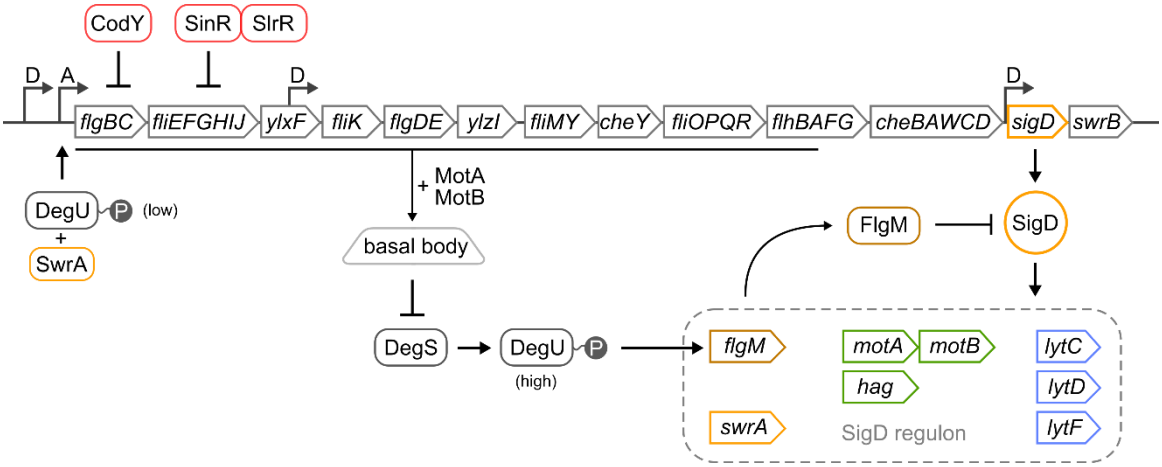

Figure 5: Transcriptional regulation of early and late flagellar genes. Transcription of the *fla-che* operon (grey arrows, top) is initiated at the (A) SigA-dependent *fla-che* promoter, as well as three (D) SigD-dependent promoters upstream of *flgB*, *fliK* and *sigD*. Transcriptional repressors are shown in red. The SigD regulon includes the autolysins *lytC*, *lytD* and *lytF*, the late flagellar genes *motA*, *motB* and *hag*, the anti-sigma factor gene *flgM* and *swrA* among others. SwrA converts DegU-P from a repressor to an activator of *fla-che* operon expression. High levels of DegU-P inhibit *fla-che* operon expression directly at the SigA promoter site (not shown) and indirectly via expression of *flgM*. Assembly of the flagellar basal body antagonizes FlgM by inhibiting DegS activity thereby promoting and stabilizing the SigD ON state required for motility.

Positive autoregulation of *fla*/*che* is particularly important, as transcription of *sigD* was shown to underly a position-dependent effect, in which transcript abundance and distance of the gene to the $P_{fla/che}$ promoter reveal a negative correlation (Cozy and Kearns 2010; Cozy *et al.* 2012). Consequently, expression of *sigD* is prone to noise in promoter activation from $P_{fla/che}$ and possibly affected by RNA polymerase processivity, mRNA turnover or the availability of nucleotides (Veening and Kuipers 2010; Cozy *et al.* 2012). Further regulators of flagellar synthesis are the global transcriptional regulator CodY

and the SinR-SlrR heterodimer (Cairns *et al.* 2014). SinR-SlrR, which is under control of Spo0A-P mediated anti-repression (see 1.3.1), directly represses transcription of *hag* and the autolysins *lytF* and *lytC*, whereas repression of the *early flagellar* genes by SinR-SlrR is presumably indirect and involves DegU-P dependent expression of the anti-SigD factor FlgM (see 1.4.2) (Caramori *et al.* 1996; Bertero *et al.* 1999; Kobayashi 2008; Chai *et al.* 2010b; Hsueh *et al.* 2011; Mukherjee and Kearns 2014). Finally, CodY binds to the *fla*/*che* and the *hag* promoter region and thereby couples flagellar synthesis to the nutritional status of the cell (Bergara *et al.* 2003; Ababneh and Herman 2015). As a result of the *fla*/*che* operon structure, elaborated regulatory feedback loops and Spo0A-P dependent repression, only a subpopulation of cells reaches the threshold level of SigD required to initiate the bistable switch further stabilizing SigD levels and the motile state (Cozy and Kearns 2010; Mukherjee and Kearns 2014). Moreover, regulation of SigD and motility underlies an intertwining post-transcriptional regulatory network (see 1.4.2).

1.4.2 Posttranslational and functional regulation of motility

Motility and matrix production are fundamentally opposing adaptations (Cairns *et al.* 2014). To ensure full commitment of individual cells to either motility or biofilm formation, several regulatory and mechanistic (functional) links have evolved (Kearns *et al.* 2005; Cairns *et al.* 2014). In addition to the elaborated transcriptional control, regulation of motility and SigD underlies an intertwining posttranslational regulatory network, which involves DegU-P dependent transcription of the anti-SigD factor FlgM (Tokunaga *et al.* 1994; Caramori *et al.* 1996; Bertero *et al.* 1999; Hsueh *et al.* 2011; Mukherjee and Kearns 2014). FlgM sequesters SigD thereby quenching intracellular levels of SigD and preventing the sigma factor from initiating the bistable switch described above (1.4.1). While the detailed mechanism remains unclear, several independent studies demonstrated a feedback mechanism, that couples phosphorylation of DegU-P to flagellar rotation and to the assembly of the flagellar apparatus (Hölscher *et al.* 2018; Diethmaier *et al.* 2017; Chan *et al.* 2014; Cairns *et al.* 2013; Hsueh *et al.* 2011; Barilla *et al.* 1994). In particular, increased levels of DegU-P and DegU-P dependent cellular functions (γ-PGA formation, *aprE* expression) were reported for mutants deficient in *hag*, *motA*/*motB*, *sigD* or genes for basal body synthesis. Moreover, DegU-P level increase upon surface sensing, artificial inhibition of flagellar rotation or growth in media with increased viscosity (Cairns *et al.* 2013; Belas 2014; Chan *et al.* 2014; Diethmaier *et al.* 2017). The resulting enhanced synthesis of FlgM prevents SigD from initiating positive autoregulation leaving cells in a non-motile SigD OFF state (Hölscher *et al.* 2018; Diethmaier *et al.* 2017; Chan *et al.* 2014; Cairns *et al.* 2013; Hsueh *et al.* 2011). In case of SigD ON state cells, phosphorylation of DegU is inhibited upon expression and assembly of the flagellar basal body and

secretion apparatus (Caramori *et al.* 1996; Aizawa *et al.* 2002; Hsueh *et al.* 2011). Consequently, transcription of *flgM* is reduced releasing SigD from FlgM, which eventually enables efficient transcription of the SigD regulon including *early* and *late flagellar genes* (*hag, motAB*; Mukherjee and Kearns 2014). In addition, transcription of *flgM* is activated by ComK via read-through from *comF* and repressed by the transition state regulator ScoC (Msadek 1999; Kodgire and Rao 2009). The flagellar clutch EpsE represents another functional regulator of motility (Blair *et al.* 2008; Guttenplan *et al.* 2010). EpsE is encoded within the *epsA-O* operon and has a bifunctional role by promoting synthesis of extracellular polysaccharides while simultaneously inhibiting motility through binding to the rotor protein FliG (Blair *et al.* 2008; Guttenplan *et al.* 2010). Thus, EpsE enables a direct and rapid functional synchronization of biofilm matrix synthesis and motility (Blair *et al.* 2008).

Further mechanism for regulation of motility including posttranscriptional regulation of flagellin expression were summarized in an excellent review by Mukherjee and Kearns (2014).

1.5 Control of exoenzyme expression by DegS-DegU

1.5.1 Function and regulation of the DegS-DegU two-component system

The DegS-DegU two-component regulatory system has a central role in controlling *Bacillus* cell physiology and cellular adaptation processes. In fact, mutations affecting either of the two genes were the first mutations described in *B. subtilis* to result in a pleiotropic phenotype and were intensively analyzed ever since (Kunst *et al.* 1974; Henner *et al.* 1988b; Marlow *et al.* 2014b). The two-component system comprises the response regulator DegU and its cognate histidine sensor kinase DegS (Msadek *et al.* 1990; Mukai *et al.* 1992). Unlike the common mode of action of sensor kinases, including ComP, DegS is not membrane-bound but located in the cytoplasm (Fabret *et al.* 1999; Meile *et al.* 2006). The second rather unusual characteristic of the DegS-DegU system is the multifunctional nature of DegU in response to its degree of phosphorylation. Unphosphorylated DegU promotes expression of ComK the master regulator for genetic competence by binding of DegU to the *comK* promoter region (Hamoen *et al.* 2000). When phosphorylated either by DegS or in an DegS independent manner, DegU-P controls the development of motility, biofilm formation and exoenzyme synthesis, with increasing levels of DegU-P required from the first to the latter (Dahl *et al.* 1992; Kobayashi 2007b; Verhamme *et al.* 2007; Cairns *et al.* 2015). Moreover, recent studies suggest that a further increase in DegU-P levels favors initiation of sporulation (Marlow *et al.* 2014b). In addition to the Spo0A-P dependent network, the DegS-DegU system provides another layer of regulation to the spatio-temporal control of cellular

differentiation, by not just activating specific cellular process depending on its degree of phosphorylation but simultaneously repressing phenotypes controlled by lower levels of DegU-P (see Figure 6; Kobayashi 2007b; Verhamme *et al.* 2007; Marlow *et al.* 2014b).

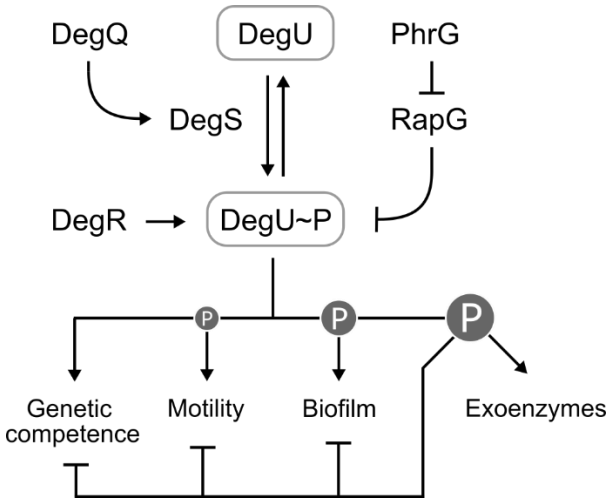

Figure 6: The DegS-DegU system controls different cellular adaptation processes. A gradual increase in the levels of phosphorylated DegU (DegU-P) activates the depicted cellular responses while simultaneously repressing developmental processes that require lower levels of DegU-P.

The intracellular level of DegU is regulated at multiple levels. Cellular mechanisms for posttranslational regulation of DegU activity include phosphorylation and dephosphorylation of DegU by DegS, interaction of DegU with ancillary factors and ClpCP dependent proteolysis (Tanaka *et al.* 1991; Ogura and Tsukahara 2010; Mordini *et al.* 2013). Although only a limited number of stimuli affecting DegS/DegU activity is known, the environmental and cellular signals are of diverse nature underlying the central role of DegU in *Bacillus* strain physiology. Kinase activity of DegS is inhibited by the SMC-ScpA-ScpA protein complex, which coordinates chromosome condensation and segregation. Upon entry into stationary growth, inhibition of DegS is relieved by depletion of the SMC-ScpA-ScpA protein complex and DegU-P dependent gene expression increases (Dervyn *et al.* 2004). Moreover, inhibition of flagellar rotation was shown to stimulate DegS-dependent phosphorylation of DegU, thereby coupling high levels of DegU-P to a sessile lifestyle (section 1.2.2) (Cairns *et al.* 2013; Diethmaier *et al.* 2017). Finally, DegS/DegU is involved in the osmotic stress response, as hyper osmotic conditions result in upregulation of genes from the DegU regulon (Ruzal and Sanchez-Rivas 1998; Steil *et al.* 2003).

Phosphorylation of DegU occurs in the N-terminal regulatory domain (NTD) of DegU at the conserved aspartate Asp56, while the C-terminal HTH luxR-type domain (CTD) mediates DNA binding of the transcription factor to its target sites (Dahl *et al.* 1991; Fabret *et al.* 1999). Moreover, the NTD is required for dimerization of DegU and protein-protein interaction of DegU with the auxiliary factors SwrA and RapG. SwrA modulates DegU-P dependent regulation of motility, γ-PGA synthesis and exoprotease

secretion by promoting expression of *fla/che* operon, *ycdA*, *pgs* and *aprE* (Ogura and Tsukahara 2012; Mordini *et al.* 2013). RapG blocks DNA binding of the corresponding response regulator by direct interaction with its DNA binding domain (Ogura *et al.* 2003; Gallego del Sol and Marina 2013). RapG activity is antagonized by secretion and uptake of the PhrG pentapeptide, and thus, in a cell density dependent manner (Ogura *et al.* 2003). Similarly, the activity of another protein from the DegS-DegU system, DegQ, is indirectly regulated by peptide pheromones. DegQ promotes phosphotransfer from DegS to DegU and thereby stimulates DegU-P dependent gene expression in *Bacillus* (Kobayashi 2007b). Expression of *degQ* is controlled by the two-component system ComP-ComA with ComA-P promoting transcription of *degQ* (Msadek *et al.* 1991). Both, the sensor kinase ComP and the response regulator ComA are regulated by quorum sensing signals. ComP senses the peptide pheromone ComX, while ComA activity is modulated by multiple Rap proteins and their corresponding Phr peptides (Core and Perego 2003; Bongiorni *et al.* 2005; Auchtung *et al.* 2006; Ogura and Fujita 2007; Smits *et al.* 2007; Shank and Kolter 2011). Thus, the RapG-PhrG system and ComA dependent *degQ* expression provide another layer of regulation for finetuning of DegU-P in a growth phase-dependent manner (Ogura *et al.* 2003). Finally, the positive effector protein DegR regulates DegU-P activity by binding to DegS thereby protecting DegU-P from DegS-dependent dephosphorylation (Mukai *et al.* 1992).

1.5.2 Genetic structure and transcriptional regulation of *degS-degU*

In addition to posttranslational regulation of DegU-P levels, expression of *degS-degU* underlies complex transcriptional control. Under non-limiting conditions during exponential growth, the expression level of *degS-degU* is low. Basal expression of the *degS-degU* operon occurs from an upstream located SigA-type promoter P1 (Msadek *et al.* 1990; Yasumura *et al.* 2008). Under these conditions, DegS-independent phosphorylation of DegU, by small molecules such as acetyl phosphate, provides low levels of DegU-P sufficient to promote the development of motility (Tokunaga *et al.* 1994; Kobayashi 2007b; Verhamme *et al.* 2007; Calvio *et al.* 2008; Mordini *et al.* 2013; Cairns *et al.* 2015). In addition to P1, transcription of *degU* but not *degS* is further enhanced by two promoters, P2 and P3, located in the 3' coding region of *degS* and the *degS-degU* intergenic region, respectively (Yasumura *et al.* 2008; Newman *et al.* 2013; Ogura *et al.* 2014). Activation of P2 occurs upon nitrogen limitation by binding of TnrA, when TnrA is released from inhibition by the glutamine synthetase GlnA (Yasumura *et al.* 2008). Thus, the *degU* specific P2 promoter allows for higher levels of DegU without necessarily increasing DegS-dependent phosphorylation of DegU. This mechanism might be crucial for developing genetic competence in *Bacillus*, a process that requires unphosphorylated DegU (Hamoen *et al.* 2000). The P3 promoter adds further complexity to the regulatory network controlling *degU* expression. P3 is inhibited by the biofilm master regulator SinR, which itself underlies indirect control by Spo0A-P, and is activated

upon binding of the carbon catabolite control protein CcpA (Ishii *et al.* 2013; Newman *et al.* 2013; Ogura *et al.* 2014). Most importantly, the P3 promoter is subjected to auto stimulation. Due to the presence of a low affinity binding site in P3, this regulation requires DegS-dependent phosphorylation of DegU to increase the DNA binding affinity of the response regulator (Kobayashi 2007b; Ogura and Tsukahara 2012). Thus, phosphorylation by DegS initiates a positive feedback loop eventually resulting in, and maintaining, high levels of DegU-P (Dahl *et al.* 1991; Yasumura *et al.* 2008; Ogura and Tsukahara 2010). Moreover, this mechanism explains and is crucial for bistability in DegU-P dependent gene expression in *B. subtilis* and related species (Veening *et al.* 2008a; Murray *et al.* 2009a).

1.5.3 Engineering of DegS-DegU for improved exoenzyme production

Among the diverse cellular functions of DegU in controlling *Bacillus* cell physiology, regulation of exoenzyme expression has gained particular interest. The wide application of *Bacilli* for secretory production of enzymes resulted in intensified work on DegS-DegU from the 1970s on, and still new functions and mechanism are assigned to the two-component system (Kunst *et al.* 1974; Ayusawa *et al.* 1975; Marlow *et al.* 2014b). Two classes of mutations have been described for DegS-DegU and DegQ, differing in the phosphorylation level of DegU. The first group is characterized by low levels of DegU-P resulting in reduced expression of exoenzymes. Strains carrying mutations from the second group share a pleiotropic phenotype, characterized by enhanced exoenzyme secretion (hypersecreting, hy), filamentous growth, loss of motility and genetic competence and the ability to to sporulate in the presence of glucose (Ayusawa *et al.* 1975; Sekiguchi *et al.* 1975; Henner *et al.* 1988b; Msadek *et al.* 1990). This pleiotropic phenotype results from increased levels of DegU-P caused by several mutations in *degS* and *degU*, of which *degU32* and *degS200* are the most prominent (Dahl *et al.* 1991; Tanaka *et al.* 1991). In strains carrying the *degU32* allele, a H12L amino acid substitution in the DegU protein stabilizes the phosphorylated form of the response regulator and extends its half-life sevenfold from 20 to 140 min (Dahl *et al.* 1992). Likewise, a coding sequence exchange of G218E in the *degS200* allele promotes high levels of DegU-P by lowering the dephosphorylation activity of DegS (Tanaka *et al.* 1991). Finally, overexpression of *degQ* and *degR* was shown to mimic the hypersecretion phenotype known from *degU32* strains by promoting phosphotransfer or lowering dephosphorylation (Nagami and Tanaka 1986; Yang *et al.* 1986; Amory *et al.* 1987; Yang *et al.* 1987; Msadek *et al.* 1991). The *degQ36* allele was identified as one of the so called 'hy' mutations in *B. subtilis* and describes a C to T mutation within the -10 region of the *degQ* promoter (Yang *et al.* 1986). But, unlike the mutations in the sensor kinase and the response regulator itself, *degQ36* was shown to represent the actual wildtype allele, which was lost during domestication of *B. subtilis* laboratory strains, in particular selecting for high genetic competence (Stanley and Lazazzera 2005; McLoon *et al.* 2011; Miras and Dubnau 2016). Due to the positive effect

on exoenzyme expression, hypersecretion mutations in the DegS-DegU two component system have been analyzed in several industrially relevant *Bacillus* species, including *B. subtilis*, *B. licheniformis* and *B. megaterium* (Tjalsma *et al.* 2004a; Borgmeier *et al.* 2011; Borgmeier *et al.* 2012). Single cells analyses unraveled the underlying physiology reason, showing strongly homogeneous activation of DegU-P dependent promoters at population level in strains carrying the *degU32* allele (Veening *et al.* 2008a; Borgmeier *et al.* 2012; Ploss *et al.* 2016). However, the effect of *degU32*, the best characterized 'hy'-mutation, on production strain performance is not limited to its direct role in controlling exoenzyme expression considering that DegU-P regulates more than 120 genes (Ogura *et al.* 2001; Mäder *et al.* 2002). Interestingly, DegU-P was shown to affect CcpA-dependent carbon catabolite repression (CCR) as genes repressed by CcpA were significantly upregulated in a *B. subtilis* 168 *degU32* mutant. Analysis of glycolytic intermediates showed lower levels of key metabolites for CCR, glucose-6-phosphate and fructose-1,6-bisphosphate, indicating more efficient glycolysis (Ishii *et al.* 2013). Importantly, only minor changes in growth behavior were observed and, thus, an indirect effect of *degU32* on CCR due to depletion of glucose and earlier entry into stationary growth is excluded. Considering the negative regulation of degradative, extracellular enzymes by CCR (Priest 1977; Hanlon *et al.* 1982; Frankena *et al.* 1986; Mao *et al.* 1992; Barbieri *et al.* 2016; Habicher *et al.* 2019b), DegU-P (*degU32*) contributes to enhanced productivity both at the local, promoter-specific, and global level by rewiring the cellular signaling network.

2 Aims

The increasing demand for biotechnological products and processes requires design and construction of optimized cell chassis that allow for economically feasible solutions. Despite the important role of various *Bacillus* species such as *B. licheniformis, B. amyloliquefaciens, B. pumilus, B. clausii* to industrial biotechnology (Schallmey *et al.* 2004), many cellular processes were investigated mainly in the Gram-positive model organism *B. subtilis*. Moreover, the cultivation conditions in most of these studies differ strongly from those applied in industrial bioprocesses.

The aim of this thesis was to analyze and reduce cellular heterogeneity in *B. licheniformis* under batch and fed-batch conditions, the latter of which is frequently applied in industry. In its natural habitat, *Bacillus* is known to form phenotypically different subpopulation, which enables pre-adaptation and thereby enhances biological fitness, although these processes are energetically unfavorable and cost intensive. This 'standby' mode is inherent to *Bacillus* and hinders exploitation of its full production potential (Fischer and Sauer 2005). Lowering this metabolic burden provides a promising strategy for strain improvement (Juhas *et al.* 2014; Marlow *et al.* 2014b). Although not fully understood, differentiation of subpopulations is well characterized in the closely related *B. subtilis* enabling knowledge-based approaches in strain optimization. Within this thesis, such a rational approach is applied to *B. licheniformis.* Mutants deficient in biofilm formation or motility are systematically constructed and evaluated regarding their physiology and capability in extracellular enzyme production. The strategies applied include the deletion of genes encoding structural components of the biofilm matrix and the flagellar apparatus and those directly involved in their biosynthesis. Moreover, by modifying central regulators, cell differentiation should be targeted at the initiation step of the corresponding developmental program thereby preventing cell heterogeneity on a global level. The resulting strains are phenotypically characterized to analyze the individual effect on biofilm formation and motility in *B. licheniformis*. Subsequently, promising mutations are combined to construct cell chassis deficient in both cellular processes. Heterologous expression of the *Bacillus lentus* alkaline protease BLAP is taken as a measure for productivity of the streamlined strains. By using fluorescence protein reporter strains, cellular heterogeneity is analyzed at single cell level under batch and simulated fed-batch conditions to further elucidate developmental processes in this non-model *Bacillus* strain. Finally, the extracellular proteome is characterized to uncover changes in the host strain physiology and potentially identify new approaches for further strain optimization.

3 Results

3.1 Strain construction and phenotypical characterization

3.1.1 Construction of *B. licheniformis* host strains

Within this thesis, two strain lineages were constructed both derived from *B. licheniformis* DSM641 (US5352604). All strains and plasmids constructed in the frame of this thesis are listed in Table S3. A detailed description of the construction of all plasmids and strains of this study can be found in section 7.8. First, the effect of individual gene deletions on biofilm formation and motility was analyzed in the wildtype-close *B. licheniformis* M308 strain background (see below). Subsequently, mutations that resulted in reduced biofilm formation or motility were combined in the sporulation-deficient *B. licheniformis* DSM641 derivative *B. licheniformis* M409 (see below). Construction of *B. licheniformis* M308 and mutants thereof was performed using pE194-based homologous recombination. To accelerate strain construction, an adapted CRISPR/Cas9 based system for genome editing in *B. licheniformis* was developed and implemented for construction of mutants based on *B. licheniformis* M409.

B. licheniformis M308 differs from the *B. licheniformis* DSM641 wildtype strain by an inactivated restriction-modification system (Δ*rms*) and deletion of the *pgsB-pgsC-pgsA-pgsE* operon required for biosynthesis of poly-γ-glutamic acid (γ-PGA, *pga*). Construction of *B. licheniformis* M308 was performed by deletion of the *pga* operon in the restrictase-deficient *B. licheniformis* P304 using plasmid pDel007, both kindly provided by BASF SE. The Δ*rms* Δ*pga* mutations were required for improved handling and genetic accessibility. Importantly, although γ-PGA was shown to promote biofilm formation in selected *B. subtilis* isolates, strains deficient in *pga* still display complex colony architecture (Branda *et al.* 2006; Yu *et al.* 2016). In line with these observations, deletion of *pga* in *B. licheniformis* M308 did not lead to loss of complex colony architecture. Instead, excess γ-PGA formation in *B. licheniformis* DSM641 hampered analysis of colony morphology (Figure 7). Therefore, the Δ*pga* background was considered suitable for evaluation of genes related to biosynthesis of the extracellular matrix.

To characterize the mutations and combinations thereof *B. licheniformis* M409 was constructed. *B. licheniformis* M409 is based on *B. licheniformis* P307 (Δ*rms*, Δ*apr*, Δ*sigF*) provided by BASF SE. Most importantly, the parental strain is deficient in the formation of endospores resulting from deletion of *sigF* (*spoIIAC*). In industrial settings spore formation is undesirable due to the risk of contamination and non-producing subpopulations. Therefore, sporulation-deficiency is taken as a pre-requisite for *Bacillus* expression hosts (Pierce *et al.* 1992; Nahrstedt *et al.* 2005; Vary *et al.* 2007). SigF is the first forespore-specific sigma factor regulating expression of early forespore specific genes as well as the late forespore specific sigma factor SigG (Stragier and Losick 1996; Errington 2003; Steil *et al.* 2005;

Hoon *et al.* 2010). Mutants deficient in *sigF* fail to inactivate the second division site during asymmetric septum formation and consequently to undergo engulfment (sporulation stage III) (Piggot and Coote 1976; Setlow *et al.* 1991; Eichenberger *et al.* 2001). Moreover, *sigF* mutants are not irreversibly committed to sporulation but can resume vegetative growth under non-limiting conditions, which may explain enhanced secretory enzyme production observed upon deletion of *sigF* in *B. subtilis* and *B. licheniformis* (Dworkin and Losick 2005; Ara *et al.* 2007; Zhou *et al.* 2019). By analyzing motility and biofilm formation in the sporulation deficient strain background both cellular processes were investigated independently from this most ultimate adaptation process. To minimize degradation of secreted target proteins as well as to avoid artificial results in the protease activity assays, *B. licheniformis* P307 lacks the major alkaline protease gene *apr* (*B. subtilis* homologue: *aprE*). Finally, to evaluate the strains regarding secretory enzyme production, the heterologous *Bacillus lentus* alkaline protease (BLAP) was expressed from a chromosomally integrated expression cassette under control of a truncated, but otherwise native 227 bp fragment of the *B. licheniformis* DSM641 *apr* promoter (Jacobs 1995). BLAP is an alkaline protease used in the detergent industry and served as a model enzyme in this thesis for secretory enzyme production (US5352604). The BLAP expression cassette was integrated into the *pga* locus using plasmid pMA110, thereby simultaneously preventing γ-PGA formation. The resulting parental strain was named *B. licheniformis* M409 (Δ*rms*, Δ*sigF*, Δ*apr*, *pga*::P*apr*-BLAP). Importantly, biofilm formation was not affected in *B. licheniformis* M409 or the strain intermediates *B. licheniformis* M321 (Δ*rms*, Δ*apr,* Δ*pga*) and *B. licheniformis* M309 (Δ*rms*, Δ*sigF*, Δ*apr*, Δ*pga*) compared to *B. licheniformis* M308 (Figure 7). *B. licheniformis* M321 and M309 were constructed by deletion of the *pga* operon in *B. licheniformis* P306 (Δ*rms*, Δ*apr*; provided by BASF SE) and *B. licheniformis* P307 (Δ*rms*, Δ*sigF*, Δ*apr*) using plasmid pMA23.

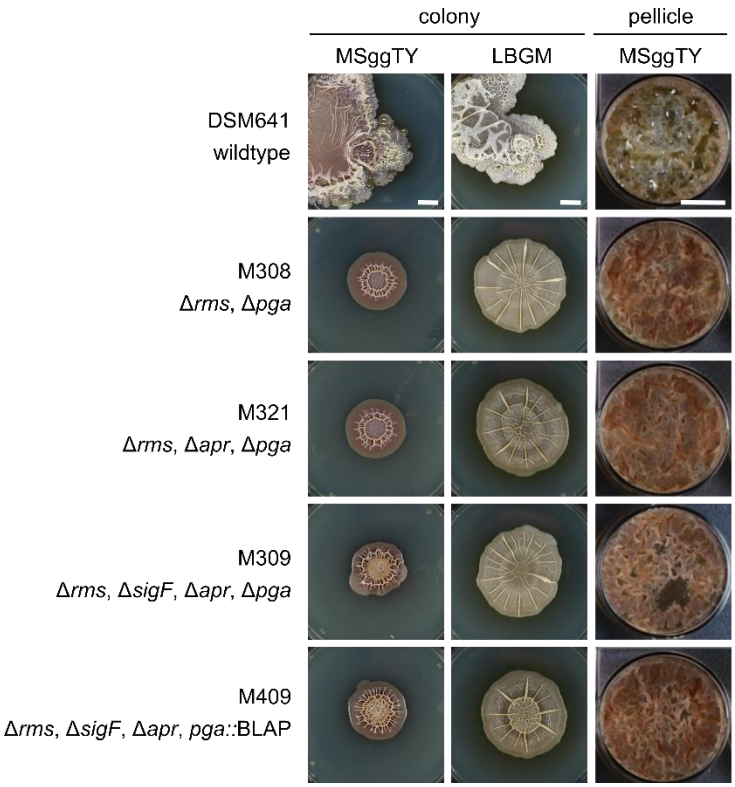

Figure 7: Biofilm formation in selected *B. licheniformis* precursor strains used in this thesis. The ability to form biofilms was analyzed by pellicle formation and colony architecture assay. **'**Colony' column depicts images of strains incubated for 5 – 7 days at 30 °C on solid MSggTY or LBGM medium. 'Pellicle' column depicts top-down images of microtiter plate wells incubated for 5 days at 30 °C without agitation. Agar plates were centrally inoculated and incubated for 18 h at 30 °C. Genotypes were as indicated below the strain number on the left. Scale bars are 1 cm. At least three biological replicates were analyzed, representative results are shown.

3.1.2 Structural and regulatory components for biofilm formation and motility in *B. licheniformis*

For the construction of biofilm and motility deficient strains, different strategies were developed ranging from the deletion of genes encoding structural components or those directly involved in their biosynthesis to deletion or modification of global regulators. With the latter, cell differentiation was targeted at the initiation step of the corresponding developmental program thereby preventing cell heterogeneity as early and global as possible. Mutations known to prevent biofilm formation or motility in *B. subtilis* were introduced and evaluated in *B. licheniformis* M308. In case of *bslA* and the *epsA-O* operon, single target evaluation was conducted in the *B. licheniformis* M409 strain background. Subsequently, the ability of the mutant strains to form biofilms was analyzed qualitatively in pellicle formation assays, in which strains proficient in matrix synthesis form a layer (pellicle) at the air-liquid interface (Branda *et al.* 2001). Moreover, the development of complex colony architecture was analyzed on solid media (Branda *et al.* 2001). Swimming motility assays was assessed using semi-solid LB

agar plates (0.4 %) as previously described (Kearns and Losick 2003; Guttenplan *et al.* 2013). Due to the closely linked regulatory network and the mutually exclusive nature of biofilm and motility in *B. subtilis* (Cairns *et al.* 2014), all strains were characterized regarding both phenotypes.

Deletion of the major *B. subtilis* matrix component TasA encoded in the *tapA-sipW-tasA* operon was conducted in *B. licheniformis* M308 using plasmid pDAN80. The resulting strain *B. licheniformis* M315 showed a less complex colony morphology and a strong reduction in the ability to form pellicles, with only a few cells attached to the polystyrene surface (Figure 8). Complete loss of biofilm formation was observed for the Δ*epsA-O* strain *B. licheniformis* M431, constructed based on *B. licheniformis* M409 using plasmid pMA112. *B. licheniformis* M431 displayed a flat colony morphology and grew exclusively as dispersed culture under static conditions without aggregation or attachment to surfaces. Similar to *B. licheniformis* M431, the Δ*epsA-O*, Δ*tapA-sipW-tasA* double mutant *B. licheniformis* M440 shows complete loss of biofilm formation (data not shown). Finally, the hydrophobic coat protein BslA was the third structural component of the *B. subtilis* biofilm matrix evaluated for its effect on biofilm formation in *B. licheniformis*. The Δ*bslA* strain *B. licheniformis* M454 was constructed based on *B. licheniformis* M409 using plasmid pMA112. Unlike Δ*epsA-O* and Δ*tapA-sipW-tasA*, deletion of *bslA* neither prevented pellicle formation nor affected colony morphology (Figure 8).

In addition to deletion of the genes most downstream in the regulatory cascade of biofilm formation, global regulators involved in biofilm formation were modified. In *B. subtilis*, both transcriptional activation and derepression is required for expression of *epsA-O* and *tapA-sipW-tasA.* Activation occurs via the shared transcriptional activator RemA (Winkelman *et al.* 2009). Moreover, SinR-dependent repression needs to be relieved, by activation of the anti-repressor SinI or SlrA, with either of the two dominating in different *B. subtilis* isolates (Kobayashi 2008; Cairns *et al.* 2014). As deletion of *remA* failed repeatedly despite varying HDR templates, inactivation was achieved by simultaneous introduction of two loss of function mutations previously described for *B. subtilis* (Blair *et al.* 2008; Winkelman *et al.* 2009). Using plasmid pMA96, the native *remA* allele was exchanged by a mutated copy resulting in the R18W and P29S amino acid exchanges. The resulting strain was named *B. licheniformis* M310.1. In addition, strain *B. licheniformis* M310.2 was constructed by disruption of the *remA* ribosome binding site with the bleomycin resistance cassette (*bleo*^{R}) from pUB110 using plasmid pMA91. The insertion site was selected based on the previously described work by Winkelmann *et al.* (2009). Both strains *B. licheniformis* M310.1 and M310.2 displayed complete loss of biofilm formation (Figure 8). To avoid usage of antibiotic resistance marker genes as well as to exclude polar effects resulting from integration of *bleo*^{R}, the *remA* loss of function mutation was selected for further strain construction and analysis. Analysis of SinI and SlrA mutants led to conflicting results regarding their role in regulating biofilm

formation in *B. licheniformis*. Inactivation of the SinR anti-repressor SinI was first conducted by complete deletion of *sinI* in *B. licheniformis* M308 using plasmid pMA30. Surprisingly, the resulting strains *B. licheniformis* M311 (Δ*sinI*) showed enhanced rather than reduced biofilm formation (Figure 8). Thus, the phenotype of *B. licheniformis* M311 resembles those of *B. subtilis* Δ*sinR* rather than Δ*sinI* strains (Kearns *et al.* 2005). As *sinI-sinR* locate in an operon polar effects of *sinI* deletion on the downstream located *sinR* were likely to cause the conflicting observations. Therefore, *sinI* was inactivated by partial deletion with plasmid pMA98 resulting in *B. licheniformis* M311.2 (Δ*sinI* p.E14-P45del). The Δ*sinI* p.E14-P45del mutation was constructed analogous to Bai *et al.* and is described as non-polar regarding expression of *sinR* (Bai *et al.* 1993). But, in contrast to the phenotype described by Bai *et al.* for *B. subtilis* Δ*sinI* (p.E14-P45del) the corresponding *B. licheniformis* strain M311.2 showed no reduction in biofilm formation. The conflicting results regarding the phenotype of *B. licheniformis* M311 and M311.2 became even more apparent when analyzing their motility, showing that both strains are non-motile. Interestingly, the formation of a subpopulation that was able to spread from the central inoculation spot was observed for both strains resulting in a heterogeneous colony morphology (see Figure 8). To further analyze the effect of *sinI* inactivation on biofilm formation, a *sinI* frameshift mutation p.L11AfsX8 (*sinI* fs) was designed leading to introduction of a translational stop codon. The resulting strain *B. licheniformis* M318 showed wildtype-like pellicle formation and motility as well as an altered but still complex colony architecture (Figure 8). As inactivation of *sinI* did not lead to loss in biofilm formation, the alternative SinR anti-repressor SlrA was evaluated regarding its role in biofilm formation in *B. licheniformis*. Construction of the Δ*slrA* strain *B. licheniformis* M317 was conducted using plasmid pMA73. Deletion of *slrA* prevented formation of complex colonies, while pellicle formation was rather wildtype-like. When analyzing the swimming motility of *B. licheniformis* strains carrying mutations in genes involved in biofilm formation, only minor differences were observed for *B. licheniformis* M315 (Δ*tapA-sipW-tasA*), M310.1 (*remA* R18W, P29S), M310.2 (*remA::bleo*^{R}), M317 (Δ*slrA*) and M318 (*sinI frameshift*). Most of these strains, showed slightly higher motility as indicated by the wider area of growth and higher cell density in regions more distal from the central inoculation spot. This became more apparent in the time resolved motility assay (Figure 8). In contrast to these strains, *B. licheniformis* M431 (Δ*epsA-O*) colonized a smaller area in the motility assay but was still able to spread on soft agar plates.

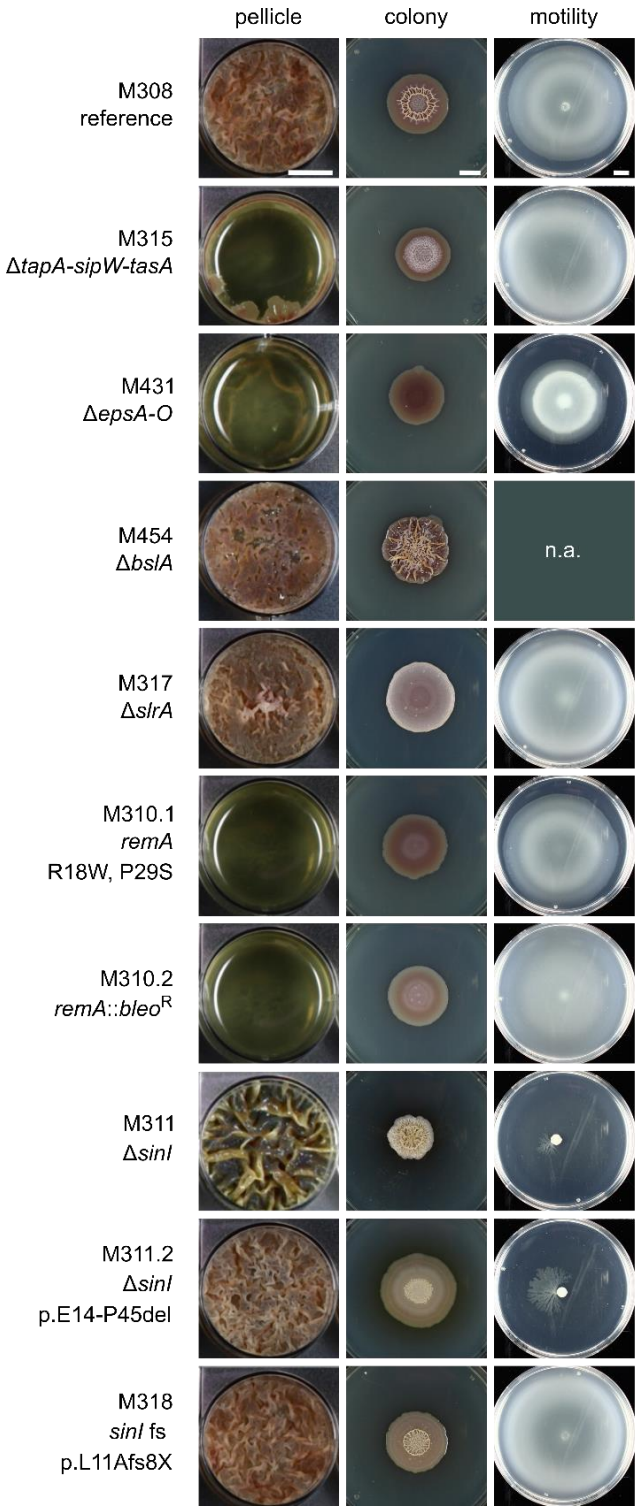

Figure 8: Phenotypical characterization of *B. licheniformis* mutants defective in biofilm formation. The ability to form biofilms was analyzed by pellicle formation and colony architecture assay. **'**Colony' column depicts images of strains incubated for 5 – 7 days at 30 °C on solid MSggTY medium. 'Pellicle' column depicts top-down images of microtiter plate wells incubated for 5 days at 30 °C without agitation. 'Motility' column depicts images of petri dishes containing LB solidified with 0.4 % agar. Agar plates were centrally inoculated and incubated for 18 h at 30 °C. White areas show zones of bacterial growth and correlate with swimming motility. Genotypes were as indicated below the strain number. Scale bars are 1 cm. At least three biological replicates were analyzed, representative results are

shown. Except for *B. licheniformis* M431 and M454 all strains are based on the wildtype-close *B. licheniformis* M308 (Δ*rms*, Δ*pga*). *B. licheniformis* M431 and M454 are based on *B. licheniformis* M409 (Δ*rms*, Δ*sigF*, Δ*apr*, *pga*::P*apr*-BLAP).

To prevent development of motility in *B. licheniformis* deletions in *hag*, *motB* and *sigD* were introduced encoding the major flagellar protein flagellin (Hag), the stator protein MotB and the sigma factor SigD. SigD controls transcription of genes required for motility, chemotaxis, and autolysis. The plasmid used for strain construction via homologous recombination were pMA92 (Δ*hag*), pMA65 (Δ*motB*) and pBW022 (Δ*sigD*). The resulting strains *B. licheniformis* M312 (Δ*sigD*), M313 (Δ*motB*) and M314 (Δ*hag*) had comparable phenotypes (Figure 9). All strains were non-motile and biofilm formation was enhanced as concluded from complex colony morphology. The pellicle formed by Δ*sigD*, Δ*motB* and Δ*hag* strains in static liquid cultures was less complex in its micro-architecture compared to the wildtype strain. It is important to note that *B. subtilis* strains deficient in motility are delayed in pellicle formation, which has not been analyzed in the context of this study (Kobayashi 2007a).

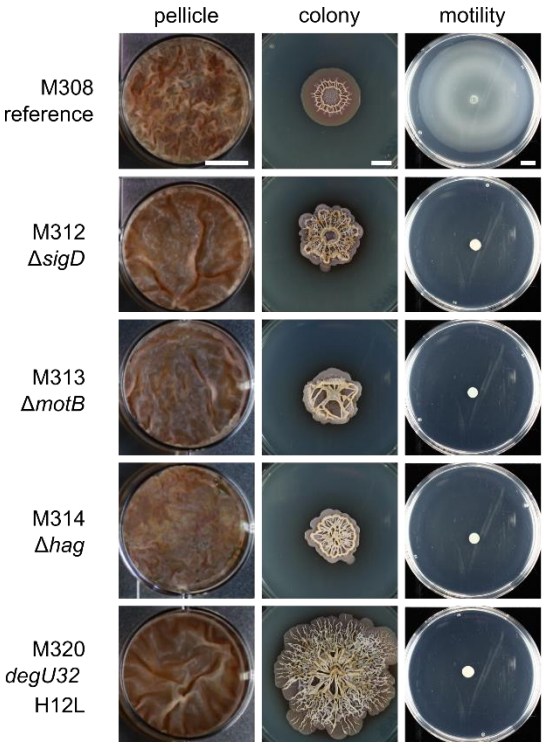

Figure 9: Phenotypical characterization of *B. licheniformis* strains mutated for genes involved in motility. The ability to form biofilms was analyzed by pellicle formation and colony architecture assay. **'**Colony' column depicts images of strains incubated for 5 – 7 days at 30 °C on solid MSggTY medium. 'Pellicle' column depicts top-down images of microtiter plate wells incubated for 5 days at 30 °C without agitation. 'Motility' column depicts images of petri dishes containing LB solidified with 0.4 % agar. Agar plates were centrally inoculated and incubated for 18 h at 30 °C. White areas show zones of bacterial growth and correlate with swimming motility. Genotypes were as indicated below the strain number on the left. All strains are based on the wildtype-close *B. licheniformis* M308 (Δ*rms*, Δ*pga*). Scale bars are 1 cm. At least three biological replicates were analyzed, representative results are shown.

The *degU32* mutation resulting in the amino acid exchange H12L in DegU was included in this thesis due to its pleiotropic effect in *B. subtilis*, including loss of motility and increased homogeneity in expression of the major alkaline protease AprE demonstrated for *B. subtilis* and *B. licheniformis* DSM13 (Msadek *et al.* 1990; Amati *et al.* 2004; Borgmeier *et al.* 2012). The native *degU* allele was exchanged by *degU32* in *B. licheniformis* M308 using plasmid pBW0654. As described for *B. subtilis*, the resulting strain *B. licheniformis* M320 is non-motile (Figure 9). Interestingly, *B. licheniformis* M320 showed a strong increase in biofilm formation under all conditions tested, including liquid and solid LB medium as well as defined media. In particular, the formation of cell aggregates in (shaking) liquid cultures (Section 3.2.3) and a strongly increased complex colony morphology was observed, while pellicle formation was altered and highly similar to the pellicles formed by Δ*sigD*, Δ*motB* and Δ*hag* strains. It is interesting to note, that in addition to the remarkably strong biofilm formation, *B. licheniformis* M320 colonized a wider surface area on solid media despite being non-motile.

The findings presented lead to the conclusion that inhibiting either of the two developmental process, motility, and biofilm formation, increases the respective other adaptation in *B. licheniformis*. However, further quantitative analyses are required to confirm this hypothesis. Consequently, construction of strains carrying multiple mutations targeting both cellular adaptation processes might be required to channel cellular resources towards product formation. Except for *sinI*, which was not successfully modified to prevent biofilm formation, all targeted genes were included in the subsequent strain engineering process.

3.1.3 Construction of combinatorial mutants deficient in biofilm and motility

While the evaluation of single genes required for biofilm formation and motility was conducted in the rather unmodified *B. licheniformis* strain M308 (Δ*rms*, Δ*pga*), *B. licheniformis* strain M409 (Δ*rms*, Δ*sigF*, Δ*apr, pga::BLAP*), was chosen for construction of combinatorial mutant strains. Most importantly, strain M409 is deficient in sporulation, thereby preventing the formation of the subpopulation with strong impact to industrial fermentation processes. By targeting motility and biofilm formation in this strain background, the impact of mutations affecting additional subpopulations was analyzed in this thesis.

A summary of the mutants constructed in this thesis is shown in Figure 10. All strains derived from *B. licheniformis* M409 were constructed using the CRISPR/Cas9 system based on pJOE-T2A. Motility was inhibited by deletion of *hag*, *sigD* or introduction of the *degU32* mutation using plasmid pMA134 (Δ*hag*), pMA114 (Δ*sigD*) and pMA117 (*degU32*). The late flagellar gene *motB* was omitted from the construction of combinatorial mutants due to the highly similar phenotype of Δ*hag*, Δ*sigD* and Δ*motB* single deletion strains (Figure 9). Biofilm deficiency was achieved by inactivation of global regulators

remA (pMA130) and *slrA* (pMA128) or the successive deletion of *epsA-O* (pMA112), *tapA-sipW-tasA* (pMA116) and *bslA* (pMA168). All strains were characterized regarding their ability to form biofilms as described above. Since all combinatorial mutants carry the *degU32*, Δ*sigD* or Δ*hag* mutation, loss of swimming motility was confirmed for selected progenitor strains only. The resulting phenotypes are summarized in Figure 11 and Figure 12. In addition to MSggTY, LBGM medium was used in the biofilm formation assay, as medium-dependent effects on biofilm formation were reported for different *B. subtilis* strains (Kobayashi 2007a; Mhatre *et al.* 2016).

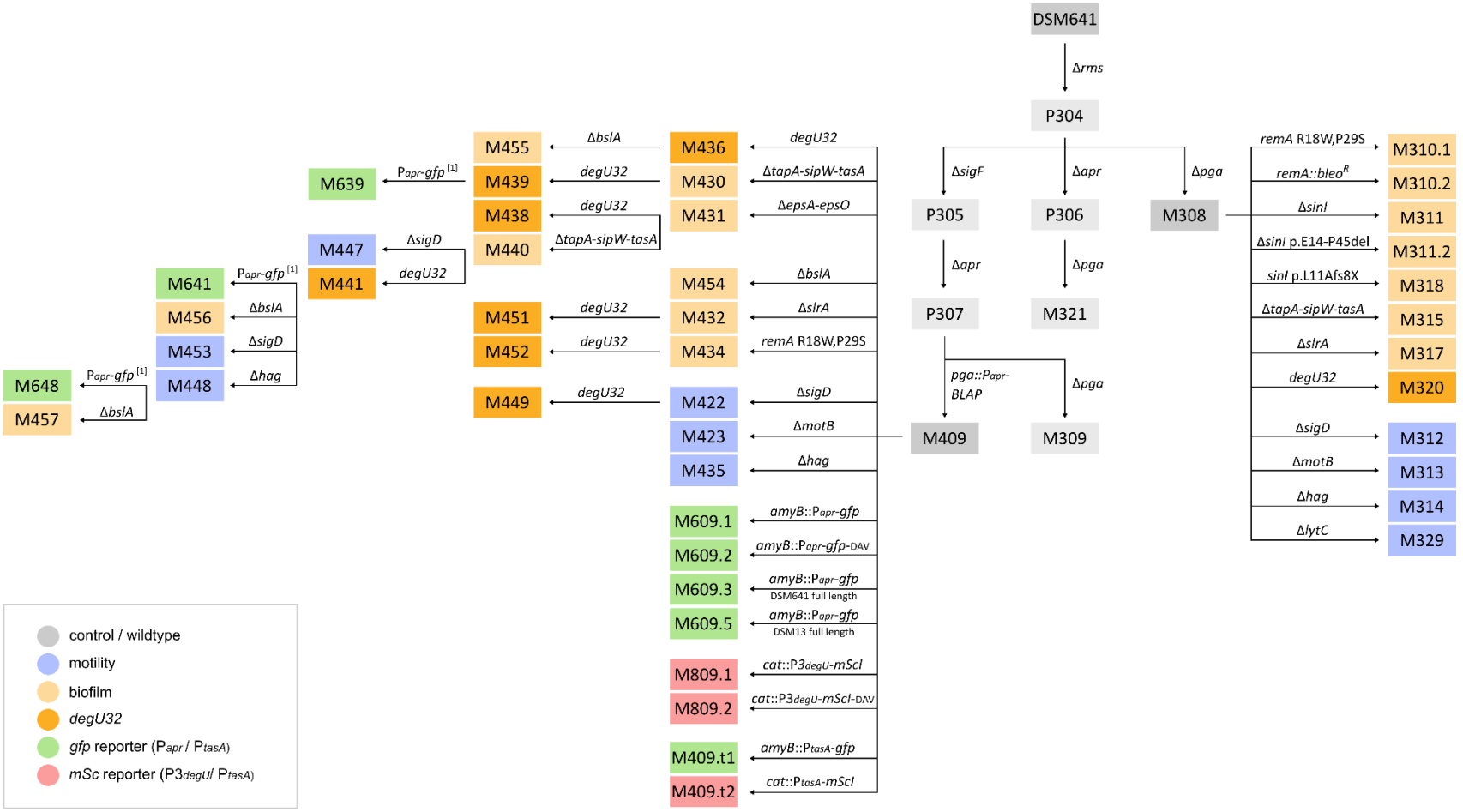

Figure 10: *B. licheniformis* strain lineage. Relevant strains constructed in this thesis are shown. Strains mutated for genes involved in biofilm formation (yellow), motility (blue, including the autolysin *lytC*), those carrying the *degU32* mutation (orange) and reporter strains carrying chromosomal integration of *gfpmut2* (P*apr*, P*tasA*; green) or *mScarletI* (P3*degU*, P*tasA*; red) are depicted. Strain number and most recent mutations introduced into the progenitor strain are as indicated. Expression of *gfpmut2* is driven by the truncated (M609.1, M609.2) or the full-length (M609.3) *B. licheniformis* DSM641 *apr* promoter or the full-length *B. licheniformis* DSM13 *apr* promoter (M609.5). Expression of *the B. lentus* alkaline protease BLAP was under control of the truncated *B. licheniformis* DSM641 *apr* promoter as used for M609.1.

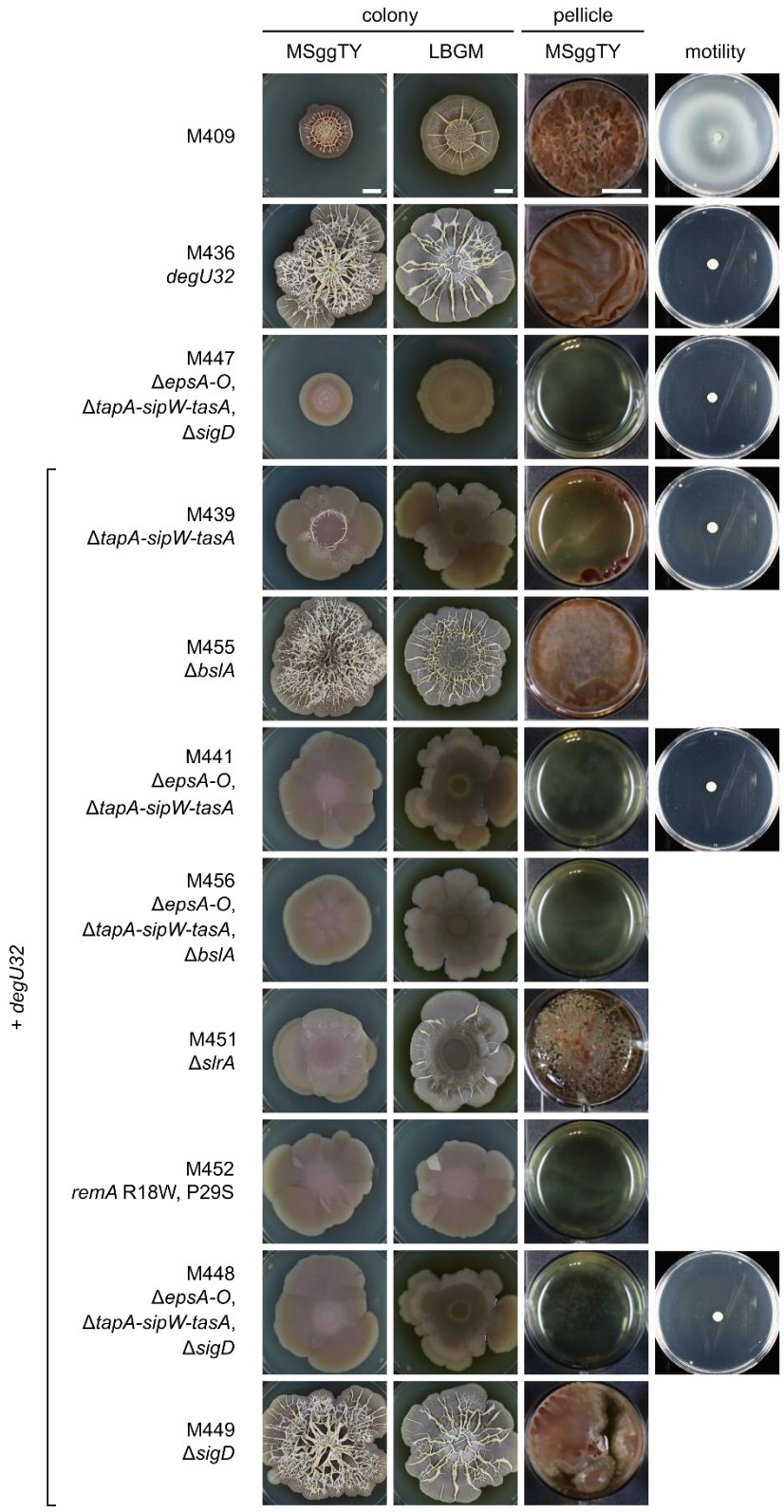

Figure 11: Biofilm formation and swimming motility of *B. licheniformis degU32* combinatorial mutants. ‘Colony’ column depicts images of strains incubated for 5 – 7 days at 30 °C on solid MSggTY or LBGM medium. ‘Pellicle’ column depicts top-down images of microtiter plate wells (diameter: 3 cm) incubated for 5 days at 30 °C without agitation. ‘Motility’ column depicts images of petri dishes containing LB solidified with 0.4 % agar centrally inoculated and incubated for 18 h at 30 °C. White areas show zones of bacterial growth and correlate with swimming motility. Assay plates were inoculated

from mid-exponential pre-cultures grown in LB medium. Genotypes were as indicated below the strain number on the left. At least three biological replicates were analyzed, representative results are shown. Scale bars are 1 cm.

The phenotype of single deletion strains derived from *B. licheniformis* M409 is in line with the target evaluation in *B. licheniformis* M308. Consequently, the Δ*apr*, Δ*sigF*, *pga*::BLAP mutations which distinguish *B. licheniformis* M409 from M308 did not influence the outcome of the phenotypical characterization (Figure 7). Loss of motility was observed for all strains carrying the *degU32* or Δ*sigD* mutation (Figure 11), and likewise for Δ*motB* and Δ*hag* (Figure 12) mutants. Motility was abolished independent from further strain modification, as shown for *B. licheniformis* M439 (Δ*tapA-sipW-tasA*, *degU32*), M441 (Δ*tapA-sipW-tasA*, Δ*epsA-O*, *degU32*) and M447 (Δ*tapA-sipW-tasA*, Δ*epsA-O*, Δ*sigD*) (Figure 11). Importantly, increased biofilm formation observed for *B. licheniformis* M320 (M308 *degU32*; Figure 9) was confirmed for *B. licheniformis* M436 (M409 *degU32*; Figure 11). Due to the known role of DegU-P in exoenzyme production and the strong morphological changes observed for *B. licheniformis degU32* single mutants, special focus was put on the construction of *degU32* strains deficient in biofilm formation. Both, complex colony architecture and the ability to form pellicles was lost or strongly reduced in *degU32* strains when simultaneously targeting structural genes for biofilm formation or regulators thereof. Similar to the results from *B. licheniformis* M315 (M308 Δ*tapA-sipW-tasA*) deletion of *tapA-sipW-tasA* did not fully prevent biofilm formation in the *degU32* strain background (*B. licheniformis* M439, Figure 11). No residual biofilm formation was observed for *B. licheniformis* M441 (Δ*tapA-sipW-tasA*, Δ *epsA-O*, *degU32*) and M451 (*remA* R18W P29S, *degU32*). Deletion of *bslA* did not affect the complex colony morphology in the *degU32*, Δ*bslA* strain *B. licheniformis* M455 (Figure 11) which is in line with the robust colony morphology of the *bslA* single deletion mutant *B. licheniformis* M454 (Figure 8). But, unlike *B. licheniformis* M454, *B. licheniformis* M455 formed less-stable pellicles, which became apparent only in LBGM medium (Figure S2). Moreover, consistent with results from pellicle formation assay of *B. licheniformis* M317 (Figure 8), deletion of *slrA* was unable to fully prevent biofilm formation in the *degU32* combinatorial mutant *B. licheniformis* M451. Both strains showed limited, but clearly visible pellicle formation and slightly elevated colonies on LBGM agar (Figure 8 and Figure 11). Similar to *degU32* single mutants *B. licheniformis* M320 (M308 *degU32*) and M436 (M409 *degU32*), introduction of *degU32* in strains deficient in biofilm formation resulted in colonization of a wider surface area (Figure 11). This effect is specific for *degU32* and not related to the non-motile phenotype in general as *B. licheniformis* M312 (Δ*sigD*), M313 (Δ*motB*) and M314 (Δ*hag*) (Figure 8) and the *sigD* combinatorial mutant *B. licheniformis* M447 (Δ*eps*, Δ*tasA*, Δ*sigD* Figure 11) displayed regular growth characteristics on solid media. Interestingly, the *sigD*, *degU32* mutant *B. licheniformis* M449

was slightly impaired in pellicle formation, which was not observed for either of the corresponding single mutant (Figure 8), while colony architecture was comparable to *B. licheniformis* M436.

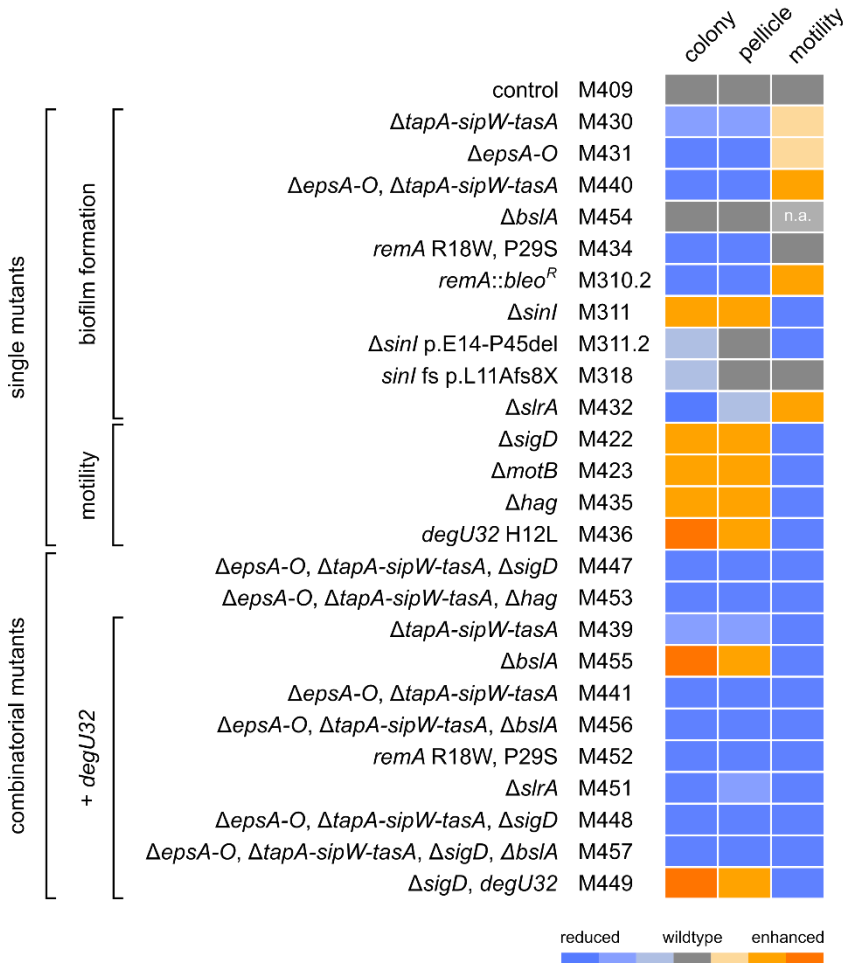

Figure 12: Summary of phenotypical analysis of *B. licheniformis* strain derivatives. Colony: Ability to develop complex colony morphology on solid medium. Pellicle: Formation of biofilms at the air-liquid interphase in liquid culture without agitation. Motility: Spreading on soft agar plates solidified with 0.4 % agar. Strain numbers and relevant genotypes are listed. Orange-blue color scheme refers to enhanced and reduced characteristics of the respective phenotype. Note, that the non-motile phenotype of *B. licheniformis* M449, M451, M452, M455, M456 and M457 was not experimentally determined but concluded from loss of motility observed for progenitor strains carrying the *degU32* or Δ*sigD* mutation.

By analyzing a comprehensive set of biofilm and motility deficient mutants as well as strains deficient in both cellular adaptations (*B. licheniformis* M447 to M457, Figure 12), the mutually exclusive character of these fundamentally opposing cellular adaptations in *B. licheniformis* was demonstrated. Null mutants deficient in either of the two processes showed upregulation of the respective other developmental program (Figure 12). This became apparent in particular, in case of motility deficient strains

displaying increased biofilm formation, while biofilm deficient strains did not necessarily show increased motility. However, further analyses are required to confirm the observations made. In summary, including the deletion of *sigF* in the parental strain *B. licheniformis* M409, the resulting most advanced strains are deficient in three cellular differentiation processes, sporulation, biofilm formation and motility.

3.2 Biofilm and motility in batch and fed-batch fermentation

The previous experiments were conducted under cultivation conditions frequently used in basic research to promote biofilm formation. While this simplifies phenotypical analysis of strains and mutants in general or may reflect limiting conditions in the natural habitat, the controlled environment in bioprocesses differs strongly regarding most parameters applied. Therefore, one aim of this thesis was to analyze cellular differentiation of *B. licheniformis* in optimized, nutrient-rich media in batch and fed-batch cultivations. To monitor the physiology and productivity on-line at the population level and at-line/off-line at the single cell level, four different promoters were transcriptional fused the genes encoding the green fluorescent protein *gfpmut2* or the red fluorescent protein *mScarletI*. Quantification of the motile subpopulation was done using the promoter sequence of the late flagellar gene *hag*, while biofilm formation was analyzed using P*tapA,* driving transcription of the gene for matrix protein synthesis (*tapA-sipW-tasA*). The exoprotease producing subpopulation was characterized by monitoring of P*apr* activity. All reporter constructs were preferably chromosomally integrated into the *amyB* or *cat* locus to prevent artificial results resulting from plasmid-based effects like altered promoter-regulator stoichiometry. The integration *loci* were previously evaluated regarding transcriptional read-through to exclude artificial results. In addition, the reporter cassettes were flanked by (bidirectional) transcriptional terminators. But, because construction of *amyB*::P*hag-gfpmut2* and *cat*::P*hag-gfpmut2* integration constructs failed repeatedly, the P*hag* reporter construct was introduced into *B. licheniformis* M409 on the low-copy vector p#0692 carrying a pBS72 derived *origin of replication*. Analysis at the population level were conducted in batch cultures using the on-line microbioreactor system BioLector®. Single cell analyses were performed with samples from batch or fed-batch cultures analyzed via flow cytometry or fluorescence microscopy.

3.2.1 Development of motility in batch and fed-batch cultivations

To investigate whether *B. licheniformis* develops a motile, chemotactic state in nutrient-rich media under batch and fed-batch conditions, the P*hag* reporter strain *B. licheniformis* M409 pWG2rH was constructed, expressing *gfpmut2* under control of a 237 bp fragment containing the *hag* promoter

region and the 3' region of the upstream located gene encoding CsrA as described before (Vlamakis *et al.* 2008). To improve translation of GFP, the native *hag* ribosome binding site was replaced with a standardized sequence GATTAACTAATAAGGAGGACAAAC (Guiziou *et al.* 2016). The plasmid-based reporter strain was cultivated in LSJ-CT and V3 medium with 20 µg/ml kanamycin sulfate. GFP fluorescence and biomass was monitored (Figure 13A, B) and P*hag* promoter activity was calculated (ΔGFP x Δt^{-1}; Figure 13C, D).

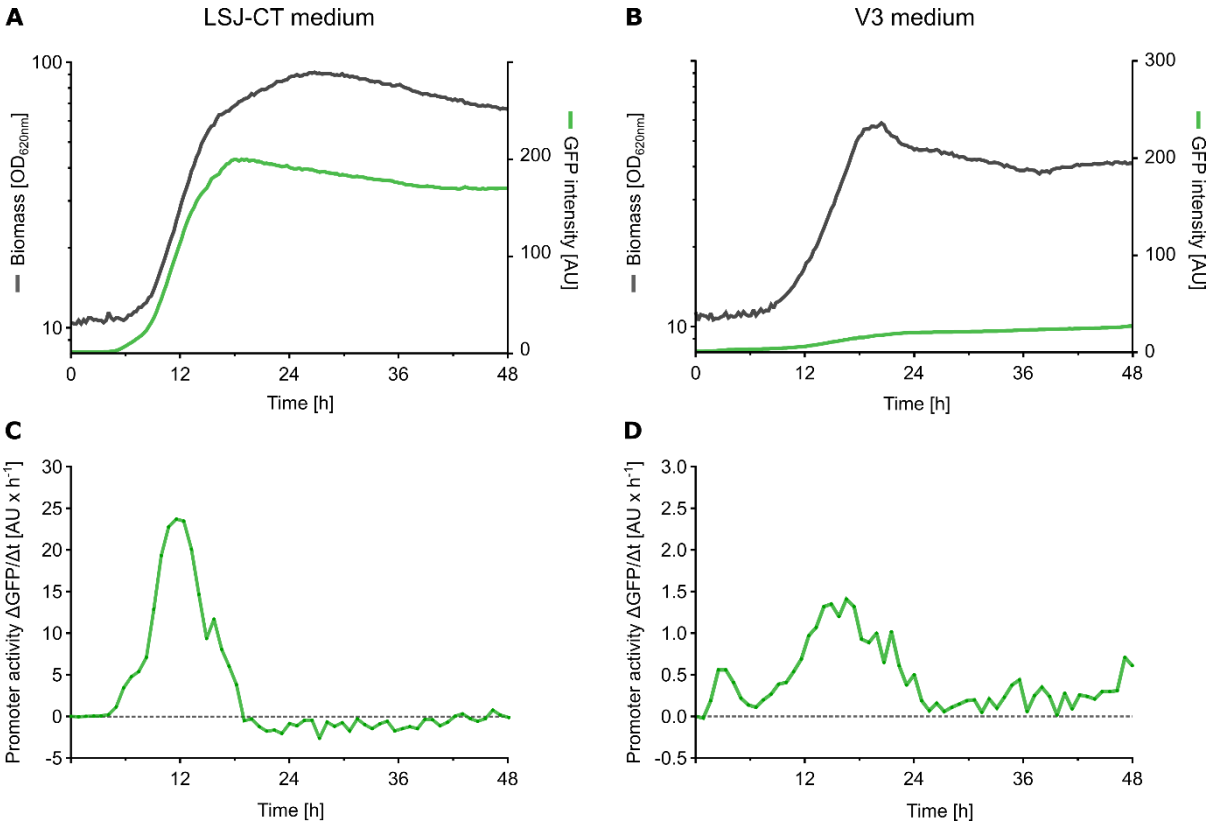

Figure 13: Development of motility in *B. licheniformis* M409 under batch conditions. The pWG2rH (Phag) reporter strain was cultivated in (A,C) LSJ-CT and (B,D) V3 medium in 48-well deep-well microtiter plates with flower geometry. (A, B) Biomass and GFP fluorescence were monitored online using the BioLector system; shaking frequency; 1,000 rpm shaking diameter, 3 mm; filling volume, 0.8 ml; temperature 30 °C. (C, D) Promoter activity was calculated from the increase in GFP fluorescence over time (ΔGFP x Δt^{-1}). Note the different vertical axis scale in C and D.

In both media, upregulation of P*hag* was observed from early exponential growth phase on, reaching maximum promoter activities during mid-exponential growth around 12 h and 15 h in LSJ-CT and V3 medium (Figure 13C, D). Entering the stationary phase promoter activity rapidly declined and no further GFP expression was observed in LSJ-CT medium while low expression occurred in V3 throughout stationary growth. Importantly, overall fluorescence and promoter activity was strongly elevated in

cultivations with complex LSJ-CT medium compared to chemically defined, but nutrient rich V3 medium. Both parameters were 8 to 16-fold higher in complex medium suggesting strong differences in the distribution of the motile subpopulation. To quantify the motile subpopulation, flow cytometry was applied (Figure 14). Based on the fluorescence distribution after 20 h of growth in LSJ-CT, in which highest fluorescence intensity were measured, GFP positive cells were divided into high and low expressing cells with a threshold of 1 x 10^4 (arbitrary units; (Figure 14C, D). The threshold value includes 90 % of all cells in the population in the 20 h sample. As *Bacillus* cells are known to exist in either a SigD ON or SigD OFF state (Cozy and Kearns 2010), cells displaying low GFP intensity have either recently activated P*hag* or promoter activity diminished and GFP turnover exceeds the synthesis rate. When grown in LSJ-CT medium, *B. licheniformis* M409 pWG2rH is characterized by bimodal distribution of cells which have activated P*hag* in the late-exponential and transition phase with the vast majority of cells showing high GFP fluorescence (85 to 90 %; Figure 14C). In fact, due to the large subpopulation, motility appears almost unimodal and homogeneous. While the total GFP positive population remains stable with 95 % of all cells expressing or having expressed GFP throughout growth, the number of cells gated as high expressing cells decreased between 24 and 40 h. The results are consistent with the global P*hag* expression profile showing a slightly decreasing GFP intensity during stationary growth (Figure 13A). Compared to samples from LSJ-CT cultures, bimodal distribution of motile cells was more pronounced and clearly detectable in defined medium, but showing the opposite trend as compared to LSJ-CT cultures as most cells (60 to 70 %) have not activated P*hag* (Figure 14B, D). The highest fraction of cells exhibiting high GFP expression was detected in samples analyzed after 24 h. Afterwards, the P*hag* expression pattern remained unchanged which is consistent with analysis at the population level (Figure 13B, D).

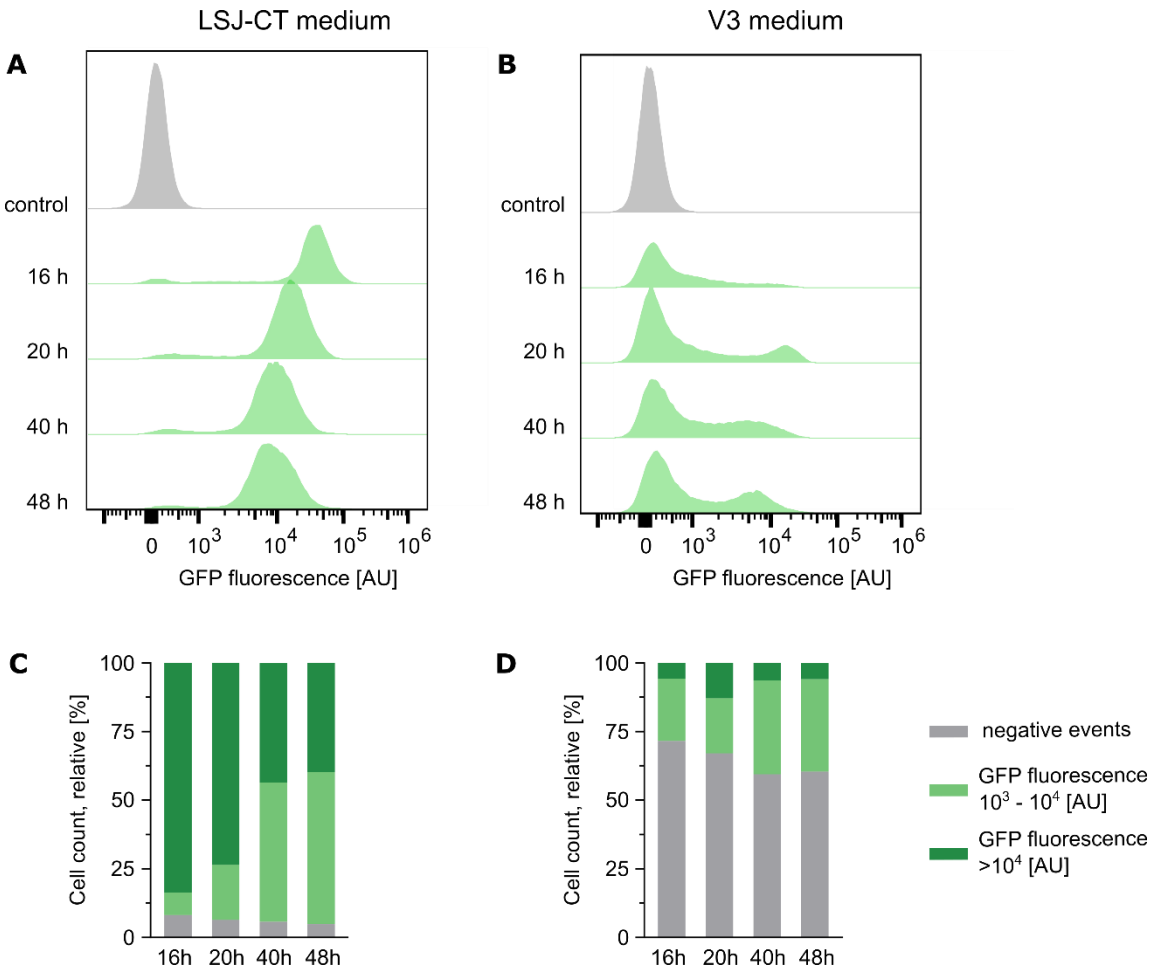

Figure 14: Quantification of the motile subpopulation in *B. licheniformis* M409 under batch conditions. The pWG2rH (P*hag*) reporter strain was cultivated in (A,C) LSJ-CT and (B,D) V3 medium in 48-well deep-well microtiter plates with flower geometry; shaking frequency, 1000 rpm; shaking diameter, 3 mm; filling volume, 0.8 ml; temperature 30 °C. Samples from late-exponential (16 h), transition state (20 h), early (40 h) and late (48 h) growth were analyzed and approximately 50,000 events were analyzed by flow cytometry. (A, B) Frequency distribution of motile cells. The Y-axis represents cell counts for each strain at 16, 24, 40, and 48 h time points. The X-axis is arbitrary units (AU) of fluorescence in a logarithmic scale. (C, D) GFP positive cells were divided in high and low expressing cells with a fluorescence intensity threshold value of 1 x 10^4.

Under fed-batch conditions the number of cells developing into a motile chemotactic state was lower compared to batch cultures. However, throughout full cultivation, GFP positive cells were detected (Figure 15). To exclude that GFP signals analyzed resulted from accumulation during growth in preculture, 1 % instead of 10 % inoculum was used, extending the batch phase to 24 h. By analyzing 700 - 2100 cells, 3.4 % were shown to have activated P_{hag} after 12 h, likely representing non-limiting growth conditions. Entering the glucose limited fed-batch phase, the number of GFP positive cells was 5.9 % (24 h) and further increased to 9.4 % after 72 h. However, it is important to note, that it was not distinguished between high and low GFP expressing cells, as maximum GFP intensity was above the

detector limit for selected cells (compare Figure 15, 72 h; fluorescence intensity (AU) ranging from 0.17 to 3.35 and signal saturated “sat.”).

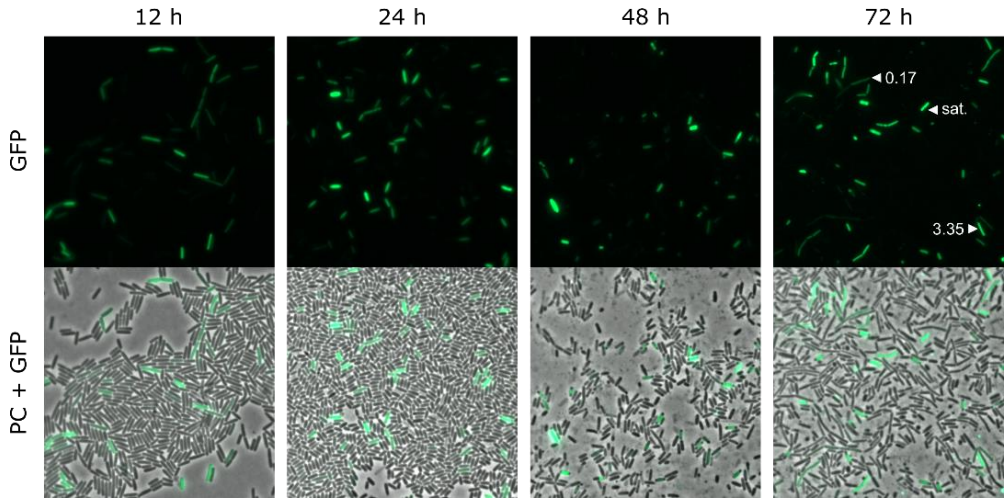

Figure 15: Development of motility in *B. licheniformis* M409 under fed-batch conditions. GFP images and phase contrast GFP overlays show frequency of cells expressing GFP under control of the flagellin promoter P*hag*. Exposure times for GFP images were 500 ms except for the 12 h sample (1000 ms). Main cultures were inoculated with 1 % of preculture resulting in a batch phase of 24 h. GFP intensities 72 h are indicated for selected cells (sat. = signal saturation).

3.2.2 Biofilm formation at population and single cell level

To investigate biofilm formation in *B. licheniformis* M409 in more detail, the P*tasA* reporter strains *B. licheniformis* M409.t1 and M409.t2 were constructed, expressing *gfpmut2* or *mScarletI* under control of a 491 bp fragment containing the *tapA-sipW-tasA* promoter region as described before (Vlamakis *et al.* 2008). To improve translation, the native ribosome binding site was replaced with a standardized sequence GATTAACTAATAAGGAGGACAAAC (Guiziou *et al.* 2016). The GFP and mScarletI expression cassettes were chromosomally integrated into the *amyB* respectively the *cat* locus, with the latter natively conferring chloramphenicol resistance to *B. licheniformis*. The GFP reporter strain *B. licheniformis* M409.t1 was analyzed in batch cultivations, while the mScarlet reporter strain *B. licheniformis* M409.t2 was used in fed-batch cultivations. In batch cultures GFP fluorescence and biomass were monitored (Figure 16A, B) and P*tasA* promoter activity was calculated (Figure 16C; $\Delta GFP \times \Delta t^{-1}$). Fed-batch samples were evaluated qualitatively only.

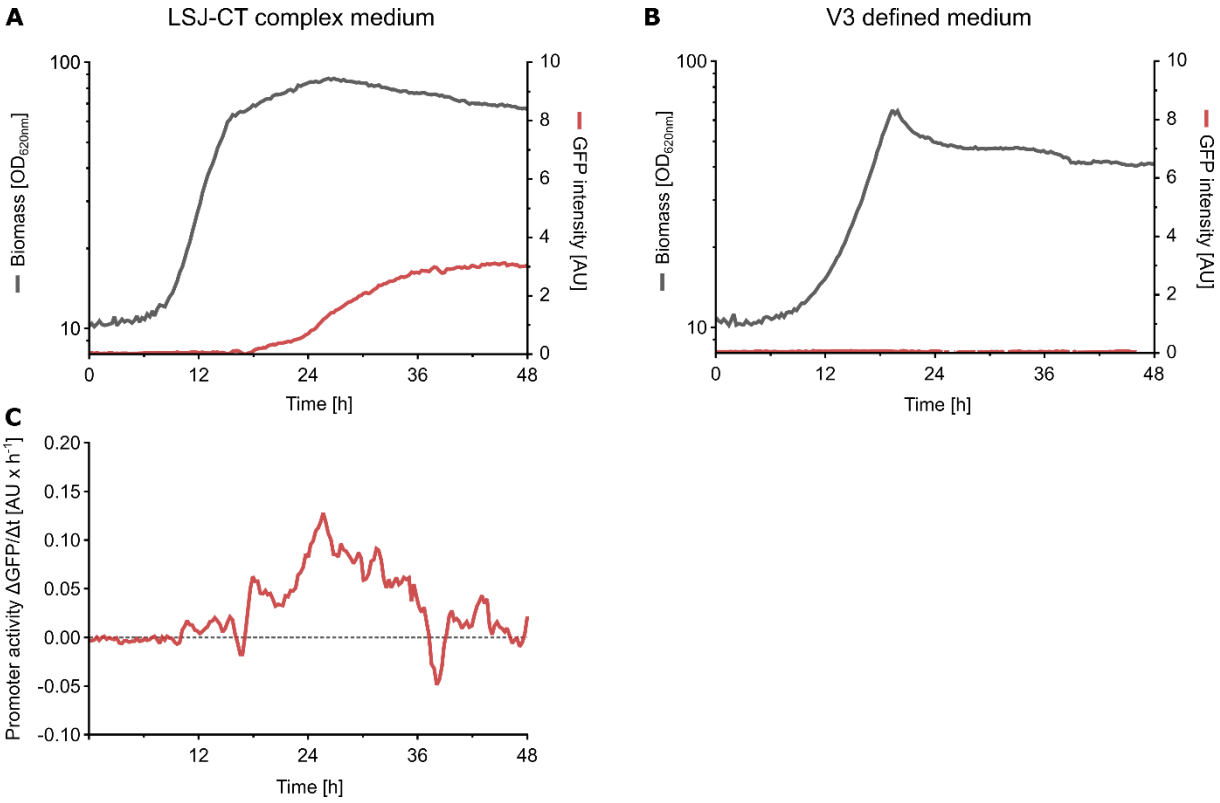

Figure 16: Biofilm formation of *B. licheniformis* M409.t1 in batch cultivations. The P*tasA* reporter strain M409.t1 was cultivated in (A,C) LSJ-CT and (B) V3 medium in 48-well deep-well microtiter plates with flower geometry. (A, B) Biomass and GFP fluorescence were monitored online using the BioLector system; shaking frequency; 1,000 rpm shaking diameter, 3 mm; filling volume, 0.8 ml; temperature 30 °C. (C) Promoter activity was calculated from the increase in GFP fluorescence over time (ΔGFP x Δt-1).

In LSJ-CT batch cultures, activation of the P*tasA* promoter leading to matrix formation occurred in transition phase (Figure 16A). Highest P*tasA* activity was determined after 24 h during early stationary growth followed by a steady decrease in promoter activity in later cultivation phases (Figure 16C). Surprisingly, no GFP expression was detected in batch culture with chemically defined medium (Figure 16B) and likewise biofilm formation was scarce in fed-batch cultures of *B. licheniformis* M409.t2 (Figure 17). However, cells expressing *mScarletI* under control of P*tasA* were occasionally detected in small clusters presumably embedded in an extracellular matrix as phase contrast images suggest (Figure 17).

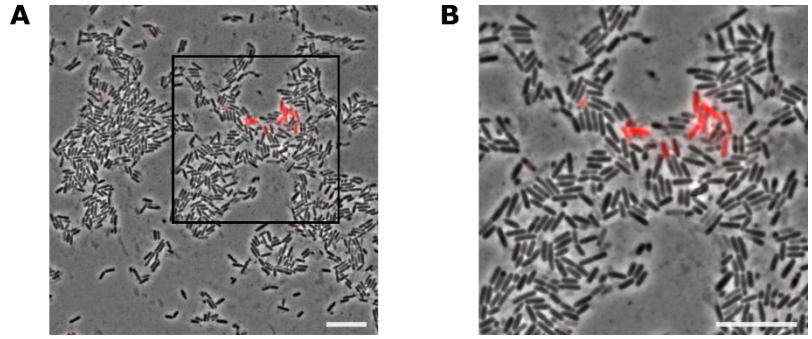

Figure 17: Development of the matrix producing subpopulation in *B. licheniformis* M409.t2 under fed-batch conditions. Phase contrast and mScarlet overlays show the frequency of cells expressing mScarlet under control of the P*tasA* promoter. Main cultures were inoculated with 1 % of preculture resulting in a batch phase of 24 h. Images were taken after 48 h. (B) Enlarged view of the cells extracted from the frame in image A. Scale bars are 10 µm.

The results presented demonstrate that phenotypical heterogeneity occurs under nutrient-rich, optimized growth conditions as differentiation. However, single cell analysis revealed a strong media-dependent effect on cellular heterogeneity, with a higher number of cells activating P*hag* in LSJ-CT medium. The difference in P*tasA* promoter activity was even more pronounced, as indicated by analysis at the population level (Figure 16). The strong differences in GFP frequency distribution indicate that V3 medium and fed-batch conditions reduce cellular heterogeneity regarding motility and biofilm formation. However, it remains to be clarified how fed-batch cultivation using complex nitrogen sources such as casitone and tryptone in LSJ-CT medium affect the formation of subpopulations, as the experimental setup using feedplates requires inorganic N-sources to enable carbon limited fed-batch cultivation.

3.2.3 Cell morphology

In *Bacillus*, developing a motile, chemotactic state is inevitable associated with cell separation and many autolysins are co-regulated with *early* and *late flagellar genes* (Márquez *et al.* 1990; Serizawa *et al.* 2004; Kearns and Losick 2005; Chai *et al.* 2010b). In contrast to planktonic growth, biofilm formation is associated with filamentous or chaining cells (Branda *et al.* 2001; Kearns *et al.* 2005; Branda *et al.* 2006; Kobayashi 2007a). Initial observations with *B. licheniformis* DSM641 derivates revealed alterations in the cell morphology of the Δ*sigD* and *degU32* mutant *B. licheniformis* M312 and M320, both causing a growth condition-dependent filamentous cell morphology. To analyze the effect of single and multiple mutations on the cell morphology in more detail, selected *B. licheniformis* M409 strains were characterized under fed-batch conditions. To exclude that the cell morphology observed results from the high inoculum with cells from the stationary pre-cultures (10% in the standard feedplate cul-

tivation), main cultures were inoculated with 1% resulting in an initial OD_{600nm} of 0.1 ± 0.01. This extends the batch phase characterized by a glucose release rate higher than the glucose uptake rate from to 24 h (Habicher *et al.* 2019c). The cell morphology was analyzed by microscopy (phase contrast and DAPI staining of nucleic acids) throughout the fed-batch phase.

As shown in Figure 18, *B. licheniformis* M409, the single deletion strains *B. licheniformis* M430 (Δ*tapA-sipW-tasA*) and *B. licheniformis* M422 (Δ*sigD*) grew exclusively as individual cells under fed-batch conditions, except for rarely observed filaments in *B. licheniformis* M409 and M422 samples after 72 h. Similar to its phenotype during the fed-batch phase, *B. licheniformis* M422 was characterized by individual cells from the transition state onwards in batch cultivations using LB medium, while cell chaining of *sigD* mutants was observed during early to mid-exponential growth only (Figure S3). Whether *B. licheniformis* M422 displays alterations in cell morphology in batch cultures with chemically defined medium remains to be clarified. In contrast to other strains analyzed, the *degU32* mutant *B. licheniformis* M436 showed a highly filamentous or rather chaining phenotype at the onset of the fed-batch phase (24h). As staining of nucleic acids using DAPI showed (Figure S4), it is important to differentiate between filamentous and chaining cells. While the latter describes individual cells, that display regular septum formation but are unable to separate, filaments are hereafter referred to as (highly) elongated, multi-nucleoid cells lacking septum formation and sharing cytoplasmic content (Takeuchi *et al.* 2005; Vejborg and Klemm 2009). At 24 h most of the *B. licheniformis* M436 cells were found in cell chains, with a few filamentous cells and both cell types diminished afterwards (Figure 18 and Figure S4). After 48 h an increasing number of cells was found in cell aggregates which was the predominant growth form at 72 h (Figure 19A). Aggregates seemed to contain single cells or duplets rather than cell chains, although multilayer aggregation impeded detailed analyses of the individual cell morphology. Moreover, adherence of cells to the polystyrene surface of shaking feedplates was observed. Thus, the increased biofilm formation observed for *B. licheniformis* M436 (*degU32*) in macroscopic analyses of static cultures using specialized media also occurred in dispersed cultures with nutrient rich media. In fact, increased biofilm formation was observed under all growth conditions tested, including complex and defined media, batch and fed-batch cultivations as well as static and dispersed cultures. Importantly, although biofilm formation did not play a major role in the parental strain *B. licheniformis* M409 under simulated fed-batch conditions, it becomes relevant in the *degU32* strain background (*B. licheniformis* M436).

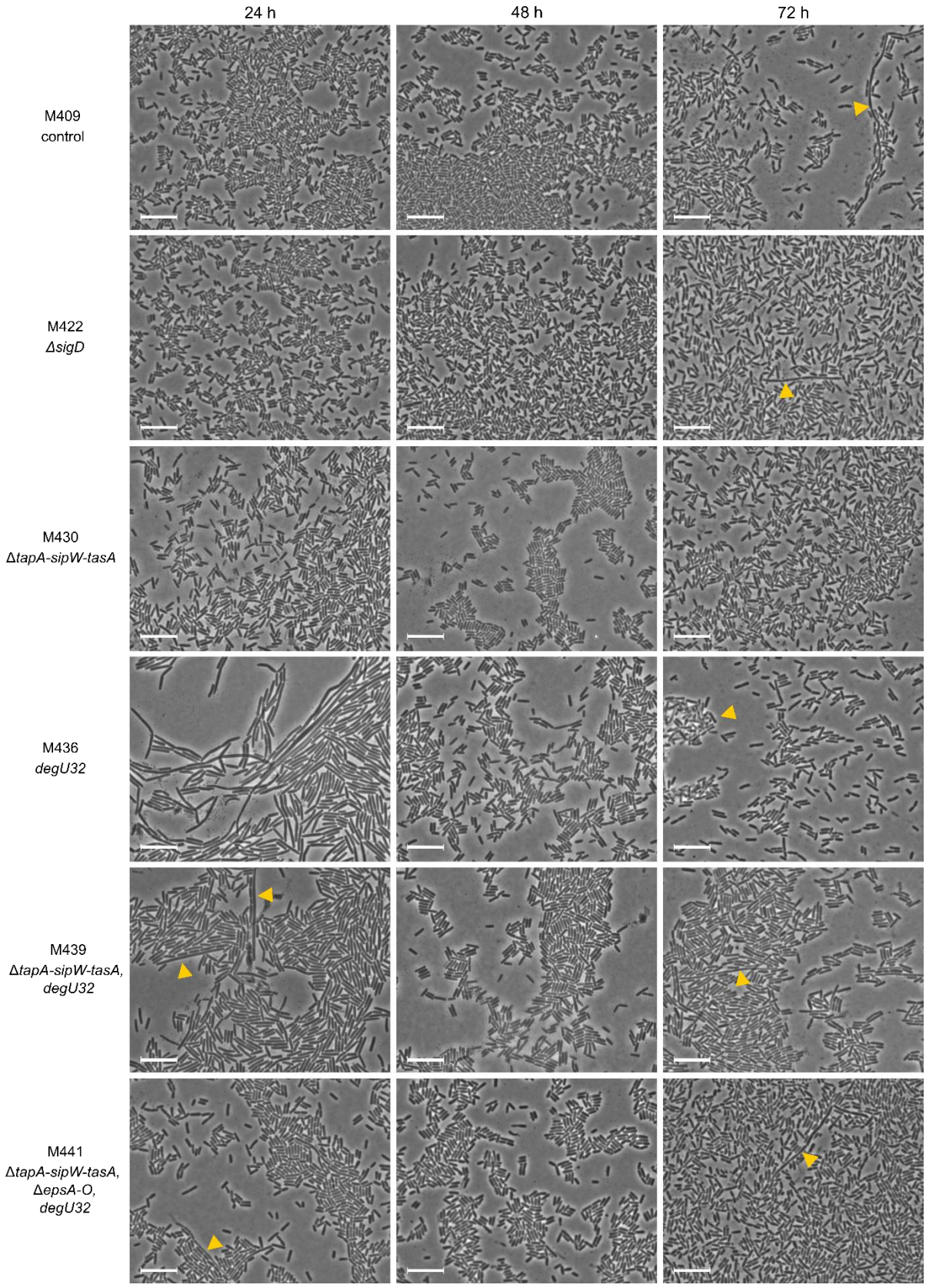

Figure 18: Cell morphology of selected *B. licheniformis* mutant strains under fed-batch conditions. Strains carrying single or multiple mutations (as indicated) were cultivated in feedplates. Samples were taken after 24, 48 and 72 h and analyzed by microscopy without further processing. Phase contrast

images are shown. Selected cell chains or aggregates are highlighted with arrow heads. White scale bars are 10 µm. Optical densities at sampling points are shown in Figure 19B.

To target biofilm formation in *degU32* mutants, the *tapA-sipW-tasA* and *epsA-O* operons were deleted, among others. Interestingly, deletion of *tapA-sipW-tasA* or in combination with Δ*epsA-O* in the *degU32* strain background (*B. licheniformis* M439 and M441) did not only reduce or prevent biofilm formation at population level (Section 3.1.3), but also strongly altered the cell morphology in microscopic analyses (Figure 18). Entering the fed-batch phase, a reduced number of filaments and cell chains was observed for the *degU32*, Δ*tasA* double mutant *B. licheniformis* M439. Most cells were individual cells but slightly elongated compared to the parental strain *B. licheniformis* M409. In case of *B. licheniformis* M441, differing from M439 by additional deletion of the *epsA-O* operon, the cell size was wildtype-like, and filaments were rare throughout the fed-batch phase. Most importantly, the formation of cell aggregates was strongly reduced in *B. licheniformis* M439 (Figure 19A) and completely abolished in *B. licheniformis* M441.

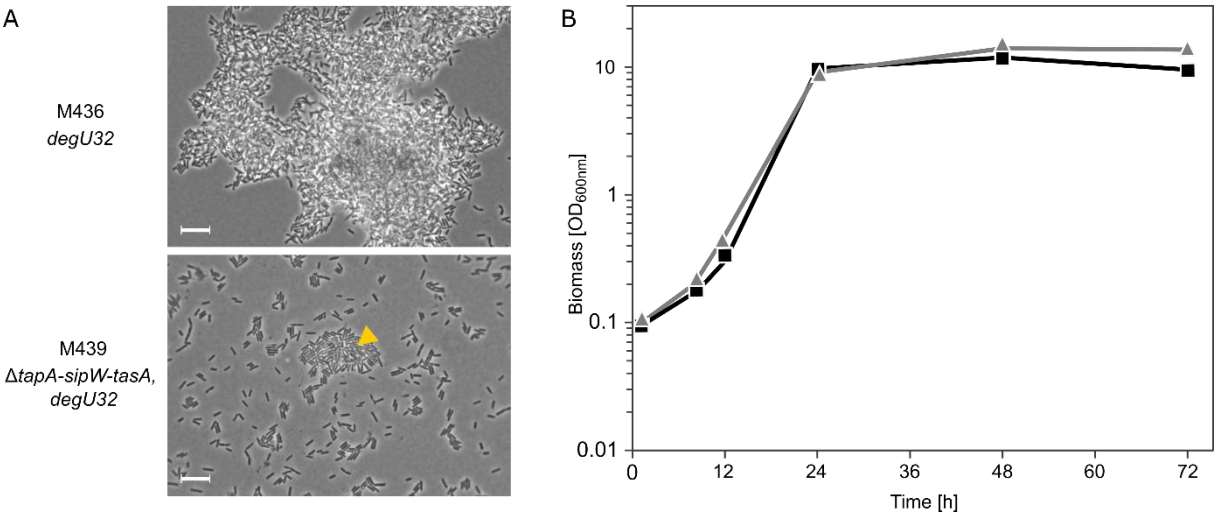

Figure 19: Formation of cell aggregates in *B. licheniformis degU32* strains. (A) Samples were taken from fed-batch cultivation after 72 h and analyzed by microscopy without further processing. Phase contrast images are shown. White scale bar is 10 µm. Cell aggregates were observed for *B. licheniformis* M436 and to limited extend for M439 and most pronounced at 48 h and 7 2h. (B) Growth of *B. licheniformis* M409 (parental strain; squares) and M439 (triangles) in the polymer-based simulated fed-batch process with 1 % inoculum.

3.2.4 Cell lysis assay

Morphological analysis revealed increased cell chaining for *B. licheniformis* M312 (Δ*sigD*) and *B. licheniformis* M320 (*degU32*) mutants, resulting at least in part from lack of SigD-dependent transcription of autolysins with DegU-P indirectly repressing SigD levels (section 1.4.2). To compare the autolysin activity between both strains in more detail, a sodium azide-based cell lysis assay was conducted. In

addition to *B. licheniformis* M312 (Δ*sigD*) and M320 (*degU32*), the *motB* and *hag* deficient strains *B. licheniformis* M313 and M314 were included in the analysis due to their highly similar phenotype (Figure 8 and Figure S6). Moreover, we were interested whether deletion of genes most downstream in the regulatory cascade for motility (*motB*, *hag*) affects host cell physiology on a more global level. Figure 20 shows the relative autolysin activity as the decrease in optical density (OD_{600nm}) after growth was inhibited by addition of sodium azide to mid-exponentially growing cultures of *B. licheniformis*. Autolysins expressed up to this point cause hydrolysis of peptidoglycan and consequently the assay shows autolysin activity at the selected time point only.

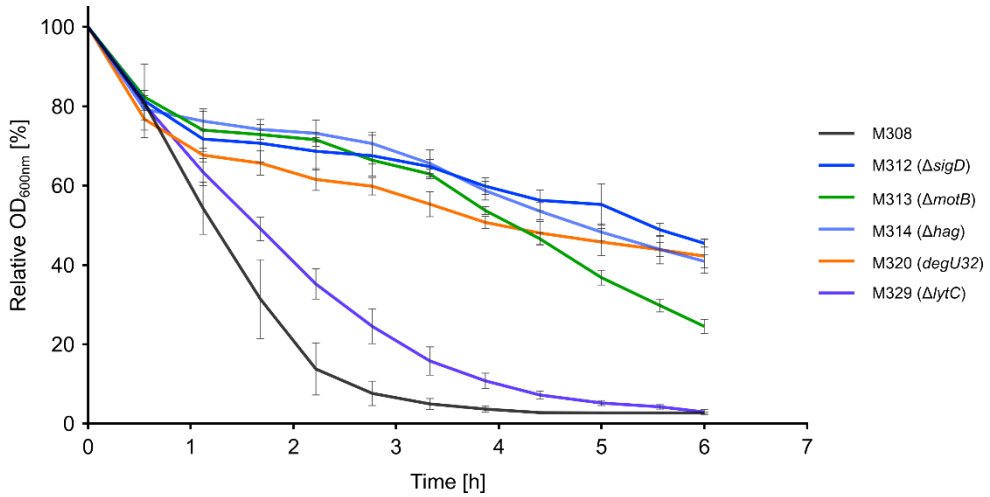

Figure 20: Cell lysis assay of motility deficient *B. licheniformis* strains. Strains were cultivated in LB medium at 37 °C until mid-exponential phase. To inhibit growth, 0.05 M sodium azide was added (t =0). The degree of cell lysis was determined by measuring the decrease in optical density. Error bars indicate the standard deviation of at least three individual replicates. Key mutations for each strain were as indicated.

Comparison of cell lysis revealed highly similar and strongly reduced autolysin activity for motility deficient strains including the *degU32* mutant *B. licheniformis* M320. After an initial decrease in optical densities to 80 % observed for all strains, OD_{600nm} values of the control strain *B. licheniformis* M308 dropped to 8 % and 4 % after 2.8 h respectively 3.9 h. In contrast, biomass of *B. licheniformis* M312, M313, M314 and M320 decreased only gradually over the course of the experiment with final OD_{600nm} values around 50 % relative to levels when sodium azide was added to the cultures, except for the *motB* mutant *B. licheniformis* M313, which showed slightly stronger cell lysis. The mutants tested are related to the SigD regulon, which also comprises the major autolysin *lytC*. As deletion of *lytC* in *B. subtilis* was shown to prevent cell lysis to a level comparable to *B. licheniformis* M312, M313 and M320,

the *lytC* deficient *B. licheniformis* M329 was included as a reference strain (Kabisch *et al.* 2013). However, unlike *B. subtilis* ATCC6051, *B. licheniformis* M329 showed only delayed cell lysis, but deletion of *lytC* did not prevent cell lysis under the conditions tested.

3.3 Growth and productivity

By targeting structural genes and regulators required for biofilm formation and motility, *B. licheniformis* strains deficient in both cellular differentiation processes were constructed. To analyze the effect of these mutations on growth and productivity, batch and fed-batch cultivations were performed. While batch cultivations are frequently applied in literature for strain characterization, fed-batch conditions represent the predominant mode of process control in industrial biotechnology. Expression of the alkaline protease BLAP served as a model enzyme for secretory enzyme production.

3.3.1 Characterization of *B. licheniformis* M409 mutants in batch cultivations

Growth in batch cultures was monitored on-line during 48 h of cultivation the on-line microbioreactor system BioLector®. Selected *B. licheniformis* strains were cultivated in rich (LSJ-CT) and chemically defined (V3) medium. Biomass (OD_{600nm}), pH and dissolved oxygen tension (DOT) were determined and the maximum specific growth rate (µmax h^{-1}) was calculated. In addition, protease expression was analyzed after 48 h of cultivation.

3.3.1.1 Growth characteristics and maximum specific growth rates

Strain specific differences were rather small in V3 cultivations while strong differences were observed for growth in LSJ-CT. However, for both media, comparison of *B. licheniformis* M409 mutants revealed three distinct types of growth curves each representing a specific subset of strains. The first group comprises the parental strain *B. licheniformis* M409 and strains deficient in biofilm formation *B. licheniformis* M430 (Δ*tasA*) and M440 (Δ*eps*, Δ*tasA*) (Figure 21 and Figure S6, grey). Additionally, further analysis showed highly similar growth characteristics for *B. licheniformis* M431 (Δ*eps*), M432 (Δ*slrA*) and M434 (*remA* missense) at least during the first 24 h of cultivation (data not shown). Secondly, strains carrying the *degU32* mutation showed similar growth behaviour independent from further strain modification as shown for *B. licheniformis* M436 (*degU32*), *B. licheniformis* M441 (Δ*eps* Δ*tasA degU32*) and *B. licheniformis* M457 (Δ*eps* Δ*tasA degU32* Δ*sigD*) (Figure 21 and Figure S6, orange). Neither inactivation of genes required for biofilm formation nor deletion of *sigD* affected growth of strains carrying the *degU32* mutation. The last group summarizes strains mutated for late flagellar genes (*motB*, *hag*) and the motility specific sigma factor SigD as well as the Δ*sigD*, Δ*eps*, Δ*tasA* combinatorial mutant *B. licheniformis* M447 (Figure 21 and Figure S6, blue).

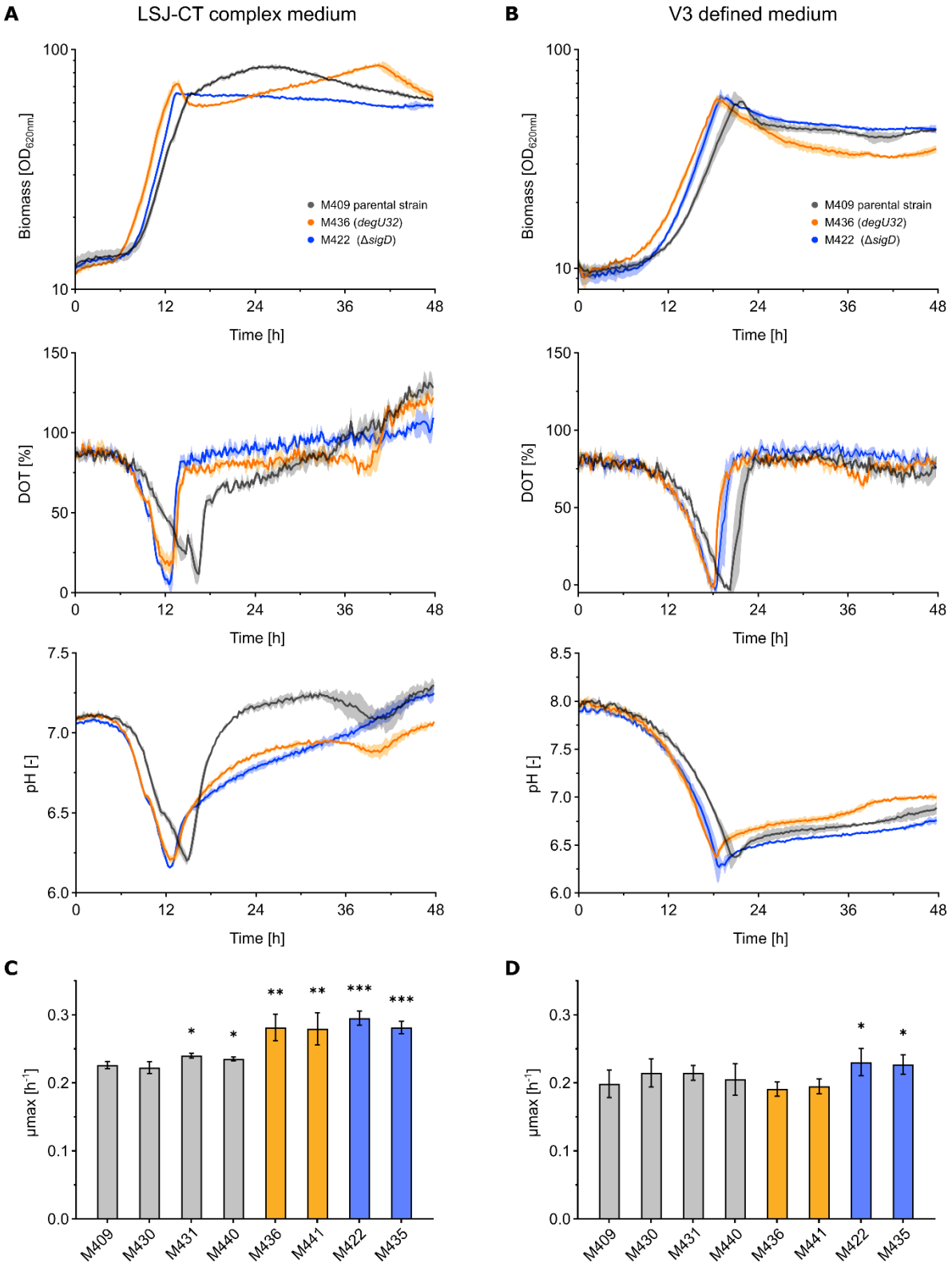

Figure 21: Batch cultivation of *B. licheniformis* strains in A) rich (LSJ-CT) and B) chemically defined (V3) medium. Biomass (scattered light, upper panel), dissolved oxygen tension (DOT, middle panel) and pH (lower panel) were monitored during 48 h of cultivation using the online microbioreactor system BioLector (1000 rpm, 3 mm shaking diameter, 30 °C, 85 % relative humidity). The growth curves shown are representative for three groups of strains: (Grey) *B. licheniformis* M409, M430 (Δ*tasA*) and M440 (Δ*eps*, Δ*tasA*). (Orange) Strains harbouring the *degU32* mutation *B. licheniformis* M436

(*degU32*), M441 (Δ*eps*, Δ*tasA, degU32*). (Blue) *B. licheniformis* M422 (Δ*sigD*) and M435 (Δ*hag*). LSJ-CT and V3 main cultures were inoculated with 0.1 % and 1 % of synchronized pre-cultures respectively. Shaded areas indicate standard deviation of three biological replicates. Maximum specific growth rate in C) LSJ-CT and D) V3 medium calculated from five individual replicates (except for M431, n = 2). Asterisks indicate the level of significance compared to the parental strain *B. licheniformis* M409.

Cultivation in LSJ-CT led to differentiation of strains during the exponential growth phase (Figure 21A). Both, *degU32* mutants and strains from the *sigD* group showed increased growth rates in LSJ-CT medium by 22 % to 30 % compared to *B. licheniformis* M409 (Figure 21C, µmax: M409 = 0.23 $h^{-}1$; M436, M441 = 0.28 h^{-1}; M422 = 0.30 h^{-1}; M435 = 0.28 h^{-1}). Moreover, *B. licheniformis* M436 (*degU32*) and related strains showed a reduced lag phase with exponential growth observed 1.5 – 2 h earlier than for strains clustering in the other two groups. However, exponential growth was not prolonged as *degU32* strains also entered the transition state earlier than *B. licheniformis* M409. It is important to note, that the initial growth phase not necessarily displays the lag phase, but possibly OD_{600nm} values were below detector limits. Nevertheless, possibly two factors contributed to improved growth of *degU32* mutants in LSJ-CT medium, a reduced lag phase and higher growth rates. Entering transition state and throughout stationary growth differences in growth were even more pronounced. While *B. licheniformis* M409 and single mutants deficient in biofilm formation (*B. licheniformis* M430, M431, M440) were characterized by a smooth transition from exponential to stationary growth, the *degU32* mutants *B. licheniformis* M436, M441 and M457 as well as *B. licheniformis* M422 (Δ*sigD*) and *B. licheniformis* M435 (Δ*hag*) showed a sharp decrease or rather abrupt stagnation in growth. Subsequently, biomass increased again for *degU32* strains reaching a second maximum in the late stationary growth phase after 40 h, while biomass of *B. licheniformis* M422 and M435 maintained stable. Interestingly, growth of *degU32* strains in LSJ-CT medium was superior to *B. licheniformis* M409 throughout the full cultivation period when increasing the inoculum from 0.1 % to 1 % (section Figure S5). Moreover, a decrease in biomass at the end of exponential growth was not observed under these conditions. Exponential growth was accompanied by a decrease in pH from 7.1 to 6.2 and a drop in DOT to 11 % (M409), 17 % (M436) and 5 % (M422). While the decrease was comparable, strains differed in the subsequent increase regarding both parameters. DOT values rapidly increased to initial values for the Δ*sigD* and *degU32* strain cluster in the transition state. In contrast, DOT values showed a slightly slower increase for *B. licheniformis* M409. The opposite trend was observed for pH values. Strains clustering with *B. licheniformis* M409 displayed a rapid increase, while only a slow, but steady increase was observed for *B. licheniformis* M422, M436 and related strains.

Compared to LSJ-CT, cultivation in V3 medium resulted in more homogeneous growth patterns (Figure 21B). All strains reached a similar maximum OD_{600nm} at the end of exponential growth followed by a decrease in biomass. Similar to cultivation in LSJ-CT, *degU32* strains showed a reduced lag phase by

about 3 h, but unlike in LSJ-CT, growth during the exponential phase was comparable to *B. licheniformis* M409 as confirmed by determination of the maximum specific growth rate (Figure 21D). In contrast to *degU32* strains, *sigD*, *hag* and *motB* mutants showed a higher growth rate in both media, although less pronounced in V3 (15 %; µmax: M409 = 0.20 h^{-1}, M422 = 0.23 h^{-1}) than in LSJ-CT medium (30 %). Like growth (OD_{600nm}), DOT and pH values were comparable in V3 medium for all three groups of strains. Compared to LSJ-CT cultures, DOT values decreased more strongly in V3 cultivations reaching 0 % DOT at the end of exponential growth.

To compare changes in growth rates between different media, relative µmax values were determined for all *B. licheniformis* M409 derived mutants. The resulting scatterplot confirmed clustering of three different groups of strains (Figure 22). Strains harboring the *degU32* mutation (Figure 22, orange) showed higher growth rates in LSJ-CT medium only, with only small differences upon introduction of further mutations that prevent biofilm formation. Highest growth rates in complex medium were observed for *B. licheniformis* M448 (Δ*eps*, Δ*tasA*, *degU32*, Δ*sigD*) and M455 (*degU32*, Δ*bslA*) which displayed a 1.4-fold increase compared to *B. licheniformis* M409. Unlike strains from the *degU32* cluster, mutations in the *sigD* regulon including the triple mutant *B. licheniformis* M447 (Δ*eps*, Δ*tasA*, Δ*sigD*) resulted in faster growth in both media, with *B. licheniformis* M423 (Δ*motB*) having the lowest growth rate from this group in LSJ-CT medium. Interestingly, growth parameters for the *degU32*, Δ*sigD* strain *B. licheniformis* M449 resembled those of the *degU32* rather than *sigD* cluster which is in line with results from phenotypical analysis (Section 3.1.3). Finally, only minor differences were observed for biofilm deficient strains harboring the wildtype *degU* allele (Figure 22, orange).

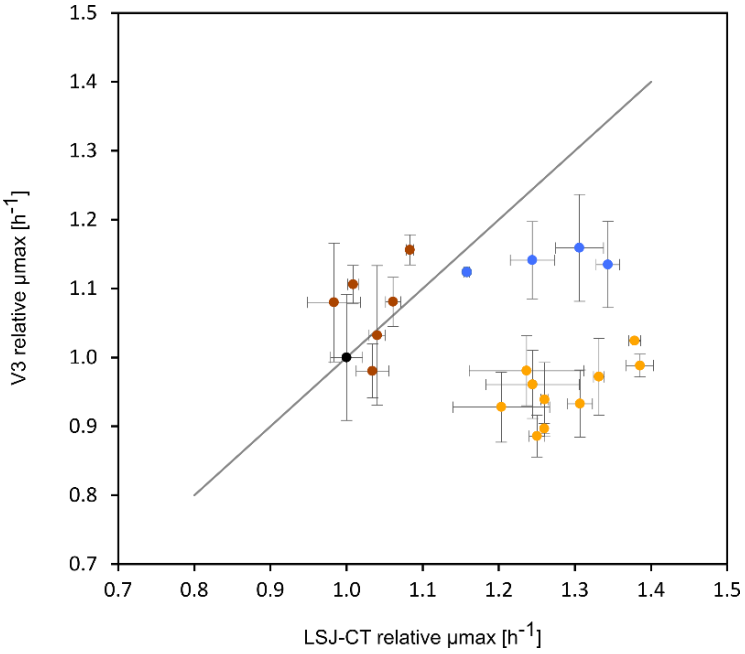

Figure 22: Correlation of relative maximum specific growth rates (µmax h^{-1}) of *B. licheniformis* strains in LSJ-CT and V3 medium. Individual growth rates were set relative to the parental strain M409 for each medium. Error bars indicate the standard deviation from at least two biological replicates. The grey trend line indicates hypothetical linear correlation of changes of the growth rate in both media. (black) parental strain M409. (brown) Biofilm deficient strains without further mutations. (blue) Strains carrying mutation in *motB*, *hag* or *sigD* (M423, M435, M422) and M447 Δ*eps* Δ*tasA* Δ*sigD* (left to right). Strains clustering down-right (orange) carry the *degU32* mutation. See Table S1 for absolute values of µmax.

3.3.1.2 Protease expression in batch cultures

Protease expression of selected *B. licheniformis* mutants was analyzed after 48 h of batch cultivation. Deletion of the *tasA* operon resulted in slightly reduced protease activity in rich medium (*B. licheniformis* M430) which was restored to wildtype-like levels upon additional deletion of *epsA-O* (*B. licheniformis* M440, Figure 23A). In V3 medium, protease expression was not affected in either of the two strains (Figure 23B). In contrast, strains carrying the *degU32* mutation displayed 1.3 to 1.6-fold higher enzyme activity in both media. Protease activity was not altered upon further strain modification as comparison of *B. licheniformis* M436 (*degU32*), *B. licheniformis* M441 (Δ*eps* Δ*tasA degU32*), and *B. licheniformis* M457 (Δ*eps* Δ*tasA degU32* Δ*hag* Δ*bslA*) showed. Moreover, protease expression of *degU32* strains in LSJ-CT medium varied depending on the inoculation strategy with lower titers resulting from higher inoculum. However, this effect was not observed in V3 cultivations and time-resolved analyses are required to investigate expression dynamics in more detail. To address this need, promoter activity was monitored on-line using fluorescence reporter constructs (Section 3.4). Surprisingly, deletion of *sigD* (*B. licheniformis* M422) or *hag* (*B. licheniformis* M435) increased protease expression

1.3 to 1.4 fold in LSJ-CT cultivations, but, unlike *degU32* strains, enzyme activity was reduced in V3 medium by 15 to 30 % (Figure 23B).

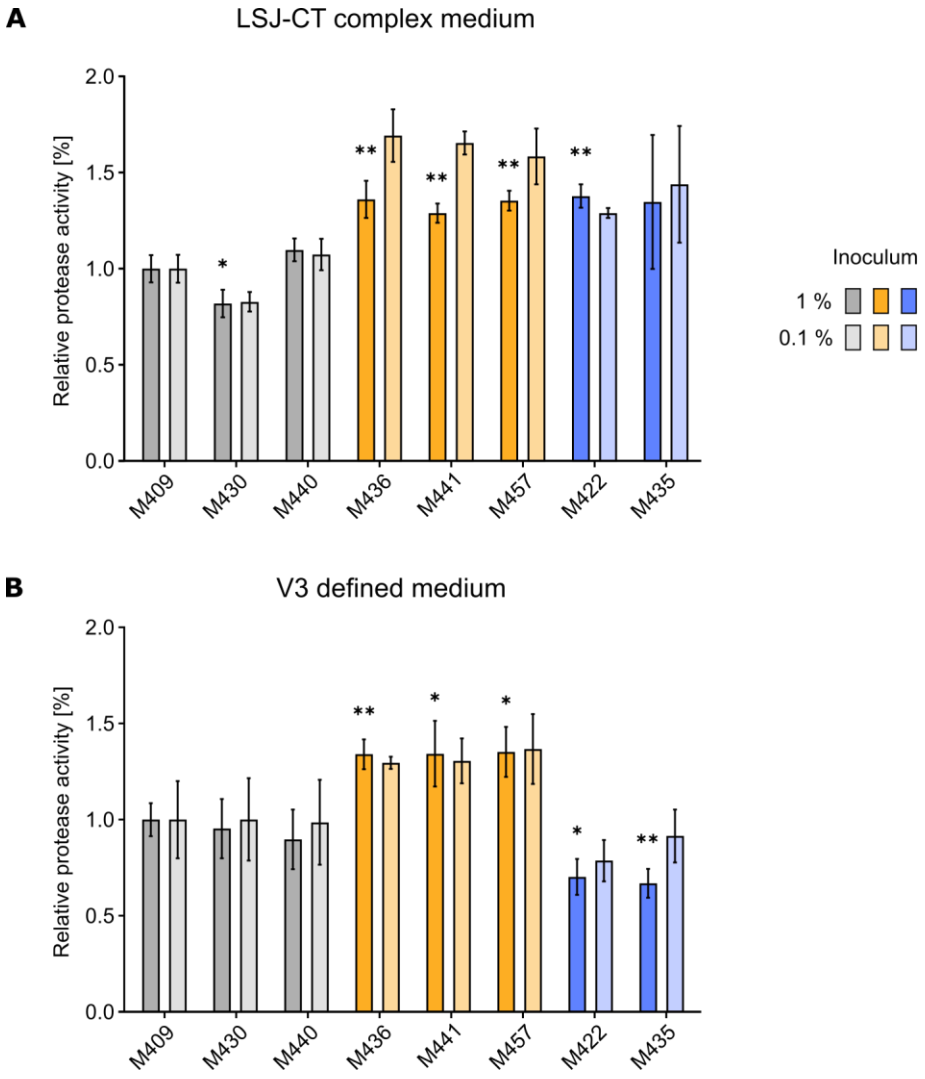

Figure 23: Protease expression of selected mutant strains in batch cultures using A) complex (LSJ-CT) and B) chemically defined (V3) medium. Protease activity was determined after 48 h. Relative protease activity is depicted, normalized for each cultivation condition (medium, inoculum) by the protease activity measured for the parental strain *B. licheniformis* M409. (Grey) *B. licheniformis* M409, M430 (Δ*tasA*) and M440 (Δ*eps*, Δ*tasA*). (Orange) Strains harbouring the *degU32* mutation *B. licheniformis* M436 (*degU32*), M441 (Δ*eps*, Δ*tasA, degU32*) and M457 (Δ*eps*, Δ*tasA, degU32*, Δ*sigD*, Δ*bslA*). (Blue) *B. licheniformis* M422 (Δ*sigD*) and M435 (Δ*hag*). Error bars indicate standard deviation of three biological replicates

3.3.2 Protease expression under simulated fed-batch conditions

In industrial biotechnology, substrate-limited fed-batch cultivation represents the predominant mode of fermentation processes allowing to minimize catabolite repression and overflow metabolism amongst other reasons (Habicher *et al.* 2019a). To avoid misinterpretation of screening results obtained from batch cultures, fed-batch cultivations need to be implemented in early phases of strain

optimization and evaluation (Habicher *et al.* 2019c). To address this requirement, the *B. licheniformis* strain derivatives constructed in this thesis were evaluated using the recently published polymer-based fed-batch system (Habicher *et al.* 2019c). The analyses include expression of the model enzyme BLAP, determination of biomass (cellular dry weight, CDW) and characterization of the extracellular proteome by applying SDS-PAGE and mass spectrometry.

3.3.2.1 Determination of biomass from fed-batch culture samples

Growth of *B. licheniformis* in the simulated fed-batch process was analyzed by measuring the optical density OD_{600nm} for *B. licheniformis* and selected mutants after 24, 24 and 72 h (Figure S8). While OD_{600nm} values were comparable in the initial cultivation phase, *B. licheniformis* M409, *B. licheniformis* M440 (Δ*tasA*, Δ*eps*) showed a decrease in biomass between 24 and 72 h. In contrast, *B. licheniformis* M439 (Δ*tasA*, *degU32*) and *B. licheniformis* M441 (Δ*tasA*, Δ*epsA*, *degU32*) showed a steady increase in OD_{600nm} throughout the microtiter plate-based fed-batch process resulting in 1.8 to 2.0-fold higher optical densities OD_{600nm} after 72 h of cultivation as compared to the parental strain *B. licheniformis* M409 (Figure 25 and Figure S8). But, as cell morphology, integrity or pigmentation may cause artificial results when measuring scattered light, cellular dry weight is considered the more accurate parameter to quantify biomass. Therefore, cellular dry weight (CDW) was determined to verify growth (Figure 24). Biomass of *B. licheniformis* strains carrying the *degU32* mutation was enhanced by 10 to 18 % for *B. licheniformis* M436 (*degU32*), M439 (Δ*tasA*, *degU32*) and M441 (Δ*tasA*, Δ*eps*, *degU32*). As a comparable increase was observed for these strains, deletion of *epsA-O* or *tapA-sipW-tasA* had no effect on final biomass in the *degU32* strain background. Surprisingly, inactivation of the transcriptional regulator RemA or SlrA in combination with the *degU32* mutation reduced biomass to wildtype levels (*B. licheniformis* M451, M452), although further verification is required. Nevertheless, the *degU32* allele was able to compensate for lower biomass of biofilm deficient single mutants of *B. licheniformis* which displayed a 20 % reduction (M430, M431, M440, M432, M434; Figure 24). Consistent with previous results from phenotypical analysis, deletion of *bslA* did not affect biomass in the single mutant *B. licheniformis* M454. Therefore, it is surprising, that targeting *bslA* in the *degU32* background (M455) further increased cellular dry weight as compared to *B. licheniformis* M436, but again further analysis is required to verify these initial observations. This also applies to the multiple mutant *B. licheniformis* M456, lacking the genes for all three major structural components of *Bacillus* biofilms, suggesting that enhanced DegU-P dependent expression of *bslA* does affect growth of *B. licheniformis degU32* strains, possibly due to the enhanced metabolic burden or process dependent effects (DOT, OTR, surface tension). Finally, single mutants deficient in *sigD*, *motB* or *hag* showed no changes in final biomass.

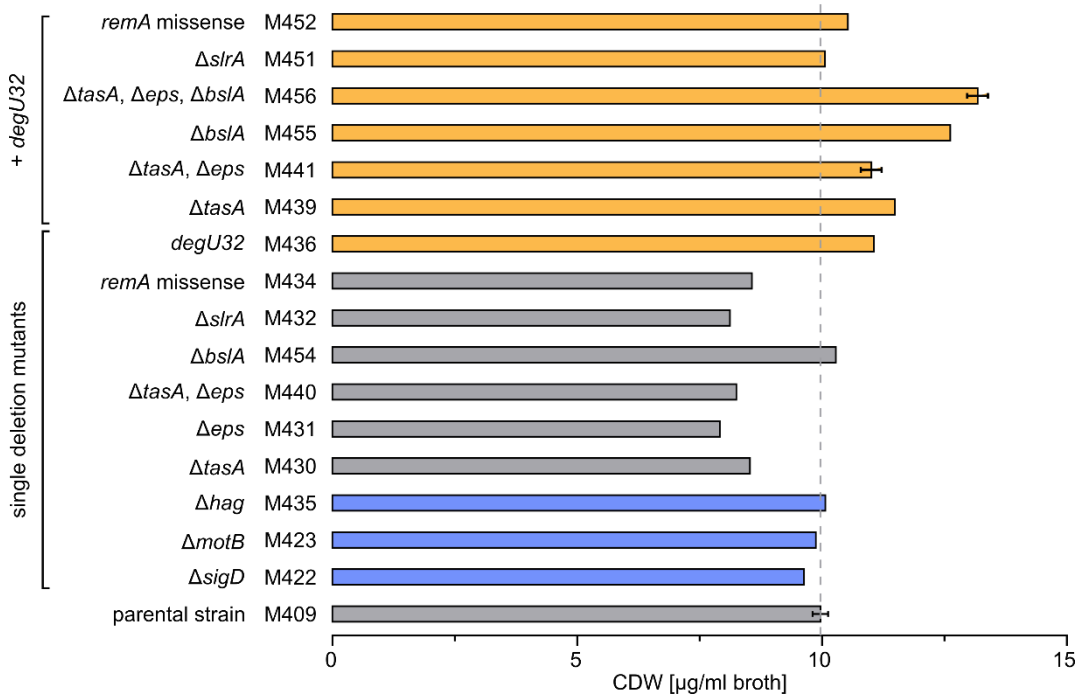

Figure 24: Biomass of *B. licheniformis* strains after 72 h of fed-batch cultivation. Samples from six biological replicates were pooled and cellular dry weight (CDW) was determined. Relevant genotypes were as indicated next to the strain number. Error bars for *B. licheniformis* M409, M441, M456 indicate standard deviation from three replicates each derived from six pooled samples.

Although higher cellular dry weight confirmed improved growth of (combinatorial) *degU32* mutants, the increase in CDW was less pronounced than measurements of optical density OD_{600nm} indicated (Figure 22, yellow cluster). Similarly, OD_{600nm} values were overrepresented for single mutants deficient in biofilm formation (Figure 22, brown cluster). In this context, it is important to note, that the low correlation of OD_{600nm} and CDW is specific for late cultivation phases (72 h) of the standardized feedplate setup with high initial inoculum of 10 % (v/v). When decreasing the inoculum to 1 % (v/v), strong correlation of OD_{600nm} and CDW was observed except for *B. licheniformis* M436 (Figure 25, grey data points and trendline). As lower initial inoculum results in prolonged batch phase, the net time in which cells face glucose limited fed-batch conditions is reduced in the experimental setup with 1 % inoculum, implying low correlation of OD_{600nm} and CDW only as the bacterial population ages. In contrast to biofilm deficient *degU32* mutants, the opposite effect was observed for the single mutant *B. licheniformis* M436 (*degU32*) and M455 (Δ*bslA*, *degU32*) in which OD_{600nm} values were underrepresented (Figure 25), possibly due to strong biofilm formation and cell aggregation affecting measurements of scattered light (Figure 11 and Figure 18). Due to the low correlation of both growth parameters in the simulated fed-batch process, specific enzyme activity was calculated based on CDW rather than OD_{600nm} values (Section 3.3.2.2, Figure 26).

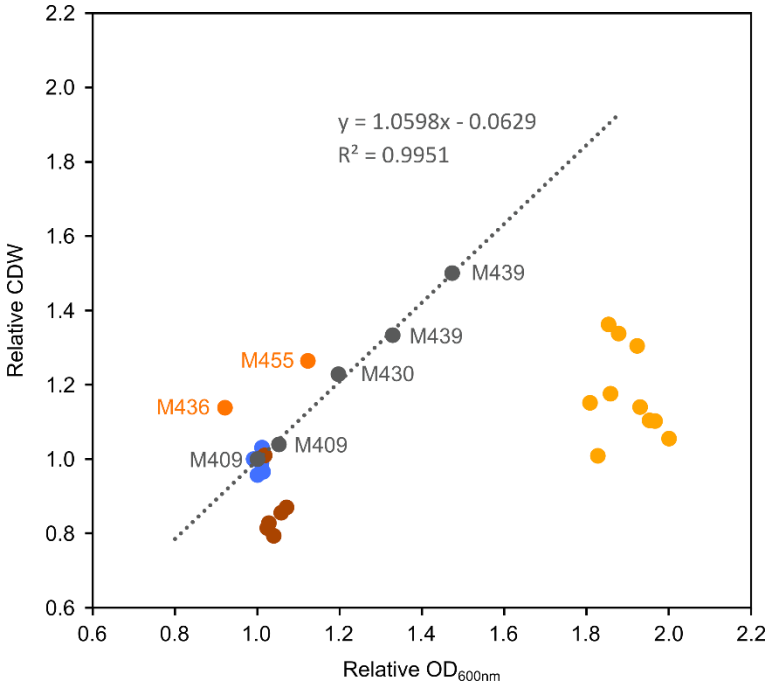

Figure 25: Correlation of relative cellular dry weight and optical density OD_{600nm} of *B. licheniformis* strains under fed-batch conditions. Samples were analyzed after 72 h of fed-batch cultivation. Dataset 1 (grey and orange): The grey trend line indicates linear correlation of CDW and OD_{600nm} experimentally obtained from feedplate cultivation with 1 % inoculum. Strain numbers are indicated next to the datapoint. M409 reference, M436 *degU32*, M455 *degU32* Δ*bslA*, M430 Δ*tasA*, M439 Δ*tasA degU32*; Dataset 2 (blue, brown, yellow): Relative OD_{600nm} and CDW values from feedplate cultivations operated in the standardized setup with 10 % inoculum. (brown) Biofilm deficient strains without further mutations. (blue) Strains carrying mutation in *motB*, *hag* or *sigD*. Strains clustering right (yellow) carry the *degU32* mutation in combination with mutations resulting in biofilm deficiency. See Table S1 for absolute values of µmax.

3.3.2.2 Targeting biofilm formation in *degU32* strains increases productivity

The productivity of *B. licheniformis* DSM641 strain derivatives was analyzed after 72 h of fed-batch cultivations. Relative as well as specific protease activity normalized by cellular dry weight were determined using N-Suc-AAPF-pNA (AAPF) as a substrate. AAPF is specific for serine proteases. As the major extracellular serine protease *apr* was deleted in *B. licheniformis* M309 and M409, no protease activity was measured for the empty control strain *B. licheniformis* M309 which lacked *pga*::BLAP present in *B. licheniformis* M409 (Figure 26). Thus, the protease activity determined for strains derived from *B. licheniformis* M409 correlates with expression of the BLAP model enzyme, while site reactivities from additional proteases usually found in the *Bacillus* secretome can be neglected. As shown in Figure 26, targeting either motility (M422 Δ*sigD*, M423 Δ*motB*, M435 Δ*hag*) or biofilm formation (M430 Δ*tasA*, M455 Δ*bslA*, M434 *remA* R18W P29S, M432 Δ*slrA*) caused only minor changes in protease activity compared to the parental strain *B. licheniformis* M409. The only exception was *B. licheniformis* M431 (Δ*epsA-O*) showing a 16.4 % higher protease expression. The specific protease activity of was even further enhanced for *B. licheniformis* M431 as biomass was lower compared to *B. licheniformis* M409.

Similarly, an increase in specific productivity was observed for the Δ*eps*, Δ*tasA* double mutant *B. licheniformis* M440, while global protease activity was comparable to the parental strain. The second single mutant characterized by improved productivity was the *degU32* strain *B. licheniformis* M436 showing 27.4 % higher protease activity. As *B. licheniformis* M436 also displayed strongly enhanced biofilm formation, construction of *degU32* strains paired with mutations preventing biofilm formation was a promising approach for further streamlining of the *B. licheniformis* expression host. The group of biofilm-deficient *degU32* strains comprises *B. licheniformis* M439 (Δ*tasA degU32*), M438 (Δ*eps degU32*), M441 (Δ*eps* Δ*tasA degU32*), M456 (Δ*eps* Δ*tasA degU32* Δ*bslA*), M451 (Δ*slrA degU32*) and M452 (*remA* R18W P29S, *degU32*). Surprisingly, all strains from this cluster showed a significant increase in protease expression under simulated fed-batch conditions (Figure 26). Compared to the parental strain, global protease activity increased by 47 to 67 %, while the increase in biomass normalized, specific activity is within the range of 23 to 58 %. More importantly, unlike in batch cultivations, BLAP expression was enhanced by 19 to 28 % compared to the *degU32* single mutant *B. licheniformis* M436. Finally, deletion of *bslA* did not improve productivity in the *degU32* strain.

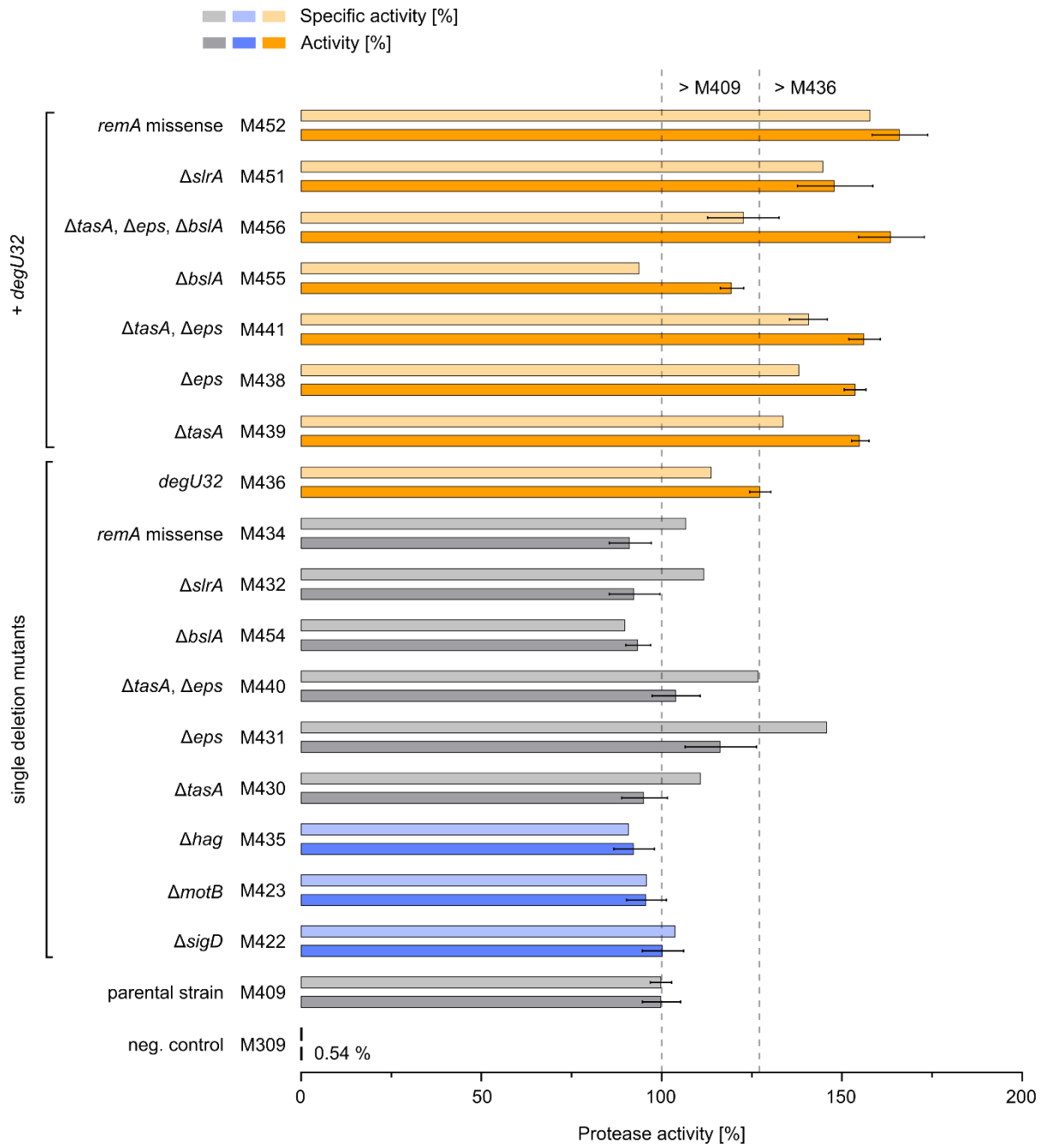

Figure 26: Protease activity of *B. licheniformis* strains in fed-batch cultivations. Protease activity was determined after 72 h of microtiter plate-based fed-batch cultivation using a N-Suc-AAPF-pNA based assay after. Relative and biomass-normalized specific protease activity is shown, both referring to the activity determined for the parental strain *B. licheniformis* M409. (Grey) *B. licheniformis* M409 and biofilm deficient strains. (Orange) Strains harboring the *degU32* mutation and (blue) motility deficient strains. Error bars indicate standard deviation of at least six biological replicates.

3.3.2.3 Increased productivity of biofilm deficient strains is specific for *degU32* but not *sigD*

The strong increase in protease expression of strains deficient in biofilm formation combined with the *degU32* allele raises the question whether this is a common feature resulting from simultaneous inactivation of biofilm formation and motility. Therefore, *B. licheniformis* M441 (Δ*tapA-sipW-tasA*, Δ*epsA-O*, *degU32*) was compared to *B. licheniformis* M447 (Δ*tapA-sipW-tasA*, Δ*epsA-O*, Δ*sigD*). Both strains are non-motile, resulting from the *degU32* allele or deletion of *sigD*, and display loss of ability to form biofilms (Section 3.1.3). Comparison of protease expression under microtiter plate-based fed-batch conditions revealed strong difference in the productivity for *B. licheniformis* M441 and M447 (Figure 27). While deletion the Δ*sigD* combinatorial mutant *B. licheniformis* M447 showed an increases in protease activity by 10 % compared to *B. licheniformis* M409, introduction of the *degU32* mutation in the Δ*tapA-sipW-tasA*, Δ*epsA-O* strain resulted in 55 % higher product formation (*B. licheniformis* M441, Figure 27A). Compared to the progenitor strain *B. licheniformis* M440, the protease titer did not significantly increase for *B. licheniformis* M447, but M441. Finally, no significant changes were observed upon additional deletion of *hag* or *sigD* (*B. licheniformis* M453 and M448) in the Δ*tapA-sipW-tasA*, Δ*epsA-O*, *degU32* strain *B. licheniformis* M441 (Figure 27).

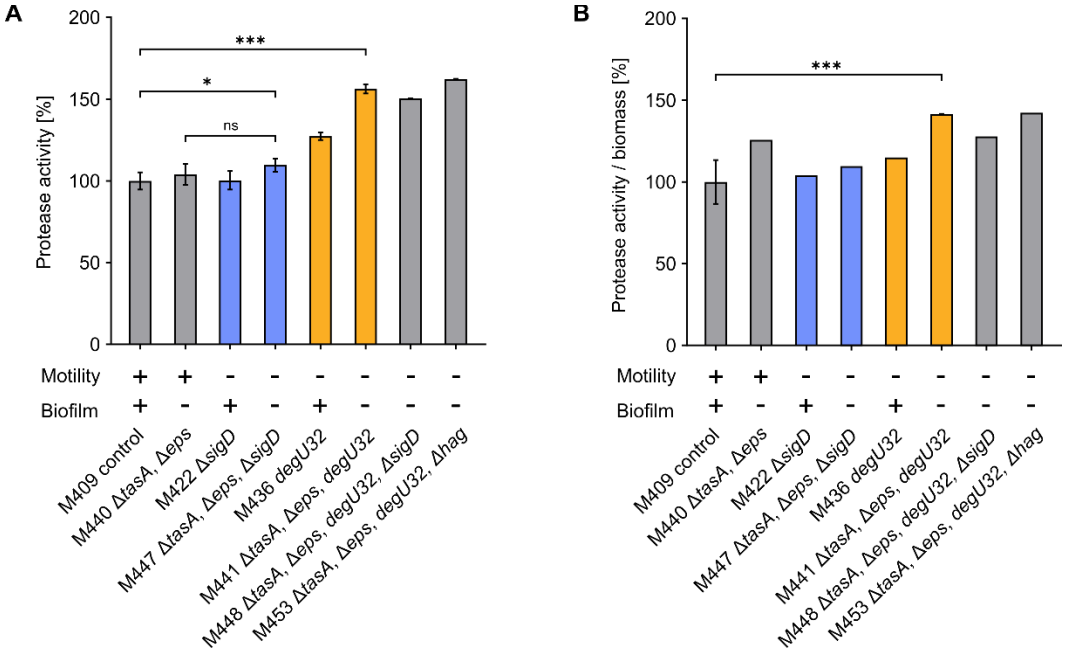

Figure 27: Productivity of biofilm and motility deficient strains regarding *degU32* or Δ*sigD* mutation. Samples are taken from microtiter plate-based fed-batch cultivation after 72 h. A) Relative protease activity from six biological replicates. B) Relative, specific protease activity calculated from the mean protease activity of six individual samples divided by the XX Asterisks indicate level of significance obtained from unpaired t-test with Welch's correction p-value (* < 0.05, ** < 0.01, *** < 0.001; ns = not significant).

3.3.2.4 Time resolved protease expression

To analyze the effect of *degU32* paired with biofilm deficiency in more detail, time resolved BLAP expression analysis was performed (Figure 28). Single mutants deficient in motility (Δ*sigD*, Δ*motB*, Δ*hag*; data not shown) or biofilm formation (*B. licheniformis* M430, M440) showed BLAP expression levels comparable to *B. licheniformis* M409 throughout fed-batch cultivation. Strikingly, strains harboring the *degU32* allele showed delayed expression of the model enzyme with 40 % lower protease activity after 24 h of cultivation. After 48 h no significant differences in protease activity were observed among all strains analyzed and, thus, *B. licheniformis* M436, M439 and M441 overcame the initial defect in product formation. Comparable to the increase in protease activity from 24 to 48 h, strains carrying the *degU32* allele continue to express BLAP, while protease activity only slightly increased for *B. licheniformis* M409 and M440. After 72 h 15 to 32 % higher protease activity was determined for *B. licheniformis* M436, M439 and M441 compared to the otherwise genotypically identical progenitor strains carrying the wildtype *degU* allele.

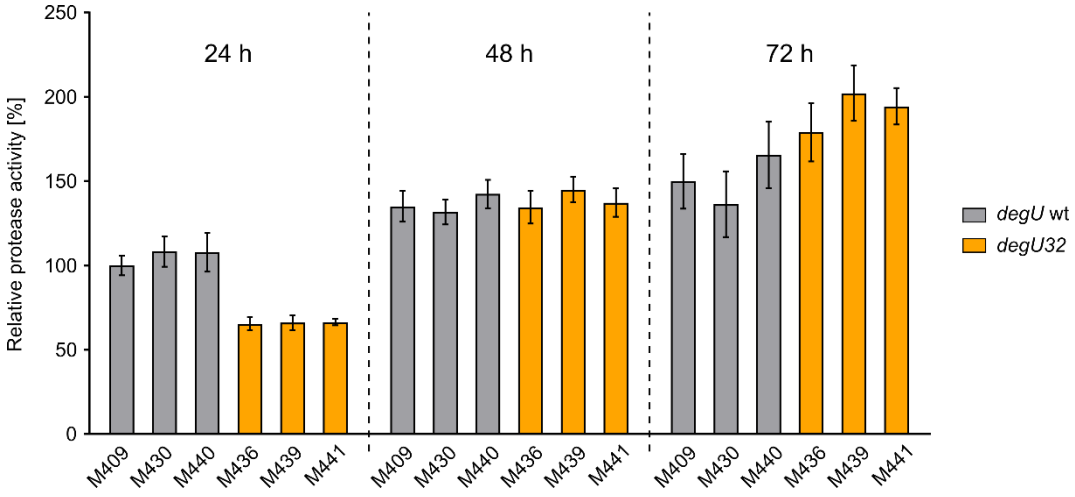

Figure 28: Time resolved protease expression. *B. licheniformis* strains harboring the wildtype *degU* (grey) or *degU32* allele (yellow) were analyzed in microtiter plate-based fed-batch cultivations. Protease expression was analyzed after 24, 48 and 72 h. Mean protease activity from six biological replicates is plotted as relative values compared to *B. licheniformis* M409 (24 h). Strains: M409 parental strain, M430 Δ*tasA*, M440 Δ*tasA* Δ*eps*, M436 *degU32*, M439 Δ*tasA degU32*, M441 Δ*tasA* Δ*eps degU32*

Expression of Apr, and likewise BLAP driven by a truncated fragment of the native *B. licheniformis* DSM641 *apr* promoter region, requires activation of two cellular pathways. First, repression of the *apr* promoter by ScoC, SinR and AbrB must be relieved through Spo0A-P. In addition, transcriptional activation by binding of DegU-P is required pathways (Veening *et al.* 2008a). To analyze whether transcription of *apr* (BLAP) was impaired due to insufficient activation of the P*apr* promoter, expression dynamics were analyzed in more detail by performing single cell (section 3.4.1).

3.4 Productivity at the single cell level

Global analysis revealed increased BLAP expression for *B. licheniformis* strains harboring the *degU32* allele in batch and fed-batch cultivations. In the fed-batch process, protease activity was further enhanced upon targeting biofilm formation int the *degU32* strain background. In contrast, protease activity was significantly lower during the early phase of the polymer-based fed-batch process (Section 3.3.2.4). To analyze *apr* expression dynamics in more detail, as well as to investigate the effect of strain modification on cellular heterogeneity, single cell analysis was performed. For this purpose, the truncated *apr* promoter fragment driving expression of BLAP was transcriptionally fused to *gfpmut2* encoding the *green fluorescent protein* GFPmut2 and integrated into the neutral *amyB* locus of *B. licheniformis* and selected mutant strains using plasmid pMA124. To prevent transcriptional read-through the reporter gene cassette was flanked by transcriptional terminators. Moreover, a promoter-less *gfpmut2* was cloned downstream of the strong ribosome binding site GATTAACTAATAAGGAGGACAAAC (Guiziou *et al.* 2016) and integrated into the *amyB* locus of *B. licheniformis* M308 using plasmid pJOE_*amyB*::G2r. As no GFP fluorescence was observed for the resulting control strain *B. licheniformis* M308::G2r, transcriptional readthrough into *amyB* does not occur (Figure S7).

3.4.1 Protease expression dynamics and heterogeneity during simulated fed-batch cultivations

To analyze the P_{apr} promoter activity under fed-batch conditions, feedplate cultivation was performed. The biofilm deficient *degU32* strain *B. licheniformis* M641 (Δ*tasA*, Δ*eps*, *degU32*) was compared to *B. licheniformis* M609.1 both carrying the *amyB*::P*apr-gfpmut2* reporter gene fusion. Samples were taken from 24 h on and analyzed by fluorescence microscopy (Figure 29; A, C, E) including quantification of GFP intensity at the single cell level to show the distribution of cells which have activated the P_{apr} promoter (Figure 29; B, D, F).

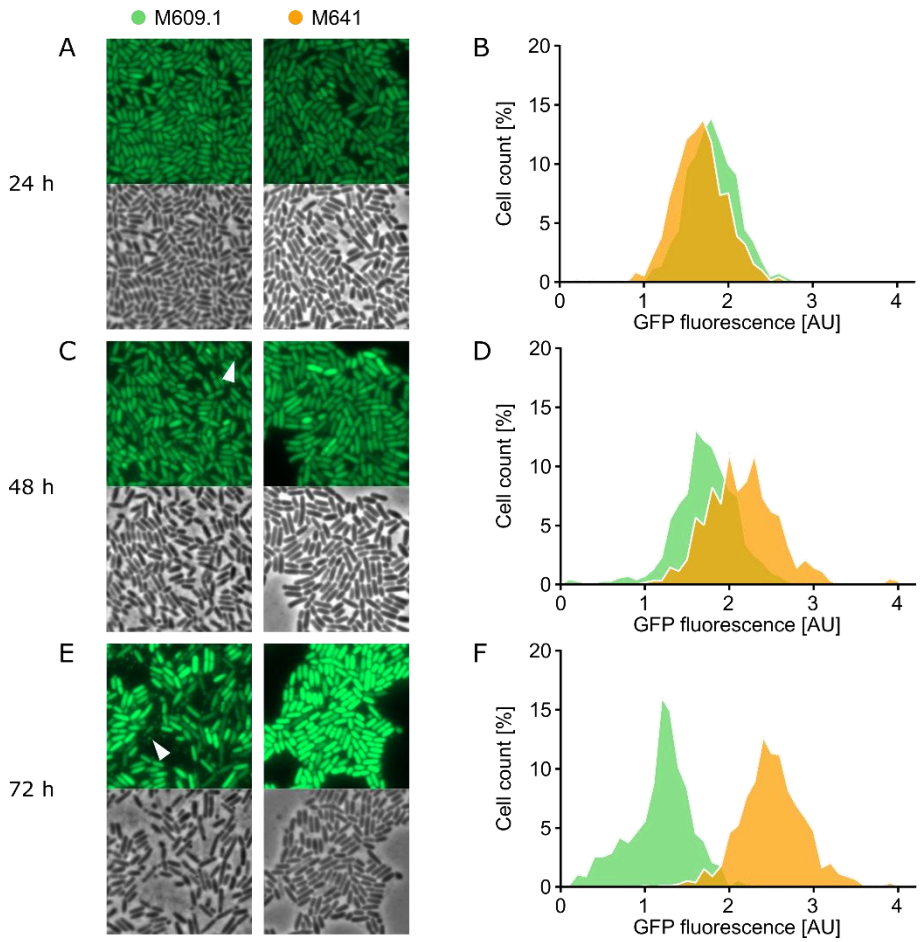

Figure 29: Protease expression dynamics and heterogeneity of *B. licheniformis* under microtiter plate-based fed-batch conditions. *B. licheniformis* M609.1 (Δ*rms*, Δ*apr*, Δ*sigF*, *pga*::BLAP, *amyB*::P*apr-gfpmut2*; green) and M641 (Δ*rms*, Δ*apr*, Δ*sigF*, *pga*::BLAP, Δ*tapA-sipW-tasA*, ΔepsA-O, *degU32*, *amyB*::P*apr-gfpmut2*; orange) were cultivated for 72 h in defined medium (V3FP) in feedplates. (A, C, E) GFP and phase contrast images of samples taken after (A) 24 h, (C) 48 h and (E) 72 h. P_{apr} promoter activity was determined by quantification of GFP fluorescence at the single cell level. GFP exposure time = 100 ms for image A, C and E, but 50 ms exposure time was used in images for quantification of samples taken after 72 h due to signal saturation (50 s images not shown). The white arrow marks noisy GFP background signals observed in samples of M609.1 from 48 h on. 600 to 800 individual cells were evaluated in ImageJ using the plugin ObjectJ. (B, D, F) Relative cell count resulting from binning of cells based on their GFP intensity (42 bins, bin width = 0.1).

Both, *B. licheniformis* M641 and the control strain *B. licheniformis* M609.1 showed P_{apr} dependent GFP expression throughout the full cultivation period and the vast majority of cells showed GFP fluorescence. In the initial fermentation phase (24 h, Figure 29A and C), GFP intensity and signal distribution was comparable between *B. licheniformis* M609.1 and M641, both showing a highly homogeneous expression pattern. However, the mean fluorescence intensity was slightly lower for *B. licheniformis* M641 (1.66 AU ± 0.31) compared to *B. licheniformis* M609.1 (1.81 AU ± 0.30). Samples analyzed after 48 h and 72 h revealed increasing cellular heterogeneity for *B. licheniformis* M609.1 at later fermentation stages, which was most pronounced after 60 h (data not shown) and 72 h of cultivation (Figure

29E and F). Higher heterogeneity was accompanied by a steady decrease in the mean fluorescence intensity to 1.19 AU ± 0.37 after 72 h. Unlike its parental strain, *B. licheniformis* M641 showed a constant increase in the mean GFP intensity and both strains are clearly distinguishable after 72 h (and 60 h). Moreover, signal distribution was homogeneous for *B. licheniformis* M641 in samples from later cultivation stages. In addition to differences in intracellular GFP intensity, an increasingly higher background fluorescence for *B. licheniformis* M609.1 became apparent from 48 h onwards. Notably, extracellular accumulation of GFP (or particles emitting light in the range of GFP) was frequently observed for *B. licheniformis* M609.1 (Figure 29C and E), while samples from *B. licheniformis* M641 showed only low background fluorescence. The higher background fluorescence was accompanied by accumulation of cell debris and more severe cell lysis for *B. licheniformis* M609.1 (Figure 29E).

The observations made are in strong contrast to previous results from *B. subtilis* and *B. licheniformis* DSM13 strains harboring the wildtype *degU* allele, in which DegU-P responsive promoters are only activated in a small subpopulation (Veening *et al.* 2008a; Borgmeier *et al.* 2012; Marlow *et al.* 2014a). Moreover, in case of these type strains homogeneous promoter activity at the single cell level was achieved only after introduction of the *degU32* mutation. These data may suggest, that the DegU-P auto stimulatory loop is intrinsically strong in *B. licheniformis* DSM641 as compared to the type strain DSM13 and other *B. subtilis* strains. Alternatively, differences in cultivation conditions or truncation of the P*apr* promoter fragment driving BLAP (and GFP) expression may account for higher homogeneity. To analyze the DegU-P dependent promoter activation in *B. licheniformis* M409, the P3 promoter fragment comprising the *degS-degU* intergenic and the DegS N-terminal coding region was transcriptionally fused to *mScarlet-I* encoding a red fluorescent protein. The P3*degU* promoter is activated by DegU-P and promotes DegU-P auto stimulation (Yasumura *et al.* 2008). The reporter gene fusion was chromosomally integrated into the *cat* locus using plasmid pMA137. The resulting strain *B. licheniformis* M809.1 and the otherwise isogenic P*apr* reporter strain *B. licheniformis* M609.1 were cultivated in feedplates and analyzed by fluorescence microscopy. Since homogeneous P*apr*-dependent GFP expression was observed in samples taken after 24 h (Figure 29A), we were interested in expression dynamics during earlier cultivation stages, in particular around 12 h marking the onset of the glucose-limited fed-batch process (see Figure 2A from Habicher *et al.* 2019). Moreover, to increase temporal resolution of the analysis, less stable fluorescence protein variants were included in the analysis. By fusing a N-terminal SsrA degradation tag to GFPmut2 (DAV tag) and mScarlet (ASV tag), higher turnover rates by ClpXP-dependent proteolysis are achieved (Guiziou *et al.* 2016). The SsrA-tag reporter gene fusions were integrated into *B. licheniformis* M409 using plasmid pMA109 and pMA138 resulting in *B. licheniformis* M609.2 (M409 *amyB*::P*aprE-gfpmut2*-DAV) and M809.2 (M409 *cat*::P*3degU-mScarletI*-ASV).

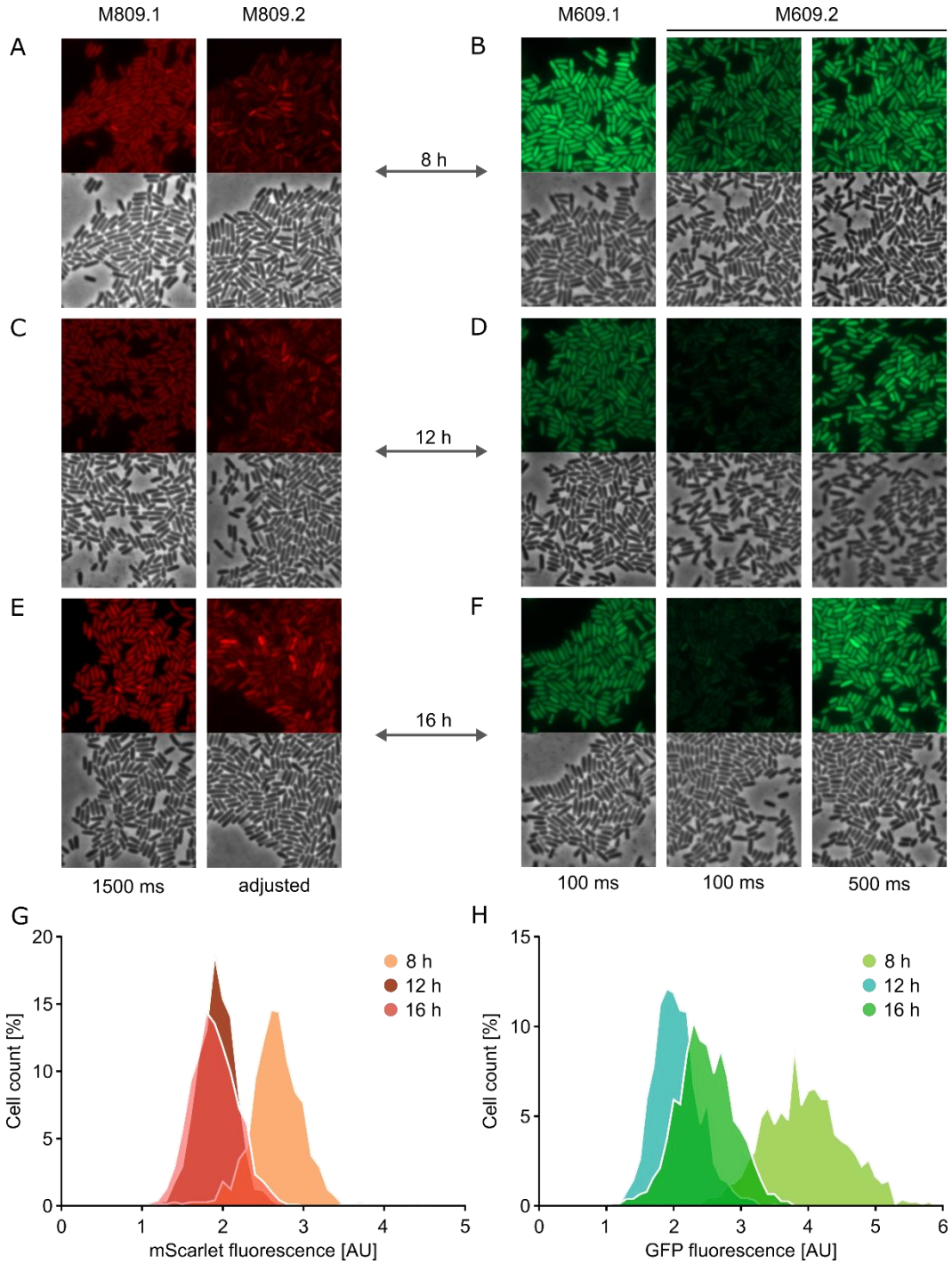

Figure 30: Expression pattern of the DegU-P dependent promoter P*apr* and P3*degU* during the initial phase of a glucose-limited fed-batch process. (A, C, E, G) P3*degU-mScarlet* reporter strains *B. licheniformis* M809.1 and M809.2 (with *ssrA* tag) and (B, D, F, H) P*apr-gfpmut2* strains M609.1 and M609.2 (with *ssrA* tag) were cultivated in defined medium (V3FP) in feedplates. Main cultures were inoculated with an initial OD_{600nm} of 0.9 ± 0.1 resulting in onset of the fed-batch phase after around 10 h of cultivation as described in Habicher *et al.* (2020). (A, C, E) mScarlet, (B, D, F) GFP and phase contrast images of samples taken after (A, B) 8 h, (C, D) 12 h and (E, F) 16 h. Exposure times for fluorescence channels are indicated below image E and F, with brightness adjusted for images M809.2 due to low signal intensity. Note, that the exposure time for M609.2 in 8 h sample was 300 ms instead of 500 ms. Promoter activity was determined by quantification of mScarlet and GFP fluorescence at the single cell level from strain M809.1 and M609.1. (G, H) Relative cell count resulting from binning of cells based on their

mScarlet and GFP intensity (bin width = 0.1). At least 700 individual cells were evaluated in ImageJ using the plugin ObjectJ.

Analysis of P*apr* and P3*degU* activity revealed homogeneous expression patterns for both DegU-P responsive promoters before (8 h; Figure 30A, B) and after (16 h; Figure 30E, F) onset of glucose starvation. Mean GFP and mScarlet signal intensities were highest after 8 h of cultivation and decreased afterwards (Figure 30 G, H). Fusion of C-terminal *ssrA* degradation tags to GFP and mScarlet resulted in lower signal intensities confirming higher turnover of both proteins. Consequently, adjustment of the brightness was required for images from *B. licheniformis* M809.2 allowing for qualitative analysis only. Heterogeneous signal distribution was more pronounced for reporter strains expressing unstable GFP (M609.2) and mScarlet (M809.2). The differences observed may result from true heterogeneous promoter activity, noise in the ClpXP system or differences in the metabolic capacity (e.g. protein synthesis) in general. In fact, noise in availability of cellular components was shown to affect signal output in particular when expression strength was low (Veening *et al.* 2008b; Cozy and Kearns 2010), suggesting that in case of *B. licheniformis* M609.2 and M809.2 where fluorescence protein levels are low, mScarlet and GFP levels are prone to cell specific fluctuations in the ClpXP system or components of the transcription and translation machinery.

The initially high fluorescence intensity under excess glucose conditions is surprising due to the known catabolite repression of protease expression in *B. licheniformis* and the closely related *B. subtilis* (Priest 1977; Hanlon *et al.* 1982; Frankena *et al.* 1986; Mao *et al.* 1992; Barbieri *et al.* 2016; Habicher *et al.* 2019b). The first 10 to 12 h of feedplate cultivation are characterized by excess glucose availability, with a glucose release rate from the polymer matrix higher than the glucose uptake rate (Habicher *et al.* 2019c). These conditions represent the batch phase with presumably high catabolite repression. However, the high initial inoculum (10 % v/v) from stationary pre-cultures in the feedplate cultivation protocol resulted in only two generation cycles before cells enter the fed-batch phase thereby minimizing the exponential growth phase (initial OD_{600nm} = 0.9 to 4.4 after 12 h). Consequently, cytoplasmic content including GFP, mScarlet and regulators of P*apr* and P3*degU* resulted in part from late stationary growth in the pre-culture and presumably caused a delay in the response to the glucose pulse during the initial batch phase. However, GFP expression dynamics in *B. licheniformis* M609.2 was comparable *B. licheniformis* M609.1 with only lower overall fluorescence intensity, and, thus *de novo* GFP (and mScarlet) synthesis during the first 8 h has occurred. After 12 h to 14 h, cells entered the fed-batch phase, characterized by reduced catabolite repression, which would explain the increase in P*apr* promoter activity between 12 h and 16 h (Figure 30H).

3.4.2 P*apr* expression dynamics and heterogeneity in batch cultures

Compared to the parental strain *B. licheniformis* M409, strains carrying the *degU32* mutation are characterized by a steady increase in protease expression and P*apr* dependent GFP expression, exceeding productivity of *B. licheniformis* M409 especially during late fermentation stages (Section 3.3.2.4 and 3.4.1). Moreover, single cell analysis during fed-batch cultivations indicated that the DegU-P autostimulatory loop is intrinsically strong in *B. licheniformis* DSM641. To analyze the underlying factors affecting P*apr* activity in more detail, batch cultivations were performed. Unlike in fed-batch cultivations, batch conditions are characterized by substrate inhibition, higher overflow metabolism and growth phase-dependent oxygen limitation all of them negatively affecting protease expression and possibly enhancing cellular heterogeneity (Hanlon *et al.* 1982; Jeude *et al.* 2006; Bähr *et al.* 2012; Ploss *et al.* 2016; Habicher *et al.* 2019b). Therefore, single cell analysis from batch cultures may provide further information on the robustness of strains in general, in particular in the context of cellular heterogeneity. P*apr* dependent GFP expression was determined in complex (LSJ-CT) and chemically defined (V3) medium at the population level using the on-line micro-bioreactor system BioLector. Based on the fluorescence intensity promoter activity was calculated ($\Delta GFP \times \Delta t^{-1}$). In addition, single cell analysis was performed by applying flow cytometry.

In addition to *B. licheniformis* M609.1 (M409 *amyB*::P*apr-gfpmut2*) and M641 (M409 Δ*tasA*, Δ*eps*, *degU32*, *amyB*::P*apr-gfpmut2*) *B. licheniformis* M639 (Δ*tasA*, *degU32*, *amyB*::P*apr-gfpmut2*) and *B. licheniformis* M648 (Δ*tasA*, Δ*eps*, *degU32*, Δ*sigD amyB*::P*apr-gfpmut2*) were included in the analyses to investigate potential effects resulting from deletion of *epsA-O* and *sigD*. Integration of the P*apr-gfpmut2* cassette into *B. licheniformis* M439 was performed by CRISPR/Cas9 using plasmid pMA124. Batch analysis of GFP reporter strains revealed strain and growth medium dependent differences in P*apr* expression strength and dynamics (Figure 31). No promoter activity was observed during exponential growth in both media tested (Figure 31A, B), indicating that the truncated P*apr* promoter underlies growth phase dependent regulation as described for native *apr* promoters in *B. subtilis* and *B. licheniformis* (Jacobs 1995). Entering stationary growth, P*apr* activity increased. Notably, in LSJ-CT medium GFP expression by *B. licheniformis* M639 (Δ*tasA*, *degU32*, *amyB*::P*apr-gfpmut2*) and M641 (Δ*tasA*, (Δ*eps*, *degU32*, *amyB*::P*apr-gfpmut2*) was observed 6 to 7 h early as compared to the reference strain *B. licheniformis* M609.1 (*amyB*::P*apr-gfpmut2*), while the corresponding growth curves were shifted by only 2 h. Moreover, GFP intensity for strains carrying the *degU32* mutation was superior to *B. licheniformis* M609.1 throughout the full cultivation period (Figure 31A). Analysis of the promoter activity showed highest activities after 18 h (M639, M641) and 22 h (M609.1) in the early stationary growth phase (Figure 31C). Subsequently, promoter activities declined before reaching a plateau and remaining constant throughout growth. Similar to the results from cultivation in complex medium, a

time shift was observed for growth and GFP synthesis in V3 medium. Differences in absolute GFP fluorescence were even more pronounced than in LSJ-CT and, notably, GFP intensities remained low for *B. licheniformis* M609.1 during stationary growth (Figure 31B). Highest promoter activity was determined in the late-stationary growth phase (Figure 31D). This was in strong contrast to *B. licheniformis* M639 and M641 which displayed higher promoter activities through the full cultivation period, temporally peaking during early stationary growth which is consistent with results from LSJ-CT cultures. It is important to note, that the onset of GFP expression or rather the increase in GFP fluorescence during late stationary growth coincided with the recovery of dissolved oxygen values (DOT; Figure 31E, F), which dropped dramatically during exponential growth.

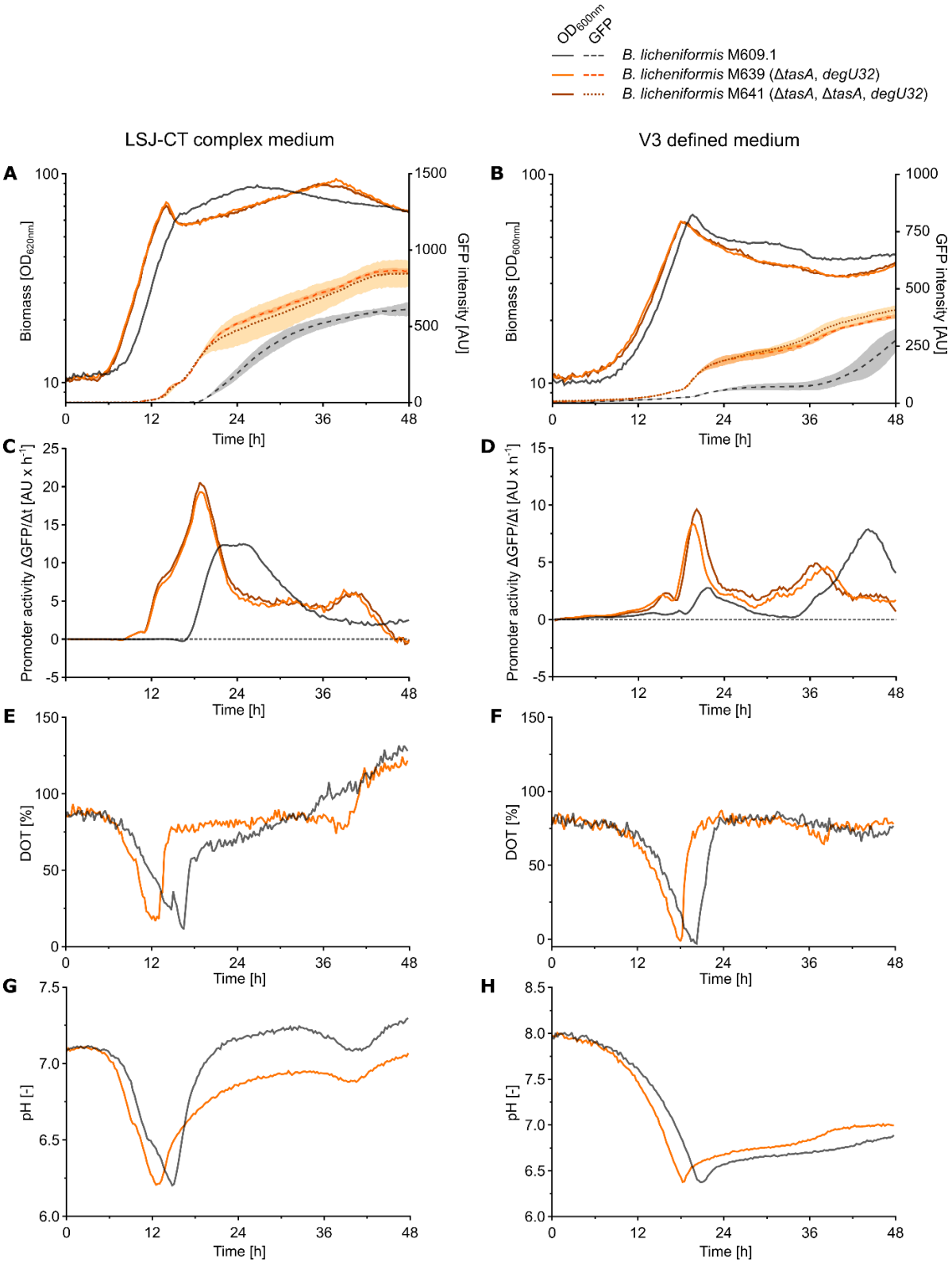

Figure 31: P*apr* promoter activity in *B. licheniformis degU32* strains in batch cultivations. Reporter strains carrying the *amyB*::P*apr-gfpmut2* reporter gene fusion were cultivated in (A, C, E, G) rich and (B, D, F, H) defined medium using the microbioreactor system BioLector (1000 rpm, 3 mm shaking diameter, 30 °C, 85 % relative humidity). Strain number and relevant genotype were as indicated. P*apr* promoter activity was determined throughout growth by measuring GFP fluorescence. (A, B) growth

(scattered light, OD_{600nm}) and GFP fluorescence are shown. pH (G, H) and DOT (E, F) profiles were derived from otherwise isogenic strains lacking reporter constructs as fluorescence-based determination of pH and DOT interfered with GFP signals. Growth between empty and reporter strains was comparable (compare Figure 21). Shaded areas indicate standard deviation from two biological replicates. (C, D) Promoter activity profiles were smoothened using GraphPad Prism 8 (12 neighbors, 2nd order). Note that *B. licheniformis* M648 (Δ*tasA*, Δ*eps*, *degU32*, Δ*sigD*) behaved identical to *B. licheniformis* M641 (Δ*tasA*, Δ*eps*, *degU32*) and is therefore not shown.

Investigation of P*apr* expression dynamics revealed higher activation of the protease promoter in strains carrying the *degU32* mutation. But promoter activity was analyzed at the population level, lacking information about cellular heterogeneity. To differentiate between either higher productivity of individual cells or a higher proportion of cells, which have activated the P*apr* promoter (or both), flow cytometry was performed (Figure 32). Samples were derived from offline cultivation in 48-well flower plates with cultivation parameters identical to previous BioLector experiments. Cells were harvested at selected time points during late-exponential, early and late stationary growth as well as the transition phase and approximately 50,000 events were analyzed by flow cytometry.

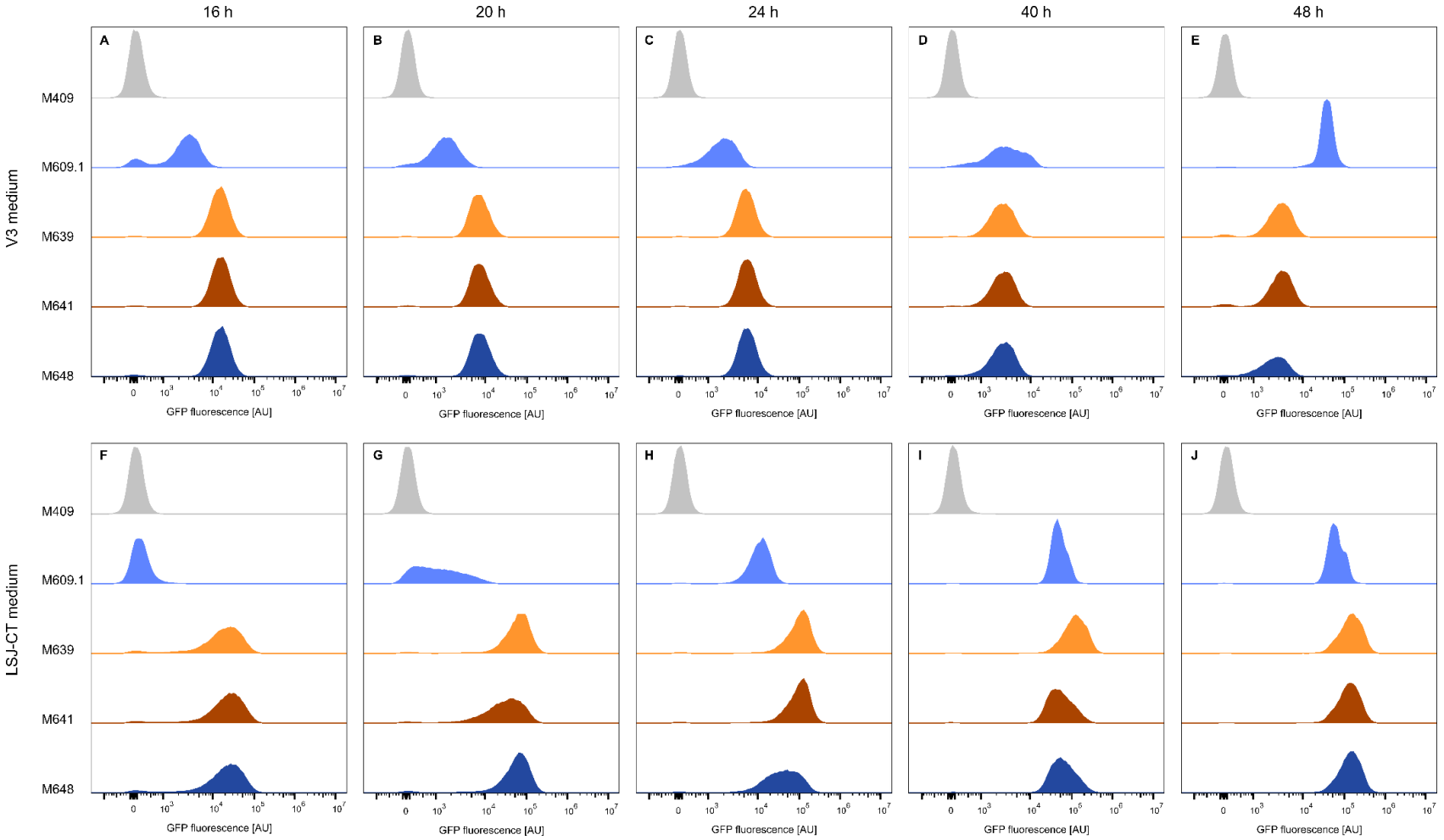

Figure 32: Protease promoter activity of *B. licheniformis degU32* strains under batch conditions. The *amyB::Papr-gfpmut2* reporter strains *B. licheniformis* M609.1 (light blue; parental strain), *B. licheniformis* M639 (orange; Δ*tasA, degU32*), *B. licheniformis* M641 (brown; Δ*tasA,* Δ*eps, degU32*) and *B. licheniformis* M648 (dark blue; Δ*tasA,* Δ*eps, degU32*, Δ*sigD*) and the negative control *B. licheniformis* M409 (grey) were cultivated in V3 chemically defined (A,B,C,D,E) and LSJ-CT complex (F,G,H,I,J) medium. Samples from (A, F) late-exponential, (B, G) transition state, (C, H) early stationary and (D, E, I, J) stationary growth were analyzed by flow cytometry. Approximately 50,000 events were analyzed.

As in fed-batch cultivations, P*apr* expression was highly homogeneous for *B. licheniformis* M639 and M641 harboring the *degU32* mutation, except for a marginal number of cells after 48 h in V3 (Figure 32E). In contrast to *degU32* mutants, a bimodal expression pattern was observed for the parental strain *B. licheniformis* M609.1 after 16 h of growth in V3 batch cultures resulting in a more homogeneous distribution after 24 h with most cells showing low to medium promoter activity. This is consistent with the small increase in GFP fluorescence between 20 and 24 h at the population level and the subsequent constant GFP intensity (Figure 31B). At 48 h, the mean fluorescence intensity of *B. licheniformis* M609.1 exceeded those from *degU32* strains, which in part resulted from a decrease in the GFP intensity of *B. licheniformis* M639, M641 and M648. Note, that *B. licheniformis* M648, differing from *B. licheniformis* M641 by additionally lacking *sigD*, behaved identical to *B. licheniformis* M639 and M641, which is in line with epistasis of *degU32* over Δ*sigD* (Figure 11; Mäder *et al.* 2002; Mukherjee and Kearns 2014). In LSJ-CT, fluorescence intensity remained high for *degU32* strains, and was superior to *B. licheniformis* M609.1 throughout the full cultivation. Moreover, single cell analysis confirmed early activation of the *apr* promoter in *degU32* strains, while no GFP expression was detected for *B. licheniformis* M609.1 after 16 h (Figure 32F). In case of the parental strain, homogeneous distribution of P*apr* positive cells was observed in the early stationary phase after 24 h, with highly heterogeneous GFP expression during the transition state (20 h; Figure 32G).

3.4.3 Analysis of the effect of P*apr* promoter variants on cellular heterogeneity

The experiments described in section 3.4.3 and 3.4.4 were conducted together with Maximilian Hilkmann within his master thesis project.

Expression of *aprE* in *B. subtilis* and *apr* in *B. licheniformis* is controlled by several global regulators namely DegU-P, SinR, ScoC, AbrB, CodY and Spo0A-P (Perego *et al.* 1988; Strauch *et al.* 1989; Shafikhani *et al.* 2002; Zhou *et al.* 2020a). The P*apr* promoter used to drive expression of BLAP in *B. licheniformis* M409 and strains derived thereof was a truncated version comprising a 227 bp fragment upstream of the translational start codon. The same promoter was used to analyze productivity at the single cell level in *B. licheniformis* M609.1 showing high homogeneity in P*apr* activity. To analyze whether the promoter truncation contributed to increased homogeneity, *B. licheniformis* M609.3 was constructed carrying *gfpmut2* under transcriptional control of the full length *apr* promoter region from *B. licheniformis* DSM641 (375 bp fragment; P*apr* (DSM641 fl.)). Moreover, the *B. licheniformis* DSM13 full length *apr* promoter region (374 bp P*apr* (DSM13 fl.)) was tested in *B. licheniformis* M409 resulting in strain *B. licheniformis* M609.5. Both promoters differ by 21 bp. *B. licheniformis* M609.3 and M609.5 were constructed by integration of the promoter reporter gene fusion into the *amyB* locus of *B. licheniformis* M409 using plasmid pMA149 and pMA147 respectively. The reporter strains were cultivated using the

microtiter plate-based fed-batch process. The initial OD_{600nm} was set to 0.9 ± 0.1 resulting in onset of the fed-batch phase after around 10 h as described in Habicher *et al.* (2020). To monitor P*apr* activity during this cultivation stage, which supposedly shows highest differences in single distribution due to growth phase dependent regulation of *apr*/*aprE* expression, sample after 8, 12 and 16 h of cultivation were analyzed by fluorescence microscopy (Figure 33 A, C, E). The distribution of cells depending on their mean GFP signal intensity is shown in Figure 33 (B, D, F).

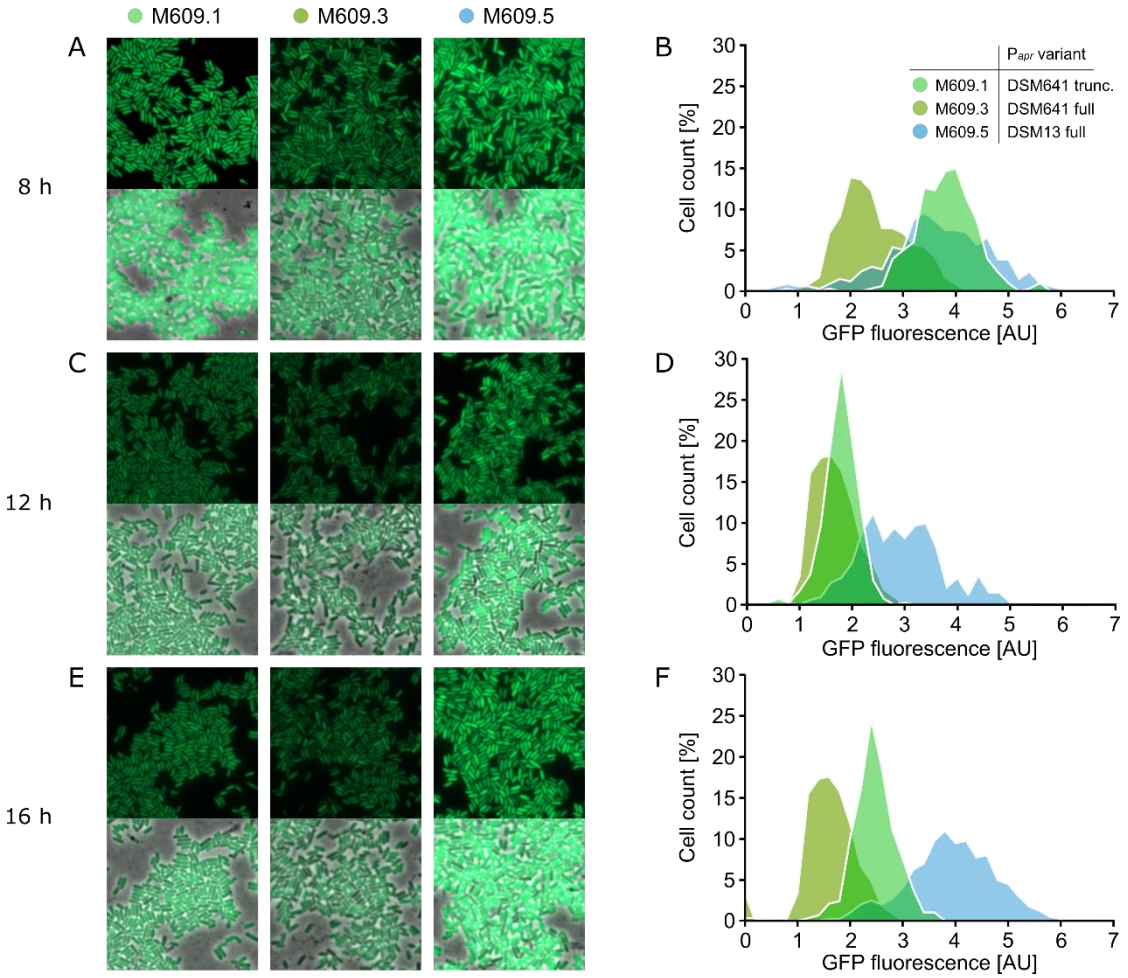

Figure 33: Promoter activity of different P*apr* variants in *B. licheniformis* under microtiter plate-based fed-batch conditions. *B. licheniformis* M609.1 (M409 *amyB*::P*apr*(DSM641 trunc.)-*gfpmut2*; green), M609.3 (M409 *amyB*::P*apr*(DSM641 full)-*gfpmut2*; olive) and M609.5 (M409 *amyB*::P*apr*(DSM13 full)-*gfpmut2*; blue) were cultivated in defined medium (V3FP) in feedplate. Main cultures were inoculated with an initial OD_{600nm} of 0.9 ± 0.1 resulting in onset of the fed-batch phase after around 10 h of cultivation as described in Habicher *et al.* (2020). (A, C, E) GFP channel and overlays of GFP and phase contrast images of samples taken after (A) 8 h, (C) 12 h and (E) 16 h are shown. P_{apr} promoter activity was determined by quantification of GFP fluorescence at the single cell level. GFP channel exposure time = 100 ms. At least 200 individual cells were evaluated in ImageJ using the plugin ObjectJ. (B, D, F) Relative cell count resulting from binning of cells based on their GFP intensity (33 bins, bin width = 0.2).

As shown in Figure 33 (A and B), *B. licheniformis* M609.1, M609.3 and M609.5 showed P*apr* dependent GFP expression already after 8 h and the vast majority of cells showed GFP fluorescence at 8, 12 and 16 h of cultivation. However, differences were observed in the fluorescence intensity and signal homogeneity depending on the P*apr* promoter and the cultivation phase. The fluorescence intensity was comparable between *B. licheniformis* M609.1 (P*apr* DSM641 trunc.; median FI = 3.8 AU) and M609.5 (P*apr* DSM13 full; median FI = 3.6 AU) in samples taken after 8 h of cultivation. In contrast, *B. licheniformis* M609.3 (P*apr* DSM641 full) showed almost 40 % lower GFP expression (median FI = 2.3 AU). The fluorescence intensity of *B. licheniformis* M609.5 remained high and clearly exceeded the values determined for *B. licheniformis* M609.1 and M609.3 after 12 and 16 h (Figure 33 C to F). The differences in GFP intensity resulted from a drop from 8 to 12 h, which was observed for all three strains but less pronounced in case of *B. licheniformis* M609.5. The median of the fluorescence intensity at 12 h was 2.9 for *B. licheniformis* M609.5 compared to 2.0 for *B. licheniformis* M609.1 and M609.3 (Figure 33 C, D). Over 50 % of all *B. licheniformis* M609.5 cells showed a higher GFP intensity than the maximum values determined for *B. licheniformis* M609.1 and M609.3. After 16 h of cultivation, the GFP intensity increased for *B. licheniformis* M609.1 (median FI = 2.5 AU) and M609.5 (median FI = 4.0 AU) but remained constant for *B. licheniformis* M609.3 (Figure 33 E, F). While the signal intensity was highest for *B. licheniformis* M609.5 throughout all samples analyzed, *B. licheniformis* M609.1 and M609.3 showed a higher signal homogeneity (i.e. lower heterogeneity) in GFP expression. However, activation of P*apr* was observed for the vast majority of cells independent from the promoter fragment used, which is in contrast to data from literature. Thus, truncation of P*apr* contributes to the GFP expression pattern, but is not the primary cause for the strong homogeneity observed. To further investigate the homogeneous P*apr* activity in *B. licheniformis* M409, two different *B. licheniformis* strains were compared regarding P*apr* activity as described in the following section.

3.4.4 Comparison of cellular heterogeneity in P*apr* activity in *B. licheniformis* DSM13 and DSM641

To analyze the effect of different strain backgrounds on P*apr* promoter activity, *B. licheniformis* M609.5 was compared to the corresponding reporter strain derived from the type strain *B. licheniformis* DSM13. Therefore, the P*apr(*DSM13 full)-*gfpmut2* expression cassette was integrated into the *amyS* locus of the methylase-deficient *B. lichenformis* DSM13 derivative MW3 using plasmid pMA147. The resulting strain was named *B. lichenformis* MH1. Both strains were cultivated and analyzed as described in the previous section (3.4.3). The results from fluorescence microscopy and the frequency distribution of cells depending on their mean GFP signal intensity are shown in Figure 34.

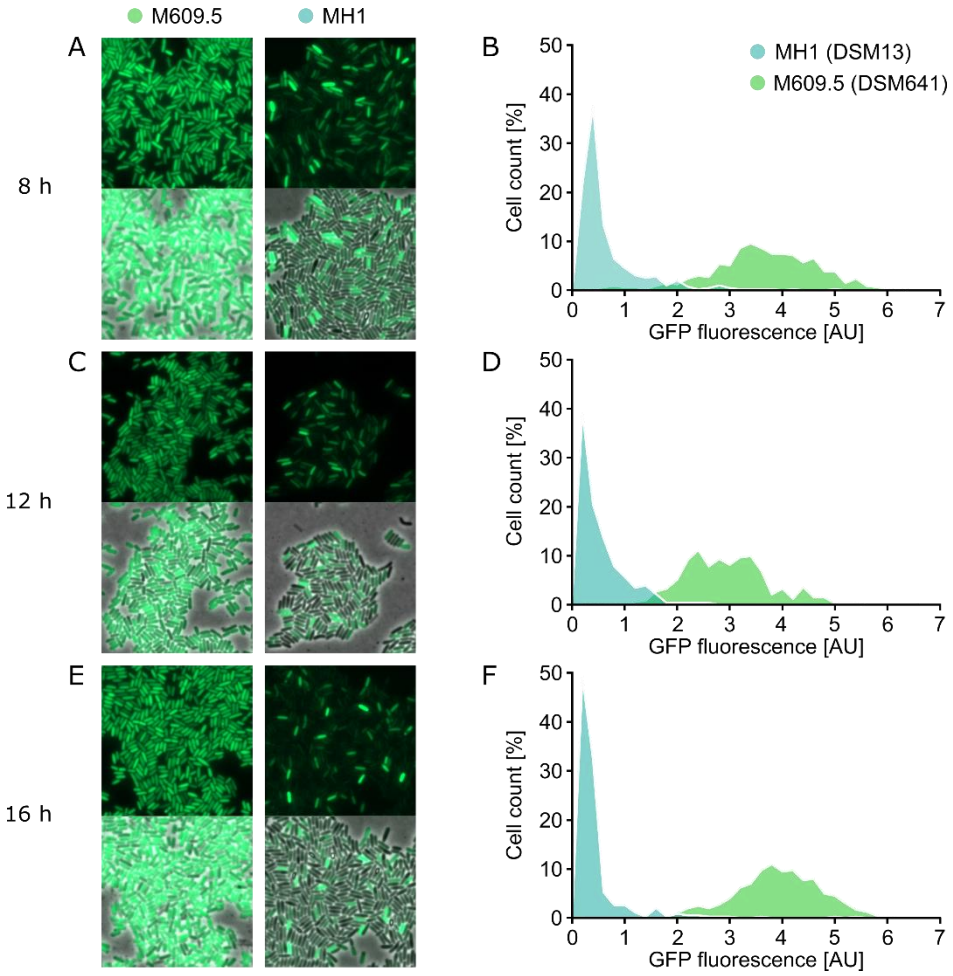

Figure 34: Comparison of P*apr* promoter activity in *B. lichenformis* DSM641 (M609.5) and DSM13 (MH1) in microtiter plate-based fed-batch cultivation. *B. licheniformis* M609.5 (M409 *amyB*::P*apr*(DSM13 full)-*gfpmut2*; green) and MH1 (MW3 *amyB*::P*apr*(DSM13 full)-*gfpmut2*; cyan) were cultivated in feedplates as described in the caption of Figure 33. (A, C, E) GFP channel and overlays of GFP and phase contrast images of samples taken after (A) 8 h, (C) 12 h and (E) 16 h are shown. P_{apr} promoter activity was determined by quantification of GFP fluorescence at the single cell level. Note: The GFP channel exposure time was 100 ms for M609.5 and 500 ms for MH1. At least 200 individual cells were evaluated in ImageJ using the plugin ObjectJ. White arrows mark endospores observed for MH1. (B, D, F) Relative cell count resulting from binning of cells based on their GFP intensity (33 bins, bin width = 0.2).

Analysis of P*apr* promoter activity in *B. licheniformis* M609.5 and MH1 (DSM13 derivative) revealed strong differences in *apr* expression at the single level between both strains. In particular, the number of cells showing GFP expression is much lower for *B. licheniformis* MH1 than for M609.5 throughout the full cultivation period (Figure 34). Whereas the majority of *B. licheniformis* M609.5 cells have activated the P*apr* promoter, only 2 % of *B. licheniformis* MH1 cells showed high GFP expression levels (FI > 3.0 AU). This pattern did not change significantly over time. Note that the exposure time for GFP channel images is five times higher for *B. licheniformis* MH1 (500 ms) than for *B. licheniformis* M609.5 (100 ms) limiting direct comparison of FI values. However, the required higher exposure time for *B.*

licheniformis MH1 underline the strong difference between both strains. In summary, although many cells of *B. licheniformis* MH1 showed GFP expression to very limited extend (Figure 34 A, C, E), the *B. licheniformis* DSM13 derived strain showed a bimodal expression pattern with a minority of that have activated the P*apr*(DSM13 full) promoter. In contrast, *B. licheniformis* M609.5 was not characterized by bimodal GFP expression and showed strong GFP expression for most cells.

3.5 Characterization of the extracellular proteome

To gain further insights into the host cell physiology, the extracellular proteome of selected *B. licheniformis* strains was analyzed by one-dimensional SDS-PAGE and subsequent mass spectrometry (Figure 35 A-D). In addition to acquisition of nutrients, secreted proteins are crucial for cell-to-cell communication, intra- and interspecies competition, detoxification of the environment, cell wall metabolism, motility, chemotaxis, and biofilm formation among others (Tjalsma *et al.* 2004a). As most of these processes affect neighboring cells, the physiological response resulting from changes in the extracellular proteome strongly depends on population density. Considering the high cell density in industrial fermentation processes, extracellular proteomics provides valuable information on the host strain physiology.

Due to the highly similar band pattern observed in the analysis of supernatant by SDS-PAGE (Figure 35 A, B), the extracellular proteome was characterized for selected strains only. In addition to *B. licheniformis* M409 (Δ*rms*, Δ*apr*, Δ*sigF*, *pga*::BLAP), the progenitor strains *B. licheniformis* M321 (Δ*rms*, Δ*pga*, Δ*apr*) and *B. licheniformis* M309 (Δ*rms*, Δ*pga*, Δ*apr*, Δ*sigF*) were included to analyze the effect of the Δ*sigF* mutation and integration of the BLAP expression cassette into the host genome. Equal volumes of supernatant were loaded to the gel allowing for estimation of protein abundance. Comparison of *B. licheniformis* M321 (Δ*rms*, Δ*pga*, Δ*apr*) and *B. licheniformis* M309 (Δ*rms*, Δ*pga*, Δ*apr*, Δ*sigF*) showed that deletion of *sigF* encoding the early-sporulation sigma factor SigF resulted in higher intensity of most protein bands while only minor changes in the band pattern were observed. In particular, deletion of *sigF* resulted in one additional protein band below the 66 kDa marker band identified as a fragment of the extracellular bacillopeptidase F (Bpr). Full length Bpr has a molecular weight of 154.9 kDa. Moreover, the intensity of the low-molecular weight band containing the bacteriocin ForD (BL00275, 14.1 kDa) increased more significantly than other protein bands identified in the secretome of *B. licheniformis* M309. Integration of the BLAP expression cassette into *B. licheniformis* M409 resulted in a prominent band below the 29 kDa reference band identified as BLAP. BLAP was also found in a faint protein band above the 29 kDa marker. Integration of BLAP decreases the intensity of selected protein bands as compared to *B. licheniformis* M309, albeit to limited extend.

B. licheniformis M409 derived-strains carrying the wildtype *degU* allele showed a similar pattern regarding the molecular weight and intensity of protein bands independent from mutations in genes required for biofilm formation or motility (*B. licheniformis* M422 to M434, Figure 35A,B). Therefore, the extracellular proteome of *B. licheniformis* M309 and M409 was considered representative for this group of strains (*B. licheniformis* M409 to M434; Figure 35 A and B). More significant changes were observed for strains carrying the *degU32* allele, but again further mutations in the *degU32* background did not affect the size or intensity of the vast majority of protein bands visualized by SDS PAGE (*B. licheniformis* M436 to M452, Figure 35 B). Thus, the extracellular proteome of *B. licheniformis* M436 (M409 *degU32*) and *B. licheniformis* M439 (M409 Δ*tapA-sipW-tasA*, *degU32*) was considered representative for *degU32* strains.

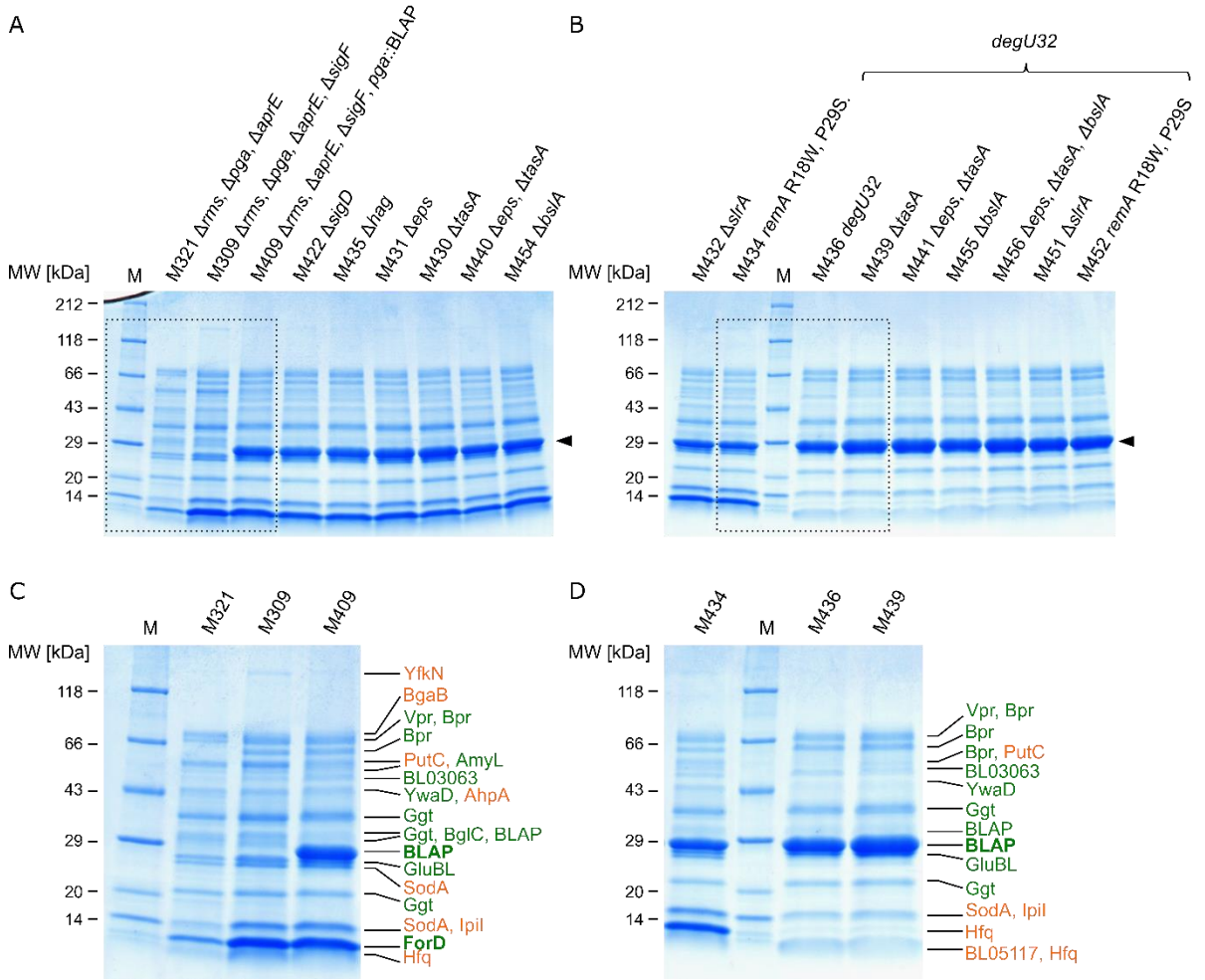

Figure 35: Characterization of the extracellular proteome of selected *B. licheniformis* strains under simulated fed-batch conditions. Biomass was separated from the culture broth by sterile filtration after 72 h of microtiter plate-based fed-batch cultivation following TCA precipitation of proteins in the

supernatant and sample preparation as described in section 7.4.2. A) and B) Proteins were separated by SDS-PAGE using a 4 - 20 % polyacrylamide Tris-Glycine gel. The extracellular proteome was characterized for C) the control strains *B. licheniformis* M309, M409 and D) the *degU32* mutants *B. licheniformis* M436 (*degU32*), M439 (Δ*tapA-sipW-tasA*, *degU32*) by MALDI-TOF. The identified extracellular (green) and cytoplasmic (orange) proteins are indicated next to the corresponding protein band. C) and D) represent closeups of the section indicated by the dotted line in A) and B) respectively. A full list of the proteins identified is shown in the supplemental material (section 6.1.11). The genotype for all strains is shown in A) and B). As *B. licheniformis* M422 to M452 are derived from *B. licheniformis* M409, only the key mutation introduced in these strains is indicated.

The secretome of *B. licheniformis* M309 and M409 comprises several peptidases. In fact, six out of nine proteins, that are known or predicted to be secreted, have proteolytic activity (Figure 35 C, highlighted in green). This includes the extracellular serine protease Vpr (85.6 kDa), the bacillopeptidase F Bpr (154.9 kDa), a putative carboxypeptidase (BL03063, 60.6 kDa), the aminopeptidases YwaD (48.2 kDa), the gamma-glutamyltranspeptidase Ggt (60.9 kDa) and the glutamyl endopeptidase GluBL (33.6 kDa). Secreted proteins not belonging to peptidases are the endo-1,4-beta-glucanase BglC (58.7 kDa), the alpha-amylase AmyL (58.5 kDa) and the bacteriocin ForD (BL00275, 14.1 kDa). While these proteins are known or predicted to be secreted in *B. licheniformis*, several cytoplasmic proteins were detected as well. The cytoplasmic proteins identified in the supernatant of *B. licheniformis* M309 and M409 were the phosphodiesterase YfkN (155.6 kDa), the beta-galactosidase BgaB (79 kDa), the 1-pyrroline-5-carboxylate dehydrogenase PutC (YcgN, 56.6 kDa), the hydroperoxide reductase AhpA (YkuU, 20.4 kDa), the superoxide dismutase SodA (22.5 kDa), the intracellular proteinase inhibitor Ipi (13.9 kDa) and the RNA chaperone Hfq (8.4 kDa) (Figure 35 C, highlighted in orange).

In *B. licheniformis* M436 (M409 *degU32*), the BLAP protein band has a higher intensity compared to strains carrying the *degU* wildtype allele (Figure 35 B and D). Except for *B. licheniformis* M455 (M409 *degU32*, Δ*bslA*), the intensity of BLAP is further enhanced in biofilm deficient *degU32* mutants (*B. licheniformis* M439, M441, M456, M451, M452). Most significant differences between wildtype *degU* and *degU32* strain were observed in the loss of high molecular weight protein bands (around 66 kDa) and loss of ForD (below 14 kDa) identified only in *degU* wildtype strains. In addition, BglC was not found in the secretome of *B. licheniformis* M436 and *B. licheniformis* M439. Finally, the number of cytoplasmic proteins was reduced in *degU32* single and combinatorial mutants (Figure 35 D) compared to the control strains *B. licheniformis* M309 and M409. The beta-galactosidase BgaB, the hydroperoxide reductase AhpA and the phosphodiesterase YfkN were not detected in *B. licheniformis* M436 and M439. But, for YfkN the band intensity already decreased when integrating the BLAP expression cassette as comparison of *B. licheniformis* M309 and M409 showed (Figure 35 C). The 1-pyrroline-5-carboxylate dehydrogenase PutC was identified in *B. licheniformis* M436 and M439 as for the control strains, but the corresponding protein band had a lower intensity. Similarly, the superoxide dismutase SodA was

less frequently found in the extracellular proteome of *B. licheniformis* M436 and M439. Only one protein identified in *B. licheniformis* M436 and M439 was absent from the samples of the control strains. The low molecular weight band migrating below the 14 kDa reference band included the protein of unknown function BL05117 (12.7 kDa).

In summary, the most significant changes in the extracellular proteome of the analyzed strains resulted from introduction of the *degU32* mutation. Strikingly, the bacteriocin ForD is absent from the secretome of *B. licheniformis* M436 and M439 both carrying the *degU32* allele, while ForD represents the most abundant protein in the extracellular proteome of *B. licheniformis* M409. Moreover, higher intensity of the BLAP protease was shown for *B. licheniformis* M436 and M439 accompanied by a lower number of cytoplasmic proteins.

4 Discussion

The aim of this thesis was to analyze and reduce cell heterogeneity in the context of strain optimization of *B. licheniformis* DSM641. Although not fully understood, differentiation of subpopulations is well characterized in the closely related *B. subtilis* enabling knowledge-based approaches in strain optimization. However, species and strain-dependent differences in the regulatory network governing cellular heterogeneity were reported and strain design 'from scratch' is still limited. Consequently, systematic analysis of potential gene targets for strain optimization is required. The strategies applied in this thesis included the deletion of genes encoding structural components of the biofilm matrix and the flagellar apparatus and those directly involved in their biosynthesis. Moreover, by modifying central regulators, cell differentiation was targeted at the initiation step of the corresponding developmental program thereby preventing cell heterogeneity on a global level.

4.1 Single target evaluation to prevent motility and biofilm formation in *B. licheniformis*

To evaluate potential targets for strain optimization in the context of cellular heterogeneity, the effect of individual gene deletions on biofilm formation and motility was analyzed. Subsequently, promising mutations were combined to construct strains deficient in both cellular adaptation mechanisms. Loss of swimming motility in *B. licheniformis* DSM641 was achieved by deletion of *hag*, *motB* and *sigD*, encoding the major flagellar protein flagellin (Hag), the proton channel MotB and the motility-specific sigma factor SigD respectively. Consequently, the corresponding mutant strains *B. licheniformis* M314/M435, M313/M423 and M312/M422 either do not synthesize flagellar or do not generate torque that drives flagellar rotation or lack both functions (Shioi *et al.* 1978; Mirel and Chamberlin 1989; Serizawa *et al.* 2004; Ito *et al.* 2005; Chen *et al.* 2009; Mukherjee and Kearns 2014). In addition to deletion of *sigD*, *motB* and *hag*, allelic exchange of the native *degU* coding region by *degU32* resulted in loss of motility in *B. licheniformis*, which is consistent with previous reports on *B. subtilis* and *B. licheniformis* (Msadek *et al.* 1990; Borgmeier *et al.* 2012). Compared to deletion of *hag* or *motB*, inactivation of *sigD* was presumed to have the most global impact on host cell physiology as the SigD regulon comprises over 150 genes related to motility, chemotaxis and autolysis (Helmann *et al.* 1988; Mirel and Chamberlin 1989; Márquez *et al.* 1990; Serizawa *et al.* 2004). But, recent findings from *B. subtilis* point towards a more global effect even when mutating early and late flagellar structural genes including *hag* and *motB*. While the detailed mechanism remains unclear, several studies on *B. subtilis* demonstrated a feedback mechanism, in which assembly of the flagellar apparatus as well as flagellar rotation is coupled to phosphorylation of DegU (Cairns *et al.* 2013; Chan *et al.* 2014; Diethmaier *et al.* 2017; Hölscher *et al.* 2018). DegU-P in turn promotes expression of the anti-SigD factor

FlgM, which sequesters SigD (Caramori *et al.* 1996; Bertero *et al.* 1999; Hsueh *et al.* 2011). Thus, by indirectly quenching intracellular levels of SigD, DegU-P prevents the sigma factor from initiating positive feedback regulation required to develop a motile, chemotactic state (Tokunaga *et al.* 1994; Allmansberger 1997; Estacio *et al.* 1998; West *et al.* 2000; Calvio *et al.* 2008; Cozy and Kearns 2010; Cozy *et al.* 2012; Mordini *et al.* 2013; Mukherjee and Kearns 2014). The highly similar phenotype of *B. licheniformis* Δ*hag*, Δ*motB* and Δ*sigD* mutants suggests a similar regulatory feedback loop in *B. licheniformis* coupling assembly of the flagellar apparatus to expression of SigD and the SigD regulon. In fact, cell lysis in *B. licheniformis* M314 (Δ*hag*) and M313 (Δ*motB*) was almost identical to *B. licheniformis* M312 (Δ*sigD*), indicating reduced expression of SigD-dependent autolysins LytC, LytD and LytF in all three strains. Consistent with this feedback mechanism involving DegU-P, cell lysis of the *degU32* mutant *B. licheniformis* M320 was comparable to *B. licheniformis* M312, M313 and M314. Moreover, the corresponding BLAP expression strains *B. licheniformis* M422, M423 and M435 displayed similar growth behavior and protease expression. As activation of the P*apr* promoter driving BLAP expression depends on DegU-P, the latter indicates comparable levels of DegU-P in Δ*hag*, Δ*motB* and Δ*sigD* mutants further confirming the hypothesized feedback mechanism. However, it remains to be clarified to which extend expression of the SigD-regulon is affected in strains deficient for *hag* or *motB*, as activation of P*hag* in *B. subtilis* Δ*hag* mutants was recently reported demonstrating functional expression of SigD in the *hag* deficient *B. subtilis* strain (Kampf *et al.* 2018; Steinberg *et al.* 2020). In addition to DegU-P dependent expression of *flgM*, the non-motile phenotype of the *degU32* mutants *B. licheniformis* M320 and M436 can be explained by a more direct role of DegU-P in regulating motility. Depending on its degree of phosphorylation, DegU is considered to regulate different cellular processes including natural genetic competence, motility, biofilm formation and secretion of exoenzymes (Kobayashi 2007b; Verhamme *et al.* 2007). The level of DegU-P required to initiate the corresponding developmental program increases from the first to the latter. While low levels of DegU-P promote expression of the *fla*/*che* operon, high levels of the response regulator inhibit motility at the transcriptional and the post-transcriptional level (Tokunaga *et al.* 1994; Msadek 1999; Mäder *et al.* 2002; Amati *et al.* 2004; Kobayashi 2007b; Verhamme *et al.* 2007; Hsueh *et al.* 2011). However, this gradual schema is complicated by the fact, that DegU-P is converted from a repressor to an activator of the *fla*/*che* operon upon interaction with SwrA (Mordini *et al.* 2013). Interestingly, this is only true for strains carrying wildtype alleles of *degSU* or *degS200*, but not for *degU32* (Mordini *et al.* 2013). Unlike wildtype DegS, DegS200 is impaired in its dephosphorylation activity leading to accumulation of DegU-P (Msadek *et al.* 1990; Tanaka *et al.* 1991; Dahl *et al.* 1992). The resulting pleiotropic phenotype of *B. subtilis degS200* mutants is indistinguishable from *degU32* mutants regarding extracellular protease activity (Msadek *et al.* 1990; Dahl *et al.* 1992; Tokunaga *et al.* 1994), transformation frequency (Msadek *et al.* 1990; Dahl *et al.* 1992)

and *pga* formation (Osera *et al.* 2009). In contrast to previous reports that *B. subtilis degS200* and *degU32* strains also share the non-motile phenotype, Mordini *et al.* (2013) demonstrated that only *degU32* mutants are impaired in motility (Msadek *et al.* 1990; Tokunaga *et al.* 1994; Mäder *et al.* 2002; Kobayashi 2007b; Verhamme *et al.* 2007; Mordini *et al.* 2013). The *degU32* allele leads to a H12L substitution in the N-terminal domain of the DegU protein stabilizing its phosphorylated form (Msadek *et al.* 1990). But, the N-terminal domain was also shown to be required for interaction with SwrA (Ogura and Tsukahara 2012). Therefore, Mordini *et al.* (2013) concluded that the level of phosphorylation attained by DegU is not the cause of motility inhibition *per se* but DegU(32)-P, unlike wildtype DegU-P, is impaired in its interaction with SwrA (Msadek *et al.* 1990; Ogura and Tsukahara 2012; Mordini *et al.* 2013). It is important to note, that conflicting observations regarding the motility of *degS200* mutants possibly result from a frameshift mutation in *swrA* present in most domesticated *B. subtilis* strains (Kearns *et al.* 2004; Zeigler *et al.* 2008; Mordini *et al.* 2013). Thus, loss of motility in *B. licheniformis degU32* strains is possibly due to the artificial nature of the DegU(32)-P protein rather than the overall DegU-P level. In addition to the regulatory function in motility, the positive effect of SwrA/DegU-P for protease (*aprE*) expression was demonstrated in the wildtype *degSU* background in a *swrA*$^{+}$ *B. subtilis* 168 derivative (Mordini *et al.* 2013). But, in contrast to control of the *fla*/*che* operon, DegU(32)-P promotes *aprE* expression and protease activity is independent from SwrA in *degU32* strains (Figure S3, Mordini *et al.* 2013; Dahl *et al.* 1992). Therefore, despite its artificial mode of action, the *degU32* mutation was included in this study as a promising target to prevent motility, while simultaneously promoting exoenzyme expression (Msadek *et al.* 1990).

While the non-motile phenotype of *B. licheniformis* DSM641 *sigD*, *motB*, *hag* and *degU32* strains was consistent with results from *B. subtilis*, phenotypical characterization of putative biofilm-deficient strains provided new insights into biofilm formation in *B. licheniformis* DSM641. As described for *B. subtilis*, deletion of the *epsA-O* and *tapA-sipW-tasA* operon abolished biofilm formation confirming their function in synthesis of the two major matrix components exopolysaccharides and amyloid fibers (Branda *et al.* 2001; Kearns *et al.* 2005; Branda *et al.* 2006). The third structural component of *Bacillus* biofilms is the amphiphilic biofilm-surface layer protein BslA (YuaB). BslA confers hydrophobicity to biofilms formed by *B. subtilis* and related strains (Kobayashi and Iwano 2012; Morris *et al.* 2017). Moreover, BslA is required for complex colony architecture independent from its function in forming the hydrophobic coat (Kobayashi 2007b; Arnaouteli *et al.* 2017). In contrast to previous reports on *B. subtilis*, deletion of *bslA* neither prevented pellicle formation (Kobayashi 2007b) nor affected complex colony architecture in *B. licheniformis* DSM641 (Arnaouteli *et al.* 2017). Thus, different from *B. subtilis, bslA* might not be required or is less important for modulating colony architecture in *B. licheniformis*

DSM641. Possibly, the *bslA* paralogue *yweA* or another yet to be identified gene may play a more important role in biofilm formation in *B. licheniformis* DSM641 (Kobayashi and Iwano 2012; Morris *et al.* 2017). Whether deletion of *bslA* affects hydrophobicity of *B. licheniformis* DSM641 biofilms remains to be clarified. First results from pellicle formation assays with *bslA* single and combinatorial mutants revealed less-stable pellicles in static liquid cultures indicating altered hydrophobicity upon deletion of *bslA*.

To prevent biofilm formation at the initiating step of the corresponding developmental pathway, global regulators were targeted. By either activating transcription of the *epsA-O* and *tapA-sipW-tasA* operon (*remA*) or mediating anti-repression of SinR (*sinI*, *slrA*) the regulators selected are essential for biofilm formation in *B. subtilis* (Kearns *et al.* 2005; Winkelman *et al.* 2013). In case of *B. subtilis*, strain dependent differences were reported regarding the role of SinI and SlrA in antagonizing SinR (Kobayashi. Similar to the phenotype observed for *epsA-O* and *tapA-sipW-tasA* mutants, inactivation of *remA* abolishes biofilm formation in *B. licheniformis* M308 and M409 which is consistent with *B. subtilis* (Winkelman *et al.* 2013). In contrast, inconclusive results were obtained for strains deficient in the SinR anti-repressors SinI and SlrA regarding their role in regulating biofilm formation in *B. licheniformis*. Both, complete and partial deletion of *sinI* resulted in enhanced rather than reduced biofilm formation. The conflicting results regarding the phenotype of *B. licheniformis sinI* deletion strains became apparent also when analyzing their motility, showing that both strains are non-motile. In contrast, *B. subtilis* Δ*sinI* mutants are deficient in biofilm formation, due to the lack of SinI antagonizing SinR and the resulting constitutive repression of biofilm matrix synthesis genes (Kearns *et al.* 2005; Chai *et al.* 2010b). Moreover, formation of the SinR-SlrR heterodimer is abolished in *B. subtilis* Δ*sinI* mutants locking cells in a motile, chemotactic state (Bai *et al.* 1993; Chai *et al.* 2010b). Unlike *sinI* deficient strains, *sinR* mutants of *B. subtilis* display robust biofilm formation and loss of motility (Kearns *et al.* 2005). Thus, the phenotype of *B. licheniformis* Δ*sinI* strains (M311, M311.2) constructed in this thesis is reminiscent of *B. subtilis* Δ*sinR* rather than Δ*sinI* strains, which likely results from the *sinI-sinR* operon structure and polar effects on *sinR* expression. To reduce potential polar effects, the *sinI* frameshift mutation p.L11AfsX8 was constructed leading to introduction of a translational stop codon. The resulting strain *B. licheniformis* M318 showed wildtype-like pellicle formation and motility as well as an altered but still complex colony architecture. In contrast to mutations in *sinI*, deletion of *slrA* prevented formation of complex colonies, while pellicle formation was wildtype-like. Moreover, time-resolved analysis of swimming motility indicated increased motility of the Δ*slrA* strain *B. licheniformis* M317 similar to the *remA* inactivation strain *B. licheniformis* M310.2, but further analyses are required to confirm these initial observations. The wildtype-like phenotype of *B. licheniformis* M318 carrying the *sinI* frameshift mutation and the reduced ability of Δ*slrA* strains to form biofilms along with their increased motility

indicate that SlrA rather than SinI antagonizes SinR in *B. licheniformis* DSM641 as observed for *B. subtilis* ATCC6051 (Kobayashi 2008). However, in *B. subtilis* ATCC6051 this was due to an inactive *ywcC* allele, encoding the SlrA transcriptional repressor YwcC (Kobayashi 2008), whereas the *ywcC* homologue of *B. licheniformis* DSM641 encodes a functional YwcC, as sequence analysis confirmed. Moreover, phenotypical analysis might be further complicated by the rapid emergence of suppressor mutations under conditions forcing biofilm formation as previously described for *B. subtilis* (Richter *et al.* 2018). Similarly, suppressor mutations cannot be excluded to cause conflicting observations regarding the phenotype of *B. licheniformis* Δ*sinI* strains as well as the ability of Δ*slrA* strains to form pellicles, but not complex colonies. In fact, suppressor mutations were observed in motility assays of *B. licheniformis* M311 and M311.2 as well as for *B. licheniformis* M318 in colony architecture analysis (Figure S1).

4.2 The mutually exclusive character of motility and biofilm development

Another challenge in engineering strains deficient in motility, biofilm formation or both processes is the underlying intertwining regulatory network controlling both developmental processes (Cairns *et al.* 2014). As described above, first results hint towards increased motility in *remA* and *slrA* mutant strains which can be explained by the SinR-SlrR developmental switch as well as functional regulation of flagellar by EpsE (Bai *et al.* 1993; Cairns *et al.* 2014). Cells that develop into a biofilm forming state, express EpsE as part of the *epsA-O* operon. EpsE inhibits motility through binding to the rotor protein FliG thereby further promoting rapid transition from planktonic to sessile lifestyle (Blair *et al.* 2008; Guttenplan *et al.* 2010). Consequently, lack of expression of EpsE in *remA* and *slrA* mutant strains could be responsible for increased motility similar to *B. subtilis* mutants lacking *epsA-O* operon expression (Bai *et al.* 1993). But, unlike the *remA* and *slrA* mutants *B. licheniformis* M310.2 and M317, the *epsA-O* (*epsE*) deficient strain *B. licheniformis* M431 did not display increased motility. However, swimming behavior was altered in the soft agar-plate based assay and further analysis are required to quantify motility in these biofilm deficient strains.

While the results from the swimming assay were less clear regarding upregulation of motility in biofilm deficient strains, upregulation of biofilm formation in motility deficient strains (Δ*hag*, Δ*motB*, Δ*sigD*, *degU32*) was clearly observed. Most severe phenotypical alterations resulted from allelic exchange of the native *degU* by the *degU32* allele in *B. licheniformis* M320 and M436. *B. licheniformis degU32* strains analyzed in this thesis showed a strong increase in biofilm formation under all conditions tested, including liquid and solid LB medium (5 g/L NaCl) as well as chemically defined media. In particular, the

formation of cell aggregates in static and shaking liquid cultures and a strongly increased complex colony morphology was observed. Pellicles at the liquid-air interphase were less structured probably due to loss of motility and the resulting dysfunctional aerotaxis (Bridier *et al.* 2011). Nevertheless, by analyzing both, colony morphology and pellicle formation the *degU32* mutation and, to lesser extent, deletion of *hag*, *motB* and *sigD* was shown to enhance biofilm formation. The *degU32* mutation is known to cause a pleiotropic phenotype in *B. subtilis* and *B. licheniformis*, including loss of motility and increased expression of exoenzymes (Msadek *et al.* 1990; Amati *et al.* 2004; Borgmeier *et al.* 2012). Moreover, it is well known that intermediate levels of DegU-P are required for biofilm formation in *B. subtilis* (Kobayashi 2007a; Verhamme *et al.* 2007; Verhamme *et al.* 2009), but an increase in biofilm robustness similar to that observed in this thesis has not been reported in literature. The role of DegU-P in biofilm formation has been linked to controlling transcription of *bslA*, *yvcA* and, although not essential for complex colony architecture, γ-PGA (Stanley and Lazazzera 2005; Kobayashi 2007a; Verhamme *et al.* 2007; Verhamme *et al.* 2009; Ostrowski *et al.* 2011; Hobley *et al.* 2013). Synthesis of γ-PGA was prevented by deletion of the complete *capB-capC-capD-capE* operon in *B. licheniformis* M308 and M409 excluding excess γ-PGA formation as the underlying biofilm enhancing mechanism in strains carrying the *degU32* allele. Similarly, DegU-P dependent expression of BslA was not responsible for the phenotype observed, as colony architecture was not affected upon deletion of *bslA* (*B. licheniformis* M454 and M455). Thus, increased expression of the lipoprotein YvcA involved in complex colony development in *B. subtilis* possibly promoted biofilm formation in the *B. licheniformis degU32* strain background. In contrast to this hypothesis, *B. subtilis* strains overexpressing *yvcA* showed wildtype-like colony morphology (Verhamme *et al.* 2007). Another possible explanation for the stronger biofilm formation in *B. licheniformis degU32* involves a previously hypothesized, yet to be identified regulatory link. In *B. subtilis* overexpression of the *degU32* allele inhibits *epsA-O* and *tapA-sipW-tasA* operon transcription (Verhamme *et al.* 2007; Marlow *et al.* 2014a), which is in contrast to the observed increase in biofilm formation in *B. licheniformis* DSM641 *degU32.* But, artificial induction of *degU32* in the complementation analysis by Marlow *et al.* limits comparability to strains constructed in this thesis, in which expression of *degU32* was under control of its native promoter. As the frequency of cells initiating sporulation increased in *B. subtilis* when expressing *degU32* under control of an IPTG-inducible promoter, DegU-P is hypothesized to promote increased levels of Spo0A-P eventually inhibiting biofilm formation as cells commence to sporulation (Cairns *et al.* 2014; Marlow *et al.* 2014b). Similarly, DegU-P levels in *B. licheniformis* M320 and M436 may promote Spo0A-P levels sufficient to trigger anti-repression of the biofilm matrix synthesis genes but not as high as in IPTG-based overexpression of *degU32* which promoted sporulation in *B. subtilis*. Thus, the results obtained in this work provide fur-

ther evidence on the previously hypothesized but still elusive link from DegU-P on Spo0A-P and consequently on *tapA-sipW-tasA* and *epsA-O* operon expression (Marlow *et al.* 2014b). Future studies should aim at analyzing Spo0A-P levels and dynamics in the *degU32* strain background to gain further insights into interaction of these central regulators shaping *Bacillus* cell physiology.
Intriguingly, introduction of the *degU32* mutation led to colonization of a wider surface area in addition to enhanced biofilm formation. Both phenotypes are genetically separable as deletion of genes encoding biofilm matrix components did not reduce surface colonization. Moreover, *B. licheniformis degU32* mutants displayed a higher maximum specific growth rate in LSJ-CT rich medium containing complex nitrogen sources, which may indicate a functional relation between growth rate and surface expansion. However, deletion of *sigD* or *hag* increased the growth rate similar to *degU32* while resulting in wildtype-like surface expansion. Considering the epistatic effect of *degU32* to Δ*sigD* and following the assumption of maximum parsimony, these data narrow down the number of genes which may cause the phenotype observed. First, the cellular mechanism causing higher maximum specific growth rates most likely resulted from deregulation of one or multiple genes within the SigD regulon, with DegU-P acting upstream of SigD. In contrast, surface expansion, exclusively observed for *degU32* mutants, presumably resulted from deregulation of genes within the DegU-P regulon that do not underly regulation by SigD.

The findings presented lead to the conclusion that inhibiting either of the two developmental process, motility, and biofilm formation, increases the respective other adaptation in *B. licheniformis* DSM641. However, further quantitative analyses are required to confirm this hypothesis (Cairns *et al.* 2014; Steinberg *et al.* 2020). Consequently, construction of strains carrying multiple mutations targeting both cellular adaptations are required to channel cellular resources towards product formation.

4.3 Cell differentiation and morphology under simulated fed-batch conditions

Previous studies on the formation of motile and biofilm forming subpopulations focused on investigating *B. subtilis* wildtype and domesticated strains under conditions promoting cellular differentiation such as in minimal MSgg medium. While this may resemble limiting conditions in nature, or empirically determined conditions inducing cellular differentiation, the controlled environment in industrial bioprocesses differs strongly regarding most parameters applied. One major goal of this thesis was to analyze cell differentiation of *B. licheniformis* in nutrient-rich media under batch and fed-batch conditions. By analyzing P*hag* and P*tasA* reporter strains using the online micro bioreactor system BioLector,

flow cytometry and fluorescence microscopy, media-dependent differences in the biofilm forming and motile subpopulation were observed. Both subpopulations were strongly enhanced in batch cultures with casitone-tryptone containing LSJ-CT medium compared to V3 with ammonium as sole nitrogen source. The expression dynamics of the P*hag* and P*tapA* promoter showed that *B. licheniformis* M409 develops a motile-chemotactic state during mid-exponential growth, as observed for *B. subtilis* wildtype strains (Kearns and Losick 2005; Chen *et al.* 2009). Moreover, motility was characterized by bimodal distribution with 40 % (V3) to 90 % (LSJ-CT) of the population expressing GFP under control of P*hag*. The lower number of motile cells in chemically defined medium compared to growth on complex nitrogen sources is in line with results from *B. subtilis* showing that *hag* is under direct and indirect negative control of CodY (Ababneh and Herman 2015). Presumably, branched chain amino acids resulting from degradation of casitone and tryptone serve as an effector of CodY increasing the affinity of the pleiotropic transcriptional regulator to its target sites (Ratnayake-Lecamwasam *et al.* 2001; Shivers and Sonenshein 2004; Brinsmade and Sonenshein 2011). Entering stationary growth, P*hag* promoter activity was no longer observed while biofilm formation increases as concluded from activation of P*tapA*. These data are consistent with previous reports from *B. subtilis*, showing precise timing in the development of these mutually exclusive adaptation processes driven by the level of Spo0A-P and DegU-P, both of which increase entering stationary growth (Mirel *et al.* 2000; Kobayashi 2007b; Verhamme *et al.* 2007; Hsueh *et al.* 2011; Mars *et al.* 2015). Unlike motility, biofilm formation was detected in LSJ-CT batch cultivations only. Likewise, analysis of the P*tapA* reporter strain *B. licheniformis* M409.t2 revealed, that only a small number of cells exhibits biofilm formation in fed-batch cultivations, while up to 9 % of the cells developed a motile chemotactic state. It is important to note, that due to the high stability and the resulting intracellular accumulation of GFPmut2 (Blokpoel *et al.* 2003), the actual number of motile cells is presumably lower. The fact, that activation of P*tapA* was low in LSJ-CT medium and not observed in chemically defined V3 medium is surprising as activation of P*tapA* requires similar conditions as P*aprE*. Transcriptional activation of both promoters requires Spo0A-P mediated anti-repression of SinR and AbrB (Gaur *et al.* 1991; Stöver and Driks 1999a; Strauch *et al.* 2007) and single cell analysis of *B. licheniformis* M609.3 confirmed strong activation under batch and fed-batch conditions. In this context, it is important to note, that M609.3 carries *gfpmut2* under control of the native, full length *B. licheniformis* DSM641 P*apr* fragment, which includes the SinR binding site located at the 5' end as described for *B. subtilis* (Gaur *et al.* 1991; Olmos *et al.* 1997; Ogura *et al.* 2003). In addition to derepression, expression of *tapA-sipW-tasA* and the likewise regulated *epsA-O* operon, but not *aprE* requires transcriptional activation by RemA (Winkelman *et al.* 2009; Winkelman *et al.* 2013). Thus, batch and fed-batch cultivation in chemically defined media may prevent RemA activity and consequently expression of matrix synthesis genes. The regulatory mechanism upstream

of RemA is yet to be discovered, but its genomic localization in an operon with the guanylate kinase *gmk* suggests a function related to stringent response and the nutrient status of the cell (Winkelman *et al.* 2013; Cairns *et al.* 2014; Steinchen and Bange 2016). Moreover, further yet to be identified environmental stimuli or a combination thereof might be required for biofilm formation. This included higher concentrations of manganese, plant derived polysaccharides and changes in osmolarity, some of which resemble conditions found in the natural habitat of *Bacilli* (Mhatre *et al.* 2014; Mhatre *et al.* 2016).

The data presented showed that only a minority of cells exhibited biofilm formation in batch and fed-batch cultures with chemically defined V3 medium, while up to 10 % of the population developed a motile-chemotactic state under simulated fed-batch conditions. Hence, preventing biofilm formation by strain engineering may have only minor effects on the host strain physiology under these conditions as the process parameter are 'epistatic' to the single gene inactivation. This applies to motility as well, although to lesser extent. However, considering the mutually exclusive character of both phenotypes and the strong intertwining regulatory network in *Bacillus* cell physiology, the distribution of subpopulations is likely to change with further strain optimization steps, as demonstrated by increased biofilm formation upon introduction of the *degU32* allele.

4.3.1 The cell morphology of *B. licheniformis degU32* strains is altered upon deletion of genes involved in biofilm formation

While biofilm formation in the progenitor strain *B. licheniformis* M409 is limited to complex or biofilm inducing media, *B. licheniformis* M436 (M409 *degU32*) displayed strong biofilm formation under all conditions tested. In fed-batch cultures, this became apparent as chaining cells during earlier cultivation phases turning into robust cell aggregates. These findings lead to the conclusion that strong biofilm formation resulted from deregulation of the gene regulatory network, and thus is intrinsic to the *B. licheniformis degU32* mutant rather than depending on extrinsic factors like growth conditions. A mechanism how DegU32/DegU(-P) may promote biofilm formation was discussed in the previous section (4.1). The strong biofilm formation in *B. licheniformis* M436 and M320 is particularly interesting as the *degU32* allele is frequently addressed in optimization of industrially relevant *Bacillus* species due to its positive impact of *degU32* on secretion of extracellular enzymes. Possible limitations due to cell chaining and aggregation resulted in special focus of this thesis on performing further strain engineering of *degU32* mutants. Importantly, improving process conditions by performing fed-batch rather than batch cultivations did not prevent matrix synthesis in *B. licheniformis* M436. Thus, avoiding biofilm formation in *B. licheniformis* M436 required further streamlining of the host genome. By deleting

tapA-sipW-tasA, *B. licheniformis* (M439) was no longer able to form cell aggregates in fed-batch cultures, which is in line with less complex colony architecture and pellicles (see section 4.1). Moreover, deletion of *tapA-sipW-tasA* resulted in loss of cell chaining and restored wildtype-like cell morphology to a *B. licheniformis degU32* mutant when combined with the Δ*epsA-O* mutation (*B. licheniformis* M441). Similar to these findings, cell chaining and the formation of cell aggregates is lost upon deletion of the *tapA-sipW-tasA* or *epsA-O* operon in the undomesticated *B. subtilis* NCIB3610, (Branda *et al.* 2001; Branda *et al.* 2006; Kobayashi 2007b; Kobayashi and Iwano 2012). Although not analyzed in detail, introduction of the *remA* or *slrA* mutation is likely to affect the cell morphology of *B. licheniformis degU32* strains in a similar manner. The detailed nature of how deletion of *tasA-sipW-tapA* and *epsA-O* affects cell chaining remains unclear, as neither of the two operons has been shown to regulate autolysin expression. In a wildtype *degU* background, functional regulation of SigD activity in response to inhibition of flagellar rotation represents the regulatory link. Both, absence of the flagellar clutch EpsE and reduced force on the flagellar motor resulting from the lack of rigid extracellular matrix promote increased levels of SigD, which in turn enhances autolysin expression (Cairns *et al.* 2013; Cairns *et al.* 2014; Diethmaier *et al.* 2017; Dragoš *et al.* 2018). But, as *Bacillus* strains carrying the *degU32* allele show strongly reduced SigD-dependent gene expression (Mäder *et al.* 2002), the regulatory link described does not explain loss of cell chaining in *B. licheniformis* M439 and M441. In this context, it remains to be clarified, if *B. licheniformis degU32* combinatorial mutants displayed cell chaining during cultivation stages earlier than 24 h or if this phenotype is completely abolished by deletion of *tapA-sipW-tasA* and *epsA-O*.

In addition to the genetic background, the cell morphology of *B. licheniformis* M436 was strongly affected by the growth phase. Cell chaining was observed during earlier cultivation phases (24 h, feedplate), whereas most cells were found in cell aggregates without showing cell chaining as the fed-batch cultivation proceeded. Cell chaining and cell separation requires remodeling of the cell wall mediated by peptidoglycan hydrolases commonly known as autolysins. *B. subtilis* and *B. licheniformis* possesses over ten different autolysins to address the diverse requirements for cell wall turnover in cell division, cell elongation, sporulation, protein secretion and insertion of proteins spanning the cell wall such as flagellin (Blackman *et al.* 1998; Smith *et al.* 2000). Growth phase-specific regulation of individual autolysins maintains cell wall homeostasis throughout exponential and stationary growth. One well known example is the SigD-dependent expression of the major vegetative growth phase autolysins LytC, LytD and LytF during exponential growth (Lazarevic *et al.* 1992; Margot *et al.* 1999; Ohnishi *et al.* 1999). Mutants deficient in *sigD* show a filamentous phenotype during exponential growth (Márquez *et al.* 1990; Chai *et al.* 2010b), which is in line with the filamentous morphology of *B. licheniformis*

M422 during LB batch cultivation. Similarly, *degU32* strains lack expression of SigD-dependent autolysins due to repression of *sigD* by DegU-P (Mäder *et al.* 2002; Mukherjee and Kearns 2014) which may explain the filamentous phenotype observed for *B. licheniformis* M436 (*degU32*) after 24 h of cultivation in the simulated fed-batch process. In contrast to this hypothesis, cell chaining was not observed for *B. licheniformis* M422 under these conditions and further analyses are required to investigate regulation of autolysins in *sigD* and *degU32* mutants. Entering stationary growth, and possibly the fed-batch phase during cultivation in feedplates, SigD-dependent gene expression decreases, and alternative autolysins become increasingly important, including CwlS and LytE. Expression of *cwlS* and *lytE* is regulated by the late stationary phase sigma factor SigH and the housekeeping sigma factor SigA (Ishikawa *et al.* 1998; Margot *et al.* 1999; Hashimoto *et al.* 2012). Thus, growth phase specific autolysin activity is likely to contribute to loss of cell chaining in *B. licheniformis* M436 during later cultivation stages.

The results discussed in this section highlight the importance of in-depth strain characterization for identification of novel strain targets. Analyses of biofilm formation and cell morphology under simulated fed-batch conditions revealed possible limitations of the *B. licheniformis degU32* mutant due to filamentous growth and cell aggregation. This phenotype is undesirable due to highly viscous fermentation broth, gradients in the availability of oxygen and nutrients along cell aggregates, and possibly increased mechanical stress due to higher stirrer speed required. To overcome similar drawbacks in production hosts, which typically grow as filaments including actinomycetes, morphological engineering approaches are frequently performed (van Wezel *et al.* 2006). Similarly, targeting biofilm formation represents a promising strategy to overcome these limitations not just in *B. licheniformis* M436 but possibly in the domestication of *Bacillus* wildtype isolates for industrial applications, many of which naturally display strong biofilm formation (Branda *et al.* 2001; Branda *et al.* 2006; Kobayashi 2007b; Kobayashi and Iwano 2012).

4.4 Productivity of optimized *B. licheniformis* mutant strains

4.4.1 Targeting biofilm formation in *B. licheniformis degU32* increases protease expression

In industrial biotechnology, substrate-limited fed-batch cultivation represents the predominant mode of fermentation processes allowing to minimize catabolite repression and overflow metabolism among other reasons (Habicher *et al.* 2019a). However, due to the simple experimental setup and low technical requirements, screening of production strains is still frequently performed in batch mode (Habicher *et al.* 2019a). To avoid misinterpretation of screening results obtained from batch cultures, fed-

batch cultivations need to be implemented in early phases of strain optimization and evaluation (Habicher *et al.* 2019c). To address this requirement, the *B. licheniformis* DSM641 strain derivatives constructed in this thesis were evaluated using the recently published polymer-based fed-batch system (Habicher *et al.* 2019c). To enable carbon limited growth, these so-called feedplates require inorganic nitrogen sources preventing utilization of complex nitrogen sources as alternative carbon sources. However, as complex media become increasingly important in the context of utilization of waste streams to create high value products, strain characterization was performed in both, chemically defined V3 medium (batch and fed-batch) and complex LSJ-CT medium (batch only). Comparison of *B. licheniformis* M409 mutants revealed three distinct subsets of strains regarding productivity. Under the three conditions tested, single deletion strains deficient in biofilm formation (Group 1) showed no changes in protease activity except for the Δ*epsA-O* strain *B. licheniformis* M431. The latter is in line with previous reports on increased exoenzyme secretion of a *epsA-O* deficient *B. licheniformis* mutant (Zhou *et al.* 2020b). Reduced viscosity of the fermentation broth is hypothesized to improve oxygen transfer leading to improved productivity. Strains deficient in motility (Group 2) are characterized by higher protease expression in LSJ-CT batch cultures. In contrast, wildtype-like or slightly reduced productivity was observed in V3 batch and fed-batch cultivations. As V3 and LSJ-CT primarily differ in the nitrogen source these findings indicate improved metabolization of complex nitrogen sources resulting from deletion of *sigD*, *hag* and possibly *motB*, but no direct or indirect role in modulating central metabolic pathways has been assigned to SigD (Márquez *et al.* 1990; Serizawa *et al.* 2004). Moreover, a higher maximum specific-growth rate observed for *B. licheniformis* M422 (Δ*sigD*) and M435 (Δ*hag*) may explain a lower productivity in V3 medium, although this does not apply to growth and productivity in LSJ-CT medium. A higher growth rate indicates increased flux through glycolysis which in turn may result in stronger carbon catabolite repression eventually repressing protease expression as shown for *B. licheniformis* S1684 (Frankena *et al.* 1986; Christiansen and Nielsen 2002). The increase in the specific growth rate upon deletion of *sigD* is in line with previous results from a *B. subtilis* Δ*sigD* mutant (Fischer and Sauer 2005). The last group summarizes strains carrying the *degU32* allele, which resulted in enhanced protease expression in batch and fed-batch cultivations (Group 3). These strains can be divided into two subgroups when comparing batch and fed-batch cultivations. Protease activity and growth in batch cultures was comparable for all *degU32* strains analyzed, independent from further genetic modification of the host cell. In contrast, introduction of mutations causing biofilm deficiency in the *degU32* strain background (Group 3.1) further enhanced protease activity in fed-batch cultivations compared to biofilm-proficient *degU32* strains (Group 3.2). The different results obtained from batch and fed-batch cultivations underline the importance of implementing fed-batch cultivations in the early phase of strain evaluation (Habicher *et al.* 2019a). It is tempting to speculate, that in

B. licheniformis M436, the high number of cellular resources spent for biofilm formation decrease the productivity compared to biofilm-deficient *degU32* strains and that relieving this metabolic burden resulted in channeling of cellular resources towards product formation. However, further factors must be considered. Only recently, deletion of the *epsA-O* operon in *B. licheniformis* 2709 was shown to improve AprE expression which was at least in part due to more homogeneous growth, lower viscosity of the growth medium and the resulting improved oxygen transfer (Zhou *et al.* 2020b). In this regard, it is important to note, that improved growth contributes only in part to higher productivity of *B. licheniformis* M438, M439, M441, M451, M452 and related strains as biomass-normalized specific activity showed. The underlying reason for the higher specific activity is discussed in section 4.5. The *degU32*, Δ*bslA* mutant *B. licheniformis* M455 represents the only exception from the group of *degU32* combinatorial mutants. Compared to its progenitor strain, deletion of *bslA* in *B. licheniformis* M436 (*degU32*) did not affect protease activity. This is surprising as the role of DegU-P in biofilm formation in *B. subtilis* was assigned to transcriptional activation of *bslA* and possibly higher BslA synthesis may represent a metabolic burden to *degU32* strains (Kobayashi 2007b; Verhamme *et al.* 2009). However, the observation that deletion of *bslA* did not affect protease expression is in line with its low impact on biofilm formation in *B. licheniformis*, as Δ*bslA* mutants still formed robust biofilms. Interestingly, time-resolved protease activity assays from fed-batch samples revealed lower productivity during earlier cultivation phases for *B. licheniformis degU32* strains, while *degU32* strains outperform d*egU* wildtype strains in the long-term (from 48 to 72 h). The initial lower product titers did not result from lower cell densities or impaired growth of *degU32* mutants, as biomass (OD_{600nm}) was comparable after 24 h (Figure S8). Furthermore, cell aggregation or higher viscosity of the fermentation broth are not the underlying reason for delayed protease expression, as cell aggregates and filaments are resolved upon deletion of the *tapA-sipW-tasA* and *epsA-O* operon, but the resulting strain *B. licheniformis* M441 showed similar BLAP activity as the *degU32* single mutant *B. licheniformis* M436. Instead, a regulatory effect specific for *degU32*, or DegU-P in general, possibly affected protease activity in the initial phase of the polymer-based fed-batch process. Expression of Apr/AprE, and likewise P*apr*-BLAP, requires activation of two cellular pathways. First, repression of the *apr* promoter by ScoC, SinR and AbrB must be relieved through Spo0A-P and only recently, Spo0A-P was shown to directly bind to and activate the *aprE* promoter (Msadek *et al.* 1993; Msadek 1999). In addition, transcriptional activation by binding of DegU-P is required (Veening *et al.* 2008a). Since the *degU32* allele is well known to increase transcription of *apr* expression by increased stability of phosphorylated DegU-P, lack of DegU-P was excluded as the reason for initially lower BLAP activity (Msadek *et al.* 1990). Possibly, insufficient levels of Spo0A-P in *degU32* mutants hampered protease expression during early

stages in the simulated fed-batch process, but this hypothesis was also rejected for the following reasons. First, *degU32* was shown to promote high levels of Spo0A-P in *B. subtilis* (Marlow *et al.* 2014b). Secondly, single cell analysis showed similar promoter activities for the P*apr-gfpmut2* reporter strain *B. licheniformis* M641 (Δ*eps*, Δ*tasA*, *degU32*) compared to the control strain M609.1 after 24 h of fed-batch cultivation. Finally, earlier activation of the protease promoter in batch cultivations was observed, which is in line with the positive effect of *degU32* on protease expression in *B. subtilis* and *B. licheniformis* (Mäder *et al.* 2002; Ogura *et al.* 2003; Verhamme *et al.* 2007; Veening *et al.* 2008a; Borgmeier *et al.* 2012). These findings clearly demonstrate that Spo0A-P levels are sufficient to trigger the P*apr* promoter. Therefore, the underlying mechanism leading to lower protease expression in *B. licheniformis degU32* strains during early stages of the simulated fed-batch conditions remains elusive.

4.4.2 Increased productivity is specific for combined mutation of biofilm forming genes and *degU32* but not Δ*sigD*

The strong increase in protease expression of strains deficient in biofilm formation combined with the *degU32* allele raises the question whether this is a common feature resulting from simultaneous inactivation of biofilm formation and motility. Therefore, *B. licheniformis* M441 (Δ*tapA-sipW-tasA*, Δ*epsA-O*, *degU32*) was compared to *B. licheniformis* M447 (Δ*tapA-sipW-tasA*, Δ*epsA-O*, Δ*sigD*). Both strains are non-motile, resulting from the *degU32* allele or deletion of *sigD*, and lost the ability to form biofilms. However, when analyzing protease activity under simulated fed-batch conditions, strong difference in the productivity became apparent. Compared to the progenitor strain *B. licheniformis* M440, protease expression did not significantly increase for *B. licheniformis* M447, unlike *B. licheniformis* M441, which showed 43 % higher protease activity under fed-batch conditions. Consequently, increased protease expression did not result from preventing motility and biofilm *per se* under the conditions tested. Instead, a yet unknown combined effect of the *degU32* mutation and biofilm deficiency led to construction of optimized *B. licheniformis* DSM641 strains. Possibly, the high amount of cellular resources spent for biofilm formation prevented *degU32* single mutants from exploiting their full protease expression capacity and inhibiting biofilm formation resulted in streamlining of these strains. Moreover, loss of cell aggregation and reduced viscosity of the fermentation broth due to deletion of *epsA-O* presumably improved oxygen transfer thereby contributing to a higher metabolic capacity and product formation (Zhou *et al.* 2020b). It is worth mentioning, that motility and biofilm formation were observed to only limited extend in the parental strain *B. licheniformis* M409 under fed-batch conditions and, thus, these cellular mechanisms do not represent a strong metabolic burden to the host cell. Therefore, it would be interesting to compare *B. licheniformis* M447 (Δ*eps* Δ*tasA* Δ*sigD*) and

B. licheniformis M441 under conditions using complex media, in which the formation of both subpopulations was more pronounced. 85 % of the population express or have expressed *gfpmut2* under control of P*hag* in LSJ-CT batch cultures. Moreover, biofilm formation was observed under these conditions. Therefore, targeting both cellular adaption process may indeed reduce the metabolic burden to the host cell and channel cellular resources towards product formation.

4.5 Productivity at the single cell level

4.5.1 The effect of *degU32* on cellular heterogeneity in batch cultures

To analyze the activity of the P*apr* promoter driving BLAP expression in more detail, the *amyB*::P*apr-gfpmut2* reporter strains *B. licheniformis* M609.1 and *B. licheniformis* M641 (Δ*tasA*, Δ*eps*, *degU32*) were compared. In batch cultivations, P*apr* activity was repressed during exponential growth and increased in the transition state. This expression profile is in line with precise timing of *aprE* expression in *B. subtilis* (and *B. licheniformis*), which underlies negative control by ScoC, SinR, AbrB and CodY under non-limiting growth conditions and transcriptional activation by DegU-P and Spo0A-P as cells enter stationary growth (Perego *et al.* 1988; Strauch *et al.* 1989; Shafikhani *et al.* 2002; Zhou *et al.* 2020a). Compared to *B. licheniformis* M609.1, *B. licheniformis* M641 showed earlier and stronger activation of the P*apr* promoter, which is in line with the known function of DegU-P in promoting exoenzyme expression in *B. subtilis* and *B. licheniformis* DSM13 (Henner *et al.* 1988a; Veening *et al.* 2008a; Borgmeier *et al.* 2012; Marlow *et al.* 2014a; Ploss *et al.* 2016). Importantly, the temporal difference in initiating protease expression in *B. licheniformis* M609.1 and M639/M641 was more pronounced than the shift in growth curves. Thus, changes in *apr* expression dynamics resulted from the regulatory role of DegU-P in promoting transcription of *apr* rather than the slightly different growth phase the samples were taken from (Henner *et al.* 1988a; Shimane and Ogura 2004). Flow cytometry of early stationary phase samples revealed high homogeneity in the exoprotease producing population for *B. licheniformis* M641, whereas the control strain *B. licheniformis* M609.1 showed heterogeneous (LSJ-CT) and bimodal (V3) expression during the transition state. Heterogeneity in P*aprE* activity is well known for *B. subtilis* and *B. licheniformis* DSM13 and results from only a small fraction of cells reaching Spo0A-P and DegU-P levels sufficient to trigger *aprE* expression. In these model strains, bimodality is maintained throughout stationary growth and the *aprE* producing cells represent only a small subpopulation (Veening *et al.* 2008a; Borgmeier *et al.* 2012; Marlow *et al.* 2014a). Presumably, exoenzyme expression by a small number of cells is sufficient to provide nutrients to the whole population allowing for division of labor and increased biological fitness (Aguilar *et al.* 2007). In contrast, the H12L amino acid substitution in the *degU32* allele stabilizes the phosphorylated form of DegU-P and increases its halftime sevenfold from 20 to 140 min (Dahl *et al.* 1992). Driven by the auto-stimulatory loop of DegU-P, the number of

cells reaching high levels of DegU-P is dramatically enhanced in the *degU32* background, which results in higher homogeneity in P*apr* activity as observed for *B. licheniformis* M641 (and M639, M648) (Yasumura *et al.* 2008; Borgmeier *et al.* 2012). As construction of the *degU32* single mutant P*apr-gfpmut2* reporter strain *B. licheniformis* M636 succeeded only at the end of this project phase, the strain was not included in the analysis. Therefore, it remains to be clarified whether deletion of *epsA-O* or *tapA-sipW-tasA* affects timing or strength of P*apr* dependent GFP expression in the *degU32* strain background. But, comparable growth characteristics and protease activity on global expression level suggest a similar behavior of *degU32* single and combinatorial mutants in batch cultures (Figure 21 and Figure 23), which is likely also reflected at single cell level.

4.5.2 Stimulation of DegU-P is intrinsically high in *B. licheniformis* M409

In case of *B. subtilis* 168 and *B. licheniformis* DSM13, homogeneous P*aprE* activity is observed only upon introduction of the *degU32* mutation (Veening *et al.* 2008a; Borgmeier *et al.* 2012; Marlow *et al.* 2014a). In strong contrast, the *B. licheniformis* DSM641 (M409) reporter strain M609.1, carrying the native *degU* allele, showed high homogeneity in *apr* activity during stationary growth in batch culture as well as in earlier stages of simulated fed-batch cultivation. These observations suggest that the DegU-P autostimulatory loop is intrinsically strong in *B. licheniformis* DSM641 (M409). This hypothesis was confirmed by single cell analysis of *B. licheniformis* M809.1 expressing *mScarletI* under control of the *degU* P3 promoter, which is subjected to auto stimulation by DegU-P (Yasumura *et al.* 2008). Further evidence came from comparison of the *B. licheniformis* DSM13 P*apr* reporter strain MH1 and *B. licheniformis* M609.5. Both strains expressed *gfpmut2* under control of the P*apr*(DSM13 full) promoter to exclude promoter-dependent effects. In line with the results from Borgmeier *et al.* (2012), the DSM13 type strain was characterized by a bimodal expression pattern with a minority of cells activating the P*apr* promoter. In contrast, *B. licheniformis* M609.5 showed strong GFP expression for the majority of cells confirming the strong impact of the strain background on protease expression. In *B. subtills*, differences between wildtype and domesticated strains are well known to affect cellular heterogeneity. For example, the presence of SwrA affects the distribution of motile and sessile cells. As many domesticated *B. subtilis* strains lack a functional *swrA* gene, including *B. subtilis* PY79, the number of cells developing a motile chemotactic state is reduced as compared to wildtype isolates such as *B. subtilis* NCIB3610 (Kearns and Losick 2005; Chen *et al.* 2009). Another example of how domestication affected cellular heterogeneity is illustrated by the *degQ36* allele (Stanley and Lazazzera 2005; McLoon *et al.* 2011). DegQ stimulates autophosphorylation of DegS, thereby facilitates higher level of DegU-P and promotes exoenzyme secretion (Msadek *et al.* 1991; Do *et al.* 2011). Moreover, genetic compe-

tence is reduced due to the requirement of unphosphorylated DegU for expression of the master regulator of genetic competence *comK* (Miras and Dubnau 2016). The *degQ36* allele was identified as one of the so called 'hy' (hypersecretion) mutation in screening for improved exoenzyme secretion in *B. subtilis* and describes a C to T mutation within the -10 region of the *degQ* promoter (Yang *et al.* 1986; Amory *et al.* 1987). The resulting higher levels of DegQ lead to a pleiotropic phenotype similar to strains carrying the *degU32* and *degS200* 'hy' mutations (Msadek *et al.* 1991). But, unlike the mutations in the sensor kinase and the response regulator itself, *degQ36* was shown to represent the actual wildtype allele, which was lost as a consequence of domestication, in particular selecting for high genetic competence (Stanley and Lazazzera 2005; McLoon *et al.* 2011; Miras and Dubnau 2016). Although the *degQ36* is native to *B. licheniformis* DSM641 and DSM13, and thus, does not explain the strain dependent differences in cellular heterogeneity, these studies exemplify how domestication, isolation, and screening of strains for desired characteristics results in strain dependent differences. It is important to note, that unlike *B. licheniformis* M409, *B. licheniformis* MH1 carries a functional *sigF* gene and initiation of spore formation may contribute to the lower number of cells activating P*apr*. However, deletion of *sigF* does not result in homogeneous expression of *aprE* in *B. subtilis* (Veening *et al.* 2008a). Thus, the underlying physiological reason for intrinsically strong DegU-P autostimulatory loop in *B. licheniformis* M409 (and DSM641) remains elusive.

4.5.3 Fed-batch cultivation and promoter engineering contribute to homogeneity in protease expression

Although the strain background had the strongest impact on protease expression in *B. licheniformis*, results from single cell analysis showed that cultivation under fed-batch conditions contributed to higher homogeneity in the protease producing subpopulation of *B. licheniformis* M409 (M609.1). The glucose limited growth results in lower catabolite repression, which otherwise inhibits protease expression in *B. subtilis* and *B. licheniformis* (Priest 1977; Hanlon *et al.* 1982; Frankena *et al.* 1986; Mao *et al.* 1992; Barbieri *et al.* 2016; Habicher *et al.* 2019b). Similarly, increased homogeneity of the DegU-P dependent P*amyQ* promoter was observed for *B. subtilis* 168 when simulated fed-batch conditions were applied (Ploss *et al.* 2016). Moreover, truncation of the P*apr* promoter fragment, driving expression of BLAP and GFPmut2, contributed to higher homogeneity in the protease producing population as well. The 227 bp promoter fragment was derived from the native *B. licheniformis* DSM641 P*apr* promoter region, but lacks the most upstream (Wilson *et al.* 1993; Jacobs 1995). In *B. subtilis*, the transcriptional repressors CodY, AbrB, ScoC and SinR bind to this 5' region of the *aprE* promoter, thereby repressing *aprE* during exponential growth (Strauch 1995; Olmos *et al.* 1997; Msadek 1999; Barbieri *et al.* 2016). Thus, lack of these repressor sites in the 227 bp promoter fragment may explain

stronger activiation of the truncated DSM641 P*apr* compared to the full-length promoter fragment present in *B. licheniformis* M609.3. Accordingly, transcriptional activity of a 154 bp promoter fragment from *B. licheniformis* 6816 *aprE* did not underly ScoC (Hpr) dependent repression (Jacobs 1995).

4.5.4 *degU32* affects cellular heterogeneity and cell viability in *B. licheniformis* during late stages of fed-batch cultivation

The initial hypothesis in this thesis, was that the *degU32* allele improves protease expression in *B. licheniformis* DSM641 by increasing the homogeneity in the *apr* expressing population, as described for *B. subtilis* and *B. licheniformis* DSM13 (Veening *et al.* 2008a; Borgmeier *et al.* 2012). While this indeed applied to *apr* expression during the transition state in batch cultivations, high homogeneity was observed even for the *degU* control strain *B. licheniformis* M609.1 under simulated fed-batch conditions. In fact, the distribution in P*apr-gfpmut2* positive cells was similar for *B. licheniformis* M609.1 (control) and *B. licheniformis* M641 (Δ*eps*, Δ*tasA*, *degU32*) after 24 h of fed-batch cultivation. Thus, higher homogeneity in activation of the protease promoter is not the cause for higher productivity of *B. licheniformis* M441/M641 *per se*. Surprisingly, single cell analysis revealed strongly improved strain characteristics for *B. licheniformis* M641 during later stages in the simulated fed-batch process. Unlike the control strain *B. licheniformis* M609.1, *B. licheniformis* M641 showed a constant increase in the mean GFP intensity, which is in line with the results from steady increase in BLAP activity. Moreover, GFP signal distribution was homogeneous for M641 throughout fed-batch cultivation, whereas high cellular heterogeneity became apparent for *B. licheniformis* M609.1 from 48 h onwards. Most importantly, strong background fluorescence was observed for *B. licheniformis* M609.1 accompanied by the accumulation of cell debris. These findings suggest, that *B. licheniformis* M609.1 is severely affected by cell lysis and that cell viability is improved upon introduction of the Δ*eps*, Δ*tasA* and *degU32* mutations. Note, that construction of the *degU32* single mutant P*apr-gfpmut2* reporter strain *B. licheniformis* M636 was finished at the end of this project phase, and therefore the effect of *degU32* single mutation was not investigated. Future work should aim at comparing *B. licheniformis* M636 and M641 to elucidate the impact of Δ*eps* and Δ*tasA* on P*apr* activity and cell viability in *B. licheniformis* strains carrying the *degU32* allele.

4.6 Analysis of the extracellular proteome of *B. licheniformis* mutant strain

To gain further insights into the host cell physiology, the extracellular proteome of selected *B. licheniformis* strains was analyzed by one-dimensional SDS-PAGE and subsequent mass spectrometry. In addition to acquisition of nutrients, secreted proteins are crucial for cell-to-cell communication, intra-

and interspecies competition, detoxification of the environment, cell wall metabolism, motility, chemotaxis and biofilm formation among others (Tjalsma *et al.* 2004b). As most of these processes affect neighboring cells, the physiological response resulting from changes in the extracellular proteome strongly depends on population density. Considering the high cell density in industrial fermentation processes, extracellular proteomics provides valuable information on the host strain physiology and potentially new approaches for further strain optimization.

4.6.1 Δ*sigF* and integration of the BLAP expression cassette in *B. licheniformis* M409 have minor effects on the extracellular proteome under simulated fed-batch conditions

In industrial biotechnology of *Bacilli*, sporulation-deficiency is a pre-requisite except for applications, which take advantage of spore formation including the spore-display technology and utilization of *Bacillus* spores as probiotics in food and feed applications or as biologicals in plant protection (Cutting 2011). Spore formation is undesirable due to the risk of contamination and non-producing subpopulations and, consequently, is among the first targets in *Bacillus* expression host optimization (Pierce *et al.* 1992; Nahrstedt *et al.* 2005; Vary *et al.* 2007). Within this thesis, the most advanced *B. licheniformis* mutants were constructed based on the sporulation-deficient *B. licheniformis* M409 (Δ*rms*, Δ*apr*, Δ*sigF*, *pga*::BLAP), in which the *sigF* (*spoIIAC*) gene, encoding the forespore-specific sigma factor SigF, was deleted (Stragier and Losick 1996; Errington 2003; Steil *et al.* 2005; Hoon *et al.* 2010). In *B. subtilis*, more than 900 genes are deregulated in a Δ*sigF* mutant under sporulation conditions and 117 gene were differentially expressed even during exponential growth in LB medium (Overkamp and Kuipers 2015). To differentiate between changes in the extracellular proteome that resulted from inactivation of SigF and those caused by the gene deletion targets evaluated within this thesis, *B. licheniformis* M321 (Δ*rms*, Δ*pga*, Δ*apr*) was included in the analysis of supernatant from simulated fed-batch cultivation by SDS-PAGE. Only minor changes in the protein band pattern were observed between *B. licheniformis* M321 and M309. However, deletion of *sigF* resulted in higher intensity of most protein bands, in particular the low-molecular weight band containing the bacteriocin ForD (BL00275, 14.1 kDa). SigF mutants are not irreversibly committed to sporulation but can resume vegetative growth under non-limiting conditions, which may explain enhanced secretory enzyme production observed upon deletion of *sigF B. subtilis* and *B. licheniformis* (Dworkin and Losick 2005; Ara *et al.* 2007; Zhou *et al.* 2019).

Integration of the BLAP expression cassette into *B. licheniformis* M409 resulted in a prominent band below the 29 kDa reference identified as the mature BLAP protein. Like all subtilisin proteases, BLAP is synthesized as a pre-pro-enzyme (ZITAT). Pre-pro-BLAP has a size of 39.6 kDa. During secretion, the

signal peptide is cleaved resulting in the 36.4 kDa pro-enzyme. Subsequently, BLAP undergoes auto-catalytic cleavage for removal of the pro-peptide resulting in a 26.9 kDa protein. Moreover, the presence of BLAP in the supernatant decreased the intensity of selected protein bands as compared to *B. licheniformis* M309. In particular, the intensity of the secreted endo-1,4-beta-glucanase BglC (58.7 kDa), alpha-amylase AmyL (58.5 kDa) and a gamma-glutamyltranspeptidase Ggt (60.9 kDa) was reduced. In addition, the protein band, in which the intracellular 1-pyrroline-5-carboxylate dehydrogenase PutC (YcgN, 56.6 kDa) was identified, had a lower intensity in *B. licheniformis* M409. Higher proteolytic activity upon expression of BLAP may resulted in stronger degradation of proteins from the supernatant, which explains the reduced intensity of selected protein bands. Moreover, shifting cellular resources, protein production and secretion capacities towards BLAP expression cannot be excluded as an underlying reason for reduced levels of natively secreted proteins. However, in strains carrying the single-copy BLAP expression cassette, protein production capacities are most likely not limiting.

4.6.2 The extracellular proteome of *B. licheniformis* under simulated fed-batch conditions

Most significant changes in the extracellular proteome of *B. licheniformis* M409 strain derivatives were observed for strains carrying the *degU32* mutation. In contrast, none of the alternative mutations preventing biofilm formation (Δ*eps*, Δ*tasA*, *remA* R19W P29S, Δ*slrA*) or motility (Δ*sigD*, Δ*hag*, Δ*motB*) had an impact on the extracellular proteome under simulated fed-batch conditions. This is surprising at first glance, as previous studies on the extracellular proteome of *B. licheniformis* DSM13 showed high abundance of proteins related to cellular heterogeneity, foremost Hag and TasA (Voigt *et al.* 2006; Voigt *et al.* 2007). However, differences in the process conditions, in particular batch cultivations with minimal medium used by compared to fed-batch cultivation with V3 medium (this thesis) may explain the contrasting observations. In fact, the lack of Hag and TasA in the secretome of *B. licheniformis* M409 single mutants is in line with the single cell analysis of *B. licheniformis* P*hag* and P*tapA* reporter strains, showing that only a minority of cells exhibited motility or biofilm formation in V3 mineral salt medium (section 4.3). As for *B. licheniformis* M409 derived single mutants, combinatorial *B. licheniformis* mutants carrying the *degU32* allele (M439, M441, M451, M452, M455 and M456), did not differ from the *degU32* single mutant *B. licheniformis* M436 under the conditions tested. Compared to strains carrying the *degU* wildtype allele, *degU32* mutants were characterized by a lower number of cytoplasmic proteins identified in the supernatant, which is likely to result from lower cell lysis (see section 4.6.3) or higher proteolytic activity causing degradation of cytoplasmic proteins. Except for

ForD, which was absent from samples taken from *B. licheniformis* M436 and M439 (discussed in section 4.6.3), only minor differences in the number of secreted proteins were detected compared to *B. licheniformis* M409. The secretome of both, *degU32* and *degU* wildtype strains, was characterized by several peptidases. In fact, six out of nine proteins, that are known or predicted to be secreted, have proteolytic activity. This includes the extracellular serine protease Vpr, the bacillopeptidase F Bpr, a putative carboxypeptidase BL03063, the aminopeptidases YwaD, the gamma-glutamyl transpeptidase Ggt and the glutamyl endopeptidase GluBL. In contrast, only a limited number of glycosyl hydrolases, AmyL and BglC, were found in the secretome of *B. licheniformis* M409, which is surprising due to the carbon limited growth conditions and a high number of genes in the genome of *B. licheniformis* encoding extracellular carbohydrate-hydrolyzing enzymes (Rey *et al.* 2004; Veith *et al.* 2004). However, expression of enzymes for metabolization of alternative carbon sources often depends on substrate induction in addition to derepression of CcpA-mediated carbon catabolite repression in *B. subtilis* and related strains (Laoide *et al.* 1989; Blencke *et al.* 2003; Görke and Stülke 2008). Thus, the absence of an inducer e.g. cellobiose as in expression of the glucomannan utilization operon *gmuBACDREFG*, may explain the low number of carbohydrate-active enzymes under the conditions tested (Sonenshein 2007; Sadaie *et al.* 2008). Moreover, these observations are in line with previous characterization of the extracellular proteome of *B. licheniformis* under glucose starvation conditions (Voigt *et al.* 2006; Voigt *et al.* 2007). The high number of peptidases may allow *B. licheniformis* to inhabit ecological niches different from *B. subtilis* by utilizing non-carbohydrate C-sources. Noticeably, Ggt was among the most abundant proteins detected in the secretome of all *B. licheniformis* strain derivatives. In *B. subtilis*, the gamma-glutamyl transpeptidase Ggt degrades poly-γ-glutamic acid (γ-PGA) natively produced by many *Bacillus* strains (Suzuki and Tahara 2003; Ashiuchi *et al.* 2006). Considering the strong γ-PGA production observed for the *B. licheniformis* DSM641 wildtype strain, expression of Ggt possibly allows the host strain to reutilize cellular resources invested into γ-PGA formation under limiting growth conditions. In line with these observations, expression of *ggt* in *B. subtilis* is upregulated upon glucose starvation (Jong *et al.* 2012; Scoffone *et al.* 2013). Alternatively, degradation of γ-PGA might be simply required for biofilm dispersal allowing cells to escape from the biofilm or mucoid colony as nutrients become limiting. A similar mechanism was postulated for disruption of the biofilm matrix proteins by upregulation of proteases (Marlow *et al.* 2014a). It is important to note, that efficient γ-PGA degradation by the exo-type hydrolase Ggt requires the presence of an endo-type γ-PGA hydrolase (Scoffone *et al.* 2013). In *B. subtilis*, the gamma-glutamyl hydrolase PgdS exerts this function, but despite being genetically encoded in the *B. licheniformis* DSM641 chromosome, PgdS was not detected in this thesis (Suzuki and Tahara 2003; Scoffone *et al.* 2013). This might be due to low activity of SigD under simulated fed-batch conditions in chemically defined medium (section 4.3), as expression of *pgdS* depends on

SigD (Serizawa *et al.* 2004). In contrast, PgdS was identified in the secretome of *B. licheniformis* DSM13 during early stationary growth in LB medium (Voigt *et al.* 2007), which is in line with increased SigD-dependent gene expression in *B. licheniformis* M409 in complex LSJ-CT medium.

In summary, analysis of the extracellular proteome revealed two subgroups of strains, carrying the *degU* or *degU32* allele, that differ by only a limited number of proteins. Independent from the strain background, a high number of extracellular degradative enzymes was detected, many of which are under direct or indirect control by catabolite repression (Kim *et al.* 1995; Blencke *et al.* 2003; Scoffone *et al.* 2013; Barbieri *et al.* 2016). The polymer-based glucose limited fed-batch process, which was developed to mimic industrial fermentations often operated in fed-batch mode, overcomes this catabolite repression (Habicher *et al.* 2019c; Habicher *et al.* 2019b). It remains to be clarified how the single and multiple gene deletions affect the extracellular proteome in cultivations using complex media, in which motile and biofilm forming cells represent a larger fraction of the cell population as demonstrated within this thesis.

4.6.3 Introduction of *degU32* into *B. licheniformis* prevents ForD expression

Most significant changes in the extracellular proteome of *B. licheniformis* resulted from introduction of the *degU32* mutation. Strikingly, the bacteriocin formosin D (ForD, BL00275) was absent from the secretome of *B. licheniformis* M436 and M439 both carrying the *degU32* allele, while ForD represented the most abundant protein in the extracellular proteome of *B. licheniformis* M409. ForD has no homology to any protein of known function and was functionally characterized by only two studies working with the *B. licheniformis* type strain DSM13 and the tropic marine isolate *B. licheniformis* D1 (Lundström 2012; Dusane *et al.* 2013). ForD is a 9.6 kDa antimicrobial peptide belonging to the lactococcin 972 family and was shown to exert bacteriolytic activity towards *B. subtilis, B. pumilus, Candida albicans* and *Pseudomonas aeruginosa* (Lundström 2012; Dusane *et al.* 2013). Bacteriocins typically target closely related species, which inhabit a similar ecological niche, thereby providing a fitness advantage to the host in inter-species competition (Tagg *et al.* 1976). A second, presumably equally important function of bacteriocins in *B. subtilis* is the killing of sensitive sibling cells to release nutrients that feed the bacteriocin-producing subpopulation. This so-called cannibalism is a common strategy to delay entry into sporulation as well as to provide nutrients to finalize the energy intensive spore formation by sacrificing a fraction of cells. This eventually provides a fitness advantage to the population (González-Pastor *et al.* 2003; Claverys and Håvarstein 2007; González-Pastor 2011). Well known examples for bacteriocins or toxins that have evolved in this way are the spore killing factor SkfA and the sporulation delay protein SdpC produced by *B. subtilis* (González-Pastor 2011). *B. licheniformis* does not synthesize SkfA or SdpC and cannibalism has not been reported for this species. But, considering

the high homology between these two closely related species and similar environmental constrains they are facing, a mechanism similar to SdpC or SkfA is likely to have evolved for *B. licheniformis*. ForD may possess such function in *B. licheniformis*, as concluded from the following observations. First, ForD is the most abundant protein in the supernatant of *B. licheniformis* M409 after 72 h of cultivation and single cell analysis revealed strong cell lysis at this cultivation stage. More importantly, a fraction of the cells in *B. licheniformis* M609.1 is seemingly not affected in cellular integrity. In this scenario, the intact cells represent the ForD producing subpopulation which co-express the immunity factors located in the *for*-operon (see below), while those struggling with cell lysis do not produce ForD on their own and are sensitive to the bacteriocin. Secondly, cell lysis after 72 h is prevented and cell integrity was highly homogeneous for *degU32* mutants, which lack ForD. Interestingly, DegU controls the expression of at least three bacteriocins and toxin/anti-toxin systems in *B. subtilis*. This includes DegU-P-dependent repression of the *wapA-wapI* operon, encoding the toxic WapA and its anti-toxin WapI as well as expression of the SdpC-paralog YitM and its anti-toxin YitQ by DegU (Kobayashi 2007b; Baptista *et al.* 2013; Stempler *et al.* 2017). YitQ is directly associated with biofilm formation in *B. subtilis* (Kobayashi and Ikemoto 2019), but neither YitM/YitQ nor WapA/WapI are encoded in the genome of *B. licheniformis*. Alternative to lack of ForD, lower autolysin activity due to repression of *sigD*/SigD in *degU32* strains cannot be excluded to affect cell integrity. However, phenotypical analysis within this thesis showed that the *degU32* and *sigD* mutation affect cell morphology and cell lysis in a media- and growth phase-dependent manner. The findings presented led to the conclusion, that inhibition of SigD-dependent autolysin expression by *degU32* most likely does not affect cell morphology and cell lysis during later fermentation stages in the simulated fed-batch process using chemically defined media. These observations are in line with the known function of SigD as a (late) exponential-phase sigma factor in *B. subtilis*, whereas SigD-dependent gene expression decreases after entering stationary growth (Kearns and Losick 2005; Chen *et al.* 2009).

The observation of reduced or complete loss of ForD expression in *B. licheniformis* strains carrying the *degU32* allele raises the question how *degU32* affects *forD* expression. In *B. subtilis*, DegU(-P) controls expression of at least three bacteriocins and toxin/anti-toxin systems. Moreover, the DegS-DegU system controls synthesis of non-ribosomal synthesized peptide antibiotics in various *Bacillus* species suggesting a conserved role of the response regulators in intra- and interspecies competition (Kobayashi 2007b; Baptista *et al.* 2013; Stempler *et al.* 2017; Kobayashi and Ikemoto 2019). ForD may represent an additional target of DegU(-P), which is specific for *B. licheniformis*, but no direct role of DegU/DegU-P in *forD* expression has been described. ForD is chromosomally encoded in the polycistronic *forD-forE-forF-forG* operon, with *forE, forF* and *forG* being involved in processing of ForD and conferring immunity to the host cell (Lundström 2012). However, only little is known about transcriptional control

and the expression profile of *forDEFG*, except for a predicted sigma factor H-type (SigH) promoter sequence (Britton *et al.* 2002; Lundström 2012). In *Bacillus*, SigH controls transcription of early stationary phase genes, many of which are involved in sporulation, genetic competence and physiological processes associated with transition to stationary phase in general (Dubnau *et al.* 1988; Grossman 1995; Britton *et al.* 2002). One central function of SigH is to initiate a positive feedback loop formed by Spo0A-P, AbrB and SigH that promotes high levels of Spo0A-P in the pre-divisional cell. Thereby, SigH exerts a direct and indirect function in sporulation initiation (Weir *et al.* 1991; Predich *et al.* 1992; Strauch 1995; Fujita and Sadaie 1998). Once polar septation is accomplished, SigH becomes dispensable for subsequent sporulation stages and SigH-dependent gene expression decreases (Healy *et al.* 1991; Nicolas *et al.* 2012; Riley *et al.* 2018). In line with the temporal expression pattern of SigH activity, analysis by Dusan *et al.* (2012) indicated, that the antimicrobial activity of supernatants obtained from *B. licheniformis* D1 increases during late exponential growth in LB cultures and maintains at a high level before decreasing during late stationary growth. However, it is unlikely that *B. licheniformis degU32* strains expressed ForD at an earlier point during cultivation, as single cell analysis showed high cell integrity throughout the full simulated fed-batch process. The lack of predicted DegU-binding site suggests an indirect role of DegU/DegU-P in regulating *forDEFG* expression. However, the exact function remains elusive and was not further studied within this thesis. Alternative to indirect or direct transcriptional control of *forDEFG* by DegU/DegU-P, higher proteolytic activity in *B. licheniformis degU32* strains may resulted in degradation of ForD, as previous analysis indicate that ForD is susceptible to proteolytic digestion (Dusane *et al.* 2013). However, no reduction in ForD was observed when introducing the BLAP expression cassette as comparison of *B. licheniformis* M309 and M409 showed.

Taken together, the findings presented suggest ForD-induced cell lysis under simulated fed-batch conditions, which is prevented upon introduction of the *degU32* allele. Future analysis should aim at analyzing whether *B. licheniformis* M409 cells, that seem vital after 72 h, maintain integrity beyond 72 h, which would indicate immunity to the bacteriocin. The presence of immune and sensitive cells is characteristic and fundamental to cannibalistic behavior in *Bacillus* as shown for SdpC and SkfA (González-Pastor 2011). In contrast, if cell lysis in *B. licheniformis* M409 is a gradual process, the coexistence of immune and sensitive cells can be excluded, and cell lysis is likely to result from induction of autolysis during later cultivation stages. To analyze potential bistability in ForD expression, *forD* promoter reporter gene fusion could complement the analysis. This setting should include a strain background defective in *forD*, as otherwise the ForD sensitive subpopulation undergoes cell lysis. Finally, single deletion of ForD would allow to demonstrate, whether reduced cell lysis in *degU32* mutants results from lack of ForD or rewiring of the global gene regulatory network. A *B. licheniformis* Δ*forD* strain is also of interest to elucidate the underlying reason for increased biofilm formation in *B. licheniformis*

M436 (*degU32*). Previous analysis showed disruption of *C. albicans*, *P. aeruginosa* and *B. pumilus* biofilms upon addition of purified ForD suggesting that loss of ForD may contribute to higher biofilm robustness in *B. licheniformis* M436 (Lundström 2012; Dusane *et al.* 2013).

5 Summary and conclusion

Bacillus species invest substantial resources in inherent cellular processes for pre-adaptation to environmental changes, many of which are dispensable in the controlled environment of industrial bioprocesses. The underlying physiological mechanisms are well characterized in *B. subtilis*, but only little is known about these processes in the closely related *B. licheniformis*. Moreover, experimental conditions in previous studies differ from industrial settings in most parameters, foremost in batch cultures or plate-based analysis over fed-batch processes. In this thesis, cellular heterogeneity was analyzed in *B. licheniformis* DSM641 in optimized, nutrient-rich media in batch and fed-batch cultivations. Systematic inactivation of genes involved in biofilm formation and synthesis of the flagellar apparatus or global regulators thereof resulted in higher protein production and provided new insights in biofilm formation and cellular heterogeneity in this strain. Unlike *B. subtilis*, the hydrophobic coat protein BslA is dispensable for complex colony architecture in *B. licheniformis* DSM641. Moreover, SlrA rather than SinI seems to be the major anti-repressor of SinR in biofilm formation in *B. licheniformis* DSM641. Characterization of mutants deficient in *sigD*, *hag* or *motB* provided further evidence for a regulatory loop in which expression of SigD and the whole SigD-regulon is coupled to functional assembly of the flagellar apparatus as can be concluded from several studies in *B. subtilis*. The strongest alterations in morphology and physiology became apparent in *B. licheniformis* DSM641 strains carrying the *degU32* allele. Although the *degU32* allele has been extensively analyzed in *B. subtilis* and related species, new findings were provided within this thesis. It is well known that DegU-P is required for biofilm formation in *B. subtilis*, but an increase in biofilm robustness similar to that observed in this thesis has not been reported. Moreover, the function of DegU-P in biofilm formation has been assigned to regulation of *yvcE*, *pga* and *bslA*, but neither of the latter two was required for the phenotype of *B. licheniformis* DSM641 *degU32* strains. Instead, DegU-P may indirectly affect expression of the major matrix components encoded by *tapA-sipW-tasA* and *epsA-O*, providing further evidence for a previously hypothesized yet unknown regulatory link to Spo0A-P in *B. subtilis*. Single cell analyses of fluorescence reporter strains showed that improved process conditions can reduce the formation of undesirable cell types and subpopulations. However, introduction of the *degU32* allele resulted in strong biofilm formation under all conditions tested and, thus, is intrinsic to *B. licheniformis* DSM641 strains carrying the *degU32* allele. To overcome possible limitations resulting from filamentation and cell aggregation, including oxygen and nutrient gradients within these microenvironments, morphological engineering was performed by deletion of *remA*, *slrA*, *epsA-O* and *tapA-sipW-tasA*. The resulting biofilm deficient strains, carrying the *degU32* allele, showed almost wildtype-like cell morphology and an increase in protease expression when compared to the already improved product titer in the *degU32* single mutant *B. li-*

cheniformis M436. Comprehensive characterization of optimized strains, including single cell experiments, analysis of P*apr* expression dynamics, and extracellular proteomics, suggest that the higher protease expression resulted from a combination of multiple factors. As expected from the known positive effect of DegU-P on exoenzyme expression, protease expression was earlier, stronger, and more homogeneous in *B. licheniformis* M441 carrying the *degU32* allele combined with deletion of *epsA-O* and *tapA-sipW-tasA* under batch conditions. However, the DegU-P autostimulatory loop was intrinsically strong in *B. licheniformis* DSM641, as concluded from single cell analysis, and *B. licheniformis* M441 (M641) was not superior to the control strain *B. licheniformis* M409 (M609.1) during the early phase of simulated fed-batch cultivation. The strongly improved strain characteristics became apparent for *B. licheniformis* M641 in later cultivation stages only, in which *B. licheniformis* M409 (M609.1) was severely affected by cell lysis and showed high heterogeneity in P*apr* activity. In contrast, *B. licheniformis* M641 was characterized by a steady increase and high homogeneity in P*apr* dependent GFP expression, which most likely results from strongly improved cell viability upon introduction of the Δ*eps*, Δ*tasA* and *degU32* mutations. Since inactivation of *remA* and *slrA* had a similar effect on protease expression, the improved strain characteristics presumably apply to biofilm-deficient *degU32* strains of *B. licheniformis* DSM641 in general. Evidence for the underlying physiological reason for improved cell viability was provided by extracellular proteomics, in which the bacteriocin ForD was among the most abundant proteins in the secretome of *B. licheniformis degU* wildtype strains. In contrast, ForD was absent from strains carrying the *degU32* allele. The functional relation of DegU(32)-P and expression of ForD was described for the first time, thereby assigning a new function to the global response regulator DegU. Finally, a potential role of the poorly characterized ForD as a cannibalism factor in *B. licheniformis* to delay commitment to sporulation was proposed.

In this thesis systematic analysis of cellular responses of *B. licheniformis* to limiting environmental conditions was performed and new targets for strain improvement were identified. Similarly, only recently systematic inactivation of stress-related genes identified new targets for improved protein production in *E. coli* (Sharma *et al.* 2020). Considering the high number of cellular adaptation processes and stress response mechanisms in *Bacillus* and beyond, the potential of similar strain development approaches in the future is emphasized.

6 Supplemental material

6.1.1 Characterization of *B. licheniformis remA*, *sinI*, *slrA* mutants

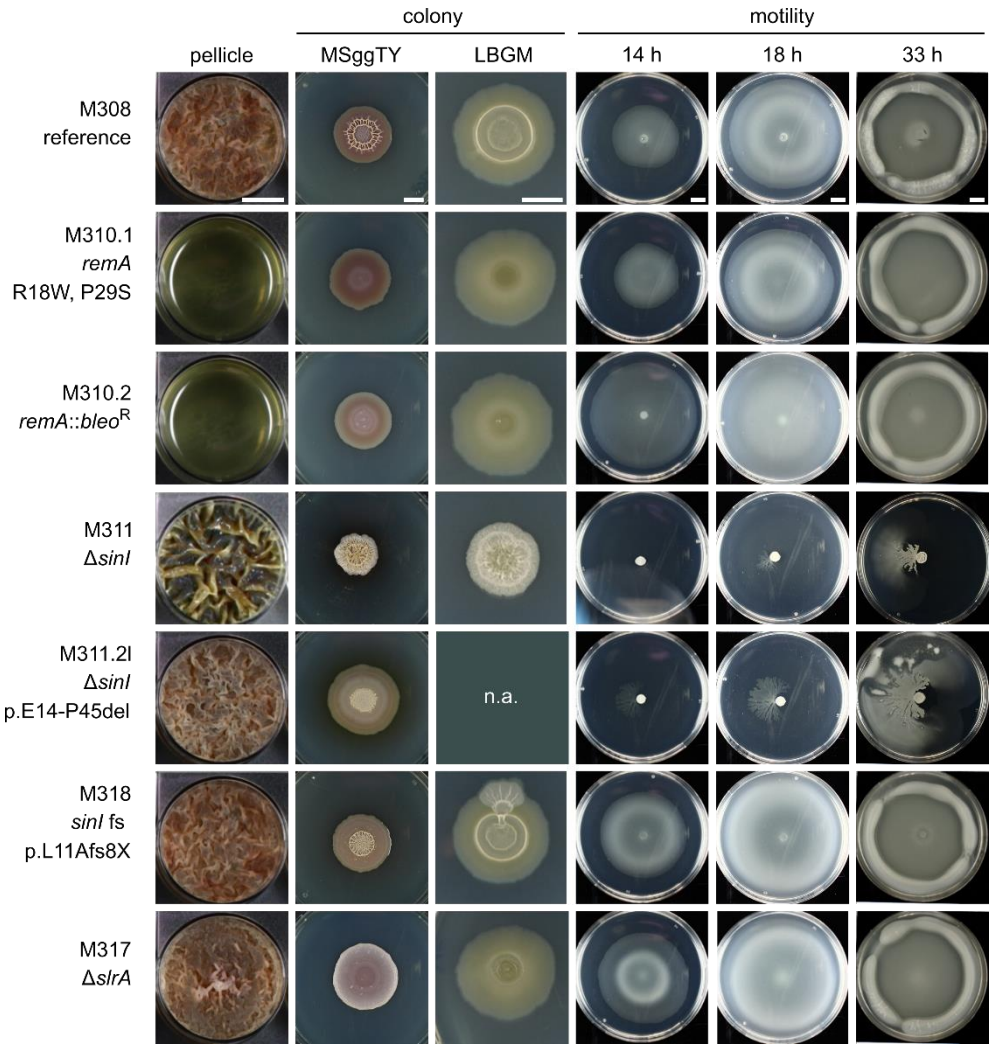

Figure S1: Biofilm formation and motility of *B. licheniformis remA* and *sinI* mutants. The ability to form biofilms was analyzed by pellicle formation and colony architecture assays using liquid and solid MSggTY medium respectively. Unlike all other samples, pellicle formation assay of the Δ*sinI* strain M311 was performed with modified LB medium containing 0.05 mM $MnSO_4$ and 1 % glycerol initially used to assess biofilm formation (LBGM). Swimming motility was analyzed after 14 h, 18 h and 33 h of growth on semi-solid LB agar (0.4 %). All strains are based on the wildtype-close *B. licheniformis* M308. White scale bars indicate 1 cm.

6.1.2 Biofilm formation assay of *B. licheniformis* Δ*bslA* mutants

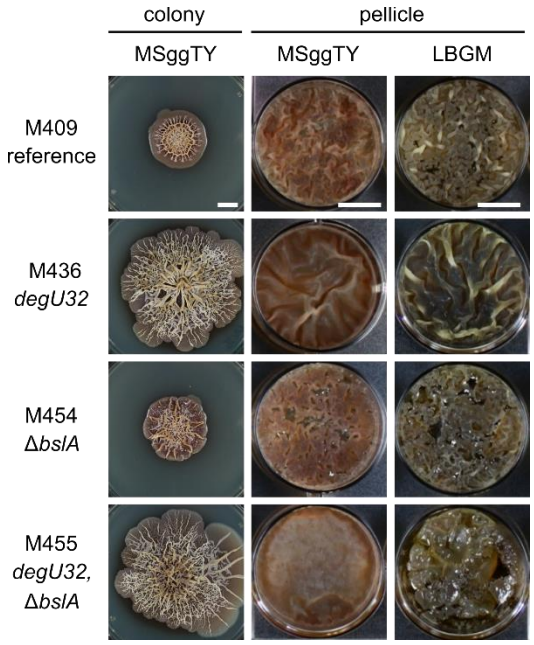

Figure S2: Biofilm formation assay of *B. licheniformis* single (M454) and combinatorial (M455) *bslA* mutants. The ability to form biofilms was analyzed by pellicle formation and colony architecture assays using liquid and solid MSggTY medium respectively. In addition to MSggTY, LBGM medium was used in the pellicle formation assay. Expression of *bslA* is the main target of DegU-P in *B. subtilis*, but deletion of *bslA* in *B. licheniformis* did not prevent biofilm formation. However, deletion of *bslA* affects pellicle structure.

6.1.3 Cell morphology of *B. licheniformis* M312 Δ*sigD* in LB medium

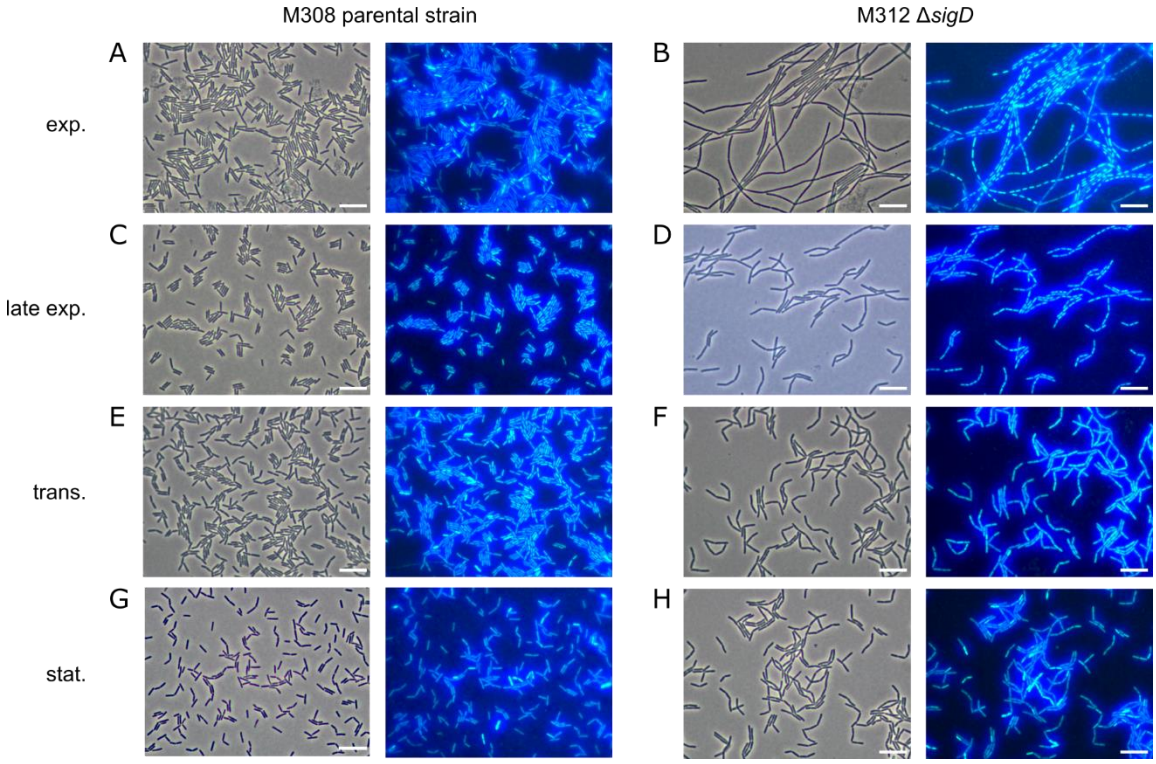

Figure S3: Cell morphology of *B. licheniformis* M312 (Δ*sigD*) in LB batch cultivations. *B. licheniformis* M308 and M312 (Δ*sigD*) were cultivated at 37 °C in shake flasks in LB medium. Phase contrast and DAPI channel images are shown. White scale bar indicates 10 µm. The filamentous phenotype resulting from deletion of *sigD* was observed most pronounced during exponential growth. Samples from stationary phase showed almost wildtype-like (M308) cell morphology.

6.1.4 Cell morphology of *degU32* mutants in fed-batch cultivation

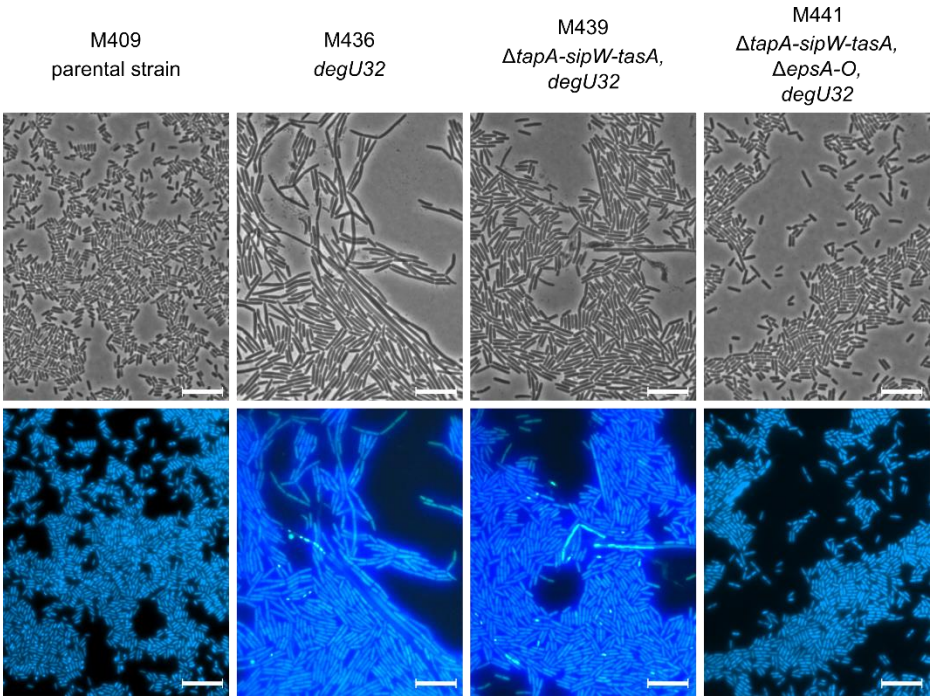

Figure S4: Cell morphology of *B. licheniformis degU32* mutants in fed-batch cultivation. Strains carrying single or multiple mutations (as indicated) were cultivated in the simulated polymer-based feedback process (feedplates). Samples were taken after 24 h and analyzed by microscopy without further processing (staining was conducted by supplementing the agarose patch with DAPI. Phase contrast (top) and DAPI staining of nucleic acid (bottom) images are shown. White scale bar indicates 10 µm. *B. licheniformis* M436 showed filamentous growth and cell chaining, which was reduced upon deletion of *tapA-sipW-tasA* (M439). Additional deletion of *epsA-O* (M441) resulted in wildtype-like cell morphology as comparison to the control strain *B. licheniformis* M409 showed.

6.1.5 Maximum specific growth rates of *B. licheniformis* mutants

Table S1: Maximum specific growth rate of *B. licheniformis* mutants in LSJ-CT and V3 medium. All strains with a M400 number are derived from *B. licheniformis* M409.

			V3 medium		LSJ-CT medium	
Strain	**Key mutation**	**N =**	**μmax h^{-1}**	**σ**	**μmax h^{-1}**	**σ**
M321	Δ*pga*, Δ*apr*	2	0.220	0.007	0.256	0.009
M409	Δ*apr*, Δ*sigF*, *pga*::BLAP	5	0.199	0.018	0.226	0.005
M422	Δ*sigD*	5	0.230	0.018	0.295	0.009
M423	Δ*motB*	2	0.224	0.000	0.262	0.001
M435	Δ*hag*	5	0.227	0.013	0.281	0.008
M430	Δ*tasA*	5	0.215	0.019	0.222	0.008
M431	Δ*eps*	2	0.215	0.008	0.240	0.002
M440	Δ*eps,* Δ*tasA*	5	0.205	0.021	0.235	0.002
N454	Δ*bslA*	2	0.195	0.008	0.234	0.005
M432	Δ*slrA*	2	0.220	0.006	0.228	0.002
M434	*remA*	2	0.230	0.005	0.245	0.001
M436	*degU32*	5	0.191	0.009	0.282	0.017
M455	Δ*bslA, degU32*	2	0.204	0.000	0.312	0.002
M439	Δ*tasA, degU32*	2	0.186	0.009	0.296	0.005
M441	Δ*eps,* Δ*tasA, degU32*	5	0.195	0.010	0.280	0.021
M447	Δ*eps,* Δ*tasA,* Δ*sigD*	2	0.226	0.014	0.304	0.005
M448	Δ*eps,* Δ*tasA,* Δ*sigD, degU32*	2	0.197	0.003	0.313	0.006
M456	Δ*eps,* Δ*tasA,* Δ*bslA, degU32*	2	n.a.	n.a.	0.283	0.010
M451	Δ*slrA*, *degU32*	2	0.178	0.001	0.285	0.002
M452	*remA, degU32*	2	0.176	0.005	0.283	0.003
M453	Δ*eps,* Δ*tasA, Δhag, degU32*	2	0.193	0.011	0.301	0.002
M457	Δ*eps,* Δ*tasA,* Δ*bslA,* Δ*sigD, degU32*	5	0.185	0.009	0.272	0.017
M449	Δ*sigD, degU32*	2	0.187	0.010	0.285	0.001

6.1.6 Inoculum dependent growth behavior of *B. licheniformis degU32* mutants

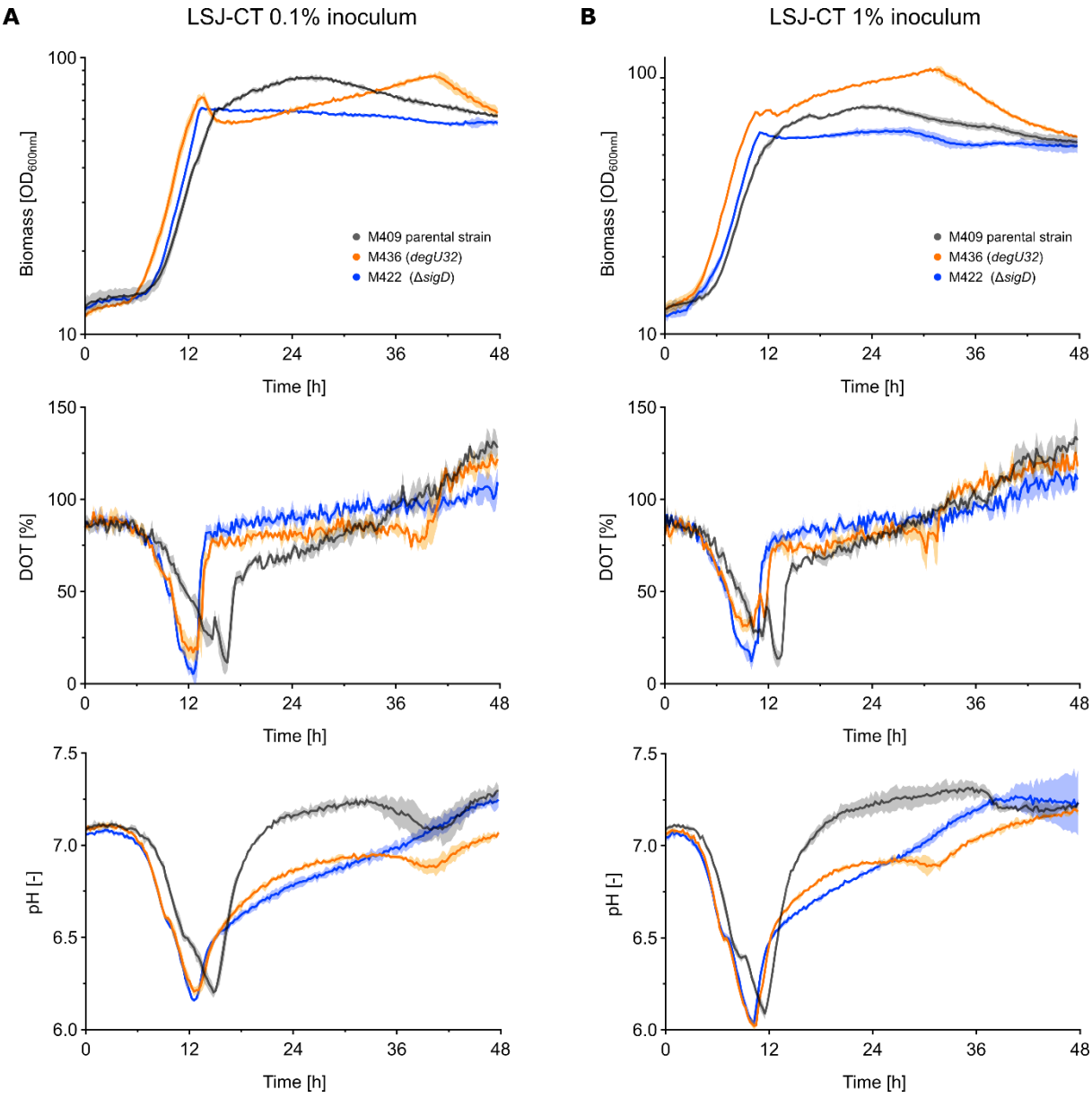

Figure S5: Effect of the inoculum on growth in LSJ-CT batch cultures of *B. licheniformis* strains. Biomass (scattered light, upper panel), dissolved oxygen tension (DOT, middle panel) and pH (lower panel) were monitored during 48 h of cultivation. LSJ-CT main cultures were inoculated with 0.1 % and 1 % of growth-synchronized pre-cultures respectively. Shaded areas indicated standard deviations of three biological replicates. The growth curves shown are representative for three groups of strains: (Grey) *B. licheniformis* M409, M430 (Δ*tasA*) and M440 (Δ*eps*, Δ*tasA*). (Orange) Strains harbouring the *degU32* mutation *B. licheniformis* M436 (*degU32*), M441 (Δ*eps*, Δ*tasA, degU32*). (Blue) *B. licheniformis* M422 (Δ*sigD*) and M435 (Δ*hag*).

6.1.7 Clustering of growth curves of *B. licheniformis* mutants

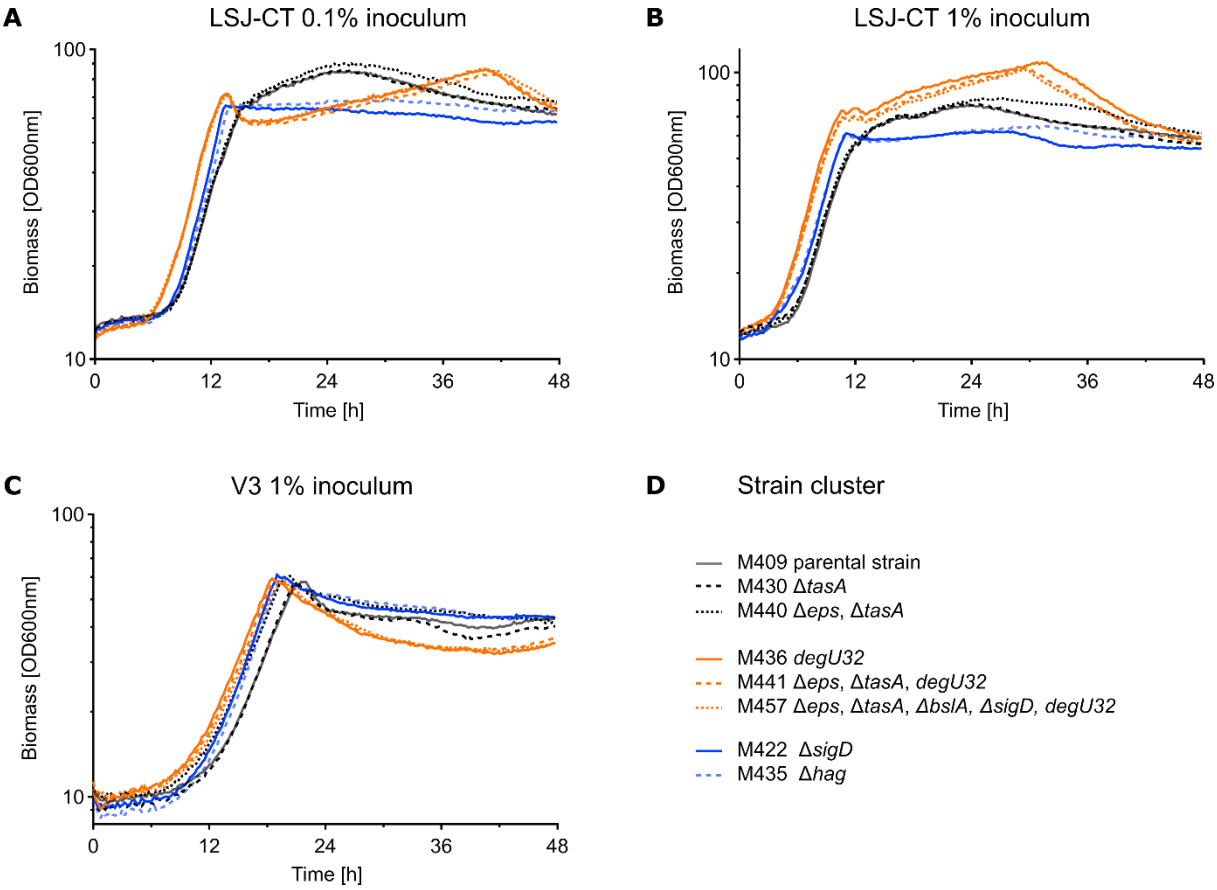

Figure S6: Growth of selected mutants in batch cultures during 48 h of cultivation using rich (LSJ-CT) and chemically defined (V3) medium. Biomass (OD600nm) was monitored online. For both media comparison of *B. licheniformis* M409 mutants revealed three distinct types of growth curves each representing a specific subset (cluster) of strains. The first group comprises the parental strain M409 and strains exclusively deficient in/for biofilm formation M430 (Δ*tasA*) and M440 (Δ*eps*, Δ*tasA*) (black, grey). Secondly, all strains harbouring the *degU32* mutation showed similar growth behaviour independent from additional mutations (orange). The last group summarizes strains mutated for *hag* or *sigD* required for motility (blue).

6.1.8 Locus evaluation in *B. licheniformis* M308 *amyB*::G2r

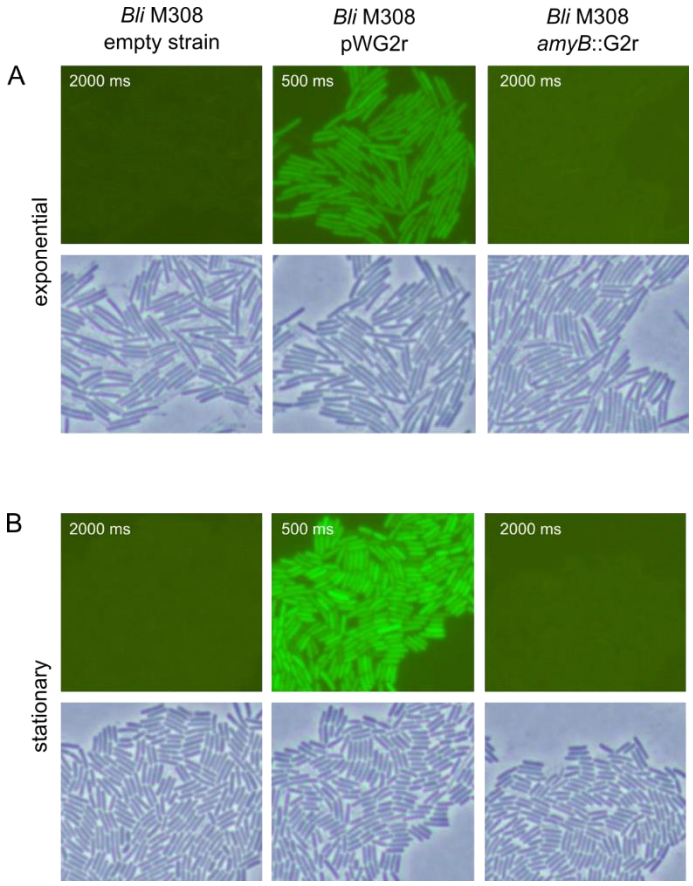

Figure S7: Evaluation of the *B. licheniformis* DSM641 *amyB* locus regarding transcriptional read-through. To evaluate the *amyB* locus for integration of promoter reporter gene cassettes potential read-through from promoters located upstream of *amyB* was analyzed. A promoter-less gfpmut2 with a standardized, strong ribosome binding site (R0, Guiziou *et al.* 2016) was integrated into *amyB* using plasmid pJOE_*amyB*::G2r. As for all reporter gene fusions constructed in this thesis, the *gfp* cassette was flanked by transcriptional terminators as described for *amyB*::P*apr-gfpmut2* constructs (see 7.8). The plasmid carrying *B. licheniformis* M308 pWG2r was used as a positive control. Previous experiments confirmed transcriptional read-through from the upstream located promoter driving expression of the kanamycin resistance gene present on the pBW944 backbone into the promoter-less R0-*gfpmut2*. All strains were cultivated in shakes flask in LB medium and GFP expression was analyzed by fluorescence microscopy during exponential (A) or stationary growth (B). For *B. licheniformis* M308 pWG2r 20 µg/ml kanamycin sulfate was added. As no GFP expression was observed for *B. licheniformis* M308 *amyB*::G2r the *amyB* locus was suitable for integration of reporter gene constructs.

6.1.9 Growth (OD_{600nm}) of *B. licheniformis* mutants at selected time points during fed-batch cultivation

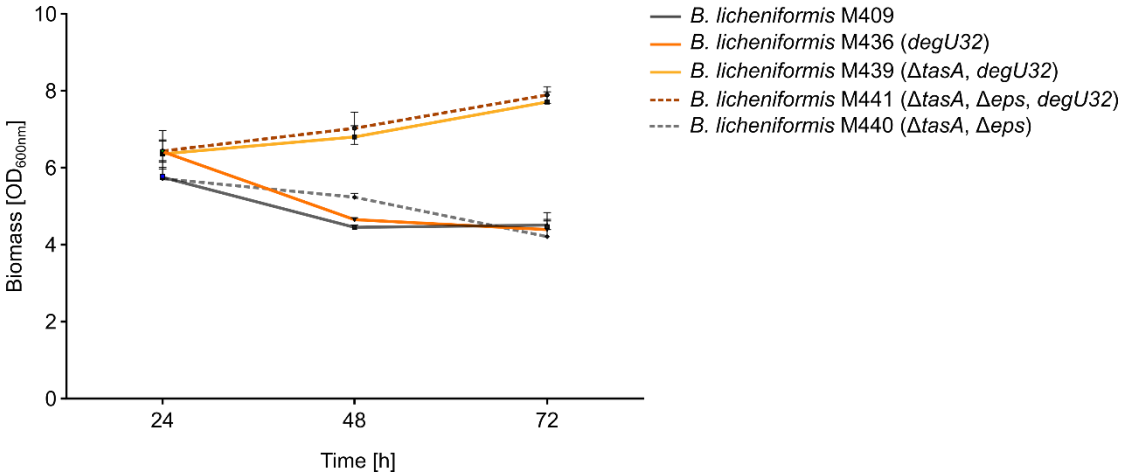

Figure S8: Growth of selected *B. licheniformis* strains during fed-batch phase. Optical density (OD_{600nm}) was determined after 24, 48 and 72 h of microtiter plate-based fed-batch cultivation. The initial OD_{600nm} (t=0) was 0.9 – 1.1 for all strains. Strain number and genotype were as indicated. Note, that the optical density of *degU32* single mutant *B. licheniformis* M436 decreased from 24 to 72 h similar to the control strain *B. licheniformis* M409 and the biofilm-deficient *B. licheniformis* M440. In contrast, the biofilm-deficient *degU32* combinatorial mutants *B. licheniformis* M439 and M441 showed a steady increase in OD_{600nm} throughout growth. But, the differences observed between *B. licheniformis* M436 and *B. licheniformis* M439/M441 are not line with the results from determination of cellular dry weight, which showed a comparable increase in biomass for these strains.

6.1.10 Normalized protease promoter activity in batch cultivation

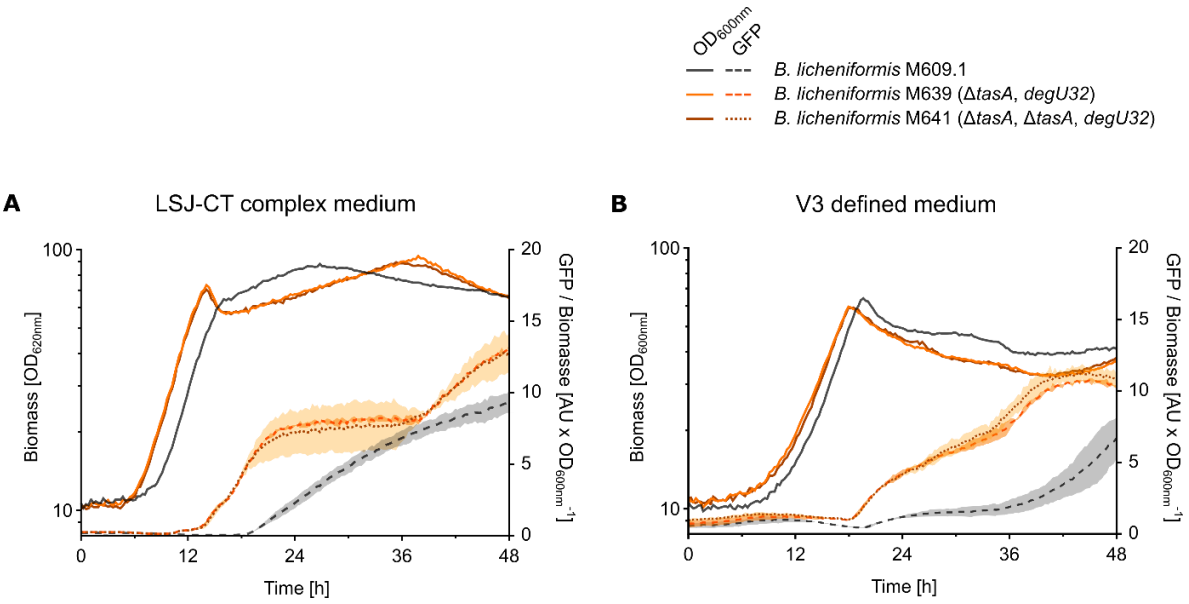

Figure S9: Normalized P*apr* promoter activity for selected *B. licheniformis* strains in batch culture. Reporter strain carrying the *amyB*::P*apr-gfpmut2* reporter gene fusion were cultivated in (A) rich and (B) defined medium using the microbioreactor system BioLector (1000 rpm, 3 mm shaking diameter, 30 °C, 85 % relative humidity). Strain number and relevant genotype were as indicated. Scattered light (OD_{600nm}) and biomass-normalized GFP fluorescence, representing P*apr* activity, are shown. Shaded areas indicate standard deviation from two biological replicates. Promoter activity profiles were smoothened using GraphPad Prism 8 (12 neighbors, 2nd order). Note that *B. licheniformis* M648 behaved identical to *B. licheniformis* M641 and is therefore not shown.

6.1.11 Extracellular proteome of *B. licheniformis* M309, M409, M436 and M409

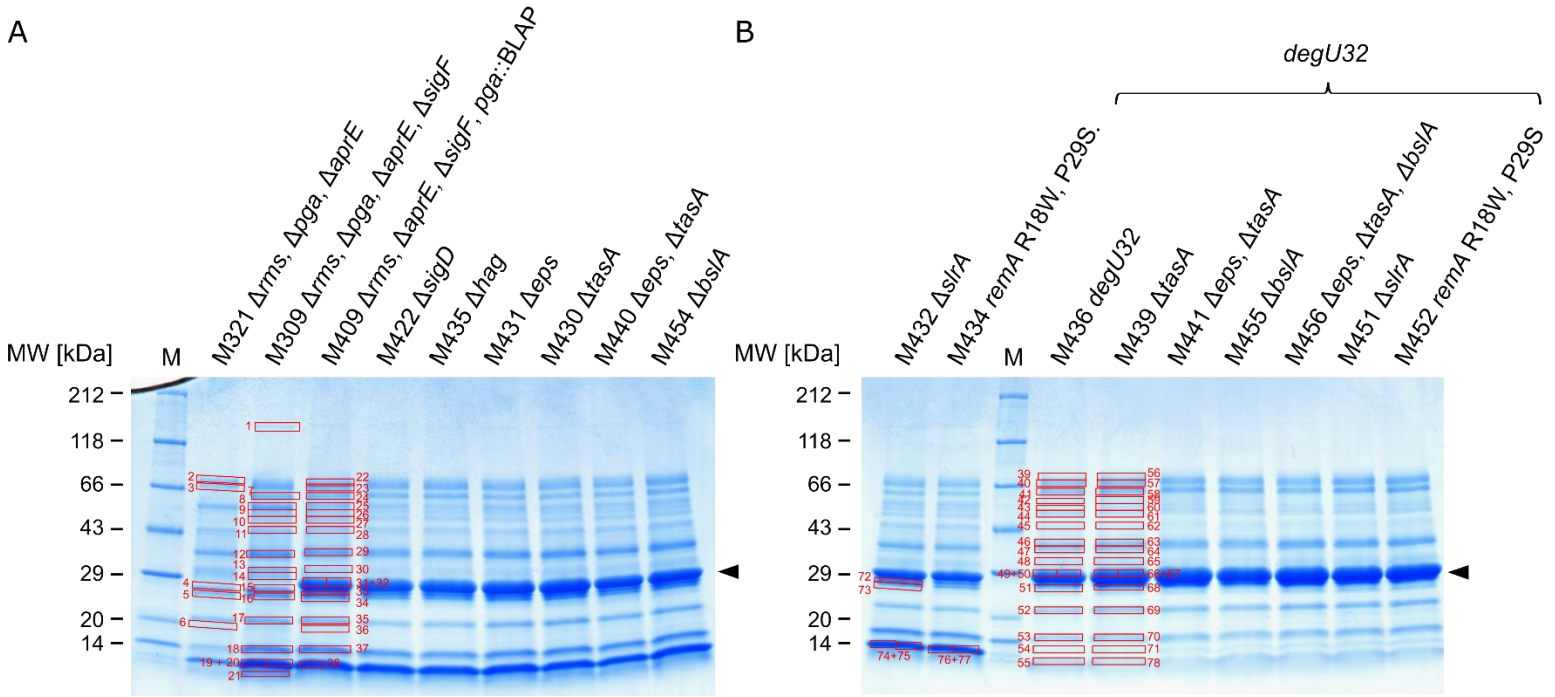

Figure S10: Sample overview of protein bands analyzed by MALDI-TOF MS/MS. Biomass was separated from the culture broth by sterile filtration after 72 h of microtiter plate-based fed-batch cultivation following TCA precipitation of proteins in the supernatant and sample preparation as described in section 7.4.2. A) and B) Proteins were separated by SDS-PAGE using a 4 - 20 % polyacrylamide Tris-Glycine gel. The extracellular proteome was characterized for the control strains *B. licheniformis* M309, M409 and the *degU32* mutants *B. licheniformis* M436 (*degU32*), M439 (Δ*tapA-sipW-tasA*, *degU32*) by MALDI-TOF. The protein bands analyzed are marked in red with the corresponding sample number next to band. The genotype for the strains is shown in A) and B). As *B. licheniformis* M422 to M452 are derived from *B. licheniformis* M409, only the key mutations introduced in these strains are indicated.

Table S2: Identification of protein bands via MALDI-TOF. Proteins with a score higher 49 are considered as significant. Only significant hits are listed. Colour code: dark green = *B. licheniformis* M321 (Δ*rms*, Δpga, Δ*apr*), blue = *B. licheniformis* M309 (Δ*rms*, Δ*pga*, Δ*apr*, Δ*sigF*), green= *B. licheniformis* M409 (Δ*rms*, Δ*apr*, Δ*sigF*, *pga*::BLAP), yellow = *B. licheniformis* M436 (Δ*rms*, Δ*apr*, Δ*sigF*, *pga*::BLAP, *degU32*), orange = *B. licheniformis* M439 (Δ*rms*, Δ*apr*, Δ*sigF*, *pga*::BLAP, Δ*tapA-sipW-tasA*, *degU32*).

Sample No.:	Rank	Protein Name; locus tag	Protein MW [Da]	Peptide Count	Protein Score	Protein Score C.I. %	Total Ion Score	Total Ion Score C.I. %	Total MS Ion Cluster Area	MS Ion Cluster Area Matched %
1	1	YfkN 5'-nucleotidase, N-terminal, degrades cyclic di-AMP; BL03110	155.603	17	190	100	142	100	130.257	88
11	2	AhpA (YkuU) alkyl hydroperoxide reductase; BL05145	20.390	5	273	100	242	100	1.378.091	27
11	1	Aminopeptidase YwaD; BL03935	48.162	10	385	100	331	100	1.378.091	127
27	2		48.162	6	101	100	81	100	575.112	65
28	1		48.162	10	354	100	301	100	402.493	140
45	1		48.162	5	223	100	208	100	248.940	116
62	1		48.162	3	190	100	182	100	125.932	49
9	1	AmyL alpha amylase; also identified in *B. licheniformis* M439 (sample 60) but protein score = 44.9; BL00499	58.493	12	114	100	53	100	642.040	37
26	2		58.493	11	104	100	50	100	536.882	26
3	2	Bacillopeptidase F; BL02253	154.934	10	152	100	136	100	467.485	20
7	1		154.934	20	230	100	161	100	368.503	44
22	1		154.934	6	214	100	206	100	390.566	38
23	1		154.934	11	230	100	209	100	499.549	69
24	1		154.934	14	478	100	446	100	405.377	55
39	1		154.934	3	123	100	123	100	123.264	17
40	1		154.934	10	213	100	195	100	325.285	84
41	1		154.934	12	370	100	347	100	403.850	58
42	1		154.934	11	188	100	169	100	250.828	26
43	1		154.934	7	99	100	89	100	140.851	36
55	3		154.934	5	64	100	64	100	264.631	14
57	1		154.934	11	199	100	177	100	250.191	89
58	1		154.934	15	294	100	257	100	544.692	63
59	1		154.934	11	221	100	202	100	616.960	45
60	3		154.934	7	78	100	69	100	72.148	16
78	3		154.934	7	128	100	120	100	1.164.635	19
2	1	BgaB, beta-galactosidase; not identified in *B. licheniformis* M436/M439 (also not with protein score < 50); BL01749	79.108	13	363	100	313	100	664.768	94
22	3		79.108	12	77	100	33	100	390.566	44
30	3	BglC, endo-1,4-beta-glucanase; BL01471	58.684	3	51	97	44	100	212.433	7
55	1	BL05117, unknown	12.699	2	344	100	331	100	264.631	73
78	1		12.699	2	219	100	206	100	1.164.635	16

Table S2, continued

Sample No.:	Rank	Protein Name; locus tag	Protein MW [Da]	Peptide Count	Protein Score	Protein Score C.I. %	Total Ion Score	Total Ion Score C.I. %	Total MS Ion Cluster Area	MS Ion Cluster Area Matched %
8	1	PutC (YcgN) delta-1-pyrroline-5-carboxylate dehydrogenase; BL01710	56.620	11	156	100	110	100	449.453	32
9	2		56.620	7	97	100	75	100	642.040	16
25	1		56.620	8	115	100	91	100	894.645	25
26	1		56.620	10	149	100	106	100	536.882	41
42	2		56.620	5	114	100	101	100	250.828	12
59	2		56.620	4	92	100	82	100	616.960	10
60	2		56.620	5	88	100	73	100	72.148	11
2	2	Extracellular serine protease Vpr; also identified in sample 7, 40 and 57 (in all strains) but with protein score < 50; BL03950	85.573	15	66	100	5	0	664.768	40
3	1		85.573	19	305	100	211	100	467.485	67
22	2		85.573	13	128	100	81	100	390.566	26
23	2		85.573	11	71	100	37	100	499.549	20
39	2		85.573	8	54	98	35	100	123.264	9
19	1	ForD bacteriocin; BL00275	14.050	6	237	100	191	100	2.302.851	63
21	2		14.050	5	116	100	79	100	4.138.330	47
75	1		14.050	4	148	100	120	100	3.495.585	6
76	1		14.050	2	89	100	79	100	1.963.735	70
77	1		14.050	5	204	100	167	100	3.026.183	66
6	3	Ggt gamma-glutamyltranspeptidase; gamma-glutamlytransferase family (EC 2.3.2.2 and EC 3.4.19.13); BL03798	60.935	12	54	98			958.604	18
12	1		60.935	14	368	100	294	100	1.483.743	145
13	1		60.935	8	228	100	200	100	908.783	44
14	1		60.935	7	111	100	88	100	505.454	22
17	1		60.935	10	155	100	113	100	3.056.831	32
29	1		60.935	13	446	100	382	100	1.332.625	148
30	1		60.935	10	121	100	82	100	212.433	42
35	1		60.935	9	145	100	108	100	2.497.401	28
46	1		60.935	14	314	100	238	100	930.173	150
47	1		60.935	12	305	100	248	100	969.163	139
52	1		60.935	10	141	100	98	100	1.585.792	37
63	1		60.935	14	359	100	284	100	996.231	151
64	1		60.935	13	351	100	286	100	1.099.295	134
65	1		60.935	9	138	100	107	100	388.238	23
69	2		60.935	10	92	100	50	100	2.016.763	20
4	2	GluBL glutamyl endopeptidase; BL01804	33.590	7	143	100	107	100	1.718.380	50
15	2		33.590	7	243	100	206	100	3.194.202	54
33	3		33.590	5	70	100	49	100	862.311	37
51	2		33.590	6	73	100	45	100	425.242	40
68	2		33.590	7	83	100	46	100	909.597	46
72	2		33.590	4	59	99	44	100	721.273	20
21	1	Hfq, host factor-1 protein, RNA chaperone; BL05175	8.482	5	218	100	171	100	4.138.330	14
55	2		8.482	3	86	100	62	100	264.631	14
71	2		8.482	2	82	100	68	100	899.106	3
78	2		8.482	4	133	100	98	100	1.164.635	30

Table S2, continued

Sample No.:	Rank	Protein Name; locus tag	Protein MW [Da]	Peptide Count	Protein Score	Protein Score C.I. %	Total Ion Score	Total Ion Score C.I. %	Total MS Ion Cluster Area	MS Ion Cluster Area Matched %
70	1	Intracellular proteinase inhibitor Ipi; BL02625	16.947	2	124	100	115	100	501.610	10
25	2	PdhD dihydrolipoamide dehydrogenase subunit; BL01619	49.650	6	97	100	77	100	894.645	21
30	2	pro-BLAP (*Bacillus lentus* alkaline protease)	36.387	1	85	100	85	100	212.433	9
48	1		36.387	7	469	100	436	100	1.584.638	59
65	2		36.387	7	106	100	73	100	388.238	24
31	1	BLAP (*Bacillus lentus* alkaline protease)	36.387	8	609	100	566	100	220.543	130
32	1		36.387	9	418	100	358	100	261.662	106
33	2		36.387	8	109	100	67	100	862.311	36
50	1		36.387	8	380	100	334	100	776.564	106
51	1		36.387	7	230	100	196	100	425.242	61
66	1		36.387	8	408	100	347	100	306.941	130
67	1		36.387	7	229	100	172	100	94.081	58
68	1		36.387	8	247	100	204	100	909.597	46
72	1		36.387	7	137	100	104	100	721.273	15
54	1		36.387	2	90	100	84	100	318.094	10
42	3		36.387	6	73	100	46	100	250.828	18
71	1		36.387	5	124	100	104	100	899.106	10
10	1	Putative carboxypeptidase; BL03063	60.645	11	438	100	388	100	1.019.471	60
27	1		60.645	13	460	100	393	100	575.112	68
44	1		60.645	16	412	100	318	100	795.516	83
45	2		60.645	7	111	100	88	100	248.940	18
60	1		60.645	9	88	100	53	100	72.148	26
61	1		60.645	13	353	100	286	100	236.699	64
69	1		60.645	5	331	100	316	100	2.016.763	22
6	1	Putative chitin binding protein; BL00145	22.641	5	221	100	191	100	958.604	37
5	1	SodA superoxide dismutase; BL03706	22.530	11	517	100	425	100	2.546.033	98
15	1		22.530	7	348	100	301	100	3.194.202	44
16	1		22.530	6	459	100	422	100	1.879.821	93
33	1		22.530	5	314	100	285	100	862.311	49
34	1		22.530	5	461	100	432	100	2.026.907	97
53	1		22.530	3	170	100	157	100	174.086	22
4	1		22.530	5	151	100	122	100	1.718.380	7
13	2	YvgN, 2,5-diketo-D-gluconic acid reductase; BL00701	31.780	9	168	100	119	100	908.783	26

7 Material and Methods

7.1 Strains, plasmids and oligonucleotides used in this study

Table S3: Strains, plasmids and oligonucleotides used in this study

Strain	Relevant genotype	Reference
E. coli DH10B	F$^-$, *mcrA,* Δ(*mrr-hsdRMS-mcrBC*), ϕ80*lacZ*ΔM15, Δ*lacX*74, *recA1*, *araD139*, Δ(*ara-leu*)7697, *galU*, *galK*, λ-, *rpsL*(Str^R), *endA1*, *nupG*	(Grant *et al.* 1990; Durfee *et al.* 2008)
E. coli INV110	F´ [*tra*Δ36, *proAB*, *lacI*^{q}, *lacZ*ΔM15], *rpsL* (Str^R), *thr*, *leu*, *endA*, *thi*-1, *lacY*, *galK*, *galT*, *ara*, *tonA*, *tsx*, *dam*, *dcm*, *supE44*, Δ(*lac-proAB*), Δ(*mcrC-mrr*)102::*Tn*10(Tet^R)	Thermo Fisher Scientific; Waltham, USA
B. licheniformis DSM641	Wildtype strain	Wilson *et al.* (1993)
B. licheniformis P304	Δ*rms*	BASF SE
B. licheniformis P305	Δ*rms*, Δ*sigF*	BASF SE
B. licheniformis P306	Δ*rms,* Δ*aprE*	BASF SE
B. licheniformis P307	Δ*rms*, Δ*sigF*, Δ*aprE*	BASF SE
B. licheniformis M308	Δ*rms*, Δ*pga*	This study
B. licheniformis M309	Δ*rms*, Δ*sigF*, Δ*aprE*, Δ*pga*	This study
B. licheniformis M321	Δ*rms*, Δ*pga*, Δ*aprE*	This study
B. licheniformis M409	Δ*rms*, Δ*sigF*, Δ*aprE*, *pga::*BLAP	This study
B. licheniformis MW3	Δ*hsdR1*, Δ*hsdR2*	Waschkau *et al.* (2008)
***B. licheniformis* M308 derivates:**		
B. licheniformis M310.1	*remA* R18W, P29S (loss of function)	This study
B. licheniformis M310.2	*remA*::*bleoR* (insertion deletion)	This study
B. licheniformis M311	Δ*sinI* (clean deletion)	This study
B. licheniformis M311.2	Δ*sinI* p.E14-P45del (partial deletion)	This study
B. licheniformis M312	Δ*sigD*	This study
B. licheniformis M313	Δ*motB*	This study
B. licheniformis M314	Δ*hag*	This study
B. licheniformis M315	Δ*tapA-sipW-tasA*	This study
B. licheniformis M317	Δ*slrA*	This study
B. licheniformis M318	Δ*sinI* p.L11Afs8X (frameshift mutation, stop codon)	This study
B. licheniformis M320	*degU32*(Hy) (H12L)	This study
B. licheniformis M329	Δ*lytC*	This study
***B. licheniformis* M409 derivates:**		
B. licheniformis M422	Δ*sigD*	This study
B. licheniformis M423	Δ*motB*	This study
B. licheniformis M430	Δ*tapA-sipW-tasA*	This study
B. licheniformis M431	Δ*epsA-epsO*	This study
B. licheniformis M432	Δ*slrA*	This study
B. licheniformis M434	*remA* R18W, P29S (loss of function)	This study
B. licheniformis M435	Δ*hag*	This study
B. licheniformis M436	*degU32* (H12L)	This study
B. licheniformis M439	Δ*tapA-sipW-tasA*, *degU32*	This study
B. licheniformis M440	Δ*epsA-epsO*, Δ*tapA-sipW-tasA*	This study
B. licheniformis M441	Δ*epsA-epsO*, Δ*tapA-sipW-tasA*, *degU32*	This study
B. licheniformis M447	Δ*epsA-epsO*, Δ*tapA-sipW-tasA*, Δ*sigD*, *degU32*	This study
B. licheniformis M448	Δ*epsA-epsO*, Δ*tapA-sipW-tasA*, *degU32*, Δ*sigD*	This study
B. licheniformis M449	*degU32*, Δ*sigD*	This study

B. licheniformis M451	Δ*slrA*, *degU32*	This study
B. licheniformis M452	*remA* R18W, P29S (loss of function), *degU32*	This study
B. licheniformis M453	Δ*eps,* Δ*tasA, Δhag, degU32*	This study
B. licheniformis M454	Δ*eps,* Δ*bslA*	This study
B. licheniformis M455	*degU32,* Δ*bslA*	This study
B. licheniformis M456	Δ*epsA-epsO*, Δ*tapA-sipW-tasA*, *degU32,* Δ*bslA*	This study
B. licheniformis M457	Δ*eps,* Δ*tasA,* Δ*bslA,* Δ*sigD, degU32*	This study
***B. licheniformis* reporter strains**		
B. licheniformis M409.t1	M409 *amyB*::P*tasA-gfpmut2*	This study
B. licheniformis M409.t2	M409 *cat*::P*tasA-mScarletI*	This study
B. licheniformis M609.1	M409 *amyB*::P*apr-gfpmut2* (P*apr* DSM641 truncated)	This study
B. licheniformis M609.2	M409 *amyB*::P*apr-gfpmut2*-DAV (P*apr* DSM641 truncated)	This study
B. licheniformis M609.3	M409 *amyB*::P*apr-gfpmut2* (P*apr* DSM641 full length)	This study
B. licheniformis M609.5	M409 *amyB*::P*apr-gfpmut2* (P*apr* DSM13 full length)	This study
B. licheniformis M639.1	M439 *amyB*::P*apr-gfpmut2* (Papr DSM641 truncated)	This study
B. licheniformis M641.1	M441 *amyB*::P*apr-gfpmut2* (Papr DSM641 truncated)	This study
B. licheniformis M648.1	M448 *amyB*::P*apr-gfpmut2* (Papr DSM641 truncated)	This study
B. licheniformis M809.1	M409 *cat*::P3*degU*-RBS-*mScarletI*	This study
B. licheniformis M809.2	M409 *cat*::P3*degU*-RBS-*mScarletI*-ASV	This study
B. licheniformis MH1	MW3 *amyS*:: P*apr-gfpmut2* (P*apr* DSM13 full length)	This study
B. li. M308 *amyB*::G2r	M308 *amyB*::RBS-*gfpmut2* (promoter-less)	This study

Plasmid	**Function**	**Reference**
pBW0034	pUC19 P*apr* type-IIs-assembly donor	BASF SE
pBW0230	HomA *amyB* type-IIs-assembly donor	BASF SE
pBW0231	HomB *amyB* type-IIs-assembly donor	BASF SE
pBW0301	HomA *cat* type-IIs-assembly donor	BASF SE
pBW0302	HomB *cat* type-IIs-assembly donor	BASF SE
pBW0304	HomA *pga* type-IIs-assembly donor	BASF SE
pBW0305	HomB *pga* type-IIs-assembly donor	BASF SE
pBW0654	pEC194RS *degU32* H12L	BASF SE
pBW0944	pBS72 ori, ColE1 ori, kanR	BASF SE
pCB56C	BLAP template	Wilson *et al.* (1993)
pDAN80	pEC194RS Δ*tapA-sipW-tasA*	Daniel Götze, Ag Schweder
pEC194RS	pE194ts-pUC18 derivative, type-IIs-assembly cassette	BASF SE
pJOE8999.1	CRISPR/Cas9 single plasmid	Altenbuchner *et al.* (2016)
pJOE-T2A	pJOE8999.1 type-IIs-assembly cassette, *mRFP* marker	This study
pJOE_amy1	pJOE-T2A with *amyB* targeting spacer (1)	This study
pJOE_amy2	pJOE-T2A with *amyB* targeting spacer (2)	This study
pJOE_cat1	pJOE-T2A with *cat* targeting spacer	This study
pJOE_*amyB*::G2r	pJOE_amy2 *amyB*::RBS-*gfpmut2* (promoter-less)	This study
pMA23	pEC194RS Δ*pgsB-pgsE*	This study
pMA73	pEC194RS Δ*slrA*	This study
pMA30	pEC194RS Δ*sinI*	This study
pMA98	pEC194RS Δ*sinI* p.E14-P45del	This study
pMA79	pEC194RS *sinI* p.L11AfsX8	This study
pMA96	pEC194RS *remA* R18W, P29S (loss of function)	This study
pMA91	pEC194RS *remA*::bleo^{R} (insertion deletion)	This study
pMA65	pEC194RS Δ*motB*	This study
pMA92	pEC194RS Δ*hag*	This study

pMA109	pJOE_amy1 *amyB*::P*apr-gfpmut2*-DAV (P*apr* DSM641 truncated)	This study
pMA110	pEC194RS *pga*::BLAP	This study
pMA112	pJOE-T2A Δ*epsA-O*	This study
pAM114	pJOE-T2A Δ*sigD*	This study
pMA116	pJOE-T2A Δ*tapA-sipW-tasA*	This study
pMA117	pJOE-T2A *degU32* H12L	This study
pMA124	pJOE_amy1 *amyB*::P*apr-gfpmut2* (P*apr* DSM641 truncated)	This study
pMA128	pJOE-T2A Δ*slrA*	This study
pMA130	pJOE-T2A *remA* R18W P29S	This study
pMA134	pJOE-T2A Δhag	This study
pMA136	pJOE-T2A ΔmotB	This study
pMA137	pJOE-T2A *cat*::P3*degU*-RBS-*mScarletI*	This study
pMA138	pJOE-T2A *cat*::P3*degU*-RBS-*mScarletI*-ASV	This study
pMA147	pJOE_amy1 *amy*B::P*apr-gfpmut2* (P*apr* DSM13 full length)	This study
pMA149	pJOE_amy2 *amy*B::P*apr-gfpmut2* (P*apr* DSM641 full length)	This study
pMA163	pJOE_amy2 *amyB*::P*tapA*-RBS-*mScarletI*	This study
pMA164	pJOE_cat1 *cat*::P*tapA*-RBS-*mScarletI*	This study
pMA168	pJOE-T2A Δ*bslA*	This study
pUC19	*E. coli* cloning vector	Yanisch-Perron *et al.* (1985)
pUCG2	pUC19 *gfpmut2* type-IIs-assembly donor	This study
pUCG22	pUC19 *gfpmut2*-DAV type-IIs-assembly donor	This study
pUCG2r	pUC19 RBS-*gfpmut2* type-IIs-assembly donor	This study
pUCS1r	pUC19 *mScarlet*I type-IIs-assembly donor	This study
pUCS11r	pUC19 *mScarlet*I-ASV type-IIs-assembly donor	This study
pUCPhag	pUC19 P*hag* type-IIs-assembly donor	This study
pWG2r	pBW0944-RBS-*gfpmut2* (promoter-less)	This study
pWt1t2t0G2r	p0692-RBS-*gfpmut2* (promoter-less)	This study
pWG2rH	p0692-P*hag*-RBS-*gfpmut2*	This study
pWG22rH	p0692-P*hag*-RBS-*gfpmut2*-DAV	This study
p0226	Δ*pgsB-pgsE* HomA-HomB	BASF SE
p0558	pUC19 derivative, type-IIs-assembly cassette from p0732	BASF SE
p0689	p0558 with *mScarletI* replaced by *lacZ*	This study
p0690	p0558 with *mScarletI* replaced by *mRFP*	This study
p0692	pBW0944 with t1t2t0 terminator downstream of *kanR*	This study
p0732	Gene synthesis of type-IIs-assembly cassette from pBSd141R	Radeck *et al.* (2017)

Oligonucleotide	**5' → 3'**
19041	CAGCGGGTGTTGGCGGGTGTCG
19042	CTGGCACGACAGGTTTCCCGACTGG
19104	GCTGCCAAAAGACAGCTTCCTTATCTAGCCATTGCTGCTGTCC
19105	GGACAGCAGCAATGGCTAGATAAGGAAGCTGTCTTTTGGCAG
19120	CCAAAATGACAAGCTTGAAGAGG
19124	GGTGGTGGTACCCAAGAGCAAATGGAAGCACG
19125	CTTCCTTTCGATATTATAGCACATTCACATACATTTCCCCCCCAAAATAC
19126	GTATTTTGGGGGGGAAATGTATGTGAATGTGCTATAATATCGAAAGGAAG
19127	GGTGGTGAATTCGAACGAAAGAGCGCACAGTG
19143	GGTGGTGAATTCGAAGACTTATATATGAGTAAAGGAGAAGAAC
19144	GGTGGTAAGCTTGAAGACCCGCTATTATTATTTGTATAGTTCATCCATGC
19156	GGTGGTAAGCTTAAGTCGCACTGTTTGCAGAC
19157	GGTGGTGGTACCTCCCTTCCGCTTTCAAGC

19168	GGTGGTAAGCTTGAAGACCCGCTATTATTAAACAGCGTCAGCAACATTTTGATTAAAT-GAATTTGTTTTGCCTGCTTTGTATAGTTCATCCATGC
19171	GGTGGTCTCGAGTTCCACTTAATGCTGATCGG
19172	ACGCTTAGGATCCCATAGCTTCCTCCAATATGATAAGAC
19173	TCTTATCATATTGGAGGAAGCTATGGGATCCTAAGCGTTTAAAAGCATCAGTTATCC
19174	CTGGAATGGGTCATGAATTCAG
19186	CAAGTCTGTCCACTCCTCATCCAAGCTTCTTCTTTCTC
19189	GCTCTTGAACAAGGCATTAGGATCCAGAGGAAATACG
19191	GTTGCAGACAAACTAGCGCGTGG
19192	GACAGCCTCGCAGAGCACAC
19202	CAAGCTATGCTTGCTCAAGC
19212	TCGATATCAGCCAATTCGCGGATATGATATTTCCAAAGC
19214	TACGTTCCCCCTGTACTTGGAC
19215	CGTATAGGATGACGATTAAACTGATC
19216	CAGGTTAAACTAGAGACGTCCAAGTACAGGGGGAACGTACGATGACCTCTAATAATTGTTAATCATGTTG
19217	CAAAGCCGATATTGATCAGTTTAATCGTCATCCTATACGATTGCTGAACAGATTAATAATAGATTTTAGC
19231	GGAGCGGCCGCTTCCTCTGTCCGATTGTCC
19232	CTGTTGGTTCGCTTGAGCAAGCATAGCTTGGACGGTTCAGCGTGTTAAGC
19233	GGAACTAGTCGATCGAAGAGCCATTCGAG
19236	TGGTAAGCTTGAAGACCTTCGACATATCGAAATTCACCGCAAGG
19237	TGGTGGATCCGAAGACTTATATTGAAATGTGTTTGATTGCACGTCC
19238	TGGTAAGCTTGAAGACCTTCGATGTGACATGGTATTGTTTGACC
19239	TGGTGGATCCGAAGACTTATATAGCGAGTATGTAATGGCTTTTG
19252	TGGTAAGCTTGAAGACCTTCGACAATGCATCGGAGAATCCGAAG
19253	TGGTGGATCCGAAGACTTATATCCATTCTCATTGTTAAACACACC
19254	GGAGGAGGTACCACTAGTCAAGAGCAAATGGAAGCACG
19255	CTCATCCAATTCTTCTTTCTC
19256	GATAAAAATGAGAAAGAAGAATTGGATGAGCCTTCCACATCAATTGAAAGAAG
19257	GGAGGAGAATTCGAACGAAAGAGCGCACAGTG
19268	GGTGGTGGATCCGAAGACTTATATGATTAACTAATAAGGAGGACAAACATGAGTAAAGGAGAAGAAC
19276	GGTGGTCTGCAGAAGACCCGCTATTATTATTTGTACAACTCGTCCATG
19293	GGTGGTGGTACCGAAGACTTATATGATTAACTAATAAGGAGGACAAACATGGTGTCAAAAGGTGAAGC
19302	GGTGGTGAATTCGAAGACTTTCGAGATTAACTAATAAGGAGGACAAACATGAGTAAAGGAGAAGAAC
19304	GAGGAGGCAGTCAAGCATGTGACAGGCGGTTTTTTTGCTATGC
19305	GCATAGCAAAAAAACCGCCTGTCACATGCTTGACTGCCTCCTC
19315	AAGCCAGCCCCGACACCCGCCAACACCCGCTGCCGCGTTTATAATGAAGACC
19316	CGCTTTCCAGTCGGGAAACCTGTCGTGCCAGCATATGTAAATCGCGGTACCG
19330	AGAATTCGAGCTCGGTACC
19332	GTTAAGCCAGCCCCGACACCCGCCAACACCCGCTGCCGCGTTTATAATGAAGACC
19342	CTTTATCCGACAAGGTACCATATGTAAATCGCGGTACCG
19343	CATAGCACAGGCGCGTAAGCCGCGTTTATAATGAAGACC
19344	GTACCGCGATTTACATATGGTACCTTGTCGGATAAAGCTG
19345	CTTCATTATAAACGCGGCTTACGCGCCTGTGCTATGTC
19352	GAAGACCCTCGACATATGTAATCTAGAGCAACGTTCTTGCCATTG
19353	CTAAAAAGGAGCGATGAGTCGCTTTTGTAAATTTGGAAAGTTAC
19354	TCCAAATTTACAAAAGCGACTCATCGCTCCTTTTTAGGTGGCAC
19355	GAACGTTGCTCTAGATTACATATGTCGAGGGTCTTCG
19362	GGAGAAGACCTTCGACCTCGGGACCTCTTTCCCTG
19363	TCCGAAGACCCGCTATTATTAGCGTGTTGCCGCTTCTGC
19377	GGAGGAGGCCAACGAGGCCTGATCGGGGAATATCGGAGTC
19378	GGAGGAGGCCTTATTGGCCCCTGTACAAGATGGGTTCTCC
19379	TACGGCATTCGGACGGTAGCCCGT

19380	AAACACGGGCTACCGTCCGAATGC
19388	TACGGACCAAATCGTCTTTATGAA
19389	AAACTTCATAAAGACGATTTGGTC
19392	GGTGGTGGTCTCTACCCGTCTCGTCCACGTCATGCTTC
19393	GGTGGTGGTCTCTTGAGTGGATGCTTCCTGCTCCTT
19394	TACGGCTAAAGCAATTGAAGCCGC
19395	AAACGCGGCTTCAATTGCTTTAGC
19396	GGTGGTGGTCTCTACCCGAAGTCATTCAATAAATCCTTTC
19397	GGTGGTGGTCTCTTGAGCTCAATGTGACATGGTATTG
19398	TACGGGATTTCGAACCTACCTTTG
19399	AAACCAAAGGTAGGTTCGAAATCC
19400	GGTGGTGGTCTCTACCCGATTTGGGATTGATACCGACGCTC
19401	GCCACTACTTCAAAGGTAGGCTCGAAATCCAAAATCC
19402	GGATTTCGAGCCTACCTTTGAAGTAGTGGCCGAAGG
19403	GGTGGTGGTCTCTTGAGTCTCCGGATTTCCGGATACAC
19424	TACGGTGCTATGCGATTTTTCATC
19425	AAACGATGAAAAATCGCATAGCAC
19430	TACGAGATTGGGTGATTTTGATGA
19431	AAACTCATCAAAATCACCCAATCT
19432	GGTGGTCTCTACCCTTCCACTTAATGCTGATCGG
19433	GGTGGTCTCTTGAGTGAATCCAGGGGCTGCAGG
19441	TACGTCCTGGATCATCCGCTTAAT
19442	AAACATTAAGCGGATGATCCAGGA
19443	TGGTGGTCTCTACCCAAGTCGCACTGTTTGCAGAC
19444	CTATAAGCATGCCTCTGTCGCGGGCATCCTGGATCATCC
19445	GATGCCCGCGACAGAGGCATGCTTATAGATGCTAC
19446	GGTGGTGGTCTCTTGAGAGTCGACGCCGTCTCTTTC
19448	GGTGGTGGTCTCTACCCCGATCGAAGAGCCATTCGAG
19449	GGTGGTGGTCTCTTGAGCTTCCTCTGTCCGATTGTCC
19452	TACGGCAATCTCTGAAAAAATGAG
19453	AAACCTCATTTTTTCAGAGATTGC
19454	GGTGGTGGTCTCTACCCGAGTAATAGAGAACAGGAAC
19455	GGTGGTGGTCTCTTGAGGATCGAAATCAACGAACTGA
19458	TACGTTTAATGCCGTATTTACCGG
19459	AAACCCGGTAAATACGGCATTAAA
19462	CGATAGAAGACCTTCGACACCCGTTTCTGTATGCG
19463	GTGATAGAAGACTTATATCTCACTCTCCTCC
19466	GGTGGTGGTCTCTACCCGGCCAACGAGGCCAGACGAGCAGGTGAGAAGTC
19467	GGTGGTGGTCTCTTGAGGGCCTTATTGGCCTCACCCTTGGCGTCCAAC
19468	TACGTGCGACCGAAGATGTAACCG
19469	AAACCGGTTACATCTTCGGTCGCA
19470	CTGGGCCTTTTTAATACGACTCACTATAGGGTCACCCTTGGCGTCCAAC
19471	CTGAAGTATATTTTAGATGAAGATTATTTCTTAATTGTCCGCTGCAGGTGAAAAG
19496	GGTGGTGGTCTCTACCCGGCCAACGAGGCCTCAATCATAAACTCGGTTCGTG
19497	GGAGCTTTTTTGCCTATTTACACAGCAATTCCCCCAAGTC
19498	GACTTGGGGGAATTGCTGTGTAAATAGGCAAAAAAGCTCCAAAG
19499	GGTGGTGGTCTCTTGAGGGCCTTATTGGCCATGTCTGCTTCTATCCGATG
19502	TACGAACTGAATCTGTCTACCGCC
19503	AAACGGCGGTAGACAGATTCAGTT
191447	TACGTCGCAGCAGAAATTAAGAGA
191448	AAACTCTCTTAATTTCTGCTGCGA

7.2 Strain cultivation, media and phenotypical characterization

7.2.1 Growth media and strain cultivation

All chemicals in this study were of analytical grade and purchased from Carl Roth GmbH & Co. KG (Karlsruhe, Germany), VWR (Darmstadt, Germany), Sigma–Aldrich Chemie GmbH (Taufkirchen, Germany), Merck (Darmstadt, Germany) and AppliChem (Darmstadt, Germany).

For cultivation of *E. coli* Lysogeny Broth medium (LB; Carl Roth, Karlsruhe) containing 10 g/L tryptone, 5 g/L yeast extract and 5 g/L $NaCl_2$ was used. *B. licheniformis* was cultivated in LB, TB (10 g/L glycerol, 12 g/L tryptone, 24 g/L yeast extract, 12,54 g/L K_2HPO_4, 2,31 g/L KH_2PO_4; pH 7.2-7.4) or LSJ-CT medium (4.44 g/L tryptone, 8.89 g/L casitone, 15 g/L glucose, 10 g/L K_2HPO_4, 10 g/L MOPS, 1 g/L $MgSO_4$ x 7 H_2O, 0.05 g/L FeSO4 x 7 H_2O, 0.1 g/L $CaCl_2$ x 2 H_2O, 0.05 g/L $MnCl_2$ x 4 H_2O). LSJ-CT was prepared freshly from separate solutions except for the casitone tryptone broth. When using mineral salt media for *B. licheniformis* V3 (batch) or V3FP (fed-batch; feedplates) was used (Wilming *et al.* 2013; Habicher *et al.* 2019c). V3 medium contained per liter: 20 g glucose, 10.6 g $(NH_4)_2SO_4$, 1.01 g $MgSO_4$ x 7 H_2O, 0.026 g $CaCl_2$ x 2 H_2O, 0.05 g MnCl2 x 4 H_2O, 0.05 g $FeSO_4$ x 7 H_2O, 41.9 g MOPS, 3.4 g K_2HPO_4, 0.53 mg CoCl2 x 6 H2O, 0.26 mg ZnCl2, 0.66 mg $NiSO_4$ x 6 H_2O, 0.31 mg $CuSO_4$ x 5 H_2O, 0.65 mg Na_2MoO_4 x 2 H_2O. V3FP was identical to V3 except for glucose which was absent from V3FP. V3 and V3FP were prepared freshly. All components were added separately. The resulting pH was 8 ± 0.1. Prior to cultivation in liquid media *Bacillus* strains were streaked freshly on LB agar plates, solidified with 12 g/L agar. If required, antibiotics where added in the following concentration. Erythromycin (10 µg/ml), kanamycin (20 µg/ml), chloramphenicol (5 µg/ml), zeocin/phleomycin (10 µg/ml) for *B. licheniformis*. When using zeocin/phleomycin the pH was adjusted to 7.5 to improve selectivity. Kanamycin (20 µg/ml), streptomycin (10 µg/ml) and ampicillin (100 µg/ml) were used for selection of *E. coli* transformants. For storage of *Bacillus* and *E. coli* at -80 °C, cryo cultures were prepared by adding 200 µl of sterile glycerol to 800 µl of cells.

7.2.2 Microtiter plate-based batch cultivation

Batch cultivations, including precultures, for on-line monitoring of cultivation parameters were performed in 48-well deep-well microtiter plates with flower geometry in the BioLector® Pro system (m2p-labs GmBH, Baesweiler, Germany; article number for microtiter plates: pre-culture: MTP-48-B, main culture: MTP-48-BOH 1) with a shaking frequency of 1000 rpm, a shaking diameter of 3 mm and a relative humidity > 75 %. The BioLector® systems enables parallel online monitoring of scattered light (OD_{620nm}), fluorescence, dissolved oxygen tension and pH (Kensy *et al.* 2009). Precultures were prepared by a two-step protocol (Habicher *et al.* 2019c). The first preculture was carried out in 800 µl

complex TB medium inoculated with a single colony from the strain streaked onto LB agar plates. After 16 -18 h at 30 °C, 8 µl were transferred to 800 µl fresh V3 mineral medium with glucose or LSJ-CT broth depending on the medium used in the main culture. In contrast to Habicher *et al.* (2019b) the second preculture was incubated for 24 h until stationary growth to synchronize growth of different strain derivates. For main cultures, each well was filled with 800 µl of V3 or LSJ-CT medium and inoculated with 1 % or 0.1 % (v/v) of the second pre-culture. The inoculum used in the experiments is indicated in the corresponding caption. Microtiter plates for batch cultivations were covered with a sterile, evaporation reducing barrier (m2p-labs GmBH, Baesweiler, Germany; article number: F-GPR48-10). In case of strains carrying plasmid-based reporter constructs 20 µg/ml kanamycin-sulfate were added to the medium. LED and bandpass filter modules used for online monitoring of fluorescence intensities were E-OP-404 (GFP, excitation 480/10 nm, emission 520/25 nm) and E-OP-419 (mScarlet, excitation 580/10 nm, emission 610/10 nm). Offline batch cultivation in microtiter plates was performed analogous to the online cultivation but plates were incubated in a standard incubator shaker (Infors HT Multitron Pro, Infors GmbH, Basel, Switzerland), with a shaking frequency of 1000 rpm, a shaking diameter of 3 mm and a relative humidity of 85 %. Growth was monitored by measurement of scattered light (OD_{600nm}) in a microplate reader (Infinite M200 or M1000, Tecan Group Ltd., Männedorf, Switzerland).

7.2.3 Microtiter plate-based fed-batch cultivation

Small scale fed-batch main cultivations were conducted as described previously (Habicher *et al.* 2019c). In brief, 48-well deep-well microtiter plates with a glucose-containing polymer (Feed Plate ® Kuhner Shaker GmbH, Herzogenrath, Germany; article number: SMFP08004) and 700 µl V3FP were inoculated with 70 µl of the second preculture (see above) and incubated for 72 h at 30 °C and 400 rpm in a standard incubator shaker with an orbit diameter of 25 mm (New Brunswick Innova 42R, Eppendorf AG, Hamburg Germany). The resulting initial OD_{600nm} in main cultures was comparable between different strains and within the range of 1.0 - 1.2. To avoid contamination and evaporation, main cultures were sealed with a sterile, gas-permeable, evaporation reducing foil (m2p-labs GmBH, Baesweiler, Germany; article number: F-GPR48-10). Precultures for fed-batch cultivations were incubated under the same conditions as the main culture in a standard incubator shaker. Offline analyses of small-scale fed-batch cultivations included measurement of scattered light (OD_{600nm}), determination of cellular dry weight (CDW) and protease activity.

7.2.4 Determination of cellular dry weight (CDW)

Determination of biomass was performed in 2 ml reaction tubes using 1.8 – 2.0 ml of cell culture. In case of feedplate cultivation six replicates were pooled to increase sample volume. Calculation of final cellular dry weight requires the following steps. The weight of the empty tube (Wt) is determined prior

to sample transfer. The weight of the filled tube (Wb) is determined followed by harvesting of the cells by centrifugation for 10 min at 10.000 xg. After removing the supernatant, the cell pellet is washed once by resuspending the cells in 500 µl of deionized water. When feedplate samples were analyzed, the water was used to wash the corresponding microtiter wells prior to resuspending the cell pellet. This step was of particularly important in case of *degU32* single mutants displaying strong biofilm formation which is accompanied by stronger surface adhesion. To minimize technical errors, the pipette tip is washed in an additional 500 µl of water in a separate tube. The wash fraction is combined with the resuspended sample. Washing of cell pellets was carried out by carefully pipetting up and down using a 1000 µl pipette to minimize shearing forces. To completely remove the supernatant after washing of the cell pellet, the reaction tube was placed upside down on a paper towel. Subsequently, the weight of the reaction tube with the wet biomass (Wpw) is determined. The samples were prepared for lyophilization by freezing the cell pellet at -20 °C over night. Freeze drying was carried out for 24 h until excess liquid was removed from biomass yielding the weight of the reaction tube including the dried sample (Wpd). The cellular dry weight (mg biomass / mg broth) is calculated as follows.

$$\mathrm{CDW} = (\mathrm{Wpd} - \mathrm{Wt})/(\mathrm{Wb} - \mathrm{wt})$$

7.2.5 Biofilm formation assay

The ability to form biofilms was analyzed using a modified MSgg medium in liquid culture (pellicle formation) and agar plates (colony architecture) (Branda *et al.* 2001). Due to poor growth of *B. licheniformis* DSM641 strains, MSgg was supplemented with 0.5 % yeast extract and 1 % Bacto tryptone yielding MSggTY. Tryptophan and phenylalanine were removed from the MSggTY formulation. Agar plates (33 ml medium per 92 x 16 mm plate) were solidified with 1.5 % Bacto agar and allowed to dry for 35 min in a laminar flow hood. Overnight cultures were diluted 100-fold in LB medium and grown for 6 hours at 30 °C and 250 rpm. From this preculture, 5 ml of fresh LB medium were inoculated adjusting the OD_{600nm} to 0.05 and incubated until the culture reached the mid-exponential growth phase (OD_{600nm} of 0.8 – 1.2). For colony architecture assays, 20 µl of cells were spotted centrally on MSggTY agar. Pellicle formation experiments were conducted in 12-well microtiter plates (Sarstedt AG & Co. KG, Nümbrecht, Germany; article number: 3921500) by inoculation of 3 ml MSggTY medium with 20 µl cell suspension. Microtiter and agar plates were incubated without agitation for respectively 7 and 5 days at 30 °C. Alternative to MSggTY, LB medium supplemented with 0.05 mM $MnCl_2$ and 1 g/L glucose was used for pellicle and colony morphology assays (LBGM). As LB medium containing glycercol frequently used in biofilm formation assays (Shemesh and Chai 2013) resulted in a mucuous colony morphology, glycerol was replaced with glucose. However, despite being less frequently used than glycerol

containing media, glucose-containing media were previously used in biofilm formation assays as well (Mhatre *et al.* 2016).

7.2.6 Motility assay

Swimming motility was analyzed as described before (Kearns and Losick 2003; Guttenplan *et al.* 2013). The following modifications were made. Precultures were prepared as described for the biofilm formation assay. LB agar plates containing 0.4 % agar (25 ml medium per 92 x 16 mm plate) were prepared freshly and dried without lid for 25 min in a laminar flow hood and centrally inoculated with 3 µl of the mid-exponential growing preculture. After drying of the cell suspension, the plates were incubated for 14 – 18 hours at 30 °C and qualitatively analyzed for motility. Non-motile strains did not spread from the central inoculation spot, whereas motile strains were able to colonize the full soft agar plate.

7.2.7 Cell lysis assay

Functional analysis of autolysin activity was analyzed as described previously (Blackman *et al.* 1998). Two subsequent pre-cultures were prepared. To synchronize growth of different strains overnight culture grown at 37 °C in LB medium were prepared. The second LB pre-culture was inoculated 1:100 and grown to an OD_{600nm} of 1. Subsequently, 50 ml LB medium in a 500 ml shaking flask without baffles were inoculated adjusting the initial OD_{600nm} to 0.05. The main culture was grown to mid-exponential phase at 37 °C, 250 rpm. Reaching an OD_{600nm} of 1.2 and 2.0, growth was inhibited by addition of 0.05 M sodium azide. Lysis of cells was followed spectrophotometrically while continuing incubation at 37 °C and 250 rpm.

7.3 Transformation methods

7.3.1 Electroporation of *E. coli*

Transformation of *E. coli* DH10B and INV110 was conducted by electroporation as described by Sambrook *et al.* (2012) with minor adjustments to the protocol. The preculture was prepared by inoculation of 10 ml LB containing 10 µg/ml streptomycin with cells from a fresh LB agar plate and incubated at 37 °C and 250 rpm overnight. Two main cultures were prepared in parallel each containing 100 ml LB medium inoculated with 2 ml of the overnight culture in a 500 ml shake flask without baffles. As soon as cells reached an OD_{600nm} of 0.5 – 0.7, growth was stopped by cooling of the cultures on ice for at least 15 min. From now on all steps were performed on ice. Cells were transferred to 50 ml reaction tubes and harvested by centrifugation for 15 min at 1500 x g and 4 °C. Subsequently, three washing steps were conducted using 40, 25 and 10 ml of sterile, ice-cooled 10 % glycerol. Two cell

pellets were combined after the first and second washing step. Finally, cells were resuspended in 700 µl of washing buffer. 50 µl aliquots of competent cells were stored at -80 °C until transformation. To transform competent *E. coli* cells, 50 µl cells per transformation mix were thawed on ice. 10 – 50 ng plasmid DNA or up to 5 µl ligation mix were added and mixed by carefully pipetting twice. The transformation mix was then transferred to a precooled electroporation cuvette (2 mm gap width; VWR, Darmstadt, Germany). An electrical field was applied setting the parameter to 2500 V, 20 µF and 200 Ω (Gene Pulser Xcell; Bio-Rad). Immediately after the electrical pulse, cells were recovered by addition of prewarmed 950 µl SOC medium (5 g/L yeast extract, 20 g/L tryptone, 10 mM NaCl, 2.5 mM KCl, 10 mM $MgCl_2$, 10 mM $MgSO_4$, 20 mM glucose, pH 7.5) to the cuvette. The cells were transferred to a 2 ml reaction tubes and incubated horizontally at 37 °C, 250 rpm, to allow for regeneration and development of antibiotic resistance. Transformants were spread on LB agar plates containing appropriate antibiotics for selection and incubated over night at 37 °C.

7.3.2 Electroporation of *B. licheniformis*

Transformation of *B. licheniformis* was performed by electroporation according to Brigidi *et al.* (1991) with following modifications. Regeneration of cells was performed using 1 ml LBSPG consisting of LB supplemented with 0.25 M sucrose, 50 mM KH_2PO_4, 10 % glycerol; (Vehmaanperä 1989). When working with temperature sensitive plasmids, regeneration was conducted for 3 h at 33 °C instead of 1 h at 37 °C. Plasmid DNA for transformation of *B. licheniformis* was isolated from the restrictase-deficient *E. coli* INV110, to overcome the *E. coli* methylation pattern-dependent restriction of DNA.

7.4 Biochemical methods

7.4.1 Protease activity assay

Protease activity was determined using N-succinyl-alanine-alanine-proline-phenylalanine-p-nitroanilide (N-Suc-AAPF-pNA) as a substrate. The assay was carried out as described in Habicher *et al.* (2019) based on the method developed by DelMar *et al.* (1979). The samples supernatant was separate from the biomass by filtration. 200 µl of culture broth to a 96-well filter plate (AcroPrep Advanced 96 well Filter Plate 0.45 µm polyethersulfone filter; Pall Biotech, Dreiech, Germany) following centrifugation at 1200 xg for 50 min at 4 °C. To avoid clogging of the filter plate, an additional centrifugation step prior to the filter plate can be included in the protocol, following filtration of the supernatant. However, this step was part of the standard operation procedure for final strain analysis resulting in the data of this thesis. Samples were then diluted with sample buffer (0.1 M Tris HCl buffer (pH 8.6), 0.1 % (w/v) Brij 35) to keep the absorption between 0.05 and 2 (see below). The concentration of the substrate stock was 60 mg/ml N-Suc-AAPF-pNA dissolved in water free dimethyl sulfoxide. If necessary,

storage of substrate stocks at -20 °C is possible for no longer than 6 months. The substrate containing starter solution was prepared freshly by 50-fold dilution of the substrate stock with 0.1 M Tris HCl buffer (pH 8.6) and 0.1 % (w/v) Brij 35. To start the reaction, 100 µl of starter solution was added to 50 µl of diluted sample in a 96-well microtiter plate (Sarstedt AG & Co. KG, Nümbrecht, Germany; article number: 1581). Release of 4-Nitroaniline was measured at 30 °C for 15 min in a microplate reader (Infinite M200, Tecan Group Ltd., Männedorf, Switzerland) at a wavelength of 405 nm. Protease activity was calculated from the change of absorption, the extinction coefficient ε = 8900 M^{-1} cm^{-1} and a path length of 0.43 cm. To allow for adjustment of the reaction temperature, values from the first 3 minutes were omitted from the calculation. If not stated otherwise, relative protease activity values were calculated in relation to the parental strain *B. licheniformis* M409.

7.4.2 SDS-PAGE procedure and sample preparation

For the analysis of secreted proteins one-dimensional sodium dodecyl sulphate polyacrylamide gel electrophoresis (SDS-PAGE) was conducted (Laemmli 1970). Samples were taken after 72 h of microtiter plate-based fed-batch cultivation. The supernatant was separated from the cells by applying 200 µl of culture broth to a 96-well filter plate (AcroPrep Advanced 96 well Filter Plate 0.45 µm polyethersulfone filter; Pall Biotech, Dreiech, Germany) following centrifugation at 1200 xg for 50 min at 4 °C. Subsequently, 180 µl supernatant were treated with 25 µl 100 % pre-cooled trichloroacetic acid (TCA) to precipitate proteins. The samples were mixed by pipetting and incubated on ice for 2 h before centrifugation for 20 min at 12000 xg. The supernatant was discarded and the resulting pellet containing the precipitated proteins was washed once with 1 ml acetone (HPLC grade; Carl Roth, Karlsruhe, Germany). After centrifugation for 20 min at 12000 xg, the pellet was dried under a fume hood. The dried pellet was dissolved in 45 µl 1x SDS sample buffer (0.02 % (w/v) Bromophenol blue, 10 mM DTT, 12.5 mM EDTA pH 8, 10 % (v/v) glycerol, 2 % (w/v) SDS, 62.5 mM Tris-HCl pH 6.8) and incubated for 15 min at 95 °C. After brief centrifugation for 15 s at 8000 xg, 7.5 µl of dissolved sample were loaded on a Tris-Glycine gradient gel (8–16% Mini-PROTEAN® TGX™ Precast Protein Gel; Bio-Rad, article number: 4561103). Proteins were separated by applying 120 V and 80 mA for 50 – 60 min. After fixation for 10 – 20 min (10 % glacial acetic acid, 40 % ethanol), proteins were stained overnight with Coomassie Brilliant Blue solution (94 µM Coomassie Brilliant Blue G250, 20 % ethanol, 605 mM ammonium sulfate, 191 mM phosphoric acid). Destaining was achieved by applying fixation solution for 10 minutes followed by several incubation steps in purified water for 4 – 8 hours at room temperature. For storage, stained gels were moistened, sealed in polypropylene foil and stored at 4 °C.

7.4.3 Protein analysis by mass spectrometry

Identification of proteins in the supernatant was performed by MALDI-TOF MS/MS essentially as described in Kabisch *et al.* (2013) and was conducted by Dr. Dirk Albrecht (Institute of Microbiology, University of Greifswald). Protein bands were excised from SDS-PAGE gels with a sterile scalpel and washed twice with 100 µl of a solution of 50 % CH_3OH and 50 mM NH_4HCO_3 for 30 min followed by third washing step using 100 µl 75 % CH_3CN for 10 min. Gel pieces were dried for 17 min at 37 °C to allow for evaporation of acetonitrile prior to tryptic digest. In gel digestion of proteins was performed by rehydration of dried gel pieces in 10 µl trypsin solution (4 µg/ml trypsin; Promega; Madison, Wisconsin, USA) and incubation for 120 min at 37 °C. For extraction of the peptides, two subsequent extraction steps were performed with 60 µl and 40 µl of a solution of 0.1 % trifluoroacetic acid (TFA) in 50 % CH_3CN was added and incubated for 30 min at 40 °C. The supernatant was transferred into a new microtiter plate and dried at 40 °C for 220 min. Samples were resuspended in 0.9 µl α-cyano-4-hydroxycinnamic acid (3.3 mg/ml in 50 % CH_3CN, 0.5 % TFA). 0.7 µl of the matrix-embedded sample was deposited on the MALDI target plate. The samples were allowed to dry for 10 - 15 min before measurement by MALDI-TOF mass spectrometry. MALDI-TOF MS/MS analysis was carried out on the AB SCIEX TOF/TOF™ 5800 Analyzer (ABSciex /MDS; Analytical Technologies, Darmstadt, Germany). Mass spectrometry data were analyzed using the Mascot search engine (version 2.4.0; Matrix Science Ltd, London, UK) with a specific user sequence database and a specific *B. licheniformis* database including the heterologous BLAP protein.

7.5 Single cell analysis

7.5.1 Fluorescence microscopy and image analysis

For the analysis of cell morphology and fluorescence protein reporter gene expression, fluorescence microscopy was performed. Samples were diluted in 0.9 % NaCl adjusting the optical density OD_{600nm} to 1 – 2. Then, 0.5 µl of cells were applied to an agarose pad prepared by moulding 1.5 % agarose in phosphate buffered saline (8 g/L NaCl, 0.2 g/L KCl, 1.78 g/L Na_2HPO_4, 0.24 g/L KH_2PO_4) in a 125 µl gene frame on a microscope slide. Storage of precast agarose slides was possible for up to 2 h. For optimal fit of the cover slide, agarose frames were cut into eight pads, each allowing for analysis of one individual sample. The cell suspension was allowed to dry before applying the cover slip. The agarose slides immobilized the cells and ensured an even focus plane thereby improving the analysis. For staining of the nucleoid, 2 µg/ml DAPI (4',6-diamidino-2-phenylindole) were added to the agarose. Microscopy images were captured with a Zeiss Axio Imager.M2 epifluorescence microscope (Carl Zeiss Microscopy GmbH; Jena, Germany) equipped with an EC Plan-Neofluar objective (100x, 1.3 Oil Ph3 M27) and a Zeiss AxioCam controlled by the ZEN software. The filter sets used were obtained from Zeiss (Carl Zeiss

Microscopy GmbH; Jena, Germany) with the indicated excitation (ex) and emission (em) spectra in nm: DAPI filter set 49 (ex 365, em 445/50), GFP filter set 38 (ex 470/40, em 525/50), mScarlet filter set 63 HE (ex 572/25 HE, em 629/62 HE). Microscopy images were analyzed using the ImageJ software running the plugin ObjectJ with the NucTracer script developed for single cell analysis (Syvertsson *et al.* 2016). 16-bit tiff files of phase-contrast, DAPI and GFP/mScarlet images were imported into ImageJ and stored in a TIFF-stack format containing the images arranged by channels. Cells were identified based on the nucleoid stained with DAPI. Subsequently, the region of interest to measure fluorescence (GFP/mScarlet) is defined and taken as a proxy for mean fluorescence of a single cell. The Nuctracer script was modified by adjusting the diameter for the region of interest to 0.5 µm. For GFP/mScarlet the measured values were blanked against the average background fluorescence of the image. At least 200 individual cells were analyzed per sample. The fluorescence intensity values were exported as comma separated values (.csv) and analyzed using the software GraphPad Prism 8 (GraphPad Software, Incorporation; San Diego, California, USA).

7.5.2 Flow cytometry

To increase sample size in single cell analysis, flow cytometry was performed using the CytoFLEX (A00-1-1102; Beckman Coulter GmbH; Krefeld, Germany), equipped with a 488 nm excitation laser and a GFP emission filter (B90303, 495 – 565 nm). Samples were taken and diluted in PBS if needed prior to analysis. 50,000 events were analyzed. All measurements were ungated. The gain was set to 25 for the side and forward scatter (SSC, FSC) and to 50 for GFP (FITC). The resulting distribution of the fluorescence intensity was analyzed using the software FlowJo (Becton, Dickinson & Company; Ashland, Oregon, USA).

7.6 DNA isolation and purification

7.6.1 Isolation of plasmid DNA

For isolation and purification of plasmid DNA from *E. coli* and *Bacillus* the High Pure Plasmid Isolation Kit (Roche, Sigma–Aldrich Chemie GmbH; Taufkirchen, Germany) was used according to the manufacturer instructions with the following changes made. For *Bacillus*, the cells suspended in suspension buffer were treated with 10 µg/ml lysozyme for 30 min at 37 °C prior to alkaline cell lysis. Lysis at room temperature was performed for 3 min. Wash buffer 1 was omitted from the protocol. 50 µl instead of 100 µl buffer were used for elution of the DNA. The elution buffer was prewarmed to 65 °C before applying to the column. After applying the buffer, the column was incubated at room temperature for 1 – 3 min prior to centrifugation. All centrifugation steps were conducted at 17000 xg. Isolated plasmid DNA was stored at 4 °C.

7.6.2 Isolation and purification of chromosomal DNA from *Bacillus*

For isolation and purification of chromosomal DNA from *Bacillus* the High Pure PCR Template Preparation Kit (Roche, Sigma–Aldrich Chemie GmbH; Taufkirchen, Germany) was used according to the manufacturer instructions with the following modifications made. 200 µl cells were harvested by centrifugation and suspended in 200 µl suspension buffer (High Pure Plasmid Isolation Kit; Roche) and treated with 10 µg/ml lysozyme for 30 min at 37 °C prior to cell lysis. 400 µl inhibitor removal buffer were used. The second wash step was performed with 200 µl wash buffer. The DNA was eluted with 65 °C prewarmed elution buffer (10 mM TRIS-HCl, pH 8.5). After applying the buffer, the column was incubated at room temperature for 3 min prior to centrifugation. All centrifugation steps were conducted at 17000 xg.

7.6.3 Extraction of crude genomic DNA from *Bacillus*

For screening of *Bacillus* colonies crude genomic DNA was extracted providing DNA sufficient for PCR analysis while increasing the throughput. The method is based on heating of cells in an alkaline ethanol solution (Vingataramin and Frost 2015). 125 µl cells from an overnight culture were treated with 210 µl extraction solution (240 mM NaOH, 74 % EtOH, 2.7 mM EDTA), 5 µl lysozyme (20 mg/ml) and 5 µl RNase (20 mg/ml) solution for 45 min at 37 °C. The sample was then incubated for 30 min at 80 °C and 1000 rpm (Eppendorf ThermoMixer; Eppendorf, Hamburg, Germany) following centrifugation for 45 min at 1300 xg and 4 °C. The supernatant was discarded. The pellet was dried for 30 min at 60 °C. Finally, the crude DNA was dissolved in elution buffer (10 mM TRIS-HCl pH 8.5) and stored at 4 °C.

7.6.4 Gel electrophoresis

Separation of DNA for analytical or purification purposes was conducted by agarose gel electrophoresis. Agarose gels contained 0.8 to 1.4 % (w/v) agarose in TAE buffer (0.8 mM Tris-HCl, 0.4 mM acetic acid, 1 mM EDTA, pH 8) and peqGREEN (VWR; Darmstadt, Germany). Samples were mixed with loading dye (BLUE, EuRx; Danzig, Poland) prior to loading the gel. As a reference, the Perfect Plus 1 kb DNA Ladder was used (EuRx; Danzig, Poland). Gel electrophoresis was performed for 15 – 30 min at 120 V.

7.6.5 Extraction of DNA from agarose gels

Extraction and purification of DNA from agarose gels was performed using the QIAquick Gel Extraction Kit (Qiagen; Hilden, Germany). All steps were conducted according to the manufacturer instructions with the following changes made. The gel slice was dissolved at 65 °C. The wash buffer (PE) volume was reduced to 500 µl. The elution buffer was prewarmed to 65 °C before applying to the column. 25 – 40 µl elution buffer were used.

7.6.6 PCR product purification

Purification of DNA from PCR or restriction digest samples was performed using the High Pure PCR Product Purification Kit (Roche, Sigma–Aldrich Chemie GmbH; Taufkirchen, Germany). All steps were conducted according to the manufacturer instructions except for the elution buffer which was pre-warmed to 65 °C before applying to the column. After applying the buffer, the column was incubated at room temperature for 1 – 3 min prior to centrifugation.

7.7 DNA manipulation

7.7.1 Polymerase chain reaction (PCR)

In vitro amplification of DNA was conducted via PCR using Taq (Roboklon; Berlin, Germany) or Q5 High-Fidelity (New England Biolabs GmbH, NEB; Frankfurt am Main, Germany) DNA polymerase for analytical and preparative purposes respectively. The composition of both PCR reaction mixes is shown in the tables below. PCR reaction conditions were as follows. Q5 polymerase: Initial denaturation at 98 °C for 30 s followed by 30 times cycling of denaturation at 98 °C for 10 s, oligonucleotide annealing for 30 s at 50 °C – 72 °C and elongation of the product at 72 °C with 30 s/kb. The final elongation was performed for 5 min at 72 °C. Taq polymerase: initial denaturation for 3 min at 95 °C was completed before 32 cycles of a denaturation for 15 s at 95 °C, annealing for 30 s at 50 °C – 72 °C, elongation at 72 °C with 1 min/kb and a final extension at 72 °C for 5 min. DNA oligonucleotides were obtained from Invitrogen (ThermoFisher Scientific Inc., Waltham, Massachusetts, USA). When using cell suspension obtained from colonies or liquid cultures as template DNA, the initial denaturation step was increased to 3 min to improve cell lysis.

Component	Volume	Final concentration
10 x Taq buffer C	2 µl	1 x
Primer 1 (100 µM)	0.2 µl	1 µM
Primer 2 (100 µM)	0.2 µl	1 µM
dNTPs (5 mM each)	0.8 µl	0.2 mM each dNTP
DNA template	variable	< 100 ng
Taq DNA Polymerase	0.1 µl	0.5 Units / 20 µl
Aqua dest.	ad 20 µl	

Component	Volume	Final concentration
5 x Q5 reaction buffer	5 µl	1 x
Primer 1 (100 µM)	0.2 µl	0.8 µM
Primer 2 (100 µM)	0.2 µl	0.8 µM
dNTPs (5 mM each)	1 µl	0.2 mM each dNTP
DNA template	variable	< 100 ng
Taq DNA Polymerase	0.25 µl	0.5 Units / 25 µl
Aqua dest.	ad 25 µl	

7.7.2 Conventional cloning (restriction, ligation, dephosphorylation)

For conventional cloning of DNA 0.5 - 2 µg of insert and vector were digested with 10 – 20 U of each restriction enzyme for 1 – 3 h according to the manufacturer's instruction (NEB; Frankfurt am Main, Germany). Alternatively, overnight digestion was performed. Digested DNA fragments were purified by gel extraction or direct column purification with the latter routinely applied for digested PCR products. In case the cloning strategy required dephosphorylation of digested vector DNA, 5 U of Antarctic Phosphatase (AnP; NEB; Frankfurt am Main, Germany and the required amount of AnP buffer (final concentration 1x) were added after the restriction digest was performed prior to purification. Dephosphorylation was conducted for 60 min at 37 °C. DNA fragments prepared for ligation were analyzed by agarose gel electrophoresis to confirm purity and determine DNA concentration. DNA ligation was conducted in 10 µl reaction volume with 0.7 µl of T4 DNA ligase (NEB; Frankfurt am Main, Germany). Vector and insert were added in the molar ratio of 1:3 using 50 ng of vector DNA and incubated at either room temperature for 1 h or 16 °C overnight. Up to 5 µl of ligation mixture was used in electroporation of *E. coli* cells.

7.7.3 Type IIs assembly

The type IIs assembly technology allows for directed cloning of DNA fragments in a single reaction (Engler *et al.* 2008; Radeck *et al.* 2017). Type IIs restriction enzymes such as *Bsa*I and *Bbs*I (*Bpi*I) cleave outside of their recognition sequence enabling the design of unique, customized restriction overhangs. Consequently, multiple fragments can be ligated in the desired order. Moreover, the reaction product does not contain the recognition sites for the specific enzyme allowing for a spatially and temporarily joined restriction ligation reaction. For assembly of two or multiple fragments, 30 – 100 ng DNA per fragment were combined in an equimolar ratio or two-fold excess of insert(s). The total reaction volume of 15 µl included 1 µl of restriction enzyme and T4 DNA ligase each and 1.5 µl of 10x T4 DNA ligase buffer. To improve initial digestion of DNA the reaction mixture was incubated for 30 min at 37 °C prior to the temperature shift applied for optimized assembly. Repetitive restriction and ligation took place in 15 cycles at 37 °C and 21 °C each applied for 10 min. Inactivation of the ligase and the restriction enzyme was performed for 10 min at 50 °C and 20 min at 80 °C. The reaction mixture was stored at 4 °C. Up to 5 µl were used for transformation of the cloning host.

7.7.4 Gibson assembly

The Gibson assembly technology allows for directed cloning of linearized DNA fragments in a single reaction independent from restriction enzymes (Gibson *et al.* 2009). Thereby, Gibson assembly overcomes potential limitations resulting from the requirement of restriction enzymes binding motifs while usually showing improved cloning efficiencies. The reaction requires complementary single-stranded 3’ overhangs for annealing of DNA fragments which are generated by an exonuclease. In addition, DNA polymerase and DNA ligase activity are required for filling of gaps and sealing nicks in the DNA. Linear DNA fragments were generated by restriction of circular plasmid DNA or amplification of DNA fragments (insert and plasmid backbone) in independent PCR reactions. In case of PCR based linearization of plasmid DNA, the reaction product was treated with *Dpn*I for 1 – 3 h to remove template DNA prior to purification. Complementary overlapping regions of 30 – 35 bp between DNA fragments were introduced as extensions to the oligonucleotides used for amplification. 10 µl assembly reactions included 5 µl of *NEBuilder® HiFi DNA Assembly Master Mix* (E2621L, NEB; Frankfurt am Main, Germany), 50 – 100 ng of vector DNA and a 2:1 molar ratio of insert to vector DNA. After incubation for 1 h at 50 °C, 3 µl of the reaction mix were transformed into competent *E. coli* DH10B cells.

7.7.5 DNA sequencing

Automated DNA sequencing was conducted by Eurofins Genomics (Ebersberg, Germany) using the chain termination method according to Sanger. This is based on the termination of DNA elongation

due to incorporation of fluorescent labeled dideoxynucleotides into the newly synthesized DNA strand. For sample preparation, 500 – 1000 ng of plasmid DNA or 75 ng of purified PCR product were transferred into a sequencing tube, filled to 17 µl with purified water and 0.7 µl of the sequencing primer (100 mM) were added. The sequencing results were analyzed using the Geneious software package (Biomatters; Auckland, New Zealand).

7.7.6 Splicing by overlap extension (SOE-) PCR

Homology directed repair (HDR) templates were synthesized by SOE-PCR (Horton *et al.* 1990) of two PCR fragments comprising the 5' and 3' flanking region of the target gene. *Bsa*I restriction sites were introduced as overhangs to the 5' region forward primer and the 3' region reverse primer. To allow for splicing of both fragments, the internal oligonucleotides were extended by 15 – 20 bp complementary to the respective other flanking region resulting in an overlap of 30 – 40 bp in total. The 5' and 3' fragments were column purified prior to SOE-PCR to remove oligonucleotides used in the first reaction. 50 – 100 ng of each fragment were added to a 100 µl SOE-PCR mix using Q5 DNA polymerase and split into four 25 µl reactions. Splicing was performed by running 15 PCR cycles without oligonucleotides. The annealing temperature was calculated based on the melting temperature of the overlapping region. Subsequently, the 5' region forward primer and the 3' region reverse primer were added allowing for amplification of the joined HDR template. After 25 PCR cycles, purification of the HDR template was conducted by agarose gel extraction.

7.8 Plasmid and strain construction

7.8.1 Plasmids for pE194-based gene deletion and integration

To allow for markerless gene deletion and integration in *B. licheniformis*, a homologous recombination method exploiting a temperature sensitive pE194-derived shuttle vector was applied similar to the pMAD system (Villafane *et al.* 1987; Dempsey and Dubnau 1989; Vehmaanperä 1989). The pE194-based shuttle vector pEC194RS (provided by BASF SE) consist of the temperature-sensitive ori and erythromycin resistance marker gene from pE194ts (Villafane *et al.* 1987) cloned into the *Sma*I site of pUC18, in which the native *Bsa*I site was removed. Moreover, pEC194RS carries a type-II-assembly mRFP cassette from pBSd141R (GenBank accession number: KY995200) integrated into the *Bam*HI site of pUC18. In the following paragraph, construction of target-specific deletion plasmids is described. The pEC194RS based gene deletion procedure is described in section 0.

For deletion of the **poly-γ-glutamic acid** (*pga*) synthesis operon which consist of *ywsC* (*pgsB*), *ywtA* (*pgsC*), *ywtB* (*pgsA*) and *ywtC* (*pgsE*), the 5' and 3' homologous flanking region was amplified by PCR

as a single fragment from plasmid p0226 (provided by BASF SE). The oligonucleotides introduce *Bsa*I restriction sites with unique overhangs. The PCR fragment was purified by agarose gel extraction and cloned into pEC194RS in a one-step type-IIS-assembly reaction. 3 µl of the reaction mix were transformed into *E. coli* DH10B. Transformants were selected on LB agar plates containing 100 µg/ml ampicillin. Positive clones were identified by screening for white colonies and verified by sequencing of the deletion cassette. The resulting plasmid was named pMA23.

For deletion of the *B. licheniformis* DSM641 ***slrA*** gene, the homologous flanking regions were amplified by PCR using oligonucleotides 19171 and 19172 for the 5' flanking region and 19173 and 19174 for the 3' flanking region and gDNA from *B. licheniformis* DSM641. Both fragments were ligated by SOE-PCR (section 7.7.6) and cloned into pEC194RS as described for pMA23. The resulting plasmid was named pMA73.

For deletion of the *B. licheniformis* DSM641 ***sinI*** gene, the homologous flanking regions were amplified by PCR using oligonucleotides 19124 and 19125 for the 5' flanking region and 19126 and 19127 for the 3' flanking region and gDNA as a template. Both fragments were ligated by SOE-PCR (section 7.7.6) and cloned into pEC194RS as described for pMA23. The resulting plasmid was named pMA30. Plasmid pMA98 for partial deletion of *sinI* was constructed as described for pMA30. However, the 5' and 3' homologous region were amplified using oligonucleotide 19254 and 19255 and 19256 and 19257 respectively. The partial Δ*sinI* p.E14-P45del mutation was constructed analogous to Bai *et al.* and is described as non-polar regarding expression of *sinR* (Bai *et al.* 1993). Finally, *sinI* was inactivated by introduction of the frameshift mutation p.L11AfsX8 resulting in a translational stop codon eight codons downstream of leucin at position 11, which was changed to alanine. To simplify screening of positive clones, and artificial *Hind*III restriction site was introduced with the L11A amino acid exchange. The inactivated *sinI* gene allele was constructed as described fpr pMA30. However, the two PCR fragments were amplified with 19124 and 19186 for the 5' region and 19126 and 19189 for the 3' region of *sinI.* The resulting plasmid was named pMA79.

Inactivation of the *B. licheniformis* DSM641 ***remA*** gene was conducted by allelic exchange with a mutated copy resulting in the R18W and P29S amino acid exchanges (Blair *et al.* 2008; Winkelman *et al.* 2009). The plasmid pMA96 was constructed as described for pMA79. However, oligonucleotides 19120 and 19212 as well as 19215 and 19157 were used for the 5' and the 3' region. Alternative to the loss of function mutation, *remA* was inactivated by disruption of the ribosome binding site with the bleomycin resistance cassette (*bleo*^{R}) from pUB110. The 5' and 3' region were amplified with oligonucleotide 19120 and 19214 as well as 19157 and 19215. The bleomycin resistance marker gene was amplified from pUB110 with oligonucleotides 19219 and 19217. Subsequently, the 5' flanking region and

bleo^{R} were ligated by SOE-PCR following purification of the desired fragment and a second SOE-PCR with the 3' flanking region. The resulting fragment was cloned into pEC194RS as described for pMA23. The *remA*::*bleo*^{R} insertion plasmid was named pMA91. The insertion site for *bleo*^{R} was selected as described for *B. subtilis* by Winkelmann *et al.* (2009).

Construction of the ***motB*** deletion plasmid for *B. licheniformis* DSM641 was performed as described for pMA73. However, oligonucleotides 19156 and 19104 for the 5' flanking region and 19105 and 19157 for the 3' flanking region were used. The resulting plasmid was named pMA65.

Construction of the ***hag*** deletion plasmid for *B. licheniformis* DSM641 was performed as described for pMA73. However, oligonucleotides 19231 and 19202 for the 5' flanking region and 19232 and 19233 for the 3' flanking region were used. The resulting plasmid was named pMA92.

Construction of **DegU** H12L hyperphosphorylation mutants was achieved by exchange of the wildtype gene with the *degU32* allele using plasmid pBW0654 (Kunst *et al.* 1974; Henner *et al.* 1988b). pBW0654 was provided by BASF SE. A *Pst*I restriction site was introduced along with the H12L amino acid exchange allowing for improved screening for positive clones.

Plasmid pMA110 for integration of the ***blap*** expression cassette into the *pga* locus was constructed by a two-step cloning strategy. The ***blap*** gene encodes the *Bacillus lentus* alkaline protease. First, the complete protease expression cassette from pCB56C (Wilson *et al.* 1993) was amplified by PCR using oligonucleotides 19362 and 19363 and subcloned into p0689 in a type-II-assembly reaction with restriction endonuclease *Bpi*I resulting in p0689_BLAP (see section 7.8.5.1 for further details on p0689). Expression of BLAP was under control of a 227 bp fragment of the native *B. licheniformis* DSM641 P*apr* promoter region present in pCB56C. In a second type-II-assembly reaction with pEC194RS, p0689-BLAP, pBW0304 and pBW0305, the *pga*::BLAP integration plasmid pMA110 was constructed using *Bsa*I. pBW0304 and pBW0305 carry the 5' and 3' homology regions of the *pga* locus (both provided by BASF SE).

7.8.2 pE194-based gene deletion procedure

To allow for marker-less gene deletion and integration in *B. licheniformis*, a homologous recombination method exploiting a temperature sensitive pE194-derived shuttle vector was performed essentially as described by Vehmaanperä *et al.* (1991). The shuttle plasmid pEC194RS used for gene deletion has a temperature-sensitive ori and carries a erythromycin resistance cassette as described in section 7.8.1. The plasmid does not replicate at temperatures higher than 42 °C. Consequently, a temperature upshift allows for integration of the plasmid into the host strain gene via a Campbell-type crossover event, when applying selective pressure, or allows for curing of the plasmid under non-selective conditions.

Deletion of the target gene started with transformation of the target-specific pEC194RS-based plasmid into *B. licheniformis* by electroporation. Regeneration and handling of transformants was performed at 33 °C enabling replication of the plasmid in the host cell. Due to slower growth at 33 °C, regeneration was conducted for at least 3 h. Transformants were spread on LB agar plates containing 10 µg/ml erythromycin and incubated at 33 °C for 1 – 2 days. Positive transformants were verified by plasmid isolation and PCR analysis of the deletion cassette. Deletion of the target gene started with a single colony grown at 33 °C over night in LB medium containing 10 µg/ml erythromycin. The next day, 40 ml of pre-warmed LB-Lennox medium with 10 µg/ml erythromycin were inoculated with 800 µl of the overnight culture in a 500 ml Erlenmeyer flask without baffles and incubated for 2 h at 45 °C and 200 rpm until an OD_{600nm} of 0.3 – 0.5 was reached. Subsequently, a second main culture with pre-warmed LB without erythromycin was inoculated with 800 µl of the first main culture and further incubated at 45 °C and 200 rpm. After 5 – 6 h, 10^{-4} and 10^{-5} dilutions were prepared, spread on LB agar plates containing 10 µg/ml erythromycin with 100 µl cell suspension per plate and incubated for 3 – 5 days at 33 °C. Putative positive mutants were identified by isolation of gDNA and PCR analysis of the modified gene locus with special focus on later growing colonies and colonies showing altered morphology. For curing of the gene deletion plasmid after successful removal of the wildtype allele from the chromosome, the clone is spread on a LB agar plate containing 10 µg/ml erythromycin and incubated overnight at 33 °C. The following day, 40 ml of prewarmed LB medium were inoculated with an inoculation loop taking one streak of cells from the agar plate and incubated for at least 8 h at 42 °C and 200 rpm. 400 µl of cells were used for inoculation of a second 40 ml LB culture, which was incubated overnight at 42 °C and 200 rpm. The next day, a third LB culture war prepared the same way. After 8 h, 10^{-5} to 10^{-7} dilutions were prepared and spread on LB agar plates without antibiotics. Following incubation overnight at 37 °C, single colonies were transferred to LB and LB agar plates containing 10 µg/ml erythromycin and incubated for 2 days at 33 °C. Finally, erythromycin-sensitive clones that have lost the plasmid were analyzed for the desired genomic modification by gDNA extraction, PCR analysis and sequencing of the target locus.

7.8.3 Construction of CRISPR/Cas9 based genome editing plasmids

Within this thesis, CRISPR/Cas9 based genome editing was established as a routine technology for modification of *B. licheniformis* DSM641. The system applied was developed by Altenbuchner (2016) and is based on a single plasmid pJOE8999.1 providing the *Streptococcus pyogenes* Cas9 (SpCas9, hereafter referred as Cas9), a single guide RNA (sgRNA) and the editing template for homology directed repair (HDR) of the Cas9-induced DNA double-strand break. Expression of Cas9 is under control of the mannose-inducible promoter P*manP.* This section describes the construction of plasmids for

CRISPR/Cas9 based genome editing. The gene deletion procedure is described in section 7.8.4 (page 156). Cloning of the target-specific 20 bp spacer and the HDR template is achieved by two consecutive steps. Applying the Type IIs Assembly method (*Bsa*I; see 7.7.3), the 20 bp target-specific spacer sequence replaces a *lacZ* reporter gene. The HDR template is inserted into the plasmid via restriction (*Sfi*I) and ligation.

7.8.3.1 Construction of the CRISPR/Cas9 pJOE-T2A basis vector

To allow for one-step cloning of spacer and HDR templates, a type-IIs-assembly compatible cloning module was ordered as a gene synthesis construct (p0732, BASF SE) and integrated into the two most distal *Sfi*I sites of pJOE8999.1. The type-IIs-assembly cassette was designed based on pBSd141R (accession number: KY995200; Radeck *et al.* 2017) and consists of a constitutively expressed *mRFP* reporter gene flanked by *Bsa*I restriction sites. The *mRFP* gene simplifies identification of putatively positive clones, which appear colorless on X-Gal (5-bromo-4-chloro-3-indolyl-β-D-galactopyranoside), IPTG (isopropyl β-d-1-thio-galactopyranoside) and kanamycin (20 µg/ml) containing transformation plates, while negative clones are either blue (*lacZ*), red (*mRFP*) or purple (*lacZ* and *mRFP*). The donor plasmid p0732 and pJOE8999.1 were digested with *Sfi*I and the desired fragments were purified by extraction from agarose gels. After ligation of both fragments using T4 DNA ligase the reaction mixture was transformed into *E. coli* DH10B cells. Transformants were spread on LB agar plates containing kanamycin (20 µg/ml) and incubated overnight at 37 °C. Plasmid DNA was isolated from individual clones and analyzed by PCR and DNA. The resulting plasmid was named pJOE-T2A.

7.8.3.2 General procedure for cloning of target specific CRISPR/Cas9 plasmids

To construct target-specific pJOE-T2A plasmids, a 20 bp spacer sequence was designed using Geneious 10.1.5 (Biomatters, Ltd.; Auckland, New Zealand). The spacer was assembled by annealing of two complementary oligonucleotides each carrying a 4 bp extension suitable for cloning into *Bsa*I sites of pJOE-T2A. Annealing of oligos was performed by heating of 2.5 µl of each primer (100 µM) in 90 µl 30 mM HEPES buffer (pH7.8) for 5 min at 95 °C and stepwise cooling to 4 °C with 0.1 °C/s (Cobb *et al.* 2015). The HDR template was synthesized by SOE-PCR of two PCR fragments comprising the 5’ and 3’ flanking region of the target gene. *Bsa*I restriction sites were introduced as overhangs to the 5’ region forward primer and the 3’ region reverse primer. The 5’ and 3’ fragments were column purified prior to SOE-PCR to remove oligonucleotides used in the first reaction. Purification of the HDR template fused by SOE-PCR was conducted by agarose gel extraction. In case of (single) point mutations, the selected flanking regions are directly adjacent to each other with the point mutation(s) located in the oligonucleotide used to amplify the fragments. For integrative reporter constructs, the promoter reporter gene fusion and the flanking regions are subcloned into p#195 followed by amplification and purifica-

tion of the full cassette prior to their usage in type-IIs-assembly reactions. The type-IIs-assembly reaction mixture was transformed into *E. coli* DH10B cells (Life technologies). Transformants were spread on LB agar plates containing kanamycin (20 µg/ml) and 60 µl IPTG (100 µM), 70 µl X-Gal (30 mg/ml) spread onto of the surface and incubated overnight at 37 °C. Plasmid DNA was isolated from individual clones and analyzed by restriction digest or PCR. All plasmids were sequence verified.

7.8.3.3 CRISPR/Cas9 plasmids for modification of biofilm genes and regulators

The **BslA** coding region (GenBank accession number AAU42812; locus tag: *B. licheniformis* DSM13 = BLi03999) was cross-checked by identification of a characteristic N-terminal sequence and the C-terminal CxC motif to distinguish BslA from its paralogue YweA (Morris *et al.* 2017). *B. licheniformis* DSM13 and DSM641 BslA differ in the L130M substitution. To construct the *bslA* deletion vector, the homologous flanking region were amplified with oligonucleotides 19496, 19497 and 19498, 19499 using gDNA of *B. licheniformis* DSM641 as a template. The *bslA* specific spacer sequence was constructed by annealing of oligonucleotides 19501 and 19502. The oligonucleotide duplex and the HDR template were prepared as described above (7.8.3.2) and cloned into pJOE-T2A in a one-step type-II-assembly reaction. The resulting plasmid was named pMA168.

To delete the ***epsABCDEFGHIJKLMNO*** operon (*yveK* – *yvfF*) the homologous flanking region were amplified with oligonucleotides 19377,19304 and 19305, 19378 using gDNA of *B. licheniformis* DSM641 as a template. The spacer sequence targeting *epsG* was constructed by annealing of oligonucleotides 19379 and 19380. The oligonucleotide duplex and the HDR template were prepared as described above (7.8.3.2) and cloned into pJOE-T2A in a one-step type-II-assembly reaction. The resulting plasmid was named pMA112.

The ***slrA*** (accession number AAU42855; locus tag: *B. licheniformis* DSM13 = BLi04042) deletion vector was constructed by amplification of the HDR template from the previously constructed *slrA* deletion plasmid pMA73 using oligonucleotides 19432 and 19433. For simplified screening of deletion mutants, an artifical *Bam*HI site was introduced between the homology flanking regions (already present in pMA73). The *slrA* specific spacer sequence was constructed by annealing of oligonucleotides 19430 and 19431. The oligonucleotide duplex and the HDR template were cloned into pJOE-T2A in a one-step type-II-assembly reaction as described above (7.8.3.2). The resulting plasmid was named pMA128.

For deletion of the ***tapA-sipW-tasA*** operon the HDR template was PCR amplified from the previously constructed *tapA-sipW-tasA* deletion plasmid pDAN80 (Daniel Götze, Ag Schweder, unpublished) using oligonucleotides 19396 and 19397. The *tapA* specific spacer sequence was constructed by annealing of oligonucleotides 19394 and 19395. The oligonucleotide duplex and the HDR template were cloned

into pJOE-T2A in a one-step type-II-assembly reaction as described above (7.8.3.2). The resulting plasmid was named pMA116.

To inactivate **RemA**, the wildtype allele was exchanged by a mutated copy of the *remA* gene at its native locus, resulting in expression of a RemA with the combined loss of function mutations R18W and P29S previously described (Blair *et al.* 2008; Winkelman *et al.* 2009). The homology flanks for *remA* R18W, P29S regions were amplified from pMA96 using oligonucleotides 19443, 19444 and 19445, 19446. In addition to the R18W and P29S mutations already present in pMA96, this step introduces a silent mutation of arginin at position 36 to remove a *Bsa*I restriction site located in *remA*. The *remA* specific spacer sequence was constructed by annealing of oligonucleotides 19441 and 19442. The binding region of the spacer is directly adjacent to the P29S mutations, with P29S simultaneously resulting in loss of the PAM sequence. The oligonucleotide duplex and the HDR template were cloned into pJOE-T2A in a one-step type-II-assembly reaction as described above (7.8.3.2). The resulting plasmid was named pMA130.

7.8.3.4 Plasmid construction for introduction of the *degU32* mutation

Construction of **DegU** H12L hyperphosphorylation mutants was achieved by exchange of the wildtype gene with the *degU32* allele (Kunst *et al.* 1974; Henner *et al.* 1988b). The mutated allele was synthesized by SOE-PCR of the *degU* region with oligonucleotides 19400, 19401 and 19402, 19403 using gDNA of *B. licheniformis* M320 (M308 *degU32*) as a template. In addition to the H12L mutation, two silent mutations in the codons of glutamic acid at positions 26 and 30 located in the PAM and spacer binding region were introduced by oligonucleotides 19401 and 19402. The *degU* spacer sequence was constructed by annealing of oligonucleotides 19398 and 19399. The oligonucleotide duplex and the HDR template were cloned into pJOE-T2A in a one-step type-II-assembly reaction as described above (7.8.3.2). The resulting plasmid was named pMA117.

7.8.3.5 Plasmids for deletion of motility related genes

To delete ***sigD***, the HDR template was amplified from pBW022 (Daniel Götze, Ag Schweder, unpublished) with oligonucleotides 19392 and 19393. The spacer sequence was constructed by annealing of oligonucleotides 19388 and 19389. The oligonucleotide duplex and the HDR template were cloned into pJOE-T2A in a one-step type-II-assembly reaction as described above (7.8.3.2). The resulting plasmid was named pMA114.

The ***motB*** deletion vector was constructed by amplification of the HDR template from the previously constructed *motB* deletion plasmid pMA65 using oligonucleotides 19454 and 19455. The spacer se-

quence was constructed by annealing of oligonucleotides 19458 and 19459. The oligonucleotide duplex and the HDR template were cloned into pJOE-T2A in a one-step type-II-assembly reaction as described above (7.8.3.2). The resulting plasmid was named pMA136.

For construction of the ***hag*** deletion vector the HDR template from the previously constructed *hag* deletion plasmid pMA92 using oligonucleotides 19448 and 19449. The spacer sequence was constructed by annealing of oligonucleotides 19452 and 19453. The oligonucleotide duplex and the HDR template were cloned into pJOE-T2A in a one-step type-II-assembly reaction as described above (7.8.3.2). The resulting plasmid was named pMA134.

7.8.4 CRISPR/Cas9 based genome editing

The protocol applied for CRISPR/Cas9 based genome editing in *B. licheniformis* was first developed by Altenbuchner 2016 and is based on a single plasmid pJOE8999.1 providing the Cas9, sgRNA and the editing template for homology directed repair (HDR) of the Cas9-induced DNA double-strand break. Expression of Cas9 is under control of the mannose-inducible promoter P*manP* (Altenbuchner 2016). The pJOE-T2A based gene editing plasmids were isolated from *E. coli* INV110 and introduced into *B. licheniformis* via electroporation. After regeneration at 37 °C transformants were selected on LB agar plates containing 20 µg/ml kanamycin and 0.2 % D-Mannose. Transformation plates were incubated for 1 – 6 days with long incubation times being required for integration of *gfp* reporter constructs. The resulting transformants were transferred to fresh LB agar plates and incubated overnight at 50 °C to promote plasmid curing. In parallel, gDNA was isolated (section 7.6.3) and analyzed by PCR. The following day, isolation streaks of positive clones were performed. This step represented the second curing step resulting in isolation of single clones. Single clones were then transferred to LB plates and LB plates containing 20 mg/ml kanamycin to confirm plasmid curing. Kanamycin-sensitive clones, which have lost the plasmid, were analyzed by PCR analysis of extracted gDNA. Successful genome editing was confirmed by sequencing of the modified locus. In case the first transformation attempt fails, the following parameters can be changed individually or in combination. The temperature for regeneration and incubation of transformation plates is reduced to 30 or 33 °C simultaneously extending the regeneration time to 3 h. 0.2 % D-Mannose can be added already and only during regeneration in liquid medium, following plating on LB plates containing 20 mg/ml kanamycin only.

7.8.5 Construction of *B. licheniformis* reporter strain

7.8.5.1 Type-IIS assembly donor and receiver plasmids

The GFPmut2 gene variant (GenBank accession number AF302837) was ordered as gene synthesis fragment (Geneart; Regensburg, Germany) with flanking BpiI restriction sites and amplified with primer

19143 and 19144 thereby introducing BamHI/HindIII restriction sites. The PCR fragment was cloned into pUC19 by restriction digest and ligation and transformed into *E. coli* DH10B. Transformants were selected on LB agar plates containing 100 µg/ml ampicillin. For blue-white selection of putatively positive clones, 60 µl IPTG (100 µM) and 70 µl X-Gal (30 mg/ml) were spread on prewarmed agar plates prior to plating. Positive clones were verified by sequencing. The resulting GFPmut2 donor plasmid was named pUCG2.

The donor plasmid carrying the GFPmut2 gene with the C-terminal SsrA degradation tag was constructed as described for pUCG2. But, primer 19143 and 19168 were used. 19168 introduced the sequence encoding a 14 amino acids SsrA proteolysis tag. Aspartic acid (D), alanine (A) and valine (V) constitute the last three C-terminal amino acids, which have the strongest impact on proteolysis. The GFPmut2-DAV donor plasmid was named pUCG22.

The donor plasmid carrying the GFPmut2 gene with the strong, standardized ribosome binding site (RBS) R0 (GATTAACTAATAAGGAGGACAAAC; Guiziou *et al.* 2016) was constructed as described for pUCG2. But, primer 19268 and 19144 were used. The resulting plasmid was named pUCG2r.

The *mScarletI* donor plasmid with the strong, standardized RBS R0 (Guiziou *et al.* 2016) was constructed as described for pUCG2r. The mScarletI gene (GenBank accession number KY021424) sites was ordered as gene synthesis fragment (Geneart; Regensburg, Germany) with flanking BpiI restriction and amplified with primer 19293 and 19276 thereby introducing BamHI/HindIII restriction sites and the standardized RBS. The resulting plasmid was named pUCS1r.

Similar to pUCS1r, pUCS11r was constructed with the SsrA proteolysis tag fused to mScarletI. The SsrA proteolysis tag with the last three C-terminal amino acids being alanine (A), serine (S) and valine (V) was introduced by amplification with primer 19287. The forward primer used was 19293.

For assembly of the *gfpmut2* and *mScarletI* reporter gene with subpopulation-specific promotors, pUCPhag, pUCPtapA and pBW0034 were used. pBW0034 was provided by BASF SE and carries a 227 bp fragment of the native *B. licheniformis* DSM641 P*apr* promoter region as described in Wilson *et al.* (1993). The TA dinucleotide upstream of the *apr* ATG codon was changed to AT to allow for standardized type-IIs-cloning.

pUCP*hag* provided the *B. licheniformis* DSM641 *hag* promoter region. pUCP*hag* was constructed was described for pUCG2. The 229 bp promoter fragment was amplified from gDNA with primer 19236 and 19237 thereby omitting the native RBS to allow for tuning of gene expression by a standardized RBS fused to the *gfpmut2* reporter gene (pUCG2r). The *hag* promoter region was selected as described by Vlamakis *et al.* (2008).

For plasmid-based read-out of promoter activity, the low-copy plasmid p0692 was constructed. p0692 is based on the shuttle vector pBW0944 provided by BASF SE. pBW0944 carries the low-copy *Bacillus* origin of replication (ori) from pBS72, the ColE1 *E. coli* ori, a kanamycin resistance marker gene for selection in both organisms and a type-IIs-assembly cloning site. To prevent transcriptional read-through form the plasmid backbone into the reporter gene cassette, the t1t2t0 terminator region from pMUTIN2 (Vagner *et al.* 1998) was cloned upstream of the type-IIs-cloning site. This was achieved by amplification of the terminator region using primer 19352 and 19353 as well as PCR-based linearization of pBW0944 using primer 19354 and 19355. After *Dpn*I treatment of the pBW0944 fragment for 1 h at 37 °C a Gibson assembly reaction was performed. 2 µl of the reaction mix were transformed into *E. coli* DH10B. Transformants were selected on LB agar plates containing 20 µg/ml kanamycin. Positive clones were verified by colony PCR and sequencing using primer 19191 and 19192. The resulting plasmid was named p0692. To confirm that the t1t2t0 terminator region prevents transcriptional read-through the promoter-less RBS-*gfpmut2* fragment from pUCG2r was amplified with primer 19302 and 19268 introducing BpiI restriction sites suitable for direct cloning into pBW0944 and p0692. The resulting plasmids were named pWG2r and pWt1t2t0G2r. Both plasmids were introduced into *B. licheniformis* M308. The reporter strains were cultivated in LB and sample were analyzed for GFP expression during exponential and stationary growth. No GFP fluorescence was observed for the p0692-based pWt1t2t0G2 (data not shown), whereas the pWG2r reporter strain showed significant GFP expression (Figure S7).

For subcloning of promoter reporter gene fusion constructs the *E. coli* plasmid p0689 and p0690 were constructed based on p0558 provided by BASF SE. p0558 carries a cloning site that consists of a *mScarletI* gene for screening of positive clones flanked by BpiI restriction sites. Due to technical reasons the *mScarletI* gene was replaced by *lacZ* (p0689) or *mRFP* (p0690). For construction of p0689, p0558 was linearized by PCR amplification using primer 19315 and 19316. The *lacZ* insert was amplified from pUC19 with primer 19041 and 19042. Ligation of both fragments was conducted by Gibson assembly. As sequencing of the resulting plasmid revealed, the BpiI / BsaI restriction site located downstream of *lacZ*, hereafter referred as C-site, was lost during cloning. The intermediate plasmid was named p0558_lacZΔC-site. To reconstruct the missing C-site, p0558_lacZΔC-site was linearized by PCR amplification using primer 19041 and 19333. The missing BpiI / BsaI site was amplified from p0558 using primer 19330 and 19332. Both fragments were ligated by Gibson assembly. 2 µl of the reaction mix were transformed into *E. coli* DH10B. Transformants were selected on LB agar plates containing 20 µg/ml kanamycin. Positive clones were verified by colony PCR. The resulting plasmid p0689 was verified by sequencing. For construction of p0690, p0558 was linearized by PCR amplification using primer 19342 and 19343. The *mRFP* insert was amplified from p0195 with primer 19344 and 19345. Ligation

of both fragments was conducted by Gibson assembly. Both plasmids were verified by functional analysis of lacZ (X-Gal plate-based test) and mRFP expression as well as sequencing of the modified region.

7.8.5.2 Plasmid-based read-out of *hag* promoter activity in *B. licheniformis*

To analyze the *hag* promoter activity at the single cell level, pWG2rH was constructed. The *hag* promoter fragment and the RBS-*gfpmut2* fragment were cloned into the low-copy vector p0692 by type-IIs-assembly of pUCPhag, pUCG2r and p0692. 2 µl of the reaction mix were transformed into *E. coli* INV110. Transformants were selected on LB agar plates containing 20 µg/ml kanamycin and screened for white or yellow clones that have lost the red-fluorescent screening marker present in the cloning site of p0692 as described previously (Radeck *et al.* 2017). Plasmid DNA was isolated and verified by sequencing. The resulting plasmid was named pWG2rH. pWG2rH was transformed into *B. licheniformis* M409 by electroporation and positive transformants were verified by amplification and sequencing of the P*hag*-RBS-*gfpmut2* cassette using primer 19191 and 19192.

7.8.5.3 CRISPR/Cas9 plasmids for chromosomal integration of reporter gene fusions

To prepare the pJOE8999.1 basis vector for cloning of expression cassettes for integration into the *B. licheniformis amyB* or *cat* locus, protospacers targeting the wildtype locus were cloned into pJOE8999.1 as described by Altenbuchner *et al.* (2016). Two different protospacer sequences were tested for *amyB*. Oligonucleotides 191447 and 191447 were aligned and cloned into pJOE8999.1 in a type-IIS-assembly reaction resulting in pJOE_amy1 as described in section 7.8.3.2. Cloning of the spacer generated by oligonucleotide 19468 and 19469 resulted in pJOE_amy2. To target the *B. licheniformis cat* locus, oligonucleotides 19424 and 19425 were aligned and cloned into pJOE8999.1 in a type-IIS-assembly reaction resulting in pJOE_cat1.

Plasmids for marker-less chromosomal integration of promoter reporter gene fusion cassettes were constructed by two consecutive type-IIs-assembly reactions. In the first step, cloning of the promoter fragment and the reporter gene into the *E. coli* plasmid p0689 or p0690 was performed using *Bpi*I. The resulting plasmids were used in a second type-IIS-assembly reaction to join the reporter cassette and the homologous flanking region required for genomic integration. The fragments were cloned into the *E. coli* plasmid p0195 using *Bsa*I. p0195 is a pSEVA141 derivative (GenBank accession number JX560324) carrying the ColE1 ori, an ampicillin resistance marker gene and a mRFP screening marker gene flanked by type-IIS cloning sites as described before (Radeck *et al.* 2017). Finally, the full expression cassette was amplified by PCR for cloning into the CRISPR/Cas9 plasmids carrying the target-specific sgRNA (pJOE_amy1, pJOE_amy2 and pJOE_cat1).

7.8.5.4 Cloning and integration of *amyB*::P*apr-gfpmut2* reporter gene cassettes

For integration of the *gfpmut2* gene under control of the truncated, but otherwise native P*apr* promoter fragment from *B. licheniformis* DSM641 plasmid, pMA124 was constructed. First, P*apr* and *gfpmut2* were cloned into p0690 using pBW0034, pUCG2 and p0690 in a type-IIs-assembly reaction with BpiI. 2 µl of the reaction mix were transformed into *E. coli* DH10B. Transformants were selected on LB agar plates containing 20 µg/ml kanamycin and screened for white or yellow clones that have lost the red-fluorescent screening marker present in the cloning site of p0690 as described previously (Radeck *et al.* 2017). Plasmid DNA was isolated and verified by sequencing. The resulting plasmid p0690_G2A was used in a second type-IIS-assembly reaction with pBW0230, pBW0231 and p0195 to insert the expression cassette between the *amyB* homologous flanking regions. pBW0230 and pBW0231 are derivatives of pSEVA250 carrying the upstream and downstream flanking regions of the *B. licheniformis amyB* gene. 2 µl of the reaction mix were transformed into *E. coli* DH10B. Transformants were selected on LB agar plates containing 100 µg/ml ampicillin and screened for white or yellow clones that have lost the red-fluorescent screening marker present in the cloning site of p0195. The resulting plasmid was named pMA119. To clone the *amyB*::P*apr-gfpmut2* cassette into the CRISPR/Cas9 vector pJOE_amy1, the corresponding fragment was amplified from pMA119 using oligonucleotides 19466 and 19467. The PCR product and pJOE_amy1 were digested with *Sfi*I at 50 °C overnight and purified by gel extraction following ligation. 3 µl of the ligation mix were transformed into *E. coli* DH10B. Transformants were selected on LB agar plates containing 100 µg/ml ampicillin and screened by colony PCR. Plasmid DNA was isolated and verified by sequencing. The resulting plasmid pMA124 was transformed into the methylase-deficient *E. coli* INV110. Plasmid DNA was isolated and used for electroporation of *B. licheniformis*. CRISPR/Cas9 based genomic integration of the *amyB*::P*apr-gfpmut2* cassette was performed as described in section 7.8.4 , but transformation plates were incubated for 4 – 6 days, as outgrowth of putative positive clones was delayed. The modified *amyB* locus was verified by sequencing.

Construction of pMA109 for integration of *gfpmut2* with the C-terminal SsrA degradation tag under control of the truncated, but otherwise native P*apr* promoter fragment from *B. licheniformis* DSM641 plasmid was performed as described for pMA124. However, pUCG22 was used instead of pUCG2.

Construction of pMA149 for integration of *gfpmut2* under control of the native, full-length *apr* promoter P*apr*(DSM641 fl.) from *B. licheniformis* DSM641 was conducted as described for pMA124. However, the *apr* promoter was amplified from genomic DNA of *B. licheniformis* DSM641 with oligonucleotides 19462 and 19463 introducing *Bpi*I sites for subsequent type-IIS-assembly of the PCR fragment with pUCG2 and p0690. Moreover, pJOE_amy2 was used instead of pJOE_amy1.

Construction of pMA147 for integration of *gfpmut2* under control of the native, full-length *apr* promoter from *B. licheniformis* DSM13 P*apr*(DSM13 fl.) was conducted as described for pMA149. However, the *apr* promoter was amplified from genomic DNA of *B. licheniformis* DSM13 with oligonucleotides 19462 and 19463. pMA147 can be used for integration of the P*apr*(DSM13)-*gfpmut2* cassette into the *amyB* locus of *B. licheniformis* DSM641 and the *amyS* locus of *B. licheniformis* DSM13.

7.8.5.5 Cloning and integration of *tapA-sipW-tasA* reporter gene cassettes

Construction of pMA163 for integration of *gfpmut2* under control of the *tapA-sipW-tasA* promoter from *B. licheniformis* DSM641 into the *amyB* locus was performed as described for pMA124, with the following modifications. A 483 bp fragment comprising the promoter region was amplified by PCR with oligonucleotides 19238 and 19239. The promoter region was selected as described by Vlamakis *et al.* (2008). The PCR fragment was directly used for a type-IIS-assembly reaction with pUCG2r and p0690. Moreover, pJOE_amy2 was used instead of pJOE_amy1.

Plasmid pM164 for integration of *mScarletI* under control of the *tapA-sipW-tasA* promoter into the *cat* locus from *B. licheniformis* DSM641 was constructed as described for pMA163 with the following modifications made. The *tapA-sipW-tasA* promoter fragment was directly used for a type-IIS-assembly reaction with pUCS1r and p0689. The resulting plasmid, named pMA160, was used in a second type-IIS-assembly reaction together with p0195 and the *cat* homologous flanking regions provided on pBW0301 and pBW0302 resulting in plasmid pMA162. pBW0301 and pBW0302 are derivatives of pSEVA250 carrying the upstream and downstream flanking regions of the *B. licheniformis* DSM641 *cat* gene. The P*tapA*-RBS-*mScarletI* expression cassette was amplified by PCR with oligonucleotide 19470 and 19471 and cloned via Gibson assembly into pJOE_cat1 linearized by restriction digest with *Xba*I and *Sal*I. The resulting plasmid pMA164 was verified by sequencing and used for integration of the promoter reporter gene fusion into *B. licheniformis* M409 as described for pMA124.

7.8.5.6 Cloning of the promoter-less RBS-*gfpmut2* gene for integration into *amyB*

Construction of pJOE_*amyB*::G2r for integration of the promoter-less *gfpmut2* with a standardized RBS was conducted as described for pMA124. However, the RBS-*gfpmut2* fragment from pUCG2r was amplified with primer 19302 and 19268 introducing *Bpi*I restriction sites suitable for direct cloning into p0690. Moreover, pJOE_amy2 was used instead of pJOE_amy1.

7.8.5.7 Cloning and integration of *cat*::P*3degU-mScarletI* reporter constructs

Construction of pMA137 for integration of *mScarletI* under control of the P3*degU* promoter region from *B. licheniformis* DSM641 into the *cat* locus was conducted as described for pMA164, with the

following modifications. The *degU* P3 promoter located in the *degS-degU* intergenic region was amplified by PCR with oligonucleotides 19252 and 19253. The promoter region was selected as described by Borgmeier *et al.* (2012).

Construction of pMA138 for integration of *mScarletI* with the C-terminal SsrA degradation tag under control of the P3*degU* promoter region from *B. licheniformis* DSM641 into the *cat* locus was conducted as described for pMA137. However, pUCS11r was used instead of pUCS1r.

7.9 Software

Cloning and sequence analysis was performed using Geneious (Version 10.1, Biomatters; Auckland, New Zealand). Data evaluation and visualization was conducted with MS Excel (Microsoft Corp.; Redmond, Washington, USA) and GraphPad Prism (Version 8, GraphPad Software; San Diego, California, USA). Flowcytometry data were analyzed with CytExpert (Version 2.3; Beckmann Coulter GmbH; Krefeld, Germany) and FlowJo (Becton, Dickinson & Company; Ashland, Oregon, USA). Fluorescence microscopy images were analyzed using the ZEN Image software (Version 2.6; Carl Zeiss, Jena, Germany) and ImageJ using the plugin ObjectJ with the NucTracer script (NIH; Syvertsson *et al.* 2016).

8 References

Ababneh, Qutaiba O.; Herman, Jennifer K. (2015): CodY Regulates SigD Levels and Activity by Binding to Three Sites in the fla/che Operon. In: *Journal of bacteriology* 197 (18), S. 2999–3006. DOI: 10.1128/JB.00288-15.

Acevedo-Rocha, Carlos G.; Gronenberg, Luisa S.; Mack, Matthias; Commichau, Fabian M.; Genee, Hans J. (2019): Microbial cell factories for the sustainable manufacturing of B vitamins. In: *Current opinion in biotechnology* 56, S. 18–29. DOI: 10.1016/j.copbio.2018.07.006.

Adams, David G. (2000): Heterocyst formation in cyanobacteria. In: *Current opinion in microbiology* 3 (6), S. 618–624. DOI: 10.1016/S1369-5274(00)00150-8.

Aguilar, Claudio; Vlamakis, Hera; Losick, Richard; Kolter, Roberto (2007): Thinking about Bacillus subtilis as a multicellular organism. In: *Current opinion in microbiology* 10 (6), S. 638–643. DOI: 10.1016/j.mib.2007.09.006.

Aguilar Suárez, Rocío; Stülke, Jörg; van Dijl, Jan Maarten (2019): Less Is More: Toward a Genome-Reduced Bacillus Cell Factory for "Difficult Proteins". In: *ACS synthetic biology* 8 (1), S. 99–108. DOI: 10.1021/acssynbio.8b00342.

Aizawa, Shin-Ichi; Zhulin, Igor B.; Márquez-Magaña, Leticia; Ordal, George W. (2002): Chemotaxis and Motility. In: Sonenshein, Losick and Hoch (Hg.): Bacillus subtilis and Its Closest Relatives. From Genes to Cells: American Society of Microbiology, S. 437–452.

Allmansberger, R. (1997): Temporal regulation of sigD from Bacillus subtilis depends on a minor promoter in front of the gene. In: *Journal of bacteriology* 179 (20), S. 6531–6535. DOI: 10.1128/jb.179.20.6531-6535.1997.

Alonso, Saúl; Rendueles, Manuel; Díaz, Mario (2012): Physiological heterogeneity of Pseudomonas taetrolens during lactobionic acid production. In: *Applied microbiology and biotechnology* 96 (6), S. 1465–1477. DOI: 10.1007/s00253-012-4254-2.

Altenbuchner, Josef (2016): Editing of the Bacillus subtilis Genome by the CRISPR-Cas9 System. In: *Applied and environmental microbiology* 82 (17), S. 5421–5427. DOI: 10.1128/AEM.01453-16.

Amati, Giuseppe; Bisicchia, Paola; Galizzi, Alessandro (2004): DegU-P represses expression of the motility fla-che operon in Bacillus subtilis. In: *Journal of bacteriology* 186 (18), S. 6003–6014. DOI: 10.1128/JB.186.18.6003-6014.2004.

Amory, A.; Kunst, F.; Aubert, E.; Klier, A.; Rapoport, G. (1987): Characterization of the sacQ genes from Bacillus licheniformis and Bacillus subtilis. In: *Journal of bacteriology* 169 (1), S. 324–333. DOI: 10.1128/jb.169.1.324-333.1987.

Ara, Katsutoshi; Ozaki, Katsuya; Nakamura, Kouji; Yamane, Kunio; Sekiguchi, Junichi; Ogasawara, Naotake (2007): Bacillus minimum genome factory: effective utilization of microbial genome information. In: *Biotechnology and applied biochemistry* 46 (Pt 3), S. 169–178. DOI: 10.1042/BA20060111.

Arnaouteli, Sofia; Ferreira, Ana Sofia; Schor, Marieke; Morris, Ryan J.; Bromley, Keith M.; Jo, Jeanyoung *et al.* (2017): Bifunctionality of a biofilm matrix protein controlled by redox state. In: *Proceedings of the National Academy of Sciences of the United States of America* 114 (30), E6184-E6191. DOI: 10.1073/pnas.1707687114.

Arnaouteli, Sofia; Matoz-Fernandez, D. A.; Porter, Michael; Kalamara, Margarita; Abbott, James; MacPhee, Cait E. *et al.* (2019): Pulcherrimin formation controls growth arrest of the Bacillus subtilis biofilm. In: *Proceedings of the National Academy of Sciences of the United States of America* 116 (27), S. 13553–13562. DOI: 10.1073/pnas.1903982116.

Ashiuchi, Makoto; Nakamura, Hisaaki; Yamamoto, Masayoshi; Misono, Haruo (2006): Novel poly-gamma-glutamate-processing enzyme catalyzing gamma-glutamyl DD-amidohydrolysis. In: *Journal of bioscience and bioengineering* 102 (1), S. 60–65. DOI: 10.1263/jbb.102.60.

Auchtung, Jennifer M.; Lee, Catherine A.; Grossman, Alan D. (2006): Modulation of the ComA-dependent quorum response in Bacillus subtilis by multiple Rap proteins and Phr peptides. In: *Journal of bacteriology* 188 (14), S. 5273–5285. DOI: 10.1128/JB.00300-06.

Avery, Simon V. (2006): Microbial cell individuality and the underlying sources of heterogeneity. In: *Nature reviews. Microbiology* 4 (8), S. 577–587. DOI: 10.1038/nrmicro1460.

Ayusawa, D.; Yoneda, Y.; Yamane, K.; Maruo, B. (1975): Pleiotropic phenomena in autolytic enzyme(s) content, flagellation, and simultaneous hyperproduction of extracellular alpha-amylase and protease in a Bacillus subtilis mutant. In: *Journal of bacteriology* 124 (1), S. 459–469.

Baert, Jonathan; Kinet, Romain; Brognaux, Alison; Delepierre, Anissa; Telek, Samuel; Sørensen, Søren J. *et al.* (2015): Phenotypic variability in bioprocessing conditions can be tracked on the basis of on-line flow cytometry and fits to a scaling law. In: *Biotechnology journal* 10 (8), S. 1316–1325. DOI: 10.1002/biot.201400537.

Bähr, Cornelia; Leuchtle, Bernd; Lehmann, Christian; Becker, Julia; Jeude, Markus; Peinemann, Frank *et al.* (2012): Dialysis shake flask for effective screening in fed-batch mode. In: *Biochemical Engineering Journal* 69, S. 182–195. DOI: 10.1016/j.bej.2012.08.012.

Bahram, Mohammad; Hildebrand, Falk; Forslund, Sofia K.; Anderson, Jennifer L.; Soudzilovskaia, Nadejda A.; Bodegom, Peter M. *et al.* (2018): Structure and function of the global topsoil microbiome. In: *Nature* 560 (7717), S. 233–237. DOI: 10.1038/s41586-018-0386-6.

Bai, U.; Mandic-Mulec, I.; Smith, I. (1993): SinI modulates the activity of SinR, a developmental switch protein of Bacillus subtilis, by protein-protein interaction. In: *Genes & development* 7 (1), S. 139–148. DOI: 10.1101/gad.7.1.139.

Bais, Harsh Pal; Fall, Ray; Vivanco, Jorge M. (2004): Biocontrol of Bacillus subtilis against infection of Arabidopsis roots by Pseudomonas syringae is facilitated by biofilm formation and surfactin production. In: *Plant physiology* 134 (1), S. 307–319. DOI: 10.1104/pp.103.028712.

Baptista, Catarina; Barreto, Hugo Condessa; São-José, Carlos (2013): High levels of DegU-P activate an Esat-6-like secretion system in Bacillus subtilis. In: *PloS one* 8 (7), e67840. DOI: 10.1371/journal.pone.0067840.

Barbe, Valérie; Cruveiller, Stéphane; Kunst, Frank; Lenoble, Patricia; Meurice, Guillaume; Sekowska, Agnieszka *et al.* (2009): From a consortium sequence to a unified sequence: the Bacillus subtilis 168 reference genome a decade later. In: *Microbiology (Reading, England)* 155 (Pt 6), S. 1758–1775. DOI: 10.1099/mic.0.027839-0.

Barbieri, Giulia; Albertini, Alessandra M.; Ferrari, Eugenio; Sonenshein, Abraham L.; Belitsky, Boris R. (2016): Interplay of CodY and ScoC in the Regulation of Major Extracellular Protease Genes of Bacillus subtilis. In: *Journal of bacteriology* 198 (6), S. 907–920. DOI: 10.1128/JB.00894-15.

Bartolini, M.; Cogliati, S.; Vileta, D.; Bauman, C.; Rateni, L.; Leñini, C. *et al.* (2018): Regulation of Biofilm Aging and Dispersal in Bacillus subtilis by the Alternative Sigma Factor SigB. In: *Journal of bacteriology* 201 (2). DOI: 10.1128/JB.00473-18.

Beauregard, Pascale B.; Chai, Yunrong; Vlamakis, Hera; Losick, Richard; Kolter, Roberto (2013): Bacillus subtilis biofilm induction by plant polysaccharides. In: *Proceedings of the National Academy of Sciences of the United States of America* 110 (17), E1621-30. DOI: 10.1073/pnas.1218984110.

Belas, Robert (2014): Biofilms, flagella, and mechanosensing of surfaces by bacteria. In: *Trends in microbiology* 22 (9), S. 517–527. DOI: 10.1016/j.tim.2014.05.002.

Bergara, F.; Ibarra, C.; Iwamasa, J.; Patarroyo, J. C.; Aguilera, R.; Márquez-Magaña, L. M. (2003): CodY is a nutritional repressor of flagellar gene expression in Bacillus subtilis. In: *Journal of bacteriology* 185 (10), S. 3118–3126. DOI: 10.1128/JB.185.10.3118–3126.2003.

Bertero, M. G.; Gonzales, B.; Tarricone, C.; Ceciliani, F.; Galizzi, A. (1999): Overproduction and characterization of the Bacillus subtilis anti-sigma factor FlgM. In: *The Journal of biological chemistry* 274 (17), S. 12103–12107. DOI: 10.1074/jbc.274.17.12103.

Blackman, S. A.; Smith, T. J.; Foster, S. J. (1998): The role of autolysins during vegetative growth of Bacillus subtilis 168. In: *Microbiology (Reading, England)* 144 (Pt 1), S. 73–82. DOI: 10.1099/00221287-144-1-73.

Blair, Kris M.; Turner, Linda; Winkelman, Jared T.; Berg, Howard C.; Kearns, Daniel B. (2008): A molecular clutch disables flagella in the Bacillus subtilis biofilm. In: *Science (New York, N.Y.)* 320 (5883), S. 1636–1638. DOI: 10.1126/science.1157877.

Blencke, Hans-Matti; Homuth, Georg; Ludwig, Holger; Mäder, Ulrike; Hecker, Michael; Stülke, Jörg (2003): Transcriptional profiling of gene expression in response to glucose in Bacillus subtilis: regulation of the central metabolic pathways. In: *Metabolic engineering* 5 (2), S. 133–149. DOI: 10.1016/s1096-7176(03)00009-0.

Blokpoel, Marian C.J.; O'Toole, Ronan; Smeulders, Marjan J.; Williams, Huw D. (2003): Development and application of unstable GFP variants to kinetic studies of mycobacterial gene expression. In: *Journal of Microbiological Methods* 54 (2), S. 203–211. DOI: 10.1016/S0167-7012(03)00044-7.

Bongiorni, Cristina; Ishikawa, Shu; Stephenson, Sophie; Ogasawara, Naotake; Perego, Marta (2005): Synergistic regulation of competence development in Bacillus subtilis by two Rap-Phr systems. In: *Journal of bacteriology* 187 (13), S. 4353–4361. DOI: 10.1128/JB.187.13.4353-4361.2005.

Borgmeier, Claudia; Biedendieck, Rebekka; Hoffmann, Kristina; Jahn, Dieter; Meinhardt, Friedhelm (2011): Transcriptome profiling of degU expression reveals unexpected regulatory patterns in Bacillus megaterium and discloses new targets for optimizing expression. In: *Applied microbiology and biotechnology* 92 (3), S. 583–596. DOI: 10.1007/s00253-011-3575-x.

Borgmeier, Claudia; Bongaerts, Johannes; Meinhardt, Friedhelm (2012): Genetic analysis of the Bacillus licheniformis degSU operon and the impact of regulatory mutations on protease production. In: *Journal of biotechnology* 159 (1-2), S. 12–20. DOI: 10.1016/j.jbiotec.2012.02.011.

Borriss, Rainer; Danchin, Antoine; Harwood, Colin R.; Médigue, Claudine; Rocha, Eduardo P. C.; Sekowska, Agnieszka; Vallenet, David (2018): Bacillus subtilis, the model Gram-positive bacterium: 20 years of annotation refinement. In: *Microbial biotechnology* 11 (1), S. 3–17. DOI: 10.1111/1751-7915.13043.

Branda, S. S.; González-Pastor, J. E.; Ben-Yehuda, S.; Losick, R.; Kolter, R. (2001): Fruiting body formation by Bacillus subtilis. In: *Proceedings of the National Academy of Sciences of the United States of America* 98 (20), S. 11621–11626. DOI: 10.1073/pnas.191384198.

Branda, Steven S.; Chu, Frances; Kearns, Daniel B.; Losick, Richard; Kolter, Roberto (2006): A major protein component of the Bacillus subtilis biofilm matrix. In: *Molecular microbiology* 59 (4), S. 1229–1238. DOI: 10.1111/j.1365-2958.2005.05020.x.

Branda, Steven S.; González-Pastor, José Eduardo; Dervyn, Etienne; Ehrlich, S. Dusko; Losick, Richard; Kolter, Roberto (2004): Genes involved in formation of structured multicellular communities by Bacillus subtilis. In: *Journal of bacteriology* 186 (12), S. 3970–3979. DOI: 10.1128/JB.186.12.3970-3979.2004.

Branda, Steven S.; Vik, Shild; Friedman, Lisa; Kolter, Roberto (2005): Biofilms: the matrix revisited. In: *Trends in microbiology* 13 (1), S. 20–26. DOI: 10.1016/j.tim.2004.11.006.

Bridier, Arnaud; Le Coq, Dominique; Dubois-Brissonnet, Florence; Thomas, Vincent; Aymerich, Stéphane; Briandet, Romain (2011): The spatial architecture of Bacillus subtilis biofilms deciphered using a surface-associated model and in situ imaging. In: *PloS one* 6 (1), e16177. DOI: 10.1371/journal.pone.0016177.

Brinsmade, Shaun R.; Sonenshein, Abraham L. (2011): Dissecting complex metabolic integration provides direct genetic evidence for CodY activation by guanine nucleotides. In: *Journal of bacteriology* 193 (20), S. 5637–5648. DOI: 10.1128/JB.05510-11.

Britton, Robert A.; Eichenberger, Patrick; Gonzalez-Pastor, Jose Eduardo; Fawcett, Paul; Monson, Rita; Losick, Richard; Grossman, Alan D. (2002): Genome-wide analysis of the stationary-phase sigma factor (sigma-H) regulon of Bacillus subtilis. In: *Journal of bacteriology* 184 (17), S. 4881–4890. DOI: 10.1128/jb.184.17.4881-4890.2002.

Burbulys, David; Trach, Kathleen A.; Hoch, James A. (1991): Initiation of sporulation in B. subtilis is controlled by a multicomponent phosphorelay. In: *Cell* 64 (3), S. 545–552. DOI: 10.1016/0092-8674(91)90238-t.

Cabeen, Matthew T.; Russell, Jonathan R.; Paulsson, Johan; Losick, Richard (2017): Use of a microfluidic platform to uncover basic features of energy and environmental stress responses in individual cells of Bacillus subtilis. In: *PLoS genetics* 13 (7), e1006901. DOI: 10.1371/journal.pgen.1006901.

Cairns, Lynne S.; Hobley, Laura; Stanley-Wall, Nicola R. (2014): Biofilm formation by Bacillus subtilis: new insights into regulatory strategies and assembly mechanisms. In: *Molecular microbiology* 93 (4), S. 587–598. DOI: 10.1111/mmi.12697.

Cairns, Lynne S.; Marlow, Victoria L.; Bissett, Emma; Ostrowski, Adam; Stanley-Wall, Nicola R. (2013): A mechanical signal transmitted by the flagellum controls signalling in Bacillus subtilis. In: *Molecular microbiology* 90 (1), S. 6–21. DOI: 10.1111/mmi.12342.

Cairns, Lynne S.; Martyn, Jessica E.; Bromley, Keith; Stanley-Wall, Nicola R. (2015): An alternate route to phosphorylating DegU of Bacillus subtilis using acetyl phosphate. In: *BMC microbiology* 15, S. 78. DOI: 10.1186/s12866-015-0410-z.

Calvio, Cinzia; Celandroni, Francesco; Ghelardi, Emilia; Amati, Giuseppe; Salvetti, Sara; Ceciliani, Fabrizio *et al.* (2005): Swarming differentiation and swimming motility in Bacillus subtilis are controlled by swrA, a newly identified dicistronic operon. In: *Journal of bacteriology* 187 (15), S. 5356–5366. DOI: 10.1128/JB.187.15.5356-5366.2005.

Calvio, Cinzia; Osera, Cecilia; Amati, Giuseppe; Galizzi, Alessandro (2008): Autoregulation of swrAA and motility in Bacillus subtilis. In: *Journal of bacteriology* 190 (16), S. 5720–5728. DOI: 10.1128/JB.00455-08.

Caramori, T.; Barilla, D.; Nessi, C.; Sacchi, L.; Galizzi, A. (1996): Role of FlgM in sigma D-dependent gene expression in Bacillus subtilis. In: *Journal of bacteriology* 178 (11), S. 3113–3118. DOI: 10.1128/jb.178.11.3113-3118.1996.

Caspi, Ron; Altman, Tomer; Billington, Richard; Dreher, Kate; Foerster, Hartmut; Fulcher, Carol A. *et al.* (2014): The MetaCyc database of metabolic pathways and enzymes and the BioCyc collection of Pathway/Genome Databases. In: *Nucleic acids research* 42 (Database issue), D459-71. DOI: 10.1093/nar/gkt1103.

Chai, Yunrong; Beauregard, Pascale B.; Vlamakis, Hera; Losick, Richard; Kolter, Roberto (2012): Galactose metabolism plays a crucial role in biofilm formation by Bacillus subtilis. In: *mBio* 3 (4), e00184-12. DOI: 10.1128/mBio.00184-12.

Chai, Yunrong; Chu, Frances; Kolter, Roberto; Losick, Richard (2008): Bistability and biofilm formation in Bacillus subtilis. In: *Molecular microbiology* 67 (2), S. 254–263. DOI: 10.1111/j.1365-2958.2007.06040.x.

Chai, Yunrong; Kolter, Roberto; Losick, Richard (2009): Paralogous antirepressors acting on the master regulator for biofilm formation in Bacillus subtilis. In: *Molecular microbiology* 74 (4), S. 876–887. DOI: 10.1111/j.1365-2958.2009.06900.x.

Chai, Yunrong; Kolter, Roberto; Losick, Richard (2010a): Reversal of an epigenetic switch governing cell chaining in Bacillus subtilis by protein instability. In: *Molecular microbiology* 78 (1), S. 218–229. DOI: 10.1111/j.1365-2958.2010.07335.x.

Chai, Yunrong; Norman, Thomas; Kolter, Roberto; Losick, Richard (2010b): An epigenetic switch governing daughter cell separation in Bacillus subtilis. In: *Genes & development* 24 (8), S. 754–765. DOI: 10.1101/gad.1915010.

Chan, Jia Mun; Guttenplan, Sarah B.; Kearns, Daniel B. (2014): Defects in the flagellar motor increase synthesis of poly-γ-glutamate in Bacillus subtilis. In: *Journal of bacteriology* 196 (4), S. 740–753. DOI: 10.1128/JB.01217-13.

Chen, Rui; Guttenplan, Sarah B.; Blair, Kris M.; Kearns, Daniel B. (2009): Role of the sigmaD-dependent autolysins in Bacillus subtilis population heterogeneity. In: *Journal of bacteriology* 191 (18), S. 5775–5784. DOI: 10.1128/JB.00521-09.

Chowdhury, Soumitra Paul; Dietel, Kristin; Rändler, Manuela; Schmid, Michael; Junge, Helmut; Borriss, Rainer *et al.* (2013): Effects of Bacillus amyloliquefaciens FZB42 on lettuce growth and health under pathogen pressure and its impact on the rhizosphere bacterial community. In: *PloS one* 8 (7), e68818. DOI: 10.1371/journal.pone.0068818.

Christiansen, Torben; Nielsen, Jens (2002): Production of extracellular protease and glucose uptake in Bacillus clausii in steady-state and transient continuous cultures. In: *Journal of biotechnology* 97 (3), S. 265–273. DOI: 10.1016/s0168-1656(02)00109-8.

Chu, Frances; Kearns, Daniel B.; Branda, Steven S.; Kolter, Roberto; Losick, Richard (2006): Targets of the master regulator of biofilm formation in Bacillus subtilis. In: *Molecular microbiology* 59 (4), S. 1216–1228. DOI: 10.1111/j.1365-2958.2005.05019.x.

Chu, Frances; Kearns, Daniel B.; McLoon, Anna; Chai, Yunrong; Kolter, Roberto; Losick, Richard (2008): A novel regulatory protein governing biofilm formation in Bacillus subtilis. In: *Molecular microbiology* 68 (5), S. 1117–1127. DOI: 10.1111/j.1365-2958.2008.06201.x.

Chumsakul, Onuma; Takahashi, Hiroki; Oshima, Taku; Hishimoto, Takahiro; Kanaya, Shigehiko; Ogasawara, Naotake; Ishikawa, Shu (2011): Genome-wide binding profiles of the Bacillus subtilis transition state regulator AbrB and its homolog Abh reveals their interactive role in transcriptional regulation. In: *Nucleic acids research* 39 (2), S. 414–428. DOI: 10.1093/nar/gkq780.

Claverys, Jean-Pierre; Håvarstein, Leiv S. (2007): Cannibalism and fratricide: mechanisms and raisons d'être. In: *Nature reviews. Microbiology* 5 (3), S. 219–229. DOI: 10.1038/nrmicro1613.

Cobb, Ryan E.; Wang, Yajie; Zhao, Huimin (2015): High-efficiency multiplex genome editing of Streptomyces species using an engineered CRISPR/Cas system. In: *ACS synthetic biology* 4 (6), S. 723–728. DOI: 10.1021/sb500351f.

Cohn, Ferdinand (1870): Beiträge zur Biologie der Pflanzen. 2017, Nachdruck der Ausgabe von 1870. Norderstedt: Hansebooks GmbH.

Coker, James A. (2019): Recent advances in understanding extremophiles. In: *F1000Research* 8. DOI: 10.12688/f1000research.20765.1.

Colledge, Vicki L.; Fogg, Mark J.; Levdikov, Vladimir M.; Leech, Andrew; Dodson, Eleanor J.; Wilkinson, Anthony J. (2011): Structure and organisation of SinR, the master regulator of biofilm formation in Bacillus subtilis. In: *Journal of molecular biology* 411 (3), S. 597–613. DOI: 10.1016/j.jmb.2011.06.004.

Core, Leighton; Perego, Marta (2003): TPR-mediated interaction of RapC with ComA inhibits response regulator-DNA binding for competence development in Bacillus subtilis. In: *Molecular microbiology* 49 (6), S. 1509–1522. DOI: 10.1046/j.1365-2958.2003.03659.x.

Courtney, Colleen R.; Cozy, Loralyn M.; Kearns, Daniel B. (2012): Molecular characterization of the flagellar hook in Bacillus subtilis. In: *Journal of bacteriology* 194 (17), S. 4619–4629. DOI: 10.1128/JB.00444-12.

Cozy, Loralyn M.; Kearns, Daniel B. (2010): Gene position in a long operon governs motility development in Bacillus subtilis. In: *Molecular microbiology* 76 (2), S. 273–285. DOI: 10.1111/j.1365-2958.2010.07112.x.

Cozy, Loralyn M.; Phillips, Andrew M.; Calvo, Rebecca A.; Bate, Ashley R.; Hsueh, Yi-Huang; Bonneau, Richard *et al.* (2012): SlrA/SinR/SlrR inhibits motility gene expression upstream of a hypersensitive and hysteretic switch at the level of σ(D) in Bacillus subtilis. In: *Molecular microbiology* 83 (6), S. 1210–1228. DOI: 10.1111/j.1365-2958.2012.08003.x.

Cutting, Simon M. (2011): Bacillus probiotics. In: *Food microbiology* 28 (2), S. 214–220. DOI: 10.1016/j.fm.2010.03.007.

Dahl, M. K.; Msadek, T.; Kunst, F.; Rapoport, G. (1991): Mutational analysis of the Bacillus subtilis DegU regulator and its phosphorylation by the DegS protein kinase. In: *Journal of bacteriology* 173 (8), S. 2539–2547. DOI: 10.1128/jb.173.8.2539-2547.1991.

Dahl, M. K.; Msadek, T.; Kunst, F.; Rapoport, G. (1992): The phosphorylation state of the DegU response regulator acts as a molecular switch allowing either degradative enzyme synthesis or expression of genetic competence in Bacillus subtilis. In: *The Journal of biological chemistry* 267 (20), S. 14509–14514.

Davey, M. E.; O'toole, G. A. (2000): Microbial biofilms: from ecology to molecular genetics. In: *Microbiology and molecular biology reviews : MMBR* 64 (4), S. 847–867. DOI: 10.1128/mmbr.64.4.847-867.2000.

Delgado-Baquerizo, Manuel; Oliverio, Angela M.; Brewer, Tess E.; Benavent-González, Alberto; Eldridge, David J.; Bardgett, Richard D. *et al.* (2018): A global atlas of the dominant bacteria found in soil. In: *Science (New York, N.Y.)* 359 (6373), S. 320–325. DOI: 10.1126/science.aap9516.

DeLoughery, Aaron; Dengler, Vanina; Chai, Yunrong; Losick, Richard (2016): Biofilm formation by Bacillus subtilis requires an endoribonuclease-containing multisubunit complex that controls mRNA levels for the matrix gene repressor SinR. In: *Molecular microbiology* 99 (2), S. 425–437. DOI: 10.1111/mmi.13240.

DeLoughery, Aaron; Lalanne, Jean-Benoît; Losick, Richard; Li, Gene-Wei (2018): Maturation of polycistronic mRNAs by the endoribonuclease RNase Y and its associated Y-complex in Bacillus subtilis. In: *Proceedings of the National Academy of Sciences of the United States of America* 115 (24), E5585-E5594. DOI: 10.1073/pnas.1803283115.

Delvigne, Frank; Baert, Jonathan; Gofflot, Sébastien; Lejeune, Annick; Telek, Samuel; Johanson, Ted; Lantz, Anna Eliasson (2015): Dynamic single-cell analysis of Saccharomyces cerevisiae under process perturbation: comparison of different methods for monitoring the intensity of population heterogeneity. In: *J. Chem. Technol. Biotechnol.* 90 (2), S. 314–323. DOI: 10.1002/jctb.4430.

Delvigne, Frank; Goffin, Philippe (2014): Microbial heterogeneity affects bioprocess robustness: dynamic single-cell analysis contributes to understanding of microbial populations. In: *Biotechnology journal* 9 (1), S. 61–72. DOI: 10.1002/biot.201300119.

Delvigne, Frank; Zune, Quentin; Lara, Alvaro R.; Al-Soud, Waleed; Sørensen, Søren J. (2014): Metabolic variability in bioprocessing: implications of microbial phenotypic heterogeneity. In: *Trends in biotechnology* 32 (12), S. 608–616. DOI: 10.1016/j.tibtech.2014.10.002.

Dempsey, L. A.; Dubnau, D. A. (1989): Identification of plasmid and Bacillus subtilis chromosomal recombination sites used for pE194 integration. In: *Journal of bacteriology* 171 (5), S. 2856–2865. DOI: 10.1128/jb.171.5.2856-2865.1989.

Dervyn, Etienne; Noirot-Gros, Marie-Françoise; Mervelet, Peggy; McGovern, Steven; Ehrlich, S. Dusko; Polard, Patrice; Noirot, Philippe (2004): The bacterial condensin/cohesin-like protein complex acts in DNA repair and regulation of gene expression. In: *Molecular microbiology* 51 (6), S. 1629–1640. DOI: 10.1111/j.1365-2958.2003.03951.x.

Díaz, Mario; Herrero, Mónica; García, Luis A.; Quirós, Covadonga (2010): Application of flow cytometry to industrial microbial bioprocesses. In: *Biochemical Engineering Journal* 48 (3), S. 385–407. DOI: 10.1016/j.bej.2009.07.013.

Diethmaier, Christine; Chawla, Ravi; Canzoneri, Alexandra; Kearns, Daniel B.; Lele, Pushkar P.; Dubnau, David (2017): Viscous drag on the flagellum activates Bacillus subtilis entry into the K-state. In: *Molecular microbiology* 106 (3), S. 367–380. DOI: 10.1111/mmi.13770.

Diethmaier, Christine; Pietack, Nico; Gunka, Katrin; Wrede, Christoph; Lehnik-Habrink, Martin; Herzberg, Christina *et al.* (2011): A novel factor controlling bistability in Bacillus subtilis: the YmdB protein affects flagellin expression and biofilm formation. In: *Journal of bacteriology* 193 (21), S. 5997–6007. DOI: 10.1128/JB.05360-11.

Do, Thi-Huyen; Suzuki, Yuki; Abe, Naoki; Kaneko, Jun; Itoh, Yoshifumi; Kimura, Keitarou (2011): Mutations suppressing the loss of DegQ function in Bacillus subtilis (natto) poly-γ-glutamate synthesis. In: *Applied and environmental microbiology* 77 (23), S. 8249–8258. DOI: 10.1128/AEM.05827-11.

Dogsa, Iztok; Brloznik, Mojca; Stopar, David; Mandic-Mulec, Ines (2013): Exopolymer diversity and the role of levan in Bacillus subtilis biofilms. In: *PloS one* 8 (4), e62044. DOI: 10.1371/journal.pone.0062044.

Dragoš, Anna; Kiesewalter, Heiko; Martin, Marivic; Hsu, Chih-Yu; Hartmann, Raimo; Wechsler, Tobias *et al.* (2018): Division of Labor during Biofilm Matrix Production. In: *Current biology : CB* 28 (12), 1903-1913.e5. DOI: 10.1016/j.cub.2018.04.046.

Drews, G. (2000): The roots of microbiology and the influence of Ferdinand Cohn on microbiology of the 19th century. In: *FEMS microbiology reviews* 24 (3), S. 225–249. DOI: 10.1111/j.1574-6976.2000.tb00540.x.

Dubnau, David; Losick, Richard (2006): Bistability in bacteria. In: *Molecular microbiology* 61 (3), S. 564–572. DOI: 10.1111/j.1365-2958.2006.05249.x.

Dubnau, E.; Weir, J.; Nair, G.; Carter, L.; Moran, C.; Smith, I. (1988): Bacillus sporulation gene spo0H codes for sigma 30 (sigma H). In: *Journal of bacteriology* 170 (3), S. 1054–1062. DOI: 10.1128/jb.170.3.1054-1062.1988.

Dubnau, Eugenie J.; Carabetta, Valerie J.; Tanner, Andrew W.; Miras, Mathieu; Diethmaier, Christine; Dubnau, David (2016): A protein complex supports the production of Spo0A-P and plays additional roles for biofilms and the K-state in Bacillus subtilis. In: *Molecular microbiology* 101 (4), S. 606–624. DOI: 10.1111/mmi.13411.

Durfee, Tim; Nelson, Richard; Baldwin, Schuyler; Plunkett, Guy; Burland, Valerie; Mau, Bob *et al.* (2008): The complete genome sequence of Escherichia coli DH10B: insights into the biology of a laboratory workhorse. In: *Journal of bacteriology* 190 (7), S. 2597–2606. DOI: 10.1128/JB.01695-07.

Dusane, Devendra H.; Damare, Samir R.; Nancharaiah, Yarlagadda V.; Ramaiah, N.; Venugopalan, Vayalam P.; Kumar, Ameeta Ravi; Zinjarde, Smita S. (2013): Disruption of microbial biofilms by an extracellular protein isolated from epibiotic tropical marine strain of Bacillus licheniformis. In: *PloS one* 8 (5), e64501. DOI: 10.1371/journal.pone.0064501.

Dworkin, Jonathan; Losick, Richard (2005): Developmental commitment in a bacterium. In: *Cell* 121 (3), S. 401–409. DOI: 10.1016/j.cell.2005.02.032.

Earl, Ashlee M.; Losick, Richard; Kolter, Roberto (2008): Ecology and genomics of Bacillus subtilis. In: *Trends in microbiology* 16 (6), S. 269–275. DOI: 10.1016/j.tim.2008.03.004.

Eichenberger, P.; Fawcett, P.; Losick, R. (2001): A three-protein inhibitor of polar septation during sporulation in Bacillus subtilis. In: *Molecular microbiology* 42 (5), S. 1147–1162. DOI: 10.1046/j.1365-2958.2001.02660.x.

Ely, Bert (1991): [17] Genetics of Caulobacter crescentus. In: Bacterial Genetic Systems, Bd. 204: Elsevier (Methods in Enzymology), S. 372–384.

Enfors, S.-O.; Jahic, M.; Rozkov, A.; Xu, B.; Hecker, M.; Jürgen, B. *et al.* (2001): Physiological responses to mixing in large scale bioreactors. In: *Journal of biotechnology* 85 (2), S. 175–185. DOI: 10.1016/s0168-1656(00)00365-5.

Engler, Carola; Kandzia, Romy; Marillonnet, Sylvestre (2008): A one pot, one step, precision cloning method with high throughput capability. In: *PloS one* 3 (11), e3647. DOI: 10.1371/journal.pone.0003647.

Epstein, Alexander K.; Pokroy, Boaz; Seminara, Agnese; Aizenberg, Joanna (2011): Bacterial biofilm shows persistent resistance to liquid wetting and gas penetration. In: *Proceedings of the National Academy of Sciences of the United States of America* 108 (3), S. 995–1000. DOI: 10.1073/pnas.1011033108.

Errington, Jeff (2003): Regulation of endospore formation in Bacillus subtilis. In: *Nature reviews. Microbiology* 1 (2), S. 117–126. DOI: 10.1038/nrmicro750.

Erskine, Elliot; Morris, Ryan J.; Schor, Marieke; Earl, Chris; Gillespie, Rachel M. C.; Bromley, Keith M. *et al.* (2018): Formation of functional, non-amyloidogenic fibres by recombinant Bacillus subtilis TasA. In: *Molecular microbiology* 110 (6), S. 897–913. DOI: 10.1111/mmi.13985.

Estacio, W.; Anna-Arriola, S. Santa; Adedipe, M.; Márquez-Magaña, L. M. (1998): Dual Promoters Are Responsible for Transcription Initiation of the fla/che Operon in Bacillus subtilis. In: *Journal of bacteriology* 180 (14), S. 3548–3555.

Fabret, C.; Feher, V. A.; Hoch, J. A. (1999): Two-component signal transduction in Bacillus subtilis: how one organism sees its world. In: *Journal of bacteriology* 181 (7), S. 1975–1983. DOI: 10.1128/JB.181.7.1975-1983.1999.

Fernandez-de-Cossio-Diaz, Jorge; Mulet, Roberto; Vazquez, Alexei (2019): Cell population heterogeneity driven by stochastic partition and growth optimality. In: *Scientific reports* 9 (1), S. 9406. DOI: 10.1038/s41598-019-45882-w.

Fiore, Gianfranco; Perrino, Giansimone; Di Bernardo, Mario; Di Bernardo, Diego (2016): In Vivo Real-Time Control of Gene Expression: A Comparative Analysis of Feedback Control Strategies in Yeast. In: *ACS synthetic biology* 5 (2), S. 154–162. DOI: 10.1021/acssynbio.5b00135.

Fira, Djordje; Dimkić, Ivica; Berić, Tanja; Lozo, Jelena; Stanković, Slaviša (2018): Biological control of plant pathogens by Bacillus species. In: *Journal of biotechnology* 285, S. 44–55. DOI: 10.1016/j.jbiotec.2018.07.044.

Fischer, Eliane; Sauer, Uwe (2005): Large-scale in vivo flux analysis shows rigidity and suboptimal performance of Bacillus subtilis metabolism. In: *Nature genetics* 37 (6), S. 636–640. DOI: 10.1038/ng1555.

Flemming, Hans-Curt; Wuertz, Stefan (2019): Bacteria and archaea on Earth and their abundance in biofilms. In: *Nature reviews. Microbiology* 17 (4), S. 247–260. DOI: 10.1038/s41579-019-0158-9.

Frankena, Jurjen; Koningstein, Gregory M.; van Verseveld, Henk W.; Stouthamer, Adriaan H. (1986): Effect of different limitations in chemostat cultures on growth and production of exocellular protease byBacillus licheniformis. In: *Applied microbiology and biotechnology* 24 (2), S. 106–112. DOI: 10.1007/BF00938779.

Froyshov, O.; Laland, S. G. (1974): On the biosynthesis of bacitracin by a soluble enzyme complex from Bacillus licheniformis. In: *European journal of biochemistry* 46 (2), S. 235–242. DOI: 10.1111/j.1432-1033.1974.tb03616.x.

Fu, Jing; Huo, Guangxin; Feng, Lili; Mao, Yufeng; Wang, Zhiwen; Ma, Hongwu *et al.* (2016): Metabolic engineering of Bacillus subtilis for chiral pure meso-2,3-butanediol production. In: *Biotechnology for biofuels* 9, S. 90. DOI: 10.1186/s13068-016-0502-5.

Fujita, M.; Sadaie, Y. (1998): Feedback loops involving Spo0A and AbrB in in vitro transcription of the genes involved in the initiation of sporulation in Bacillus subtilis. In: *Journal of biochemistry* 124 (1), S. 98–104. DOI: 10.1093/oxfordjournals.jbchem.a022103.

Fujita, Masaya; González-Pastor, José Eduardo; Losick, Richard (2005): High- and low-threshold genes in the Spo0A regulon of Bacillus subtilis. In: *Journal of bacteriology* 187 (4), S. 1357–1368. DOI: 10.1128/JB.187.4.1357-1368.2005.

Gallego del Sol, Francisca; Marina, Alberto (2013): Structural basis of Rap phosphatase inhibition by Phr peptides. In: *PLoS biology* 11 (3), e1001511. DOI: 10.1371/journal.pbio.1001511.

Gallegos-Monterrosa, Ramses; Mhatre, Eisha; Kovács, Ákos T. (2016): Specific Bacillus subtilis 168 variants form biofilms on nutrient-rich medium. In: *Microbiology (Reading, England)* 162 (11), S. 1922–1932. DOI: 10.1099/mic.0.000371.

Gao, Tantan; Greenwich, Jennifer; Li, Yan; Wang, Qi; Chai, Yunrong (2015): The Bacterial Tyrosine Kinase Activator TkmA Contributes to Biofilm Formation Largely Independently of the Cognate Kinase PtkA in Bacillus subtilis. In: *Journal of bacteriology* 197 (21), S. 3421–3432. DOI: 10.1128/JB.00438-15.

Gaur, N. K.; Cabane, K.; Smith, I. (1988): Structure and expression of the Bacillus subtilis sin operon. In: *Journal of bacteriology* 170 (3), S. 1046–1053. DOI: 10.1128/jb.170.3.1046-1053.1988.

Gaur, N. K.; Oppenheim, J.; Smith, I. (1991): The Bacillus subtilis sin gene, a regulator of alternate developmental processes, codes for a DNA-binding protein. In: *Journal of bacteriology* 173 (2), S. 678–686. DOI: 10.1128/jb.173.2.678-686.1991.

Gerwig, Jan; Kiley, Taryn B.; Gunka, Katrin; Stanley-Wall, Nicola; Stülke, Jörg (2014): The protein tyrosine kinases EpsB and PtkA differentially affect biofilm formation in Bacillus subtilis. In: *Microbiology (Reading, England)* 160 (Pt 4), S. 682–691. DOI: 10.1099/mic.0.074971-0.

Gibson, Daniel G.; Young, Lei; Chuang, Ray-Yuan; Venter, J. Craig; Hutchison, Clyde A.; Smith, Hamilton O. (2009): Enzymatic assembly of DNA molecules up to several hundred kilobases. In: *Nature methods* 6 (5), S. 343–345. DOI: 10.1038/nmeth.1318.

González-Cabaleiro, Rebeca; Mitchell, Anca M.; Smith, Wendy; Wipat, Anil; Ofiţeru, Irina D. (2017): Heterogeneity in Pure Microbial Systems: Experimental Measurements and Modeling. In: *Frontiers in microbiology* 8, S. 1813. DOI: 10.3389/fmicb.2017.01813.

González-Pastor, José E.; Hobbs, Errett C.; Losick, Richard (2003): Cannibalism by sporulating bacteria. In: *Science (New York, N.Y.)* 301 (5632), S. 510–513. DOI: 10.1126/science.1086462.

González-Pastor, José Eduardo (2011): Cannibalism: a social behavior in sporulating Bacillus subtilis. In: *FEMS microbiology reviews* 35 (3), S. 415–424. DOI: 10.1111/j.1574-6976.2010.00253.x.

Görke, Boris; Stülke, Jörg (2008): Carbon catabolite repression in bacteria: many ways to make the most out of nutrients. In: *Nature reviews. Microbiology* 6 (8), S. 613–624. DOI: 10.1038/nrmicro1932.

Grant, S. G.; Jessee, J.; Bloom, F. R.; Hanahan, D. (1990): Differential plasmid rescue from transgenic mouse DNAs into Escherichia coli methylation-restriction mutants. In: *Proceedings of the National Academy of Sciences of the United States of America* 87 (12), S. 4645–4649. DOI: 10.1073/pnas.87.12.4645.

Grossman, A. D. (1995): Genetic networks controlling the initiation of sporulation and the development of genetic competence in Bacillus subtilis. In: *Annual review of genetics* 29, S. 477–508. DOI: 10.1146/annurev.ge.29.120195.002401.

Gu, Yang; Xu, Xianhao; Wu, Yaokang; Niu, Tengfei; Liu, Yanfeng; Li, Jianghua *et al.* (2018): Advances and prospects of Bacillus subtilis cellular factories: From rational design to industrial applications. In: *Metabolic engineering* 50, S. 109–121. DOI: 10.1016/j.ymben.2018.05.006.

Guiziou, Sarah; Sauveplane, Vincent; Chang, Hung-Ju; Clerté, Caroline; Declerck, Nathalie; Jules, Matthieu; Bonnet, Jerome (2016): A part toolbox to tune genetic expression in Bacillus subtilis. In: *Nucleic acids research* 44 (15), S. 7495–7508. DOI: 10.1093/nar/gkw624.

Gundlach, Jan; Rath, Hermann; Herzberg, Christina; Mäder, Ulrike; Stülke, Jörg (2016): Second Messenger Signaling in Bacillus subtilis: Accumulation of Cyclic di-AMP Inhibits Biofilm Formation. In: *Frontiers in microbiology* 7, S. 804. DOI: 10.3389/fmicb.2016.00804.

Guttenplan, Sarah B.; Blair, Kris M.; Kearns, Daniel B. (2010): The EpsE flagellar clutch is bifunctional and synergizes with EPS biosynthesis to promote Bacillus subtilis biofilm formation. In: *PLoS genetics* 6 (12), e1001243. DOI: 10.1371/journal.pgen.1001243.

Guttenplan, Sarah B.; Shaw, Sidney; Kearns, Daniel B. (2013): The cell biology of peritrichous flagella in Bacillus subtilis. In: *Molecular microbiology* 87 (1), S. 211–229. DOI: 10.1111/mmi.12103.

Habicher, Tobias; Czotscher, Vroni; Klein, Tobias; Daub, Andreas; Keil, Timm; Büchs, Jochen (2019a): Glucose-containing polymer rings enable fed-batch operation in microtiter plates with parallel online measurement of scattered light, fluorescence, dissolved oxygen tension, and pH. In: *Biotechnology and bioengineering* 116 (9), S. 2250–2262. DOI: 10.1002/bit.27077.

Habicher, Tobias; John, Arian; Scholl, Niklas; Daub, Andreas; Klein, Tobias; Philip, Priya; Büchs, Jochen (2019b): Introducing substrate limitations to overcome catabolite repression in a protease producing Bacillus licheniformis strain using membrane-based fed-batch shake flasks. In: *Biotechnology and bioengineering* 116 (6), S. 1326–1340. DOI: 10.1002/bit.26948.

Habicher, Tobias; Rauls, Edward K. A.; Egidi, Franziska; Keil, Timm; Klein, Tobias; Daub, Andreas; Büchs, Jochen (2019c): Establishing a Fed-Batch Process for Protease Expression with Bacillus licheniformis in Polymer-Based Controlled-Release Microtiter Plates. In: *Biotechnology journal*, e1900088. DOI: 10.1002/biot.201900088.

Hamoen, L. W.; van Werkhoven, A. F.; Venema, G.; Dubnau, D. (2000): The pleiotropic response regulator DegU functions as a priming protein in competence development in Bacillus subtilis. In:

Proceedings of the National Academy of Sciences of the United States of America 97 (16), S. 9246–9251. DOI: 10.1073/pnas.160010597.

Hamoen, Leendert W.; Venema, Gerard; Kuipers, Oscar P. (2003): Controlling competence in Bacillus subtilis: shared use of regulators. In: *Microbiology (Reading, England)* 149 (Pt 1), S. 9–17. DOI: 10.1099/mic.0.26003-0.

Hamon, M. A.; Lazazzera, B. A. (2001): The sporulation transcription factor Spo0A is required for biofilm development in Bacillus subtilis. In: *Molecular microbiology* 42 (5), S. 1199–1209. DOI: 10.1046/j.1365-2958.2001.02709.x.

Hanlon, G. W.; Hodges, N. A.; Russell, A. D. (1982): The influence of glucose, ammonium and magnesium availability on the production of protease and bacitracin by Bacillus licheniformis. In: *Journal of general microbiology* 128 (4), S. 845–851. DOI: 10.1099/00221287-128-4-845.

Hashimoto, Masayuki; Ooiwa, Seika; Sekiguchi, Junichi (2012): Synthetic lethality of the lytE cwlO genotype in Bacillus subtilis is caused by lack of D,L-endopeptidase activity at the lateral cell wall. In: *Journal of bacteriology* 194 (4), S. 796–803. DOI: 10.1128/JB.05569-11.

Healy, J.; Weir, J.; Smith, I.; Losick, R. (1991): Post-transcriptional control of a sporulation regulatory gene encoding transcription factor sigma H in Bacillus subtilis. In: *Molecular microbiology* 5 (2), S. 477–487. DOI: 10.1111/j.1365-2958.1991.tb02131.x.

Helmann, J. D.; Márquez, L. M.; Chamberlin, M. J. (1988): Cloning, sequencing, and disruption of the Bacillus subtilis sigma 28 gene. In: *Journal of bacteriology* 170 (4), S. 1568–1574. DOI: 10.1128/jb.170.4.1568-1574.1988.

Henner, D. J.; Ferrari, E.; Perego, M.; Hoch, J. A. (1988a): Location of the targets of the hpr-97, sacU32(Hy), and sacQ36(Hy) mutations in upstream regions of the subtilisin promoter. In: *Journal of bacteriology* 170 (1), S. 296–300. DOI: 10.1128/jb.170.1.296-300.1988.

Henner, D. J.; Yang, M.; Ferrari, E. (1988b): Localization of Bacillus subtilis sacU(Hy) mutations to two linked genes with similarities to the conserved procaryotic family of two-component signalling systems. In: *Journal of bacteriology* 170 (11), S. 5102–5109. DOI: 10.1128/jb.170.11.5102-5109.1988.

Hirota, Norifumi; Kitada, Makio; Imae, Yasuo (1981): Flagellar motors of alkalophilic bacillus are powered by an electrochemical potential gradient of Na +. In: *FEBS Letters* 132 (2), S. 278–280. DOI: 10.1016/0014-5793(81)81178-7.

Hobley, Laura; Ostrowski, Adam; Rao, Francesco V.; Bromley, Keith M.; Porter, Michael; Prescott, Alan R. *et al.* (2013): BslA is a self-assembling bacterial hydrophobin that coats the Bacillus subtilis biofilm. In: *Proceedings of the National Academy of Sciences of the United States of America* 110 (33), S. 13600–13605. DOI: 10.1073/pnas.1306390110.

Hoffmann, Tamara; Bremer, Erhard (2017): Guardians in a stressful world: the Opu family of compatible solute transporters from Bacillus subtilis. In: *Biological chemistry* 398 (2), S. 193–214. DOI: 10.1515/hsz-2016-0265.

Hohmann, Hans-Peter; van Dijl, Jan M.; Krishnappa, Laxmi; Prágai, Zoltán (2017): Host Organisms: Bacillus subtilis. In: Christoph Wittmann and James C. Liao (Hg.): Industrial Biotechnology, Bd. 16. Weinheim, Germany: Wiley-VCH Verlag GmbH & Co. KGaA, S. 221–297.

Hölscher, Theresa; Schiklang, Tina; Dragoš, Anna; Dietel, Anne-Kathrin; Kost, Christian; Kovács, Ákos T. (2018): Impaired competence in flagellar mutants of Bacillus subtilis is connected to the regulatory network governed by DegU. In: *Environmental microbiology reports* 10 (1), S. 23–32. DOI: 10.1111/1758-2229.12601.

Hoon, Michiel J. L. de; Eichenberger, Patrick; Vitkup, Dennis (2010): Hierarchical evolution of the bacterial sporulation network. In: *Current biology : CB* 20 (17), R735-45. DOI: 10.1016/j.cub.2010.06.031.

Horton, R. M.; Cai, Z. L.; Ho, S. N.; Pease, L. R. (1990): Gene splicing by overlap extension: tailor-made genes using the polymerase chain reaction. In: *BioTechniques* 8 (5), S. 528–535.

Hsueh, Yi-Huang; Cozy, Loralyn M.; Sham, Lok-To; Calvo, Rebecca A.; Gutu, Alina D.; Winkler, Malcolm E.; Kearns, Daniel B. (2011): DegU-phosphate activates expression of the anti-sigma factor FlgM in Bacillus subtilis. In: *Molecular microbiology* 81 (4), S. 1092–1108. DOI: 10.1111/j.1365-2958.2011.07755.x.

İrigül-Sönmez, Öykü; Köroğlu, Türkan E.; Öztürk, Büşra; Kovács, Ákos T.; Kuipers, Oscar P.; Yazgan-Karataş, Ayten (2014): In Bacillus subtilis LutR is part of the global complex regulatory network governing the adaptation to the transition from exponential growth to stationary phase. In: *Microbiology (Reading, England)* 160 (Pt 2), S. 243–260. DOI: 10.1099/mic.0.064675-0.

Irnov, Irnov; Winkler, Wade C. (2010): A regulatory RNA required for antitermination of biofilm and capsular polysaccharide operons in Bacillales. In: *Molecular microbiology* 76 (3), S. 559–575. DOI: 10.1111/j.1365-2958.2010.07131.x.

Ishii, Hiroshi; Tanaka, Teruo; Ogura, Mitsuo (2013): The Bacillus subtilis response regulator gene degU is positively regulated by CcpA and by catabolite-repressed synthesis of ClpC. In: *Journal of bacteriology* 195 (2), S. 193–201. DOI: 10.1128/JB.01881-12.

Ishikawa, S.; Hara, Y.; Ohnishi, R.; Sekiguchi, J. (1998): Regulation of a new cell wall hydrolase gene, cwlF, which affects cell separation in Bacillus subtilis. In: *Journal of bacteriology* 180 (9), S. 2549–2555. DOI: 10.1128/JB.180.9.2549-2555.1998.

Ito, Masahiro; Hicks, David B.; Henkin, Tina M.; Guffanti, Arthur A.; Powers, Benjamin D.; Zvi, Lior *et al.* (2004): MotPS is the stator-force generator for motility of alkaliphilic Bacillus, and its homologue is a second functional Mot in Bacillus subtilis. In: *Molecular microbiology* 53 (4), S. 1035–1049. DOI: 10.1111/j.1365-2958.2004.04173.x.

Ito, Masahiro; Terahara, Naoya; Fujinami, Shun; Krulwich, Terry Ann (2005): Properties of motility in Bacillus subtilis powered by the H+-coupled MotAB flagellar stator, Na+-coupled MotPS or hybrid stators MotAS or MotPB. In: *Journal of molecular biology* 352 (2), S. 396–408. DOI: 10.1016/j.jmb.2005.07.030.

Jacobs, M. F. (1995): Expression of the subtilisin Carlsberg-encoding gene in Bacillus licheniformis and Bacillus subtilis. In: *Gene* 152 (1), S. 69–74. DOI: 10.1016/0378-1119(94)00655-c.

Jeude, M.; Dittrich, B.; Niederschulte, H.; Anderlei, T.; Knocke, C.; Klee, D.; Büchs, J. (2006): Fed-batch mode in shake flasks by slow-release technique. In: *Biotechnol. Bioeng.* 95 (3), S. 433–445. DOI: 10.1002/bit.21012.

Jiang, M.; Shao, W.; Perego, M.; Hoch, J. A. (2000): Multiple histidine kinases regulate entry into stationary phase and sporulation in Bacillus subtilis. In: *Molecular microbiology* 38 (3), S. 535–542. DOI: 10.1046/j.1365-2958.2000.02148.x.

Jong, Imke G. de; Veening, Jan-Willem; Kuipers, Oscar P. (2012): Single cell analysis of gene expression patterns during carbon starvation in Bacillus subtilis reveals large phenotypic variation. In: *Environmental microbiology* 14 (12), S. 3110–3121. DOI: 10.1111/j.1462-2920.2012.02892.x.

Juhas, Mario; Reuß, Daniel R.; Zhu, Bingyao; Commichau, Fabian M. (2014): Bacillus subtilis and Escherichia coli essential genes and minimal cell factories after one decade of genome engineering. In: *Microbiology (Reading, England)* 160 (Pt 11), S. 2341–2351. DOI: 10.1099/mic.0.079376-0.

Kabisch, Johannes; Thürmer, Andrea; Hübel, Tanno; Popper, Lutz; Daniel, Rolf; Schweder, Thomas (2013): Characterization and optimization of Bacillus subtilis ATCC 6051 as an expression host. In: *Journal of biotechnology* 163 (2), S. 97–104. DOI: 10.1016/j.jbiotec.2012.06.034.

Kaiser, Kristin; Wemheuer, Bernd; Korolkow, Vera; Wemheuer, Franziska; Nacke, Heiko; Schöning, Ingo *et al.* (2016): Driving forces of soil bacterial community structure, diversity, and function in temperate grasslands and forests. In: *Scientific reports* 6, S. 33696. DOI: 10.1038/srep33696.

Kalamara, Margarita; Spacapan, Mihael; Mandic-Mulec, Ines; Stanley-Wall, Nicola R. (2018): Social behaviours by Bacillus subtilis: quorum sensing, kin discrimination and beyond. In: *Molecular microbiology* 110 (6), S. 863–878. DOI: 10.1111/mmi.14127.

Kampf, Jan; Gerwig, Jan; Kruse, Kerstin; Cleverley, Robert; Dormeyer, Miriam; Grünberger, Alexander *et al.* (2018): Selective Pressure for Biofilm Formation in Bacillus subtilis: Differential Effect of Mutations in the Master Regulator SinR on Bistability. In: *mBio* 9 (5). DOI: 10.1128/mBio.01464-18.

Kearns, Daniel B.; Chu, Frances; Branda, Steven S.; Kolter, Roberto; Losick, Richard (2005): A master regulator for biofilm formation by Bacillus subtilis. In: *Molecular microbiology* 55 (3), S. 739–749. DOI: 10.1111/j.1365-2958.2004.04440.x.

Kearns, Daniel B.; Chu, Frances; Rudner, Rivka; Losick, Richard (2004): Genes governing swarming in Bacillus subtilis and evidence for a phase variation mechanism controlling surface motility. In: *Molecular microbiology* 52 (2), S. 357–369. DOI: 10.1111/j.1365-2958.2004.03996.x.

Kearns, Daniel B.; Losick, Richard (2003): Swarming motility in undomesticated Bacillus subtilis. In: *Molecular microbiology* 49 (3), S. 581–590. DOI: 10.1046/j.1365-2958.2003.03584.x.

Kearns, Daniel B.; Losick, Richard (2005): Cell population heterogeneity during growth of Bacillus subtilis. In: *Genes & development* 19 (24), S. 3083–3094. DOI: 10.1101/gad.1373905.

Kensy, Frank; Zang, Emerson; Faulhammer, Christian; Tan, Rung-Kai; Büchs, Jochen (2009): Validation of a high-throughput fermentation system based on online monitoring of biomass and fluorescence in continuously shaken microtiter plates. In: *Microbial cell factories* 8, S. 31. DOI: 10.1186/1475-2859-8-31.

Kim, J. H.; Guvener, Z. T.; Cho, J. Y.; Chung, K. C.; Chambliss, G. H. (1995): Specificity of DNA binding activity of the Bacillus subtilis catabolite control protein CcpA. In: *Journal of bacteriology* 177 (17), S. 5129–5134. DOI: 10.1128/jb.177.17.5129-5134.1995.

Kobayashi, Kazuo (2007a): Bacillus subtilis pellicle formation proceeds through genetically defined morphological changes. In: *Journal of bacteriology* 189 (13), S. 4920–4931. DOI: 10.1128/JB.00157-07.

Kobayashi, Kazuo (2007b): Gradual activation of the response regulator DegU controls serial expression of genes for flagellum formation and biofilm formation in Bacillus subtilis. In: *Molecular microbiology* 66 (2), S. 395–409. DOI: 10.1111/j.1365-2958.2007.05923.x.

Kobayashi, Kazuo (2008): SlrR/SlrA controls the initiation of biofilm formation in Bacillus subtilis. In: *Molecular microbiology* 69 (6), S. 1399–1410. DOI: 10.1111/j.1365-2958.2008.06369.x.

Kobayashi, Kazuo; Ikemoto, Yukako (2019): Biofilm-associated toxin and extracellular protease cooperatively suppress competitors in Bacillus subtilis biofilms. In: *PLoS genetics* 15 (10), e1008232. DOI: 10.1371/journal.pgen.1008232.

Kobayashi, Kazuo; Iwano, Megumi (2012): BslA(YuaB) forms a hydrophobic layer on the surface of Bacillus subtilis biofilms. In: *Molecular microbiology* 85 (1), S. 51–66. DOI: 10.1111/j.1365-2958.2012.08094.x.

Kodgire, Prashant; Rao, K. Krishnamurthy (2009): A dual mode of regulation of flgM by ScoC in Bacillus subtilis. In: *Canadian journal of microbiology* 55 (8), S. 983–989. DOI: 10.1139/w09-049.

Kohlstedt, Michael; Sappa, Praveen K.; Meyer, Hanna; Maaß, Sandra; Zaprasis, Adrienne; Hoffmann, Tamara *et al.* (2014): Adaptation of Bacillus subtilis carbon core metabolism to simultaneous nutrient limitation and osmotic challenge: a multi-omics perspective. In: *Environmental microbiology* 16 (6), S. 1898–1917. DOI: 10.1111/1462-2920.12438.

Kovács, Akos T.; Kuipers, Oscar P. (2011): Rok regulates yuaB expression during architecturally complex colony development of Bacillus subtilis 168. In: *Journal of bacteriology* 193 (4), S. 998–1002. DOI: 10.1128/JB.01170-10.

Kubori, T.; Okumura, M.; Kobayashi, N.; Nakamura, D.; Iwakura, M.; Aizawa, S. I. (1997): Purification and characterization of the flagellar hook-basal body complex of Bacillus subtilis. In: *Molecular microbiology* 24 (2), S. 399–410. DOI: 10.1046/j.1365-2958.1997.3341714.x.

Kumpfmüller, Jana; Methling, Karen; Fang, Lei; Pfeifer, Blaine A.; Lalk, Michael; Schweder, Thomas (2016): Production of the polyketide 6-deoxyerythronolide B in the heterologous host Bacillus subtilis. In: *Applied microbiology and biotechnology* 100 (3), S. 1209–1220. DOI: 10.1007/s00253-015-6990-6.

Kunst, F.; Ogasawara, N.; Moszer, I.; Albertini, A. M.; Alloni, G.; Azevedo, V. *et al.* (1997): The complete genome sequence of the gram-positive bacterium Bacillus subtilis. In: *Nature* 390 (6657), S. 249–256. DOI: 10.1038/36786.

Kunst, F.; Pascal, M.; Lepesant-Kejzlarova, J.; Lepesant, J. A.; Billault, A.; Dedonder, R. (1974): Pleiotropic mutations affecting sporulation conditions and the syntheses of extracellular enzymes in Bacillus subtilis 168. In: *Biochimie* 56 (11-12), S. 1481–1489. DOI: 10.1016/s0300-9084(75)80270-7.

Küppers, Tobias; Steffen, Victoria; Hellmuth, Hendrik; O'Connell, Timothy; Bongaerts, Johannes; Maurer, Karl-Heinz; Wiechert, Wolfgang (2014): Developing a new production host from a blueprint: Bacillus pumilus as an industrial enzyme producer. In: *Microbial cell factories* 13 (1), S. 46. DOI: 10.1186/1475-2859-13-46.

Laemmli, U. K. (1970): Cleavage of structural proteins during the assembly of the head of bacteriophage T4. In: *Nature* 227 (5259), S. 680–685. DOI: 10.1038/227680a0.

Lakowitz, Antonia; Krull, Rainer; Biedendieck, Rebekka (2017): Recombinant production of the antibody fragment D1.3 scFv with different Bacillus strains. In: *Microbial cell factories* 16 (1), S. 14. DOI: 10.1186/s12934-017-0625-9.

Laoide, B. M.; Chambliss, G. H.; McConnell, D. J. (1989): Bacillus licheniformis alpha-amylase gene, amyL, is subject to promoter-independent catabolite repression in Bacillus subtilis. In: *Journal of bacteriology* 171 (5), S. 2435–2442. DOI: 10.1128/jb.171.5.2435-2442.1989.

Lara, Alvaro R.; Galindo, Enrique; Ramírez, Octavio T.; Palomares, Laura A. (2006): Living With Heterogeneities in Bioreactors: Understanding the Effects of Environmental Gradients on Cells. In: *MB* 34 (3), S. 355–382. DOI: 10.1385/MB:34:3:355.

Lazarevic, V.; Margot, P.; Soldo, B.; Karamata, D. (1992): Sequencing and analysis of the Bacillus subtilis lytRABC divergon: a regulatory unit encompassing the structural genes of the N-acetylmuramoyl-L-alanine amidase and its modifier. In: *Journal of general microbiology* 138 (9), S. 1949–1961. DOI: 10.1099/00221287-138-9-1949.

Leaver, M.; Domínguez-Cuevas, P.; Coxhead, J. M.; Daniel, R. A.; Errington, J. (2009): Life without a wall or division machine in Bacillus subtilis. In: *Nature* 457 (7231), S. 849–853. DOI: 10.1038/nature07742.

Lee, Ki-Sung; Kim, Jun-Seob; Heo, Paul; Yang, Tae-Jun; Sung, Young-Je; Cheon, Yuna *et al.* (2013): Characterization of Saccharomyces cerevisiae promoters for heterologous gene expression in Kluyveromyces marxianus. In: *Applied microbiology and biotechnology* 97 (5), S. 2029–2041. DOI: 10.1007/s00253-012-4306-7.

Liu, Yanfeng; Li, Jianghua; Du, Guocheng; Chen, Jian; Liu, Long (2017): Metabolic engineering of Bacillus subtilis fueled by systems biology: Recent advances and future directions. In: *Biotechnology advances* 35 (1), S. 20–30. DOI: 10.1016/j.biotechadv.2016.11.003.

Lopez, Daniel; Vlamakis, Hera; Kolter, Roberto (2009): Generation of multiple cell types in Bacillus subtilis. In: *FEMS microbiology reviews* 33 (1), S. 152–163. DOI: 10.1111/j.1574-6976.2008.00148.x.

López, Daniel; Fischbach, Michael A.; Chu, Frances; Losick, Richard; Kolter, Roberto (2009a): Structurally diverse natural products that cause potassium leakage trigger multicellularity in Bacillus subtilis. In: *Proceedings of the National Academy of Sciences of the United States of America* 106 (1), S. 280–285. DOI: 10.1073/pnas.0810940106.

López, Daniel; Kolter, Roberto (2010): Extracellular signals that define distinct and coexisting cell fates in Bacillus subtilis. In: *FEMS microbiology reviews* 34 (2), S. 134–149. DOI: 10.1111/j.1574-6976.2009.00199.x.

López, Daniel; Vlamakis, Hera; Losick, Richard; Kolter, Roberto (2009b): Paracrine signaling in a bacterium. In: *Genes & development* 23 (14), S. 1631–1638. DOI: 10.1101/gad.1813709.

Lord, Nathan D.; Norman, Thomas M.; Yuan, Ruoshi; Bakshi, Somenath; Losick, Richard; Paulsson, Johan (2019): Stochastic antagonism between two proteins governs a bacterial cell fate switch. In: *Science (New York, N.Y.)* 366 (6461), S. 116–120. DOI: 10.1126/science.aaw4506.

Love, Kerry Routenberg; Panagiotou, Vasiliki; Jiang, Bo; Stadheim, Terrance A.; Love, J. Christopher (2010): Integrated single-cell analysis shows Pichia pastoris secretes protein stochastically. In: *Biotechnology and bioengineering* 106 (2), S. 319–325. DOI: 10.1002/bit.22688.

Lundström, Sara (2012): Characterization of a Bacillus licheniformis gene cluster required for functional expression of a bacteriocin. University of Copenhagen. Faculty of Science.

Maaβ, Sandra; Wachlin, Gerhild; Bernhardt, Jörg; Eymann, Christine; Fromion, Vincent; Riedel, Katharina *et al.* (2014): Highly precise quantification of protein molecules per cell during stress and starvation responses in Bacillus subtilis. In: *Molecular & cellular proteomics : MCP* 13 (9), S. 2260–2276. DOI: 10.1074/mcp.M113.035741.

Mäder, U.; Antelmann, H.; Buder, T.; Dahl, M. K.; Hecker, M.; Homuth, G. (2002): Bacillus subtilis functional genomics: genome-wide analysis of the DegS-DegU regulon by transcriptomics and proteomics. In: *Molecular genetics and genomics : MGG* 268 (4), S. 455–467. DOI: 10.1007/s00438-002-0774-2.

Magnuson, Roy; Solomon, Jonathan; Grossman, Alan D. (1994): Biochemical and genetic characterization of a competence pheromone from B. subtilis. In: *Cell* 77 (2), S. 207–216. DOI: 10.1016/0092-8674(94)90313-1.

Manabe, Kenji; Kageyama, Yasushi; Morimoto, Takuya; Ozawa, Tadahiro; Sawada, Kazuhisa; Endo, Keiji *et al.* (2011): Combined effect of improved cell yield and increased specific productivity enhances recombinant enzyme production in genome-reduced Bacillus subtilis strain MGB874. In: *Applied and environmental microbiology* 77 (23), S. 8370–8381. DOI: 10.1128/AEM.06136-11.

Mao, Weiying; Pan, Renrui; Freedman, David (1992): High production of alkaline protease byBacillus licheniformis in a fed-batch fermentation using a synthetic medium. In: *Journal of Industrial Microbiology* 11 (1), S. 1–6. DOI: 10.1007/BF01583724.

Margot, Philippe; Pagni, Marco; Karamata, Dimitri (1999): Bacillus subtilis 168 gene lytF encodes a gamma-D-glutamate-meso-diaminopimelate muropeptidase expressed by the alternative vegetative sigma factor, sigmaD. In: *Microbiology (Reading, England)* 145 (Pt 1), S. 57–65. DOI: 10.1099/13500872-145-1-57.

Marlow, Victoria L.; Cianfanelli, Francesca R.; Porter, Michael; Cairns, Lynne S.; Dale, J. Kim; Stanley-Wall, Nicola R. (2014a): The prevalence and origin of exoprotease-producing cells in the Bacillus subtilis biofilm. In: *Microbiology (Reading, England)* 160 (Pt 1), S. 56–66. DOI: 10.1099/mic.0.072389-0.

Marlow, Victoria L.; Porter, Michael; Hobley, Laura; Kiley, Taryn B.; Swedlow, Jason R.; Davidson, Fordyce A.; Stanley-Wall, Nicola R. (2014b): Phosphorylated DegU manipulates cell fate differentiation in the Bacillus subtilis biofilm. In: *Journal of bacteriology* 196 (1), S. 16–27. DOI: 10.1128/JB.00930-13.

Márquez, L. M.; Helmann, J. D.; Ferrari, E.; Parker, H. M.; Ordal, G. W.; Chamberlin, M. J. (1990): Studies of sigma D-dependent functions in Bacillus subtilis. In: *Journal of bacteriology* 172 (6), S. 3435–3443. DOI: 10.1128/jb.172.6.3435-3443.1990.

Mars, Ruben A. T.; Nicolas, Pierre; Ciccolini, Mariano; Reilman, Ewoud; Reder, Alexander; Schaffer, Marc *et al.* (2015): Small regulatory RNA-induced growth rate heterogeneity of Bacillus subtilis. In: *PLoS genetics* 11 (3), e1005046. DOI: 10.1371/journal.pgen.1005046.

McLoon, Anna L.; Guttenplan, Sarah B.; Kearns, Daniel B.; Kolter, Roberto; Losick, Richard (2011): Tracing the domestication of a biofilm-forming bacterium. In: *Journal of bacteriology* 193 (8), S. 2027–2034. DOI: 10.1128/JB.01542-10.

Meile, Jean-Christophe; Wu, Ling Juan; Ehrlich, S. Dusko; Errington, Jeff; Noirot, Philippe (2006): Systematic localisation of proteins fused to the green fluorescent protein in Bacillus subtilis: identification of new proteins at the DNA replication factory. In: *Proteomics* 6 (7), S. 2135–2146. DOI: 10.1002/pmic.200500512.

Mhatre, Eisha; Monterrosa, Ramses Gallegos; Kovács, Akos T. (2014): From environmental signals to regulators: modulation of biofilm development in Gram-positive bacteria. In: *Journal of basic microbiology* 54 (7), S. 616–632. DOI: 10.1002/jobm.201400175.

Mhatre, Eisha; Troszok, Agnieszka; Gallegos-Monterrosa, Ramses; Lindstädt, Stefanie; Hölscher, Theresa; Kuipers, Oscar P.; Kovács, Ákos T. (2016): The impact of manganese on biofilm development of Bacillus subtilis. In: *Microbiology (Reading, England)* 162 (8), S. 1468–1478. DOI: 10.1099/mic.0.000320.

Milias-Argeitis, Andreas; Rullan, Marc; Aoki, Stephanie K.; Buchmann, Peter; Khammash, Mustafa (2016): Automated optogenetic feedback control for precise and robust regulation of gene expression and cell growth. In: *Nature communications* 7, S. 12546. DOI: 10.1038/ncomms12546.

Milton, Morgan E.; Draughn, G. Logan; Bobay, Benjamin G.; Stowe, Sean D.; Olson, Andrew L.; Feldmann, Erik A. *et al.* (2020): The Solution Structures and Interaction of SinR and SinI: Elucidating the Mechanism of Action of the Master Regulator Switch for Biofilm Formation in Bacillus subtilis. In: *Journal of molecular biology* 432 (2), S. 343–357. DOI: 10.1016/j.jmb.2019.08.019.

Miras, Mathieu; Dubnau, David (2016): A DegU-P and DegQ-Dependent Regulatory Pathway for the K-state in Bacillus subtilis. In: *Frontiers in microbiology* 7, S. 1868. DOI: 10.3389/fmicb.2016.01868.

Mirel, D. B.; Chamberlin, M. J. (1989): The Bacillus subtilis flagellin gene (hag) is transcribed by the sigma 28 form of RNA polymerase. In: *Journal of bacteriology* 171 (6), S. 3095–3101. DOI: 10.1128/jb.171.6.3095-3101.1989.

Mirel, D. B.; Estacio, W. F.; Mathieu, M.; Olmsted, E.; Ramirez, J.; Márquez-Magaña, L. M. (2000): Environmental regulation of Bacillus subtilis sigma(D)-dependent gene expression. In: *Journal of bacteriology* 182 (11), S. 3055–3062. DOI: 10.1128/jb.182.11.3055-3062.2000.

Mitsui, Nobuo; Murasawa, Hisashi; Sekiguchi, Junichi (2009): Development of natto with germination-defective mutants of Bacillus subtilis (natto). In: *Applied microbiology and biotechnology* 82 (4), S. 741–748. DOI: 10.1007/s00253-009-1894-y.

Moens, S.; Vanderleyden, J. (1996): Functions of bacterial flagella. In: *Critical reviews in microbiology* 22 (2), S. 67–100. DOI: 10.3109/10408419609106456.

Mordini, Serena; Osera, Cecilia; Marini, Simone; Scavone, Francesco; Bellazzi, Riccardo; Galizzi, Alessandro; Calvio, Cinzia (2013): The role of SwrA, DegU and P(D3) in fla/che expression in B. subtilis. In: *PloS one* 8 (12), e85065. DOI: 10.1371/journal.pone.0085065.

Morris, Ryan J.; Schor, Marieke; Gillespie, Rachel M. C.; Ferreira, Ana Sofia; Baldauf, Lucia; Earl, Chris *et al.* (2017): Natural variations in the biofilm-associated protein BslA from the genus Bacillus. In: *Scientific reports* 7 (1), S. 6730. DOI: 10.1038/s41598-017-06786-9.

Msadek, T. (1999): When the going gets tough: survival strategies and environmental signaling networks in Bacillus subtilis. In: *Trends in microbiology* 7 (5), S. 201–207.

Msadek, T.; Kunst, F.; Henner, D.; Klier, A.; Rapoport, G.; Dedonder, R. (1990): Signal transduction pathway controlling synthesis of a class of degradative enzymes in Bacillus subtilis: expression of the regulatory genes and analysis of mutations in degS and degU. In: *Journal of bacteriology* 172 (2), S. 824–834. DOI: 10.1128/jb.172.2.824-834.1990.

Msadek, T.; Kunst, F.; Klier, A.; Rapoport, G. (1991): DegS-DegU and ComP-ComA modulator-effector pairs control expression of the Bacillus subtilis pleiotropic regulatory gene degQ. In: *Journal of bacteriology* 173 (7), S. 2366–2377. DOI: 10.1128/jb.173.7.2366-2377.1991.

Msadek, Tarek; Kunst, Frank; Rapoport, Georges (1993): Two-Component Regulatory Systems. In: Abraham L. Sonenshein, James A. Hoch and Richard Losick (Hg.): Bacillus subtilis and Other Gram-Positive Bacteria, Bd. 264. Washington, DC, USA: ASM Press, S. 727–745.

Mukai, K.; Kawata-Mukai, M.; Tanaka, T. (1992): Stabilization of phosphorylated Bacillus subtilis DegU by DegR. In: *Journal of bacteriology* 174 (24), S. 7954–7962. DOI: 10.1128/jb.174.24.7954-7962.1992.

Mukherjee, Sampriti; Kearns, Daniel B. (2014): The structure and regulation of flagella in Bacillus subtilis. In: *Annual review of genetics* 48, S. 319–340. DOI: 10.1146/annurev-genet-120213-092406.

Muñoz-Dorado, José; Marcos-Torres, Francisco J.; García-Bravo, Elena; Moraleda-Muñoz, Aurelio; Pérez, Juana (2016): Myxobacteria: Moving, Killing, Feeding, and Surviving Together. In: *Frontiers in microbiology* 7, S. 781. DOI: 10.3389/fmicb.2016.00781.

Muntel, Jan; Fromion, Vincent; Goelzer, Anne; Maaβ, Sandra; Mäder, Ulrike; Büttner, Knut *et al.* (2014): Comprehensive absolute quantification of the cytosolic proteome of Bacillus subtilis by data independent, parallel fragmentation in liquid chromatography/mass spectrometry (LC/MS(E)). In: *Molecular & cellular proteomics : MCP* 13 (4), S. 1008–1019. DOI: 10.1074/mcp.M113.032631.

Murray, Ewan J.; Kiley, Taryn B.; Stanley-Wall, Nicola R. (2009a): A pivotal role for the response regulator DegU in controlling multicellular behaviour. In: *Microbiology (Reading, England)* 155 (Pt 1), S. 1–8. DOI: 10.1099/mic.0.023903-0.

Murray, Ewan J.; Strauch, Mark A.; Stanley-Wall, Nicola R. (2009b): SigmaX is involved in controlling Bacillus subtilis biofilm architecture through the AbrB homologue Abh. In: *Journal of bacteriology* 191 (22), S. 6822–6832. DOI: 10.1128/JB.00618-09.

Mustafi, Nurije; Grünberger, Alexander; Mahr, Regina; Helfrich, Stefan; Nöh, Katharina; Blombach, Bastian *et al.* (2014): Application of a genetically encoded biosensor for live cell imaging of L-valine production in pyruvate dehydrogenase complex-deficient Corynebacterium glutamicum strains. In: *PloS one* 9 (1), e85731. DOI: 10.1371/journal.pone.0085731.

Nagami, Y.; Tanaka, T. (1986): Molecular cloning and nucleotide sequence of a DNA fragment from Bacillus natto that enhances production of extracellular proteases and levansucrase in Bacillus subtilis. In: *Journal of bacteriology* 166 (1), S. 20–28. DOI: 10.1128/jb.166.1.20-28.1986.

Nahrstedt, Hannes; Waldeck, Jens; Gröne, Mark; Eichstädt, Renée; Feesche, Jörg; Meinhardt, Friedhelm (2005): Strain development in Bacillus licheniformis: construction of biologically contained mutants deficient in sporulation and DNA repair. In: *Journal of biotechnology* 119 (3), S. 245–254. DOI: 10.1016/j.jbiotec.2005.04.003.

Nakamura, L. K.; Roberts, M. S.; Cohan, F. M. (1999): Relationship of Bacillus subtilis clades associated with strains 168 and W23: a proposal for Bacillus subtilis subsp. subtilis subsp. nov. and Bacillus subtilis subsp. spizizenii subsp. nov. In: *International journal of systematic bacteriology* 49 Pt 3, S. 1211–1215. DOI: 10.1099/00207713-49-3-1211.

Nakano, M. M.; Magnuson, R.; Myers, A.; Curry, J.; Grossman, A. D.; Zuber, P. (1991): srfA is an operon required for surfactin production, competence development, and efficient sporulation in Bacillus subtilis. In: *Journal of bacteriology* 173 (5), S. 1770–1778. DOI: 10.1128/jb.173.5.1770-1778.1991.

Newman, Joseph A.; Rodrigues, Cecilia; Lewis, Richard J. (2013): Molecular basis of the activity of SinR protein, the master regulator of biofilm formation in Bacillus subtilis. In: *The Journal of biological chemistry* 288 (15), S. 10766–10778. DOI: 10.1074/jbc.M113.455592.

Nicolas, Pierre; Mäder, Ulrike; Dervyn, Etienne; Rochat, Tatiana; Leduc, Aurélie; Pigeonneau, Nathalie *et al.* (2012): Condition-dependent transcriptome reveals high-level regulatory architecture in Bacillus subtilis. In: *Science (New York, N.Y.)* 335 (6072), S. 1103–1106. DOI: 10.1126/science.1206848.

Norman, Thomas M.; Lord, Nathan D.; Paulsson, Johan; Losick, Richard (2013): Memory and modularity in cell-fate decision making. In: *Nature* 503 (7477), S. 481–486. DOI: 10.1038/nature12804.

Ogura, M.; Yamaguchi, H.; Yoshida, Ki; Fujita, Y.; Tanaka, T. (2001): DNA microarray analysis of Bacillus subtilis DegU, ComA and PhoP regulons: an approach to comprehensive analysis of B.subtilis two-component regulatory systems. In: *Nucleic acids research* 29 (18), S. 3804–3813. DOI: 10.1093/nar/29.18.3804.

Ogura, Mitsuo; Fujita, Yasutaro (2007): Bacillus subtilis rapD, a direct target of transcription repression by RghR, negatively regulates srfA expression. In: *FEMS Microbiology Letters* 268 (1), S. 73–80. DOI: 10.1111/j.1574-6968.2006.00559.x.

Ogura, Mitsuo; Shimane, Kana; Asai, Kei; Ogasawara, Naotake; Tanaka, Teruo (2003): Binding of response regulator DegU to the aprE promoter is inhibited by RapG, which is counteracted by extracellular PhrG in Bacillus subtilis. In: *Molecular microbiology* 49 (6), S. 1685–1697. DOI: 10.1046/j.1365-2958.2003.03665.x.

Ogura, Mitsuo; Tsukahara, Kensuke (2010): Autoregulation of the Bacillus subtilis response regulator gene degU is coupled with the proteolysis of DegU-P by ClpCP. In: *Molecular microbiology* 75 (5), S. 1244–1259. DOI: 10.1111/j.1365-2958.2010.07047.x.

Ogura, Mitsuo; Tsukahara, Kensuke (2012): SwrA regulates assembly of Bacillus subtilis DegU via its interaction with N-terminal domain of DegU. In: *Journal of biochemistry* 151 (6), S. 643–655. DOI: 10.1093/jb/mvs036.

Ogura, Mitsuo; Yoshikawa, Hirofumi; Chibazakura, Taku (2014): Regulation of the response regulator gene degU through the binding of SinR/SlrR and exclusion of SinR/SlrR by DegU in Bacillus subtilis. In: *Journal of bacteriology* 196 (4), S. 873–881. DOI: 10.1128/JB.01321-13.

Ohnishi, R.; Ishikawa, S.; Sekiguchi, J. (1999): Peptidoglycan hydrolase LytF plays a role in cell separation with CwlF during vegetative growth of Bacillus subtilis. In: *Journal of bacteriology* 181 (10), S. 3178–3184.

Olmos, J.; Anda, R. de; Ferrari, E.; Bolívar, F.; Valle, F. (1997): Effects of the sinR and degU32 (Hy) mutations on the regulation of the aprE gene in Bacillus subtilis. In: *Molecular & general genetics : MGG* 253 (5), S. 562–567. DOI: 10.1007/s004380050358.

Olmos, Jorge; Bolaños, Victor; Causey, Stuart; Ferrari, Eugenio; Bollvar, Francisco; Valle, Fernando (1996): A functional Spo0A is required for maximal aprE expression in Bacillus subtilis. In: *FEBS Letters* 381 (1-2), S. 29–31. DOI: 10.1016/0014-5793(96)00070-1.

Osera, Cecilia; Amati, Giuseppe; Calvio, Cinzia; Galizzi, Alessandro (2009): SwrAA activates poly-gamma-glutamate synthesis in addition to swarming in Bacillus subtilis. In: *Microbiology (Reading, England)* 155 (Pt 7), S. 2282–2287. DOI: 10.1099/mic.0.026435-0.

Ostrowski, Adam; Mehert, Angela; Prescott, Alan; Kiley, Taryn B.; Stanley-Wall, Nicola R. (2011): YuaB functions synergistically with the exopolysaccharide and TasA amyloid fibers to allow biofilm formation by Bacillus subtilis. In: *Journal of bacteriology* 193 (18), S. 4821–4831. DOI: 10.1128/JB.00223-11.

Otto, Andreas; Bernhardt, Jörg; Meyer, Hanna; Schaffer, Marc; Herbst, Florian-A; Siebourg, Juliane *et al.* (2010): Systems-wide temporal proteomic profiling in glucose-starved Bacillus subtilis. In: *Nature communications* 1, S. 137. DOI: 10.1038/ncomms1137.

Overkamp, Wout; Kuipers, Oscar P. (2015): Transcriptional Profile of Bacillus subtilis sigF-Mutant during Vegetative Growth. In: *PloS one* 10 (10), e0141553. DOI: 10.1371/journal.pone.0141553.

Perego, M.; Hoch, J. A. (1996): Cell-cell communication regulates the effects of protein aspartate phosphatases on the phosphorelay controlling development in Bacillus subtilis. In: *Proceedings of the National Academy of Sciences of the United States of America* 93 (4), S. 1549–1553. DOI: 10.1073/pnas.93.4.1549.

Perego, M.; Spiegelman, G. B.; Hoch, J. A. (1988): Structure of the gene for the transition state regulator, abrB: regulator synthesis is controlled by the spo0A sporulation gene in Bacillus subtilis. In: *Molecular microbiology* 2 (6), S. 689–699. DOI: 10.1111/j.1365-2958.1988.tb00079.x.

Pierce, J. A.; Robertson, C. R.; Leighton, T. J. (1992): Physiological and genetic strategies for enhanced subtilisin production by Bacillus subtilis. In: *Biotechnology progress* 8 (3), S. 211–218. DOI: 10.1021/bp00015a006.

Piersma, Sjouke; Denham, Emma L.; Drulhe, Samuel; Tonk, Rudi H. J.; Schwikowski, Benno; van Dijl, Jan Maarten (2013): TLM-Quant: an open-source pipeline for visualization and quantification of gene expression heterogeneity in growing microbial cells. In: *PloS one* 8 (7), e68696. DOI: 10.1371/journal.pone.0068696.

Piggot, P. J.; Coote, J. G. (1976): Genetic aspects of bacterial endospore formation. In: *Bacteriological reviews* 40 (4), S. 908–962.

Piggot, Patrick J.; Hilbert, David W. (2004): Sporulation of Bacillus subtilis. In: *Current opinion in microbiology* 7 (6), S. 579–586. DOI: 10.1016/j.mib.2004.10.001.

Pittelkow, Marco; Bremer, Erhard (2011): Cellular Adjustments of Bacillus subtilis and Other Bacilli to Fluctuating Salinities. In: Antonio Ventosa, Aharon Oren and Yanhe Ma (Hg.): Halophiles and Hypersaline Environments, Bd. 126. Berlin, Heidelberg: Springer Berlin Heidelberg, S. 275–302.

Ploss, Tina N.; Reilman, Ewoud; Monteferrante, Carmine G.; Denham, Emma L.; Piersma, Sjouke; Lingner, Anja *et al.* (2016): Homogeneity and heterogeneity in amylase production by Bacillus subtilis under different growth conditions. In: *Microbial cell factories* 15, S. 57. DOI: 10.1186/s12934-016-0455-1.

Pottathil, Mridula; Lazazzera, Beth A. (2003): The extracellular Phr peptide-Rap phosphatase signaling circuit of Bacillus subtilis. In: *Frontiers in bioscience : a journal and virtual library* 8, d32-45. DOI: 10.2741/913.

Predich, M.; Nair, G.; Smith, I. (1992): Bacillus subtilis early sporulation genes kinA, spo0F, and spo0A are transcribed by the RNA polymerase containing sigma H. In: *Journal of bacteriology* 174 (9), S. 2771–2778. DOI: 10.1128/jb.174.9.2771-2778.1992.

Priest, F. G. (1977): Extracellular enzyme synthesis in the genus Bacillus. In: *Bacteriological reviews* 41 (3), S. 711–753.

Rabbee, Muhammad Fazle; Ali, Md Sarafat; Choi, Jinhee; Hwang, Buyng Su; Jeong, Sang Chul; Baek, Kwang-Hyun (2019): Bacillus velezensis: A Valuable Member of Bioactive Molecules within Plant Microbiomes. In: *Molecules (Basel, Switzerland)* 24 (6). DOI: 10.3390/molecules24061046.

Radeck, Jara; Meyer, Daniel; Lautenschläger, Nina; Mascher, Thorsten (2017): Bacillus SEVA siblings: A Golden Gate-based toolbox to create personalized integrative vectors for Bacillus subtilis. In: *Scientific reports* 7 (1), S. 14134. DOI: 10.1038/s41598-017-14329-5.

Rasmussen, Simon; Nielsen, Henrik Bjørn; Jarmer, Hanne (2009): The transcriptionally active regions in the genome of Bacillus subtilis. In: *Molecular microbiology* 73 (6), S. 1043–1057. DOI: 10.1111/j.1365-2958.2009.06830.x.

Ratnayake-Lecamwasam, M.; Serror, P.; Wong, K. W.; Sonenshein, A. L. (2001): Bacillus subtilis CodY represses early-stationary-phase genes by sensing GTP levels. In: *Genes & development* 15 (9), S. 1093–1103. DOI: 10.1101/gad.874201.

Reuß, Daniel R.; Altenbuchner, Josef; Mäder, Ulrike; Rath, Hermann; Ischebeck, Till; Sappa, Praveen Kumar *et al.* (2017): Large-scale reduction of the Bacillus subtilis genome: consequences for the transcriptional network, resource allocation, and metabolism. In: *Genome research* 27 (2), S. 289–299. DOI: 10.1101/gr.215293.116.

Rey, Michael W.; Ramaiya, Preethi; Nelson, Beth A.; Brody-Karpin, Shari D.; Zaretsky, Elizabeth J.; Tang, Maria *et al.* (2004): Complete genome sequence of the industrial bacterium Bacillus licheniformis and comparisons with closely related Bacillus species. In: *Genome biology* 5 (10), R77. DOI: 10.1186/gb-2004-5-10-r77.

Richter, Anne; Hölscher, Theresa; Pausch, Patrick; Sehrt, Tim; Brockhaus, Franziska; Bange, Gert; Kovács, Ákos T. (2018): Hampered motility promotes the evolution of wrinkly phenotype in Bacillus subtilis. In: *BMC evolutionary biology* 18 (1), S. 155. DOI: 10.1186/s12862-018-1266-2.

Riley, Eammon P.; Trinquier, Aude; Reilly, Madeline L.; Durchon, Marine; Perera, Varahenage R.; Pogliano, Kit; Lopez-Garrido, Javier (2018): Spatiotemporally regulated proteolysis to dissect the role of vegetative proteins during Bacillus subtilis sporulation: cell-specific requirement of σH and σA. In: *Molecular microbiology* 108 (1), S. 45–62. DOI: 10.1111/mmi.13916.

Romero, Diego; Vlamakis, Hera; Losick, Richard; Kolter, Roberto (2011): An accessory protein required for anchoring and assembly of amyloid fibres in B. subtilis biofilms. In: *Molecular microbiology* 80 (5), S. 1155–1168. DOI: 10.1111/j.1365-2958.2011.07653.x.

Russell, Jonathan R.; Cabeen, Matthew T.; Wiggins, Paul A.; Paulsson, Johan; Losick, Richard (2017): Noise in a phosphorelay drives stochastic entry into sporulation in Bacillus subtilis. In: *The EMBO journal* 36 (19), S. 2856–2869. DOI: 10.15252/embj.201796988.

Ruzal, S. M.; Sanchez-Rivas, C. (1998): In Bacillus subtilis DegU-P is a positive regulator of the osmotic response. In: *Current microbiology* 37 (6), S. 368–372.

Sadaie, Yoshito; Nakadate, Hisashi; Fukui, Reiko; Yee, Lii Mien; Asai, Kei (2008): Glucomannan utilization operon of Bacillus subtilis. In: *FEMS Microbiology Letters* 279 (1), S. 103–109. DOI: 10.1111/j.1574-6968.2007.01018.x.

Schallmey, Marcus; Singh, Ajay; Ward, Owen P. (2004): Developments in the use of Bacillus species for industrial production. In: *Canadian journal of microbiology* 50 (1), S. 1–17. DOI: 10.1139/w03-076.

Schweder, Thomas; Krüger, Elke; Xu, Bo; Jürgen, Britta; Blomsten, Gustav; Enfors, Sven-Olof; Hecker, Michael (1999): Monitoring of genes that respond to process-related stress in large-scale bioprocesses. In: *Biotechnol. Bioeng.* 65 (2), S. 151–159. DOI: 10.1002/(sici)1097-0290(19991020)65:2<151::aid-bit4>3.0.co;2-v.

Scoffone, Viola; Dondi, Daniele; Biino, Ginevra; Borghese, Giovanni; Pasini, Dario; Galizzi, Alessandro; Calvio, Cinzia (2013): Knockout of pgdS and ggt genes improves γ-PGA yield in B. subtilis. In: *Biotechnol. Bioeng.* 110 (7), S. 2006–2012. DOI: 10.1002/bit.24846.

Scott, D. J.; Leejeerajumnean, S.; Brannigan, J. A.; Lewis, R. J.; Wilkinson, A. J.; Hoggett, J. G. (1999): Quaternary re-arrangement analysed by spectral enhancement: the interaction of a sporulation repressor with its antagonist. In: *Journal of molecular biology* 293 (5), S. 997–1004. DOI: 10.1006/jmbi.1999.3221.

Sekiguchi, J.; Takada, N.; Okada, H. (1975): Genes affecting the productivity of alpha-amylase in Bacillus subtilis Marburg. In: *Journal of bacteriology* 121 (2), S. 688–694.

Serizawa, Masakuni; Yamamoto, Hiroki; Yamaguchi, Hirotake; Fujita, Yasutaro; Kobayashi, Kazuo; Ogasawara, Naotake; Sekiguchi, Junichi (2004): Systematic analysis of SigD-regulated genes in Bacillus subtilis by DNA microarray and Northern blotting analyses. In: *Gene* 329, S. 125–136. DOI: 10.1016/j.gene.2003.12.024.

Serrano, M.; Zilhão, R.; Ricca, E.; Ozin, A. J.; Moran, C. P.; Henriques, A. O. (1999): A Bacillus subtilis secreted protein with a role in endospore coat assembly and function. In: *Journal of bacteriology* 181 (12), S. 3632–3643.

Setlow, B.; Magill, N.; Febbroriello, P.; Nakhimovsky, L.; Koppel, D. E.; Setlow, P. (1991): Condensation of the forespore nucleoid early in sporulation of Bacillus species. In: *Journal of bacteriology* 173 (19), S. 6270–6278. DOI: 10.1128/jb.173.19.6270-6278.1991.

Shafikhani, Sasha H.; Mandic-Mulec, Ines; Strauch, Mark A.; Smith, Issar; Leighton, Terrance (2002): Postexponential regulation of sin operon expression in Bacillus subtilis. In: *Journal of bacteriology* 184 (2), S. 564–571. DOI: 10.1128/jb.184.2.564-571.2002.

Shank, Elizabeth Anne; Kolter, Roberto (2011): Extracellular signaling and multicellularity in Bacillus subtilis. In: *Current opinion in microbiology* 14 (6), S. 741–747. DOI: 10.1016/j.mib.2011.09.016.

Sharma, Ashish K.; Shukla, Esha; Janoti, Deepak S.; Mukherjee, Krishna J.; Shiloach, Joseph (2020): A novel knock out strategy to enhance recombinant protein expression in Escherichia coli. In: *Microbial cell factories* 19 (1), S. 148. DOI: 10.1186/s12934-020-01407-z.

Shemesh, Moshe; Chai, Yunrong (2013): A combination of glycerol and manganese promotes biofilm formation in Bacillus subtilis via histidine kinase KinD signaling. In: *Journal of bacteriology* 195 (12), S. 2747–2754. DOI: 10.1128/JB.00028-13.

Shimane, Kana; Ogura, Mitsuo (2004): Mutational analysis of the helix-turn-helix region of Bacillus subtilis response regulator DegU, and identification of cis-acting sequences for DegU in the aprE and comK promoters. In: *Journal of biochemistry* 136 (3), S. 387–397. DOI: 10.1093/jb/mvh127.

Shioi, J. I.; Imae, Y.; Oosawa, F. (1978): Protonmotive force and motility of Bacillus subtilis. In: *Journal of bacteriology* 133 (3), S. 1083–1088.

Shivers, Robert P.; Sonenshein, Abraham L. (2004): Activation of the Bacillus subtilis global regulator CodY by direct interaction with branched-chain amino acids. In: *Molecular microbiology* 53 (2), S. 599–611. DOI: 10.1111/j.1365-2958.2004.04135.x.

Smith, Thomas J.; Blackman, Steve A.; Foster, Simon J. (2000): Autolysins of Bacillus subtilis: multiple enzymes with multiple functions. In: *Microbiology (Reading, England)* 146 (Pt 2), S. 249–262. DOI: 10.1099/00221287-146-2-249.

Smits, Wiep Klaas; Bongiorni, Cristina; Veening, Jan-Willem; Hamoen, Leendert W.; Kuipers, Oscar P.; Perego, Marta (2007): Temporal separation of distinct differentiation pathways by a dual specificity Rap-Phr system in Bacillus subtilis. In: *Molecular microbiology* 65 (1), S. 103–120. DOI: 10.1111/j.1365-2958.2007.05776.x.

Sonenshein, Abraham L. (2007): Control of key metabolic intersections in Bacillus subtilis. In: *Nature reviews. Microbiology* 5 (12), S. 917–927. DOI: 10.1038/nrmicro1772.

Spencer, R. C. (2003): Bacillus anthracis. In: *Journal of clinical pathology* 56 (3), S. 182–187. DOI: 10.1136/jcp.56.3.182.

Stanley, Nicola R.; Lazazzera, Beth A. (2005): Defining the genetic differences between wild and domestic strains of Bacillus subtilis that affect poly-gamma-dl-glutamic acid production and biofilm formation. In: *Molecular microbiology* 57 (4), S. 1143–1158. DOI: 10.1111/j.1365-2958.2005.04746.x.

Steil, Leif; Hoffmann, Tamara; Budde, Ina; Völker, Uwe; Bremer, Erhard (2003): Genome-wide transcriptional profiling analysis of adaptation of Bacillus subtilis to high salinity. In: *Journal of bacteriology* 185 (21), S. 6358–6370. DOI: 10.1128/JB.185.21.6358-6370.2003.

Steil, Leif; Serrano, Mónica; Henriques, Adriano O.; Völker, Uwe (2005): Genome-wide analysis of temporally regulated and compartment-specific gene expression in sporulating cells of Bacillus subtilis. In: *Microbiology (Reading, England)* 151 (Pt 2), S. 399–420. DOI: 10.1099/mic.0.27493-0.

Steinberg, Nitai; Keren-Paz, Alona; Hou, Qihui; Doron, Shany; Yanuka-Golub, Keren; Olender, Tsviya *et al.* (2020): The extracellular matrix protein TasA is a developmental cue that maintains a motile subpopulation within Bacillus subtilis biofilms. In: *Science signaling* 13 (632). DOI: 10.1126/scisignal.aaw8905.

Steinchen, Wieland; Bange, Gert (2016): The magic dance of the alarmones (p)ppGpp. In: *Molecular microbiology* 101 (4), S. 531–544. DOI: 10.1111/mmi.13412.

Stempler, Ofer; Baidya, Amit K.; Bhattacharya, Saurabh; Malli Mohan, Ganesh Babu; Tzipilevich, Elhanan; Sinai, Lior *et al.* (2017): Interspecies nutrient extraction and toxin delivery between bacteria. In: *Nature communications* 8 (1), S. 315. DOI: 10.1038/s41467-017-00344-7.

Stöver, Axel G.; Driks, Adam (1999a): Regulation of Synthesis of the Bacillus subtilis Transition-Phase, Spore-Associated Antibacterial Protein TasA. In: *Journal of bacteriology* 181 (17), S. 5476–5481.

Stöver, Axel G.; Driks, Adam (1999b): Secretion, Localization, and Antibacterial Activity of TasA, a Bacillus subtilis Spore-Associated Protein. In: *Journal of bacteriology* 181 (5), S. 1664–1672.

Stragier, P.; Losick, R. (1996): Molecular genetics of sporulation in Bacillus subtilis. In: *Annual review of genetics* 30, 297-41. DOI: 10.1146/annurev.genet.30.1.297.

Strauch, M. A. (1995): Delineation of AbrB-binding sites on the Bacillus subtilis spo0H, kinB, ftsAZ, and pbpE promoters and use of a derived homology to identify a previously unsuspected binding site in the bsuB1 methylase promote. In: *Journal of bacteriology* 177 (23), S. 6999–7002. DOI: 10.1128/jb.177.23.6999-7002.1995.

Strauch, M. A.; Spiegelman, G. B.; Perego, M.; Johnson, W. C.; Burbulys, D.; Hoch, J. A. (1989): The transition state transcription regulator abrB of Bacillus subtilis is a DNA binding protein. In: *The EMBO journal* 8 (5), S. 1615–1621.

Strauch, Mark A.; Bobay, Benjamin G.; Cavanagh, John; Yao, Fude; Wilson, Angelo; Le Breton, Yoann (2007): Abh and AbrB control of Bacillus subtilis antimicrobial gene expression. In: *Journal of bacteriology* 189 (21), S. 7720–7732. DOI: 10.1128/JB.01081-07.

Suzuki, Takao; Tahara, Yasutaka (2003): Characterization of the Bacillus subtilis ywtD gene, whose product is involved in gamma-polyglutamic acid degradation. In: *Journal of bacteriology* 185 (7), S. 2379–2382. DOI: 10.1128/jb.185.7.2379-2382.2003.

Syvertsson, Simon; Vischer, Norbert O. E.; Gao, Yongqiang; Hamoen, Leendert W. (2016): When Phase Contrast Fails: ChainTracer and NucTracer, Two ImageJ Methods for Semi-Automated Single Cell Analysis Using Membrane or DNA Staining. In: *PloS one* 11 (3), e0151267. DOI: 10.1371/journal.pone.0151267.

Szurmant, Hendrik; Ordal, George W. (2004): Diversity in chemotaxis mechanisms among the bacteria and archaea. In: *Microbiology and molecular biology reviews : MMBR* 68 (2), S. 301–319. DOI: 10.1128/MMBR.68.2.301-319.2004.

Tagg, J. R.; Dajani, A. S.; Wannamaker, L. W. (1976): Bacteriocins of gram-positive bacteria. In: *Bacteriological reviews* 40 (3), S. 722–756.

Takeuchi, Shoji; DiLuzio, Willow R.; Weibel, Douglas B.; Whitesides, George M. (2005): Controlling the shape of filamentous cells of Escherichia coli. In: *Nano letters* 5 (9), S. 1819–1823. DOI: 10.1021/nl0507360.

Tanaka, T.; Kawata, M.; Mukai, K. (1991): Altered phosphorylation of Bacillus subtilis DegU caused by single amino acid changes in DegS. In: *Journal of bacteriology* 173 (17), S. 5507–5515.

Terra, Rebecca; Stanley-Wall, Nicola R.; Cao, Guoqiang; Lazazzera, Beth A. (2012): Identification of Bacillus subtilis SipW as a bifunctional signal peptidase that controls surface-adhered biofilm formation. In: *Journal of bacteriology* 194 (11), S. 2781–2790. DOI: 10.1128/JB.06780-11.

Thaxter, Roland (1892): On the Myxobacteriaceæ, a New Order of Schizomycetes. In: *Botanical Gazette* 17 (12), S. 389–406. DOI: 10.1086/326866.

Thompson, Luke R.; Sanders, Jon G.; McDonald, Daniel; Amir, Amnon; Ladau, Joshua; Locey, Kenneth J. *et al.* (2017): A communal catalogue reveals Earth's multiscale microbial diversity. In: *Nature* 551 (7681), S. 457–463. DOI: 10.1038/nature24621.

Tjalsma, H.; Koetje, E. J.; Kiewiet, R.; Kuipers, O. P.; Kolkman, M.; van der Laan, J. *et al.* (2004a): Engineering of quorum-sensing systems for improved production of alkaline protease by Bacillus subtilis. In: *Journal of applied microbiology* 96 (3), S. 569–578. DOI: 10.1111/j.1365-2672.2004.02179.x.

Tjalsma, Harold; Antelmann, Haike; Jongbloed, Jan D. H.; Braun, Peter G.; Darmon, Elise; Dorenbos, Ronald *et al.* (2004b): Proteomics of protein secretion by Bacillus subtilis: separating the "secrets" of the secretome. In: *Microbiology and molecular biology reviews : MMBR* 68 (2), S. 207–233. DOI: 10.1128/MMBR.68.2.207-233.2004.

Tokunaga, T.; Rashid, M. H.; Kuroda, A.; Sekiguchi, J. (1994): Effect of degS-degU mutations on the expression of sigD, encoding an alternative sigma factor, and autolysin operon of Bacillus subtilis. In: *Journal of bacteriology* 176 (16), S. 5177–5180. DOI: 10.1128/jb.176.16.5177-5180.1994.

Tracy, Bryan P.; Gaida, Stefan M.; Papoutsakis, Eleftherios T. (2008): Development and application of flow-cytometric techniques for analyzing and sorting endospore-forming clostridia. In: *Applied and environmental microbiology* 74 (24), S. 7497–7506. DOI: 10.1128/AEM.01626-08.

Tsukahara, Kensuke; Ogura, Mitsuo (2008): Promoter selectivity of the Bacillus subtilis response regulator DegU, a positive regulator of the fla/che operon and sacB. In: *BMC microbiology* 8, S. 8. DOI: 10.1186/1471-2180-8-8.

Vagner, V.; Dervyn, E.; Ehrlich, S. D. (1998): A vector for systematic gene inactivation in Bacillus subtilis. In: *Microbiology (Reading, England)* 144 (Pt 11), S. 3097–3104. DOI: 10.1099/00221287-144-11-3097.

van Wezel, Gilles P.; Krabben, Preben; Traag, Bjørn A.; Keijser, Bart J. F.; Kerste, Rob; Vijgenboom, Erik *et al.* (2006): Unlocking Streptomyces spp. for use as sustainable industrial production platforms by morphological engineering. In: *Applied and environmental microbiology* 72 (8), S. 5283–5288. DOI: 10.1128/AEM.00808-06.

Vary, Patricia S.; Biedendieck, Rebekka; Fuerch, Tobias; Meinhardt, Friedhelm; Rohde, Manfred; Deckwer, Wolf-Dieter; Jahn, Dieter (2007): Bacillus megaterium--from simple soil bacterium to industrial protein production host. In: *Applied microbiology and biotechnology* 76 (5), S. 957–967. DOI: 10.1007/s00253-007-1089-3.

Veening, Jan-Willem; Igoshin, Oleg A.; Eijlander, Robyn T.; Nijland, Reindert; Hamoen, Leendert W.; Kuipers, Oscar P. (2008a): Transient heterogeneity in extracellular protease production by Bacillus subtilis. In: *Molecular systems biology* 4, S. 184. DOI: 10.1038/msb.2008.18.

Veening, Jan-Willem; Kuipers, Oscar P. (2010): Gene position within a long transcript as a determinant for stochastic switching in bacteria. In: *Molecular microbiology* 76 (2), S. 269–272. DOI: 10.1111/j.1365-2958.2010.07113.x.

Veening, Jan-Willem; Smits, Wiep Klaas; Kuipers, Oscar P. (2008b): Bistability, epigenetics, and bet-hedging in bacteria. In: *Annual review of microbiology* 62, S. 193–210. DOI: 10.1146/annurev.micro.62.081307.163002.

Veening, J-W; Smits, W. K.; Hamoen, L. W.; Kuipers, O. P. (2006): Single cell analysis of gene expression patterns of competence development and initiation of sporulation in Bacillus subtilis grown on chemically defined media. In: *Journal of applied microbiology* 101 (3), S. 531–541. DOI: 10.1111/j.1365-2672.2006.02911.X.

Vehmaanperä, J. (1989): Transformation of Bacillus amyloliquefaciens by electroporation. In: *FEMS Microbiology Letters* 61 (1-2), S. 165–169. DOI: 10.1016/0378-1097(89)90190-0.

Veith, Birgit; Herzberg, Christina; Steckel, Silke; Feesche, Jörg; Maurer, Karl Heinz; Ehrenreich, Petra *et al.* (2004): The complete genome sequence of Bacillus licheniformis DSM13, an organism with great industrial potential. In: *Journal of molecular microbiology and biotechnology* 7 (4), S. 204–211. DOI: 10.1159/000079829.

Vejborg, Rebecca Munk; Klemm, Per (2009): Cellular chain formation in Escherichia coli biofilms. In: *Microbiology (Reading, England)* 155 (Pt 5), S. 1407–1417. DOI: 10.1099/mic.0.026419-0.

Verhamme, Daniel T.; Murray, Ewan J.; Stanley-Wall, Nicola R. (2009): DegU and Spo0A jointly control transcription of two loci required for complex colony development by Bacillus subtilis. In: *Journal of bacteriology* 191 (1), S. 100–108. DOI: 10.1128/JB.01236-08.

Verhamme, Daniël T.; Kiley, Taryn B.; Stanley-Wall, Nicola R. (2007): DegU co-ordinates multicellular behaviour exhibited by Bacillus subtilis. In: *Molecular microbiology* 65 (2), S. 554–568. DOI: 10.1111/j.1365-2958.2007.05810.x.

Villafane, R.; Bechhofer, D. H.; Narayanan, C. S.; Dubnau, D. (1987): Replication control genes of plasmid pE194. In: *Journal of bacteriology* 169 (10), S. 4822–4829. DOI: 10.1128/jb.169.10.4822-4829.1987.

Vingataramin, Laurie; Frost, Eric H. (2015): A single protocol for extraction of gDNA from bacteria and yeast. In: *BioTechniques* 58 (3), S. 120–125. DOI: 10.2144/000114263.

Vlamakis, Hera; Aguilar, Claudio; Losick, Richard; Kolter, Roberto (2008): Control of cell fate by the formation of an architecturally complex bacterial community. In: *Genes & development* 22 (7), S. 945–953. DOI: 10.1101/gad.1645008.

Vlamakis, Hera; Chai, Yunrong; Beauregard, Pascale; Losick, Richard; Kolter, Roberto (2013): Sticking together: building a biofilm the Bacillus subtilis way. In: *Nature reviews. Microbiology* 11 (3), S. 157–168. DOI: 10.1038/nrmicro2960.

Voigt, Birgit; Le Hoi, Thi; Jürgen, Britta; Albrecht, Dirk; Ehrenreich, Armin; Veith, Birgit *et al.* (2007): The glucose and nitrogen starvation response of Bacillus licheniformis. In: *Proteomics* 7 (3), S. 413–423. DOI: 10.1002/pmic.200600556.

Voigt, Birgit; Schweder, Thomas; Sibbald, Mark J. J. B.; Albrecht, Dirk; Ehrenreich, Armin; Bernhardt, Jörg *et al.* (2006): The extracellular proteome of Bacillus licheniformis grown in different media and under different nutrient starvation conditions. In: *Proteomics* 6 (1), S. 268–281. DOI: 10.1002/pmic.200500091.

Wang, Congya; Cao, Yingxiu; Wang, Yongping; Sun, Liming; Song, Hao (2019): Enhancing surfactin production by using systematic CRISPRi repression to screen amino acid biosynthesis genes in Bacillus subtilis. In: *Microbial cell factories* 18 (1), S. 90. DOI: 10.1186/s12934-019-1139-4.

Waschkau, Bianca; Waldeck, Jens; Wieland, Susanne; Eichstädt, Renèe; Meinhardt, Friedhelm (2008): Generation of readily transformable Bacillus licheniformis mutants. In: *Applied microbiology and biotechnology* 78 (1), S. 181–188. DOI: 10.1007/s00253-007-1278-0.

Weinrauch, Y.; Penchev, R.; Dubnau, E.; Smith, I.; Dubnau, D. (1990): A Bacillus subtilis regulatory gene product for genetic competence and sporulation resembles sensor protein members of the bacterial two-component signal-transduction systems. In: *Genes & development* 4 (5), S. 860–872. DOI: 10.1101/gad.4.5.860.

Weir, J.; Predich, M.; Dubnau, E.; Nair, G.; Smith, I. (1991): Regulation of spo0H, a gene coding for the Bacillus subtilis sigma H factor. In: *Journal of bacteriology* 173 (2), S. 521–529. DOI: 10.1128/jb.173.2.521-529.1991.

West, J. T.; Estacio, W.; Márquez-Magaña, L. (2000): Relative roles of the fla/che P(A), P(D-3), and P(sigD) promoters in regulating motility and sigD expression in Bacillus subtilis. In: *Journal of bacteriology* 182 (17), S. 4841–4848. DOI: 10.1128/jb.182.17.4841-4848.2000.

Westers, Helga; Dorenbos, Ronald; van Dijl, Jan Maarten; Kabel, Jorrit; Flanagan, Tony; Devine, Kevin M. *et al.* (2003): Genome engineering reveals large dispensable regions in Bacillus subtilis. In: *Molecular biology and evolution* 20 (12), S. 2076–2090. DOI: 10.1093/molbev/msg219.

Wilming, Anja; Begemann, Jens; Kuhne, Stefan; Regestein, Lars; Bongaerts, Johannes; Evers, Stefan *et al.* (2013): Metabolic studies of γ-polyglutamic acid production in Bacillus licheniformis by small-scale continuous cultivations. In: *Biochemical Engineering Journal* 73, S. 29–37. DOI: 10.1016/j.bej.2013.01.008.

Wilson, Charles R.; Ladin, Beth F.; Mielenz, Jonathan R.; Hom, Sherman S. M.; Hansen, Dieter; Reynolds, Robert B. *et al.* (1993): Alkaline proteolytic enzyme and method of production. Angemeldet durch Henkel Research Corp. [US] am 10.03.1993. Veröffentlichungsnr: US5352604.

Winkelman, Jared T.; Blair, Kris M.; Kearns, Daniel B. (2009): RemA (YlzA) and RemB (YaaB) regulate extracellular matrix operon expression and biofilm formation in Bacillus subtilis. In: *Journal of bacteriology* 191 (12), S. 3981–3991. DOI: 10.1128/JB.00278-09.

Winkelman, Jared T.; Bree, Anna C.; Bate, Ashley R.; Eichenberger, Patrick; Gourse, Richard L.; Kearns, Daniel B. (2013): RemA is a DNA-binding protein that activates biofilm matrix gene expression in Bacillus subtilis. In: *Molecular microbiology* 88 (5), S. 984–997. DOI: 10.1111/mmi.12235.

Wyre, Chris; Overton, Tim W. (2014): Use of a stress-minimisation paradigm in high cell density fed-batch Escherichia coli fermentations to optimise recombinant protein production. In: *Journal of industrial microbiology & biotechnology* 41 (9), S. 1391–1404. DOI: 10.1007/s10295-014-1489-1.

Xiao, Yi; Bowen, Christopher H.; Di Liu; Zhang, Fuzhong (2016): Exploiting nongenetic cell-to-cell variation for enhanced biosynthesis. In: *Nature chemical biology* 12 (5), S. 339–344. DOI: 10.1038/nchembio.2046.

Xu, Xiaofeng; Thornton, Peter E.; Post, Wilfred M. (2013): A global analysis of soil microbial biomass carbon, nitrogen and phosphorus in terrestrial ecosystems. In: *Global Ecology and Biogeography* 22 (6), S. 737–749. DOI: 10.1111/geb.12029.

Yang, M.; Ferrari, E.; Chen, E.; Henner, D. J. (1986): Identification of the pleiotropic sacQ gene of Bacillus subtilis. In: *Journal of bacteriology* 166 (1), S. 113–119. DOI: 10.1128/jb.166.1.113-119.1986.

Yang, M.; Shimotsu, H.; Ferrari, E.; Henner, D. J. (1987): Characterization and mapping of the Bacillus subtilis prtR gene. In: *Journal of bacteriology* 169 (1), S. 434–437. DOI: 10.1128/jb.169.1.434-437.1987.

Yang, Taowei; Rao, Zhiming; Zhang, Xian; Xu, Meijuan; Xu, Zhenghong; Yang, Shang-Tian (2015): Enhanced 2,3-butanediol production from biodiesel-derived glycerol by engineering of cofactor regeneration and manipulating carbon flux in Bacillus amyloliquefaciens. In: *Microbial cell factories* 14, S. 122. DOI: 10.1186/s12934-015-0317-2.

Yanisch-Perron, C.; Vieira, J.; Messing, J. (1985): Improved M13 phage cloning vectors and host strains: nucleotide sequences of the M13mp18 and pUC19 vectors. In: *Gene* 33 (1), S. 103–119. DOI: 10.1016/0378-1119(85)90120-9.

Yasumura, Ayako; Abe, Sadanobu; Tanaka, Teruo (2008): Involvement of nitrogen regulation in Bacillus subtilis degU expression. In: *Journal of bacteriology* 190 (15), S. 5162–5171. DOI: 10.1128/JB.00368-08.

Yu, Yiyang; Yan, Fang; Chen, Yun; Jin, Christopher; Guo, Jian-Hua; Chai, Yunrong (2016): Poly-γ-Glutamic Acids Contribute to Biofilm Formation and Plant Root Colonization in Selected Environmental Isolates of Bacillus subtilis. In: *Frontiers in microbiology* 7, S. 1811. DOI: 10.3389/fmicb.2016.01811.

Zeigler, Daniel R.; Prágai, Zoltán; Rodriguez, Sabrina; Chevreux, Bastien; Muffler, Andrea; Albert, Thomas *et al.* (2008): The origins of 168, W23, and other Bacillus subtilis legacy strains. In: *Journal of bacteriology* 190 (21), S. 6983–6995. DOI: 10.1128/JB.00722-08.

Zhou, Cuixia; Zhou, Huiying; Fang, Honglei; Ji, Yizhi; Wang, Hongbin; Liu, Fufeng *et al.* (2020a): Spo0A can efficiently enhance the expression of the alkaline protease gene aprE in Bacillus licheniformis by specifically binding to its regulatory region. In: *International journal of biological macromolecules* 159, S. 444–454. DOI: 10.1016/j.ijbiomac.2020.05.035.

Zhou, Cuixia; Zhou, Huiying; Li, Dengke; Zhang, Huitu; Wang, Hongbin; Lu, Fuping (2020b): Optimized expression and enhanced production of alkaline protease by genetically modified Bacillus licheniformis 2709. In: *Microbial cell factories* 19 (1), S. 45. DOI: 10.1186/s12934-020-01307-2.

Zhou, Cuixia; Zhou, Huiying; Zhang, Huitu; Lu, Fuping (2019): Optimization of alkaline protease production by rational deletion of sporulation related genes in Bacillus licheniformis. In: *Microbial cell factories* 18 (1), S. 127. DOI: 10.1186/s12934-019-1174-1.